REACTIONS OF TOLUENE AND OXYGEN

IN AN ELECTRICAL DISCHARGE

By

Karl Ronny Eriksson, M.Sc. (Chem. Eng.)

A DOCTORAL THESIS

Submitted in partial fulfilment of the requirements for the award of

degree of Doctor of Philosophy of Loughborough University of

Technology   September, 1975

Supervisors: Mr. J. Glover

Department of Chemical Engineering

Loughborough University of Technology

Dr. B. Brooks

Department of Chemical Engineering

Loughborough University of Technology

(i)

ACKNOWLEDGEMENTS

SUMMARY

The chemical reactions of toluene and oxygen in a 50 Hz ac discharge have been studied in a capacitive coupled discharge reactor.

The variables investigated were partial pressure of the reactants, reactor pressure, reactor temperature, reactant ratios, applied reactor voltage, discharge current, capacitive current, breakdown voltage, and the phase shift.

The thermal reaction was negligible at temperatures below $300^{\circ}C$.

The major products of the reaction between toluene and oxygen were benzaldehyde, o-cresol, benzene, m+p-cresol, phenol and benzyl alcohol. The reaction was controlled by the electric field and the total reactor pressure.

The threshold energy for the chemical reaction was found to be about 10 eV.

The reaction was found to be of first order with respect to oxygen. The effect of the electric field was correlated by the parameter E/N.

The selectivity of benzene was mainly determined by the ratio of toluene to oxygen. Cresol, benzaldehyde, benzyl alcohol and phenol were mainly controlled by the parameter E/N and the partial pressure of oxygen and were all first order with respect to oxygen.

A rate expression for bimolecular reactions in cold plasmas was derived and found to agree well with the experimental results.

A model was proposed to explain some unusual features of the discharge current, and a circuit for measuring the discharge current was described.

The energy yield obtained was about 1 kWhr per mole toluene.

CONTENTS

LIST OF SYMBOLS

Symbol		CGS Units	SI Units
V	Electric potential	volt	volt
V_B	Breakdown voltage	volt	volt
V_E	Extinguishing voltage	volt	volt
i	Electric current	ampere	ampere
i_e	Electron current	ampere	ampere
i_c	Capacitive current	ampere	ampere
i_d	Discharge current	ampere	ampere
λ_e	Mean free path of electron	cm	m
α	Townsend first ionization coefficient	cm^{-1}	m^{-1}
γ	Townsend second coefficient		
η	Attachment coefficient		
ε	Kinetic energy	erg/mole	kJ/kgmole
E_a, ε_0	Activation energy	erg/mole	kJ/kgmole
l	Length	cm	m
L	Reactor length	cm	m
d	Electrode separation	cm	m
d_i	Inner diameter of reactor	cm	m
d_y	Outer diameter of reactor	cm	m
d_0	Molecular diameter	cm	m
q, δ	Cross-section	cm^2	m^2
v	Scalar velocity	cm/s	m/s
m	Mass	g	kg
ρ	Gas density	g/cm^3	kg/m^3
n, N	Particle density	cm^{-3}	m^{-3}
P	Total gas pressure	torr	pascal
k_r	Bimolecular reaction rate constant	$\dfrac{cm^3}{sec.gmole}$	$\dfrac{m^3}{sec.kgmole}$
Pb	Probability	—	—
T	Temperature	$^\circ K$	$^\circ K$

ϕ	Phase shift between applied and discharge voltage	radians	radians
r_a, r_b, r_c, r_d	Reactor radius	cm	m
θ	Run time	sec	sec
U_b, U_i	Breakdown voltage	volts	volts
U_e	Extinguishing voltage	volts	volts
C	Capacitance	Farad	Farad
V_r	Rms voltage	volt	volt
V_{peak}	Peak voltage	volt	volt
V	Reactor volume	cm^3	m^3
$N(i)$	Concentration of i	$\dfrac{gmoles}{cm^3}$	$\dfrac{kgmoles}{m^3}$
$\phi_x, \mathscr{S}_x$	Instantaneous selectivity	–	–
T_g	Gas temperature	^oK	^oK
T_e	Electron temperature	^oK	^oK
ln	Natural logarithm	–	–
E	Electric field strength	$V\ cm^{-1}$	$V\ m^{-1}$

LIST OF CONSTANTS

Constant		CGS Units	SI Units
e	Base of the natural logarithm	2.7183	2.7183
e_0	Charge of the electron	1.6×10^{-19} As	1.6×10^{-19} As
h	Planck's constant	6.625×10^{-27} erg-sec	6.63×10^{-34} J-sec.
k_0	Boltzmann constant	1.38×10^{-16} erg/$^{\circ}$K	1.38×10^{-23} J/$^{\circ}$K
m_e	Rest mass of the electron	9.11×10^{-28} g	9.11×10^{-31} kg
π	Pi	3.14159	3.14159
R	Universal gas constant	8.414×10^{7} erg/gmole-$^{\circ}$K	8.314×10^{3} J/kgmole$^{\circ}$K
ε_0	Permitivity constant	1.0 (by definition)	8.85×10^{-12} Farad/m
N_A	Avagadro's number	$6.023 \times 10^{23} \dfrac{\text{molecules}}{\text{gmole}}$	$6.023 \times 10^{26} \dfrac{\text{molecules}}{\text{kgmole}}$
eV	Electron volt	1.6×10^{-12} erg	1.60×10^{-19} Joule
πa_0^2	Atomic unit of cross-section	0.88×10^{-16} cm^2	0.88×10^{-20} m^2

CHAPTER ONE

CHAPTER 1

INTRODUCTION

Chemical reactions in an electrical discharge have been
extensively studied during the sixties. |42, 1, 8, 61, 71|
Despite this effort the only commercial process in use is the
production of ozone.

There are several different types of electrical discharge.
The two basic discharges are the electrodeless r.f. discharge
(microwave discharge) and the low frequency discharge utilizing
electrodes (capacitive discharge, corona discharge, arc discharge).
All these types of electrical discharge have different character-
istics. The major interest from a chemical reaction point of view
is whether the electrons can be considered to be in thermal equi-
librium with the gas or not.

In a cold plasma, where the electron and the gas temperature
are different, it is possible to produce more active molecules, which
would otherwise be impossible if thermal equilibrium was established.

The plasma consist largely of free radicals, ions, molecules
and molecular fragments. It has often been described as a fourth
state having almost metallic properties in some respects. It is
therefore hardly surprising that compounds like oxygen fluoride
and ozone can be produced in an electrical discharge. Even the
noble gases react to form fluorides.

The reaction chosen for this particular study was the reaction
between toluene and oxygen. A literature survey revealed that this
particular system has not been investigated previously. The elec-
trical discharge reaction is a possible alternative to thermal or

catalytic oxidation of toluene for production of technically important intermediates such as benzaldehyde, benzoic acid and phenols. Also the technique may be of use in other partial oxidation processes which are at present used on a large scale in the petrochemical industry.

The research undertaken is directed to the understanding of chemical reactions in an electrical discharge and the influence of the process variables such as temperature, pressure, residence time and electric field upon reaction rate, conversion, energy yield and selectivity.

The reactor properties such as electric capacitance and breakdown voltage were measured. The power dissipation and the discharge current were recorded by introduction of an electric circuit.

Brooks |43|, studying the reactions of benzene in a microwave discharge, found that the high energy dissipation per unit volume completely broke the benzene ring to yield acetylenes. On this basis it was thought that a capacitive discharge, having a lower power dissipation, would result in a milder attack on the benzene ring than an r.f. discharge. There are quite a number of configurations to choose from like a.c. or d.c., electrodes inside or outside the vessel. The system preferred was an annular reactor with double dielectric barriers. Although this leads to higher operating voltages there is the advantage of avoiding direct contact of the reactants with the electrodes.

Discharge simulations were carried out in order to gain a better understanding of the basic principles governing a discharge.

Preliminary runs were made in a batch reactor. The main purpose of these experiments was to give guidance for the final design

of a flow reactor and to establish the range of operating conditions.

The thesis has been divided into two parts: chapters one to four give a background of the accumulated theoretical and experimental knowledge whereas chapters five to nine describe the reactor properties and the experimental results.

CHAPTER TWO

FUNDAMENTALS OF ELECTRICAL DISCHARGES

A gas in its normal state is a good insulator. However, if an electric field of sufficient strength is applied, the gas becomes conducting. This phenomena is called electrical breakdown. There are several types of discharges depending on voltage and operating pressure. Fig. 2.1 shows some types of discharges.

From the chemical point of view we differentiate between thermal (equilibrium) and non-thermal (where the electron temperature is higher than the gas temperature) discharges. The latter is also termed cold plasma and this is the type of discharge formed from capacitive coupling of the electrodes. Fig. 2.2 shows the a.c. inductive resp. capacitive coupling as given by Spedding |42|. Llewellyn-Jones |4| has described the conditions for breakdown at different circumstances in gases. At lower gas pressures the break-down voltage follows Paschen's law and is a unique function of pressure times electrode separation. The Townsend criterion (2.1.2) and Paschen's law are only concerned with the steady state. If the frequency is high we must allow for the time lag, e.g. the time it takes from the moment when the external electric field is applied until breakdown occurs.
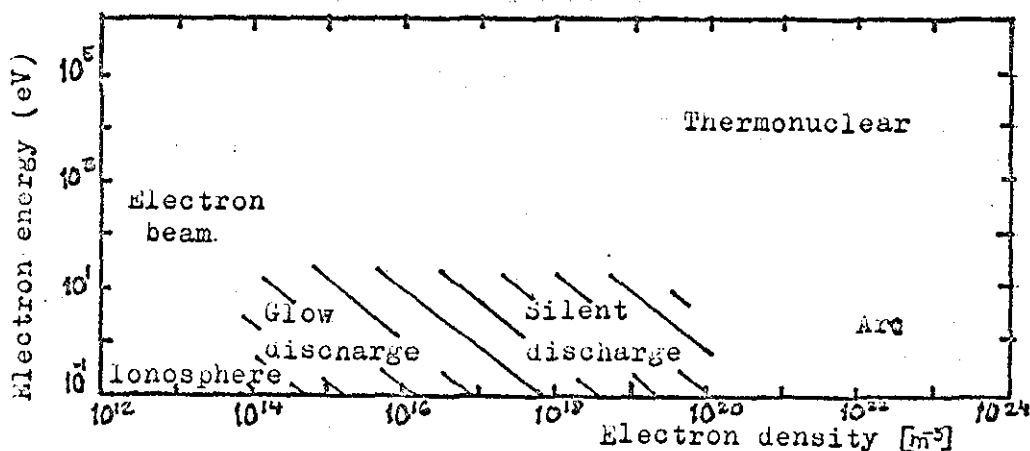
Fig. 2.1.   Classification of discharge types
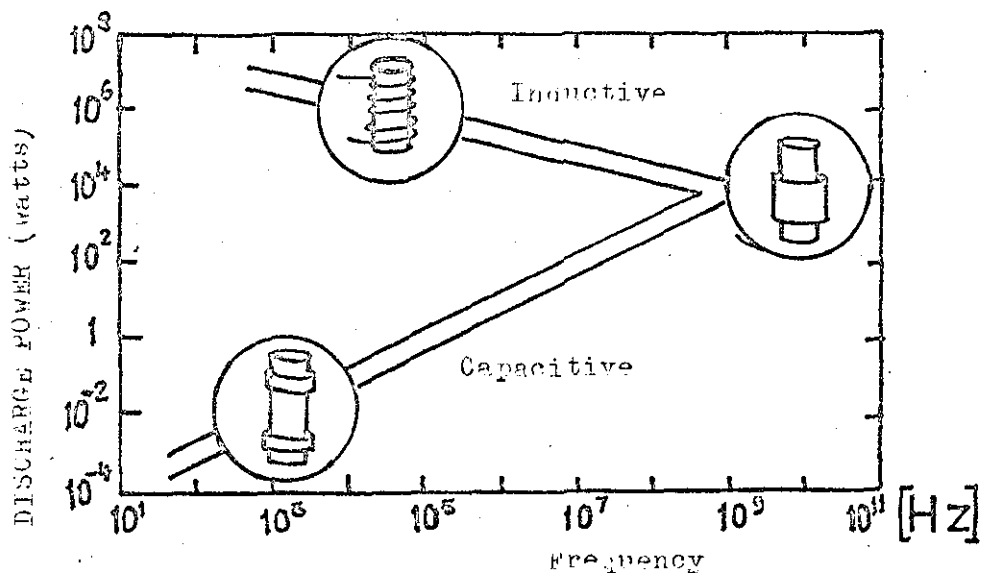
Fig. 2.2.   Power dissipation in electrical discharges

The self-sustaining discharges are formed when the applied

voltage is accelerating the few stray electrons that are always

present because of background radiation.   These electrons acquire

kinetic energy as they move in the electric field.   In this travel-

ling they will collide with gas molecules.   Most collisions are

elastic, but occasionally some electron will have sufficient energy

to ionize the gas and an avalanche of electrons builds up, following

a breakdown of the gas.   Fig. 2.3 shows a typical voltage-current

characteristic for a low pressure d.c. discharge.
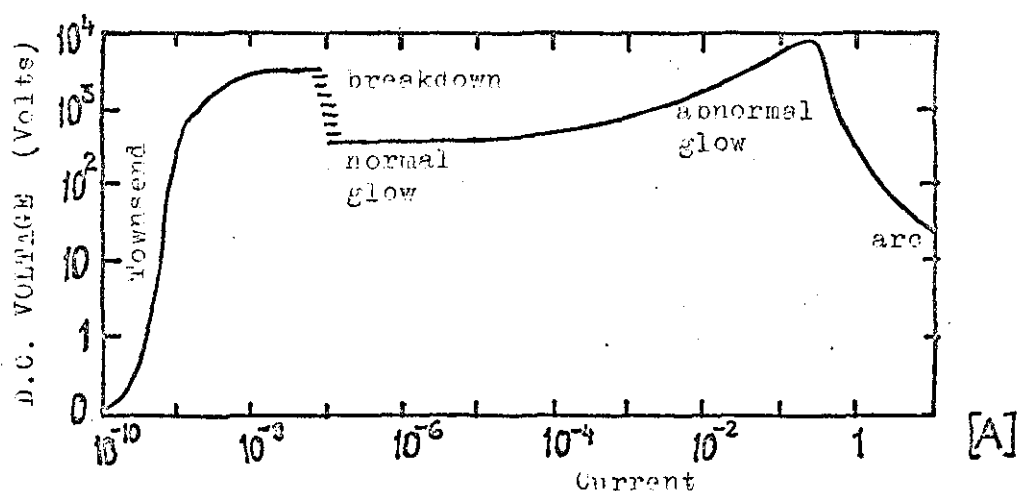
Fig. 2.3.   Glow discharge characteristic |42|

7

If we look closer at the visual appearance of the discharge we may
see something like fig. 2.4 depending on the operating conditions
like pressure, etc.
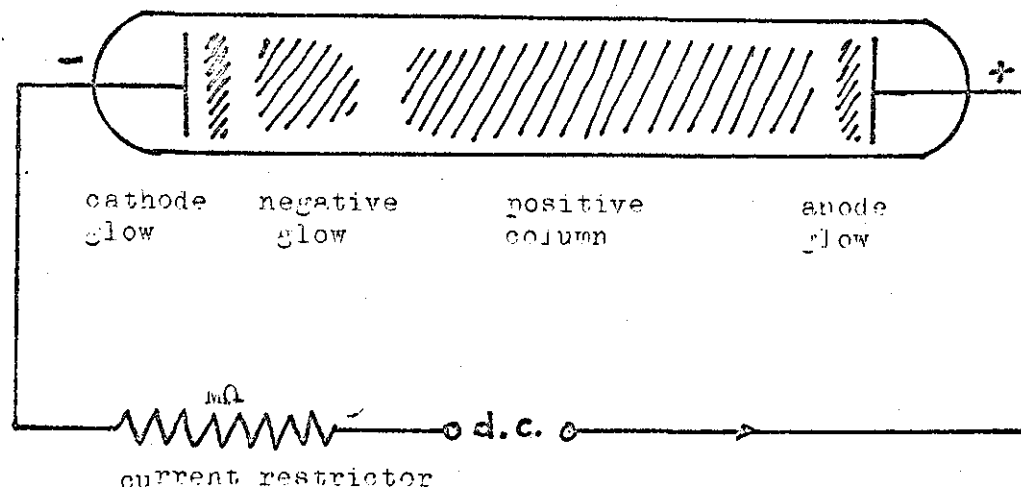
Fig. 2.4.   Glow discharge at low pressure

The discharge is not as homogeneous as it first looks. It consists
of several distinct zones. Brewer and Westhaver |55| studied the
synthesis of NH_3 and found that NH_3 was formed only in the luminous
discharge regions and preferably in the negative glow where the
electric field is largest. This also means that the kinetic energy
has its highest value in the negative glow. The disadvantage of
having zones of different energy and product reactivity is overcome
by using alternating current, the frequency of which may be 50Hz to
several kHz obtained from the main supply resp. solid state con-
verters or generators.

Many research workers have found that the reaction kinetics
often are complicated by secondary reaction with the electrodes or
deposition on the electrodes. This problem can be avoided by with-
drawing the electrodes from the discharge tubes. A typical ozonizer
is shown overleaf in fig. 2.5.
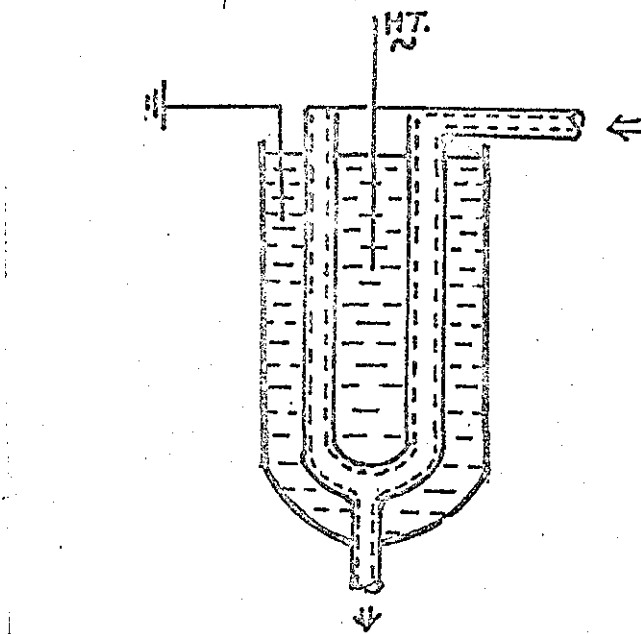
Fig. 2.5.   Ozonizer

2.1   ELECTRICAL BREAKDOWN

When the applied voltage between two electrodes is increased beyond a certain value, the current rises steeply, and further increase in voltage leads to a spark or stepwise current increase (fig. 2.3) called electrical breakdown. The step increase in current marks the beginning of ionization by collision. The actual voltage at which this occurs depends on such variables as electrode shape (point electrodes give lower voltage), spacing, pressure and type of gas.

The kinetic energy gained by an electron is $E\lambda_e e$, but since λ_e is proportional to $1/p$ the gained energy is proportional to E/p. Thus, whatever the secondary processes are, the critical field will depend on the ratio E/p. Critical values for E/p are given below for a few gases.

Gas	E/p $[Volt\ cm^{-1} mmHg^{-1}]$
Air	20
Hydrogen	10
Argon	5
Neon	2

9

2.1.1 The Townsend discharge

Townsend |44| studied the variation of current with the applied potential between two parallel plates when ultraviolet light was falling on the negative electrode. If the gas was at high pressure, the current increased with the electric force and attained a maximum value, which was not exceeded unless very large forces were used. However, by reducing the pressure of the gas, a large increase in current was obtained even at low voltage. Fig. 2.6 shows the relation of current and voltage at low pressure.
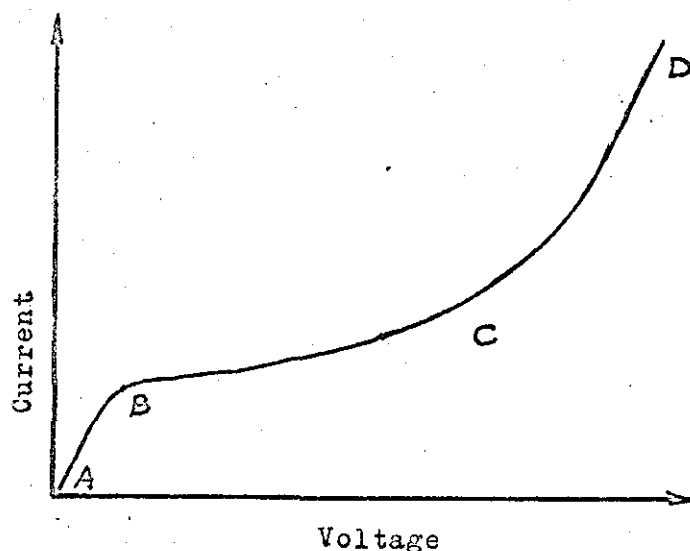
Fig. 2.6.a.   Voltage and current characteristics
of a discharge

In the first stage, AB, the current increases linearly with the applied voltage. The rate decreases at higher voltage and the current reaches a saturation value at stage BC. In the third stage, CD, when the electric force is still further increased, there is a large increase in the conductivity. This was explained by the hypothesis that new ions and electrons were produced by collisions, at first practically by electrons alone, but as the

voltage increased and the sparking potential is approached, the positive ions also acquire the property of producing others to an appreciable extent.

2.1.2 Secondary ion production

At the critical value of E/p the most energetic electrons have sufficient energy to cause ionization when they collide with an atom or molecule, producing an extra electron plus an ion. The additional electrons may, under favourable circumstances, themselves produce more electrons and positive ions. This process gives rise to an avalanche of electrons initiated by a single electron.

Suppose one electron on average makes α ionizing collisions by travelling 1 cm in the direction of the field. The increase in the number of electrons (dn_e) caused by travelling dx cm in the electric field is then

$$dn_e = n_e \, \alpha dx$$

if n_e^0 is the number of electrons we start with at $x = 0$.

We get $n_e = n_e^0 \, e^{\alpha x}$ and $i = i_0 \, e^{\alpha x}$ where $i_0 = n_e^0 \, e_0$

is the current at the cathode and dependent only on photoelectric or radioactive radiation.

α is called the first Townsend ionization coefficient and is not a constant but $\dfrac{\alpha}{p} = f(E/p)$. The function is often expressed as $\dfrac{\alpha}{p} = Ae^{-B \, p/E}$, where A and B are constants depending on the gas used.

At higher E/p there are two processes that can occur: production of photoelectrons at the cathode and collision of positive

11

ions with the cathode. A highly energetic electron may not only ionize an atom or a molecule but also leave it in an excited state. When the atom falls back in its normal state, the excess energy is given off in the form of radiation. If this energy falls on the cathode it can free an electron that gives rise to a new avalanche as it travels to the anode. Electrons emitted by the anode are pulled back by the electric field.

Electrons may also be produced when positive ions collide with the cathode, and some of its kinetic energy is transferred to electrons in the metal surface. Let γ be the probability that a secondary electron will be emitted from the cathode by secondary processes associated with each primary multiplication event. Therefore there must be $n_0 + n_s$ electrons leaving the cathode/sec and $n = (n_0 + n_s)e^{\alpha x}$ electrons reaching the anode. Now the number of secondary processes taken place is the difference between the number of electrons arriving at the anode and the number of electrons leaving the cathode, i.e. $n - (n_0 + n_s)$.

The number of secondary electrons produced is then

$$n_s = \gamma(n-(n_0 + n_s))$$

$$n_s + n_0 = \frac{\gamma n + n_0}{1 + \gamma} \qquad \text{since} \qquad n = (n_0 + n_s)e^{\alpha x}$$

$$n = \frac{\gamma n + n_0}{1 + \gamma} e^{\alpha x}$$

$$n + n\gamma = \gamma n\, e^{\alpha x} + n_0 e^{\alpha x}$$

$$n\left[1 + \gamma(1-e^{\alpha x})\right] = n_0 e^{\alpha x}$$

$$n = n_0 \frac{e^{\alpha x}}{1 - \gamma(e^{\alpha x} - 1)}$$

and

$$i = i_0 \frac{e^{\alpha x}}{1 - \gamma(e^{\alpha x} - 1)}$$ (2.1.a)

This equation gives the criterion for self-sustaining conductivity in a gas. As the denominator approaches zero, the current is increased and finally flows regardless of i_0. The criterion for breakdown is thus

$$1 = \gamma e^{\alpha x} .$$ (2.1.b)

This means that starting with one electron at the cathode enough ion pairs are formed in the electric field so that at least one new pair is formed by secondary processes. Depending on the conditions this can be a glow discharge (at low pressure), corona or an arc.

2.1.3 Attachment

In electronegative gases, like oxygen, electrons can combine with molecules or atoms to form negative ions. Negative ions can be formed by an electron capture process

$$AB + e \rightarrow (AB^-)^* \rightarrow AB^- + h\nu$$
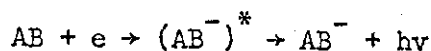
or by a dissociation process to form ion pairs

$$AB + e \rightarrow AB^* + e \rightarrow A^+ + B^- + e$$
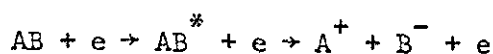
The latter reaction requires higher energy, because it must break the A-B bond, which requires about 4-5eV.

The effect of attachment on electron multiplication can be found from a similar treatment as the first Townsend coefficient.

Let η be the attachment coefficient, defined as the number of attachments per electron per cm drift, by analogy with the first coefficient α. Since the effective electron multiplication is $\alpha - \eta$ we obtain $n_e = n_o e^{(\alpha-\eta)d}$. The current consists partly of negative ions arriving at the anode. The total current is therefore

$$i = e \ (n_e + n_-)$$
$$= e \ n_0 e^{(\alpha-\eta)d} + \int_0^d \eta n dx$$

$$= e \ n_o \ e^{(\alpha-\eta)d} + \frac{n_0}{\alpha - \eta} \left[e^{(\alpha-\eta)d} - 1 \right]$$

Hence

$$i = \frac{i_0}{\alpha - \eta} \left[\alpha e^{(\alpha-\eta)d} - \eta \right] \tag{2.1.c}$$

and if we include γ in our calculations we obtain

$$i = i_0 \ \frac{\alpha e^{(\alpha-\eta)d} - \eta}{\alpha - \eta - \alpha\gamma \left[e^{(\alpha-\eta)d} - 1 \right]} \tag{2.1.d}$$

In absence of attachment 2.1.c reduces to $i = i_0 e^{\alpha d}$ and a plot of log i vs d gives a straight line of slope α, fig. 2.6.b. The upcurving of the slope, due to Townsend's second ionization coefficient, γ, is not likely to be found in an electronegative gas. Instead the slope of the curve decreases as the current increases.
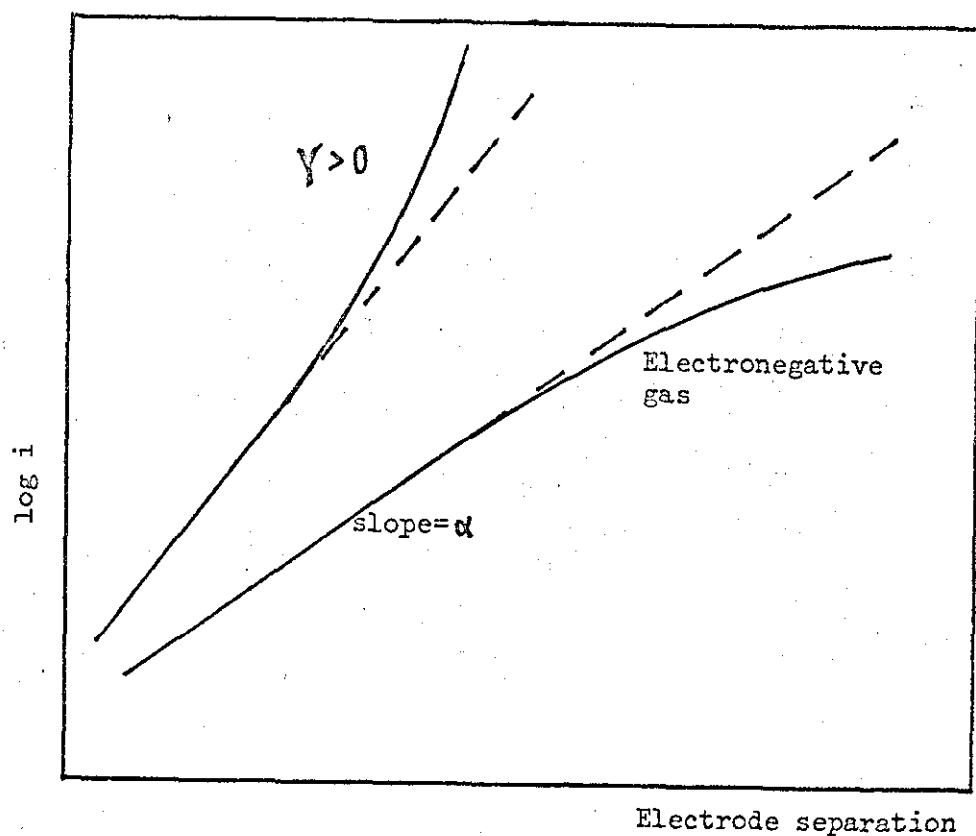
Fig. 2.6.b.   Effect of attachment
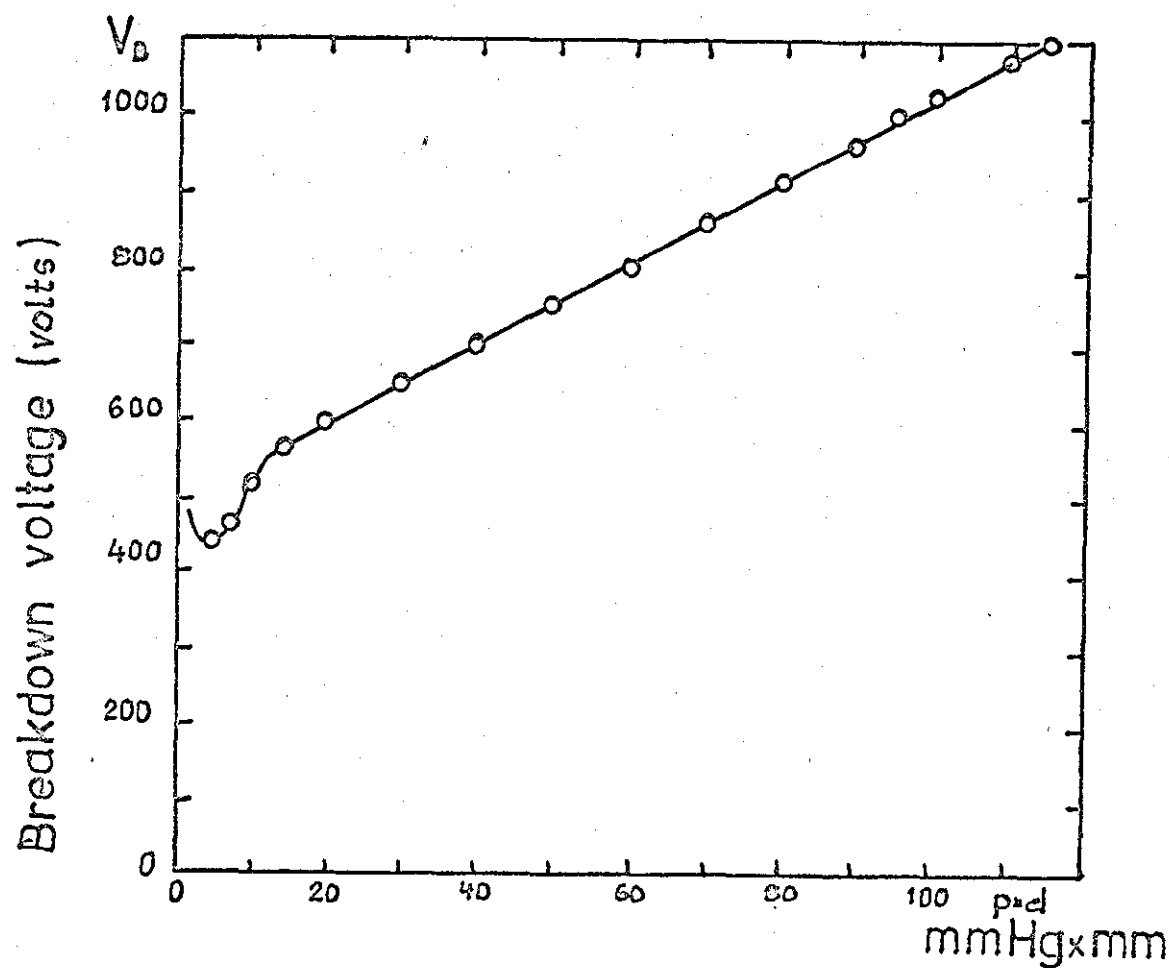
Fig. 2.7.   Breakdown voltage for oxygen |14|

15

2.1.4 Paschen's law

For short gaps at lower pressure good agreements have been obtained from the Townsend criteria, $\gamma e^{\alpha d} = 1$. If the first and second ionization coefficients, α, γ, are expressed as a function of E/p and inserted in 2.1.b we get the following expressions:

$$\frac{\alpha}{p} = f_1(E/p)$$

$$\gamma = f_2(E/p)$$

$$f_2(E/p)\exp\left[pd\ f_1(E/p)\right] = 1$$

and

$$V_s = \text{func}(pd) \qquad\qquad (2.2.a)$$

This relation is known as Paschen's law and was established experimentally as early as 1889. A graph of the breakdown voltage for oxygen is shown in fig. 2.7.

According to Townsend's theory the formative time lag should equal the ion transit time. However, practical experiments around atmospheric pressure and above have given much shorter time lag. To explain this Meek |51| and Raether |52| independently postulated the streamer theory. The theory is based on the following principles. An avalanche is initiated by an electron leaving the cathode. Due to the high mobility, electrons are swept away leaving positive ions behind, with its highest concentration near the anode. The positive charge will distort the electric field. Auxiliary avalanches are produced from photoelectrons in the vicinity of the avalanche head, thus extending the positive charge and ionizing the gap.

Meek obtained the following criteria for breakdown

$$\alpha d + \log_e(\alpha/p) = 14.46 + \log_e(E/p) + \tfrac{1}{2}\log_e(d/p) \qquad (2.2.b)$$

Raether gives the criteria for streamer formation as $\alpha d \geqslant 20$. There has been some criticism of the criterion of Meek and

16

Raether $|53|$. The equation is empirical, giving values of V_s which differ very little from the simpler form, $\exp(\alpha d) = \text{constant} \ |54|$.

2.1.5 Charge transfer

In some gas mixtures or impure gases there is a significant reduction in breakdown voltage. The explanation for this behaviour is that excited metastable atoms can ionize another molecule or atom by virtue of its excitation energy, if the latter is larger than the required ionization energy. Fig. 2.8 shows the breakdown voltage in an argon-neon mixture. In this case neon, excitation energy $(3S^3P2)$ 16.62 eV, is colliding at thermal velocity with argon in ground state, ionization energy 15.76 eV, with a probability close to unity. This effect is known as the Penning Effect.
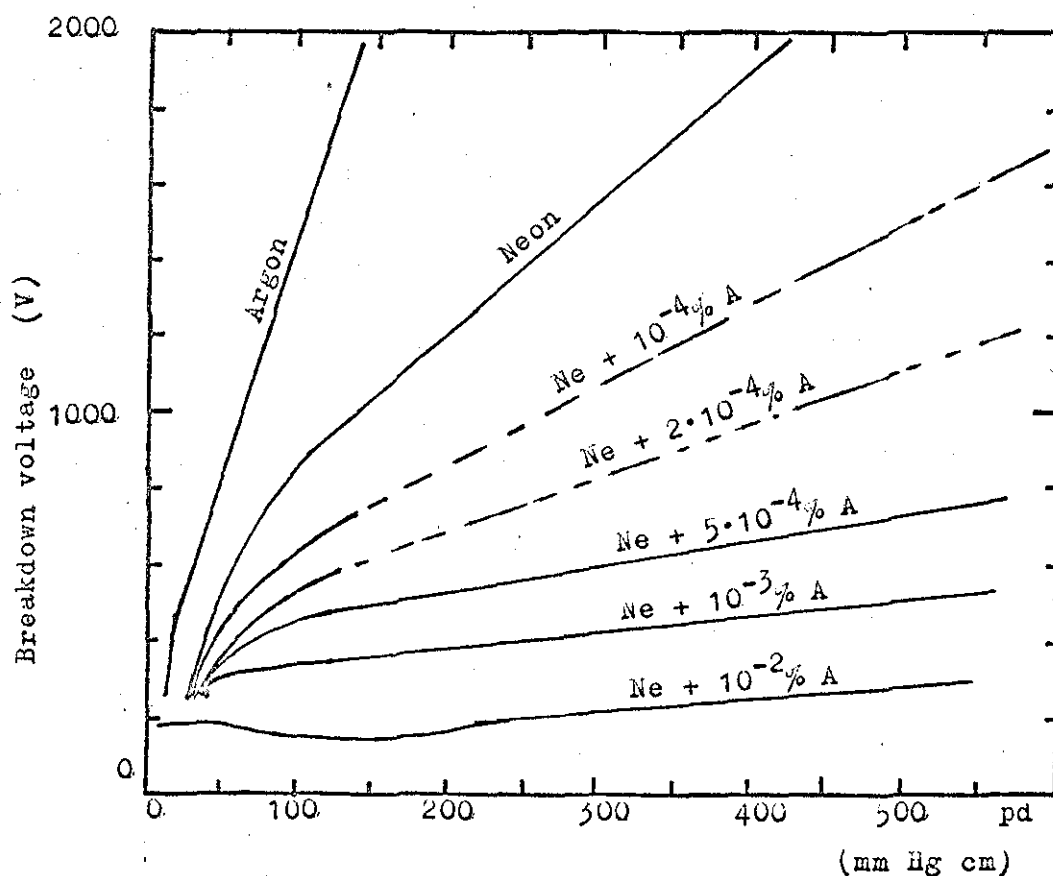
Fig. 2.8. The Penning Effect in Ar-Ne mixtures $|17|$

2.1.6 Corona discharge

In non-uniform fields, e.g. point to plane, sphere to plane or coaxial cylinders, the applied field and Townsend's ionization coefficient vary across the gap. The Townsend criterion therefore takes the following form:

$$\gamma \left\{ \exp \left(\int_0^d \alpha dx \right) \right\} - 1 = 1 \qquad (2.3)$$

which simplifies to

$$\int_0^d \alpha dx = \log_e \left(1 + \frac{1}{\gamma} \right)$$

For coaxial geometry the integration limits become the inner and outer radii of the cylinder.

Peek |56| expressed the electric field at a surface required for production of a visual corona in air between two coaxial cylinders as:

$$E = 31m\rho \left(1 + \frac{0.308}{\sqrt{\rho a}} \right) \qquad \text{peak kV/cm} \qquad (2.4)$$

where a is the inner radius in cm, m is a surface roughness factor $= 1$ for polished surfaces. ρ is the relative density factor given by

$$\rho = \frac{0.392b}{(273 + t)}$$

b is the barometric pressure in mm Hg, t is the temperature in $^\circ$C.

At high pressures there is a distinct difference in visual appearance of the two polarities. Under positive corona a bluish white light covers the entire area, whereas the negative corona appears as reddish glowing spots distributed along the surface. The first investigations of negative corona were made by Trichel |57|,

who observed that the current flows in irregular pulses, which have been named after their discoverer as Trichel Pulses. The repetition frequency (5kHz/μA) was found to increase with increasing current and point sharpness. An interpretation of these pulses was given by Hudson and Bennett |58| who ascribed the process to accumulation of negative ions outside the positive space charge. The negative space charge grows faster than the positive space charge as positive ions are withdrawn from the field into the point.

The positive corona has been studied extensively and has recently been reviewd by Loeb |59|.

The breakdown of the electric field is in the form of pulses with a repetition frequency of about 1 kHz. Loeb called this form of corona, burst corona. The average current increases steadily with voltage until the discharge becomes self-sustained. The burst pulses are generally preceded by a streamer starting from the point towards the plate. Near the corona threshold potential, two discharge forms are usually observed corresponding to streamers and bursts.

Once a streamer, which has crossed part of the gap but not its full length, has formed, adequate negative space charge can form which inhibits the formation of further streamers but not formation of coronas within the short region near the point.

The breakdown voltage for nitrogen between a wire and a coaxial cylinder (radii 0.083 and 2.3 cm) is shown overleaf in fig. 2.9 |17|.
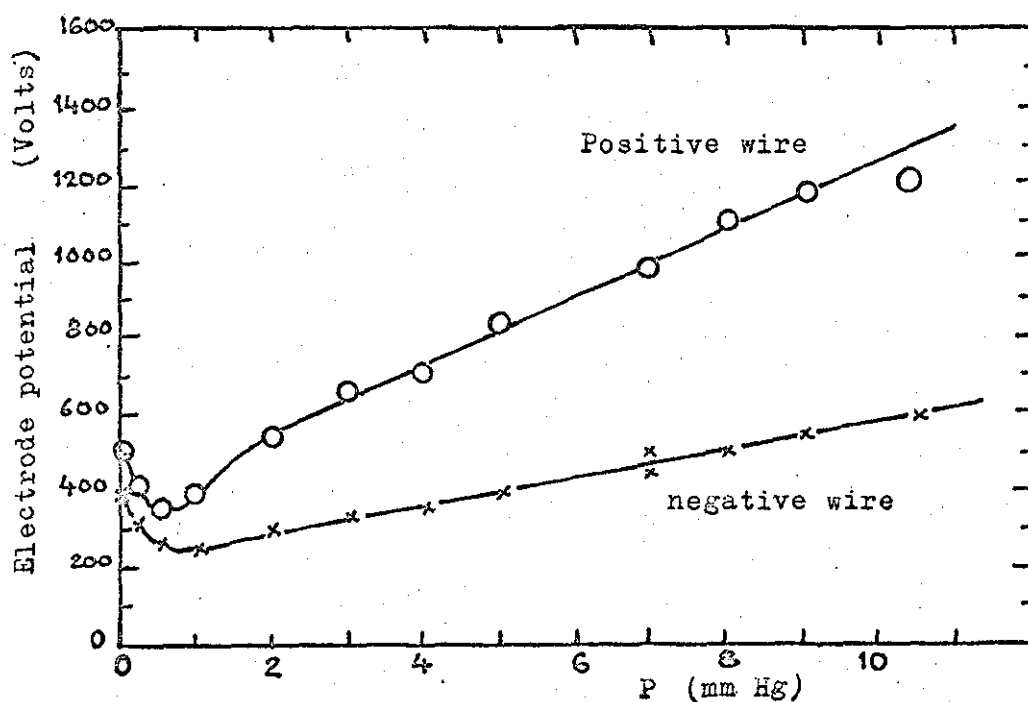
Fig. 2.9. Effect of polarity on breakdown voltage

2.2 COLLISION PROCESSES

A collision is defined as an encounter between particles that constitutes a change in mass, momentum, or kinetic energy of any of the particles. From this definition it follows that more than one type of collision can occur. Two types are distinguished: elastic collisions where translational energy is changed, and inelastic collisions where the internal energy as well as the kinetic energy of a particle are changed.

An inelastic collision can result in excitation, ionization and in some cases in chemical reactions. When we calculate the rate of chemical reaction we must know the collision frequency, which is determined by velocity and concentration. Furthermore,

we must also know the probability of the reaction to take place, which can be found from the cross-section. Unfortunately, both the velocity and cross-section are not constants. As a result of collisions some particles have a higher velocity than others. However, we can assign a mean value and a standard deviation of the scalar velocity based upon a sufficiently large population. Thus, the fraction of particles having a velocity between v and v + dv can be found from a distribution function. The cross-section cannot be calculated from microscopic data and has therefore to be measured. To achieve this we cannot use the reaction rate in reverse, since the accuracy would not be sufficient and also we do not have monoenergetic particles. There are two basic ways in which the reaction cross-section is measured. The most common is the molecular beam method. In this method one of the reactants is heated to very high temperature and then allowed to diffuse through a collimator into a beam of molecules with high translational energy. The second reactant is introduced as a second beam at right angles to the first.

The other method is irradiation of molecules with uv-light causing fragments to recoil at high energy. If these hot atoms react in their first few encounters, they can be used to measure the cross-section.

In the classical rate theory, as Steinfeld and Kinsey |5| point out, the Arrhenius parameter is a reflection of the Boltzmann distribution and not a specific property of the reactants. Thus much information about the encounter is hidden in an irretrievable form. To give a complete picture of the collision one would like to have access to the cross-section as well as the rate constant.

The main application of the collision rate theory has been in atomic physics of elementary particle bombardment in vacuum.

21

The classical rate theory is used in an overwhelming number of cases among chemists due to its simplicity of measurement and straightforward calculations.

In the case of chemical reaction in electrical discharges where we have particles with different kinetic energy, the electron temperature can often reach 20-30,000°K. Perhaps a more meaningful way of describing the particles is in terms of electron volts (eV). 1 eV is about 23 kcal/mole. Also the kinetic energy gained between collisions is a function of the mean free path of the electrons. It seems therefore more logical to present the influence of electrical variables in terms of the collision theory.

2.2.1   Cross-sections

We can define a cross-section if we think of the particles as spheres. If the particle has a diameter d_0, any one will collide which lies with its centre within a cylindrical volume $\pi d_0^2 l$ whose axis is in the path of the first particle. This volume is πd_0^2 per unit length of path. If the number density is n, this volume contains $\pi d_0^2 n$ particles per unit length, which is therefore the number of collisions per particle per unit length. Hence the mean free path between collisions is

$$\lambda = \frac{1}{\pi m d_0^2} \qquad (2.5)$$

For a mixture of gases the mean free path of particle 1 with any other type of particle is:

$$\lambda_1 = \frac{1}{\pi \sum_r m_r d_{1r}^2 \sqrt{1 + \frac{m_1}{m_r}}}$$

where $d_{1r} = \frac{1}{2}(d_1 + d_r)$ and m_r is the mass of an r-type particle.

Specifically for an electron (2.5) reduces to $\lambda_e = \dfrac{4}{\pi n d_o^2}$

where n and d refer to ions or neutral particles.

The above expression fails in practice because the particles do not behave as elastic spheres of a fixed diameter. An important result however is that the mean free path varies inversely as density or at constant temperature, as pressure.

The probability of a particle making a collision in unit distance is the reciprocal of its mean free path. Hence $Pb = 1/\lambda = nq$ where q is the cross-section. Depending on what changes take place we define more specifically a cross-section for ionization, excitation, elastic collision, and so on. If necessary q can also be subdivided, i.e. $q_{ex1}, q_{ex2}, \ldots$

Every collision must fall into one of these categories and we can therefore define an overall cross-section as $q_{tot} = \sum_x q_x$. The ratio q_x/q_{tot} gives the probability for x to occur. Thus q_i/q_{tot} is the probability of ionization. The probability depends on concentration n. For this reason values of Pb are usually referred to a standard state at 0^oC and 1 mm Hg, at which n = 3.56 10^{16}cm^{-3}. Now q_x is not constant but varies with the kinetic energy of the particles. For example, if the ionization potential of a particle is V_i volts, then when $V < V_i$ $q_i = 0$, and when $V > V_i$ we find that q_i is not constant but varies with eV_i.

Elastic collisions behave in a similar way but lack the threshold value. Hence cross-sections are often given as curves with energy, expressed as voltage or velocity, as abscissa.

2.2.2   Distribution laws

Due to frequent collisions of the molecules there will be an equilibrium distribution of velocities. This distribution can be expressed as

$$\frac{dn}{n} = f(v)dv \tag{2.6}$$

where $\frac{dn}{n}$ is the fraction of particles with velocity between v and $v + dv$. $f(v)$ is called the distribution function. Similarly there is an equilibrium distribution of energy. The Boltzmann's law expresses the number of particles in a given state as

$$\frac{n_j}{n} = \frac{g_j \; \exp(-e_j/kT)}{\sum\limits_{r=0}^{\infty} g_r \; \exp(-e_r/kT)} \tag{2.7}$$

The denominator is often called the partition function. In obtaining Boltzmann's law it is assumed that the particles are distinguishable. If instead it is assumed that the particles are indistinguishable, it is found that there are two solutions which will be independent of permutation. These are called the symmetric and antisymmetric combinations. The first leads to the Einstein-Bose statistics and the second to the Fermi-Dirac statistics. Fortunately, these cases do represent limiting cases of the Boltzmann law, and are applicable at low temperature. The Einstein-Bose and Fermi-Dirac statistics both converge to the Boltzmann law if

$$(2\pi mkT)^{3/2} >> nh^3 \tag{2.8}$$

The Maxwell distribution

Meek |15| has established the condition for a Maxwellian distribution in a gas discharge as

$$\lambda \frac{\partial T_g}{\partial r} \ll T_g \quad , \quad \lambda \frac{\partial n}{\partial r} \ll n \quad , \quad e_o \cdot E \cdot \lambda_e \ll \tfrac{1}{2} mv^2 \qquad (2.9)$$

where λ, λ_e, are the mean free path of gas particles and electrons respectively, $\tfrac{1}{2}mv^2$ the mean kinetic energy of the electrons, T_g the gas temperature and r represents a distance. The first of these conditions implies a small temperature gradient, i.e. small heat flow. The second condition stipulates a small concentration gradient. And the third condition stipulates small energy transport in a field of force, i.e. mobility of electrons in an electric field. When these conditions hold, it can be assumed that the equilibrium laws hold at any point with sufficient accuracy. The simplest definition of temperature is a constant of equilibrium such that the mean particle energy is $= \frac{3}{2} kT$. Without equilibrium the definition of temperature has no real meaning.

The distribution function for a Maxwellian distribution is

$$f(v) = 4\pi \left(\frac{m}{2\pi kT}\right)^{3/2} v^2 \exp\left\{\frac{-mv^2}{2kT}\right\} \qquad (2.10)$$

or in terms of kinetic energy ($\varepsilon = \tfrac{1}{2}mv^2$)

$$f(\varepsilon) = \sqrt{(m/\pi)} \left(\frac{2}{kT}\right)^{3/2} \varepsilon \exp(-\varepsilon/kT) \qquad (2.11)$$

The Druyvesteyn distribution

The existence of an electric field in a discharge tends to upset the equilibrium, and the energy gained by collision may not be completely randomized as assumed. Druyvesteyn [16] derived an expression for electrons that have a considerable drift in addition to their random velocity. This distribution assumes a constant cross-section and a uniform electric field and finally that only elastic collision takes place. The Druyvesteyn distribution is

$$f(E) = \frac{1.04}{\bar{\epsilon}} \ (\epsilon/\bar{\epsilon})^{\frac{1}{2}} \ \exp\left\{-0.55(\epsilon/\bar{\epsilon})^2\right\} \qquad\qquad (2.12)$$

where $\bar{\epsilon}$ is the mean of the electron kinetic energy ϵ. The mean

energy $\bar{\epsilon}$ is determined by the electric field strength and the

mean free path of the electrons. λ_e is typically 0.001 cm at

50 mmHg |3|. The distribution can also be expressed as velocity

by making the substitution $\epsilon = \frac{1}{2}mv^2$ and $dv = \dfrac{d\epsilon}{\sqrt{2me}}$.

The Druyvesteyn distribution is narrower than the Maxwellian dis-

tribution.

2.2.3 Cross-section for ionization of toluene

J. G. Gomet [22] determined the total ionization cross-section for water, benzene, toluene and naphthalene for an ionizing electron energy increasing from 20eV to 250eV in steps of 10eV. Also given is the mean free path of electrons between two ionizing collisions at 10^{-4} mm Hg. The method employed by Gomet was ionization by electron impact.

$$P_i = \frac{1}{\lambda_e} = 3.29 \; 10^{12} q_i$$

U_{volts}	$\sigma_T \; 10^{-16} \; cm^2$	$\Delta\sigma_T \; 10^{-16} \; cm^2$	$\sigma_T \, \pi a_0^2$	$\Delta\sigma_T \, \pi a_0^2$	λ_{cm}	$\Delta\lambda_{cm}$
20	0,329	0,300	0,374	0,341	8 589	7 832
30	4,952	1,681	5,636	1,913	571	193
40	8,089	2,274	9,205	2,587	349	98
50	12,744	0,981	14,503	1,116	222	17
60	15,538	0,921	17,682	1,048	182	11
70	17,572	1,221	19,997	1,389	161	11
80	18,625	1,393	21,195	1,585	152	11
90	19,932	1,778	22,683	2,023	142	13
100	20,350	1,773	23,158	2,018	139	12
110	21,319	1,254	24,261	1,427	133	8
120	20,843	0,945	23,719	1,075	136	6
130	20,621	0,806	23,467	0,917	137	5
140	20,421	0,759	23,239	0,864	138	5
150	19,367	0,804	22,040	0,915	146	6
170	17,532	0,896	19,951	1,020	161	8
200	15,112	1,069	17,197	1,217	187	13
250	12,388	0,979	14,098	1,114	228	18

Cross section (q_i)   Mean free path (λ_e)
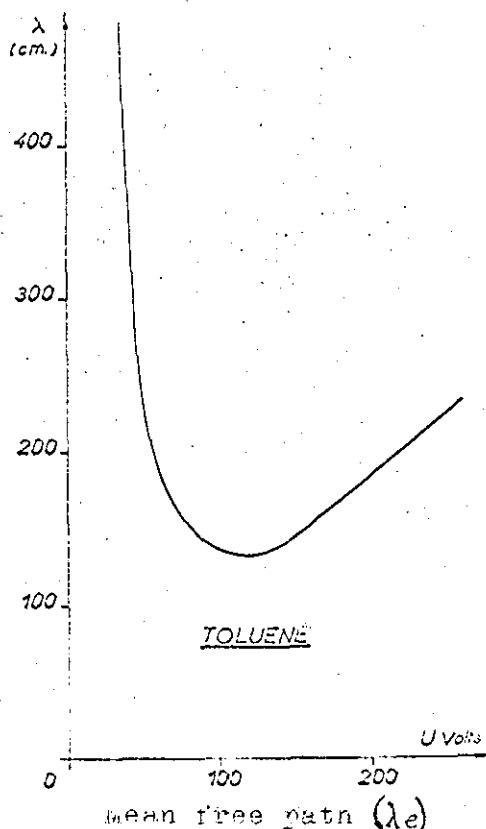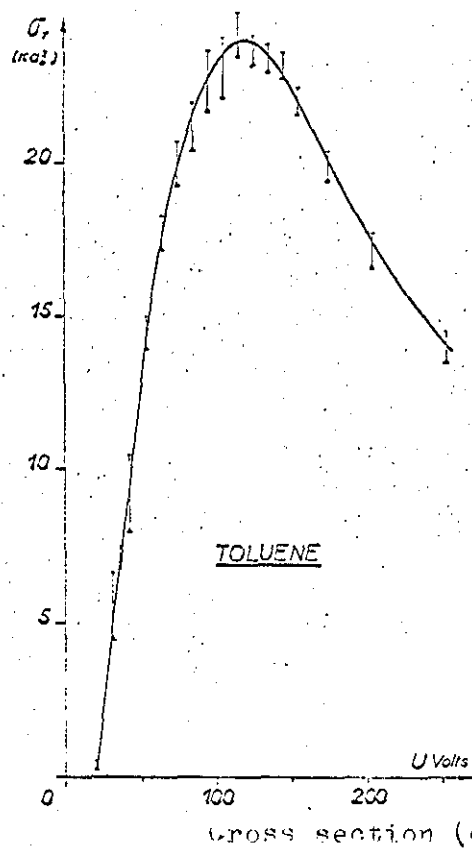
Fig. 2.10.   Cross-section for ionization of toluene

2.2.4   Cross-section for ionization of oxygen

Tate and Smith |60| studied the ionization cross-section of oxygen and several other gases by electron impact. These ionization curves as shown in fig. 2.11 have the typical shape - they rise steeply from the threshold energy up to a maximum and thereafter decay more slowly. The maximum cross-section occurs at an energy several times the threshold value. The cross-section in fig. 2.11 is related to the probability of ionization by

$$P_i = \frac{1}{\lambda_e} = n_0 q_i$$

P_i is usually quoted at 1 mm Hg and 0°C for which $n_0 = 3.56 \ 10^{16} cm^{-3}$. Such a value is also known as the efficiency of the process, in this case ionization.
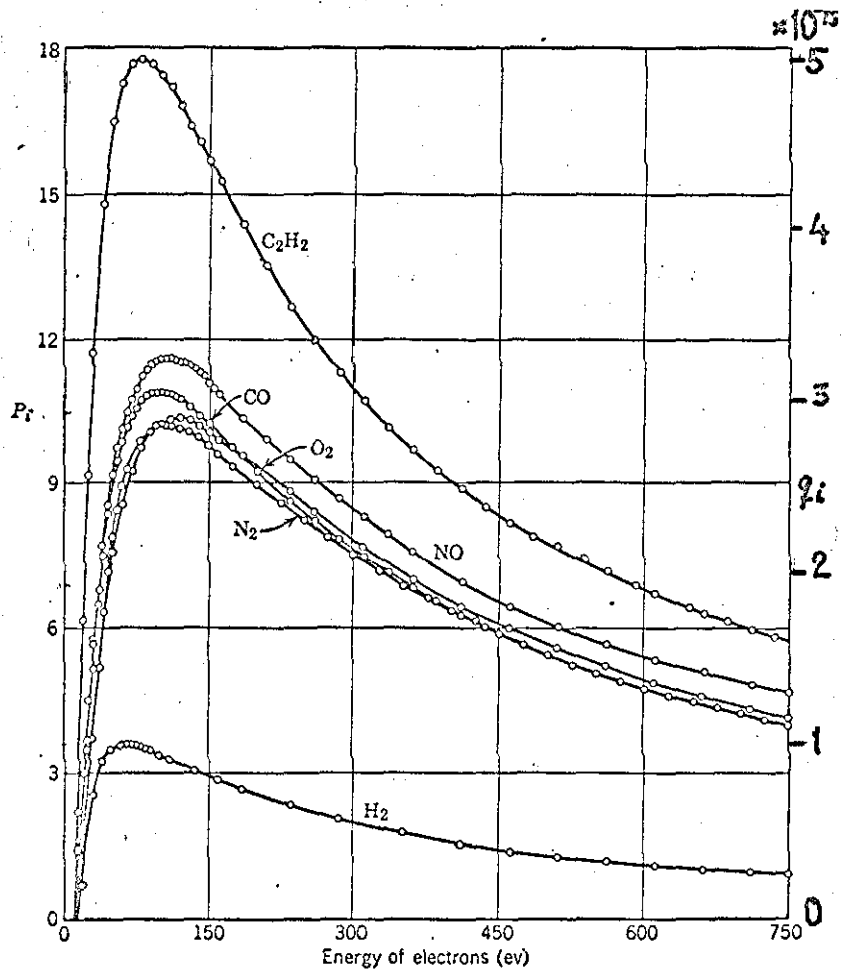
FIG. 2.11 The probability of ionization of N_2, CO, O_2, NO, H_2 and C_2H_2. The ordinate represents the number of positive charges per electron per cm path at 1 mm Hg pressure and 0°C. J. T. Tate and P. T. Smith, *Phys. Rev.* 39, 270 (1932).

2.2.5   Reaction rate from collision theory

For a second order reaction: $A + B \rightarrow$ products, the reaction rate is expressed as

$$-\frac{dCA}{dt} = \delta_r(v)vC_A C_B \qquad (2.13)$$

therefore $k_r(v) = v\delta_r(v)$ where $k(v)$ is the bimolecular reaction rate constant for a particular value of the relative velocity. Let $f(v)$ represent the distribution of velocities, section 2.2.2. The total reaction rate is found by integration over all velocities.

$$k_r = \int_0^\infty f(v)\delta_r(v)vdv \quad, \qquad (2.14a)$$

or expressed in terms of kinetic energy $\varepsilon = \tfrac{1}{2}mv^2$

$$k_r = \frac{1}{m}\int_0^\infty f(\varepsilon)\delta_r(\varepsilon)d\varepsilon \ . \qquad (2.14b)$$

To calculate the rate constant we must know the distribution law and the cross-section $\delta_r(\varepsilon)$. For a Maxwellian distribution we have, according to section 2.2.2,

$$f(\varepsilon) = \sqrt{(m/\pi)}(2/kT)^{3/2}\varepsilon \exp(-\varepsilon/kT) \ . \qquad (2.15)$$

The simplest cross-section is the hard sphere model for which:

$$\delta_r(\varepsilon) = 0 \qquad\qquad \text{when} \quad \varepsilon \leqslant E_a$$

$$\delta_r(\varepsilon) = \pi d_{12}^2 \qquad\qquad \text{when} \quad \varepsilon > E_a \quad .$$

Inserting these values in (2.14b) we get

$$k_r = \frac{1}{m}\sqrt{(m/\pi)}(2/kT)^{3/2}\pi d_{12}^2 \int_{E_a}^\infty \varepsilon \exp(-\varepsilon/kT)d\varepsilon \ .$$

After integration we obtain

$$k_r = (8kT/\pi m)^{\frac{1}{2}}(\pi d_{12}^2)(1 + (E_a/kT))\exp(-E_a/kT) . \qquad (2.16)$$

The numerical value of k from the collision theory is normally slightly higher than that predicted from transition state theory. However, in our case it will be shown later that the collision theory does provide us with an interpretation of effects of the electric field on the reaction rate.

CHAPTER THREE

CHAPTER 3

CHEMICAL REACTIONS IN ELECTRICAL DISCHARGES

The chemistry of chemical reactions in electrical discharges has been reviewed by McTaggart [1] and Kondrat'ev [71]. It is accepted that free radicals are formed in the discharge some of which are longlived, e.g. the benzylradical. The energy yield obtained is about 1 kWhr/mole, which is about ten times less than that of aqueous electrolysis.

Since the conjugated hydrocarbon radicals often have relatively long lifetimes they often combine to give polymeric substances in some cases as the major product. If we consider the vast number of reactions for organic radicals, we can appreciate the complex situation that must exist in the discharge region for higher hydrocarbons.

There are very little data published on organic reaction in gas phase utilizing the collision theory with measurement of the reactive cross-section. No such data could be found for reactions taking place in an electrical discharge.

The ionization potential for most hydrocarbons and radicals is in the range 9-10 electron volts (appendix 1.1). The excitation energies will of course be less since the electron(s) are not completely removed but merely brought out further from the centre of the molecule to a higher orbital. In a discharge therefore we find not only molecules and free radicals but also excited molecules and ions. Figure 3.1 has been taken from Kondrat'ev [71] and shows the different energy levels for oxygen. If we have a mixture of a non-condensable gas with an organic compound, there are several possibilities. Either the non-condensable gas is excited or the

organic compound or possibly both. Section 3.1 is an account of reactions reported in the literature for non-condensable gases. Reactions occurring in a discharge with only the organic compound present are described in section 3.2.

3.1 REACTIONS OF SOME ATOMIC GASES

There are two ways that the atomic gases can combine. By homogeneous recombination we mean the homogeneous reaction (only one phase present) to form the molecule.

$$X + X = X_2$$
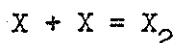
Since this is a reaction common to all the atomic gases it has been described separately in section 3.1.1.

When recombination takes place at the wall of the reactor (or at a solid interface) we have what we call a heterogeneous recombination, section 3.1.2.

Another type of reaction occurs when an atomic gas reacts with an organic compound in its normal state. This normally consists of abstraction, hydrogen abstraction being the most usual case, but abstraction of other atoms may be possible. This hydrogen abstraction that occurs is interesting in thermolecular reactions, since it is responsible for the branching in many reactions. The recombination, whether it is homogeneous or heterogeneous, is often the terminating step. The information of atomic species is indeed very valuable since it can provide a clue to the reaction mechanism.

The reaction of an atomic gas with itself and also the reaction with a hydrocarbon in its normal state is described in section 3.1.3 to 3.1.5.

3.1.1 Homogeneous recombination

The homogeneous recombination of atoms can be represented by:

$$X + X + M \rightarrow X_2 + M \qquad (1)$$

where M is a third body, such as inert gas. The mechanism is thought to proceed in two stages over an activated complex.

$$X + M \underset{K_b}{\overset{K_a}{\rightleftharpoons}} XM^* \qquad (2)$$

$$XM^* + X \underset{K_c}{\rightarrow} X_2 + M^* \qquad (3)$$

The third body (M) must be present to remove the heat of reaction (or part of it) otherwise the complex will fall apart to atomic species again very rapidly. The mechanism of the two stages is often referred to as the Lindemann-Hinshelwood mechanism. Since the activated complex rapidly falls apart it will quickly reach a steady state concentration.

$$(-r_{XM})^* = k_a [X] [M] - k_b [XM]^* - k_c [XM]^* [X] = 0$$

thus

$$(XM)^* = \frac{k_a [X] [M]}{k_b + k_c [X]}$$

and

$$\frac{d(X_2)}{dt} = \frac{k_a k_c}{k_b + k_c [X]} [X]^2 [M] \qquad (4)$$

when the radiative lifetime of the complex $(XM)^*$ is short compared with the time between collisions then $k_b \gg k_c [X]$

and

$$\left(r_{X_2} \right) = k_t [X]^2 [M].$$

k_t can be estimated

$$k_t = \frac{k_a k_c}{k_b} \approx \frac{10^{14} \cdot 10^{14}}{10^{13}}$$

The lifetime of $[XM]^*$ is set to about a period of molecular vibration (10^{-13}sec).

Thus the magnitude of k_t for recombination of O, H, N are all in the order of 10^{15} cm^6 $mole^{-2} sec^{-1}$ at $300^\circ K$ when M is a simple

molecule. For a more complex molecule this value will increase [2].

Table 3.1 lists a number of third body collision recombinations [1].

M	H	N	O	I	Br
He	-	0.8	-	2	3
Ar	4	3.0	1	3	7
H_2	7	-	-	6	-
CO_2	-	-	-	13	20
N_2	-	10	-	9	7
O_2	-	-	1	7	-
toluene	-	-	-	194	-

Table 3.1   Values of $k_t \cdot 10^{15} (cm^6 mole^{-2} sec^{-1})$

3.1.2 Heterogeneous recombination

The excess energy is released as heat when recombination occurs at the solid wall. Heterogeneous recombination is commonly found to be of first order, and are often described in terms of a recombination coefficient γ. γ is defined as the fraction of the total collision leading to recombination. The recombination coefficients for H, N, O are shown in table 3.2. [16,17]

Surface	H	O	$N \cdot 10^3$
silica	7	0.2	-
pyrex	5	0.02	0.02
H_3PO_4	0.02	0.12	-
silver	50	200	-
platina	-	-	20

Table 3.2   Recombination coefficients at 0.1 mm Hg

The state of the surface is extremely important and any surface contamination will change the value of γ very drastically. Acid surfaces are much less reactive than alkaline surfaces.

Linnett has measured the recombination coefficients, γ, at room temperature for 30 elements. Further, Linnett also determined the reaction order and the temperature dependence for silica up to 600°C. The recombination was found to be of first order with respect to oxygen. The value of γ was found to be $1.6 \; 10^{-4}$ at 20°C rising to $1.4 \; 10^{-2}$ at 600°C. Voevodskii reported an activation energy of 6.5 kcal/mole, whereas Linnett finds 1 kcal/mole at 20°C rising to 13 at 300°C and decreasing to zero at 500°C.

If we neglect the radial concentration gradient and assume a first order decay of oxygen atoms we get the following differential equation.

$$\bar{v} \frac{dc}{dx} = D_{O-M} \frac{d^2 c}{dx^2} - kc \tag{3.1}$$

with boundary conditions $c = c_0$ at $x = 0$ and $\frac{dc}{dx} = 0$ at $x = r$ for a cylindrical vessel.

If the diffusion term $kD/\bar{v}^2$ is small then $k = k'(1 + \frac{k'D}{\bar{v}^2})$ where $k' = -\bar{v} \frac{d(\ln c)}{dx} = -\frac{d(\ln c)}{dt}$.

The number of wall recombinations is given by γNc, where N is the total number of collisions per unit area, unit time and unit concentration. But $N = \bar{v}/4$. Then $k_w = -\frac{d(\ln c)}{dt} = \frac{\gamma \bar{v} S}{4V}$.

For a cylindrical vessel we have $S/V = r/2$ and therefore

$$k_w = \gamma \bar{v}/2r \tag{3.2}$$

3.1.3   Oxygen

There are two basic ways of homogeneous recombination of oxygen atoms |61| - the ozone mechanism and the direct recombination. The reactions for the ozone mechanism are:

$$O + O_2 + M \rightarrow O_3 + M \qquad (5)$$

$$O_3 + M \rightarrow O + O_2 + M \qquad (6)$$

$$O + O_3 \rightarrow 2\,O_2 \qquad (7)$$
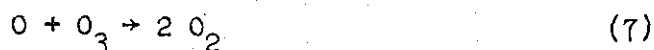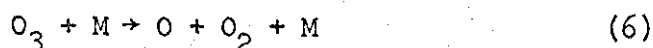
The corresponding rate constants as reported by Benson and Axworthy |70| at $100^{\circ}C$ are:

$$k_5 = 6.0 \cdot 10^7 \exp(+600/RT)$$

$$k_6 = 4.6 \cdot 10^{12} \exp(-24,400/RT)\,l.mole^{-1}sec^{-1}$$

$$|\text{modified to } H^{\circ}_{298}\ \ O(^3P) = 59.56 kcal/mole|$$

$$k_7 = 3.0 \cdot 10^{10} \exp(-6,000/RT)\,l.mole^{-1}sec^{-1}$$

For the direct recombination of oxygen we have

$$O + O + M \rightarrow O_2 + M \qquad (8)$$

$$k_8 \approx 1 \cdot 10^9\ l.^2 mole^{-2}sec^{-1}$$

The activation energy for this reaction have not been found in the literature, but since this is a recombination of two radicals it should be close to zero.

At low pressure and temperature, below $100^{\circ}C$, reaction (6) is not important and may therefore be neglected. In case of high surface to volume ratio (S/V) the heterogeneous recombination is by far the dominant reaction. Although these recombinations seemingly are simple they are far from simple. In all these reactions there is the problem of quantum energy transfer in form of rotation, vibration and electronic energy which are not sufficiently understood. There is also the deviations from the Boltzman distribution.

Unlike hydrogen there is evidence that oxygen and nitrogen produce metastable excited molecules in a discharge. Herron and Sciff |27| using microwave discharge and a mass spectrograph for identification of the positive ions, found 8% O atoms at 1 mm Hg and 10-20% of excited O_2 probably in the $^1\Delta g$ state. The ozone concentration was less than 0.02%. A similar experiment by Foner and Hudson confirms the results. |46| This also confirms the result of Mearns |45| that ozone is not formed in the discharge zone, but rather by recombination after the discharge zone. Possible reactions are:

$$O_2^*(\,^3\Sigma\mu\,) + O_2 = O + O_3 \qquad \text{collision deactivation}$$

$$O_2^- + O_2^+ = O + O_3 + h\nu \qquad \text{recombination}$$

$$O + O_2 + M = O_3 + M$$
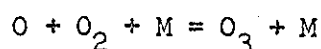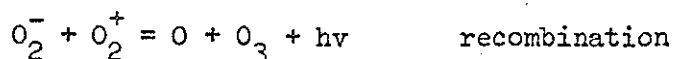
The main reaction of oxygen with saturated hydrocarbons is hydrogen abstraction. Harteck and Kopsch |48| found that CH_4 reacted to give H_2O, and CO_2. At $190^\circ C$ the conversion was 6% and it was concluded that the initial step was likely to be

$$O + CH_4 \rightarrow OH\cdot + CH_3\cdot$$
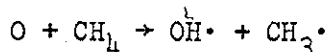
followed by rapid reaction of the radical and atomic oxygen. Cvetanovic |33| investigated benzene and toluene using oxygen atoms produced by photosensitized decomposition of nitrous oxide. The reactions of atomic oxygen with aromatics are presented in section 4.2.

The second type of reaction with oxygen on hydrocarbons is the addition to a double bond. Cvetanovic et al |64-69| examined several hydrocarbons. They concluded that the main reaction for olefines are addition of oxygen to the double bond to give epoxy and carbonyl compounds.

The observed product by addition of atomic oxygen to cis-pentene-2
and the yields are shown below YIELD

cis-β-pentene oxide   0.23

trans-β-pentene oxide   0.31

methylpropylketone

diethylketone   } 0.25

2 methylbutanal   0.21

as given by Cvetanovic |67,68|. The rate constants for oxidation
of hydrocarbons with atomic oxygen in the 3p state, generated from
photosensisitized decomposition of nitrous oxide, are shown in
table 3.3.

For saturated hydrocarbons, where hydrogen abstraction is
presumably the initial step, there is a significant slower reaction
rate - several hundred times slower. Since all these experiments
were performed at room temperature (295 ±3°K) this is merely a
reflection on the difference in activation energy.

TABLE 3.3   RATE CONSTANTS FOR REACTIONS OF ATOMIC OXYGEN

Reactant	Rel. k (isobutene = 1)	$k \, 10^{-12}$ ($cm^3 mole^{-1} sec^{-1}$)
Ethylene	0.038	0.17
Propylene	0.23	1.05
Butene-1	0.24	1.1
cis-butene-2	0.84	3.8
tr.-butene-2	1.13	5.3
isobutene	1.00	4.6
n-pentene-1		2.8
cis-pentene-2	0.90	4.1
2,3dimethylbutene2	4.18	19.0
Butadiene1,3	0.95	4.4
n-butane	0.0017	0.0078
3methylheptane	0.021	0.096
Acetaldehyde	0.027	0.12
cyclopentene	1.20	5.5
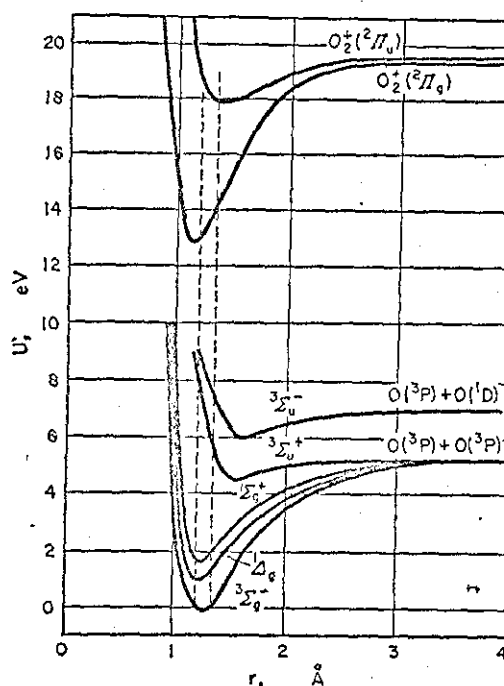
FIG. 3.3. Energy levels of O_2 and O_2^+ and the energy of the most probable transitions from the ground state of the oxygen molecule (from the point of view of the Franck–Condon principle).

3.1.4   Nitrogen

In a discharge with oxygen there will always be traces of nitrogen present if no precaution has been taken to remove it.   The normal impurity level of nitrogen is 0.3% in oxygen bottles. Kaufman found that the purity of oxygen is of utmost importance for the yield of atomic oxygen.   If 0.01-0.05% nitrogen was added to the oxygen the yield increased with about 80 atoms per molecule nitrogen added [1].   It is not yet clear whether this effect is due to heterogeneous or homogeneous effect on recombination. Effects like these will have their implications on the reproducibility which will depend on oxygen purity and geometrical dimensions of the reactor.

However, the presence of nitrogen atoms makes it desirable to include some molecule/radical reactions of nitrogen in this text. The recombination has been described in previous sections.   Nitrogen atoms will react with oxygen according to:

$$N + O_2 \rightarrow NO + O \tag{9}$$

$$N + O + M \rightarrow NO + M \tag{10}$$

$$N + NO \rightarrow N_2 + O \tag{11}$$

with rate constants

$$k_9 = 8 \cdot 10^9 \exp(-7100/RT) \; l.mole^{-1}sec^{-1}$$

$$k_{10} = 1.6 \; 10^9 \qquad\qquad l^2mole^{-2}sec^{-1}$$

$$k_{11} = 1.3 \; 10^{10} \qquad\qquad l.mole^{-1}sec^{-1}$$

Reaction (11) forms a basis for titration of nitrogen atoms in a number of investigations.   The main reaction of nitrogen atoms with hydrocarbons is the production of HCN.   The reaction of atomic nitrogen with ethylene yields: 75% HNC, 10% C_2H_6, 3% C_2H_2, and 2% $(CN)_2$. Dewhurst [47] found NH_3 in addition to the usual products in reaction with cyclic hydrocarbons.   There is no evidence of hydrogen ab-

straction in reactions with atomic nitrogen. The question whether
activated molecules and ions, e.g. N_2^*, N_2^+, play an important part
in reactions with hydrocarbons is still not clear. The major type
of reaction seems to be the formation of the $C \equiv N$ bond.

Electrical discharge in air gives minor quantities of NO, which
increases when traces of water vapour is present.

The reaction $\qquad O + NO_2 \rightarrow O_2 + NO \qquad$ (fast)

$$O + NO \rightarrow NO_2 + h\nu$$
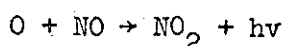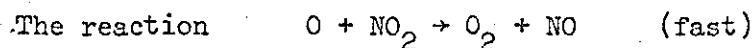
provides a method for determination of atomic oxygen by titration.
The NO produced will react with some of the oxygen atoms to give a
yellow-green glow. The end point of titration is reached when the
glow is extinguished.

Nitrogen produced from an electrical discharge [71] is a mix-
ture of molecular nitrogen in the normal state, excited molecules
in the $^3\Sigma$ state, activation energy 170 kcal nitrogen atoms in the
normal state and in the ^2D and ^2P with excitation energies 54.5, 82 kcal
respectively. That there is a considerable concentration of nitrogen
atoms is supported by the absorption of light in the 400-800Å region.

3.1.5   Hydrogen

Hydrogen radicals are very important in termolecular reactions.
It is one of the most abundant intermediates and responsible for the
propagation in many chain reactions. It is readily formed in an
electrical discharge and was first produced by Wood. The slow re-
combination makes it possible to react the hydrogen atoms several cm
away from the discharge zone. The life time of H atoms at 0.1 torr
is about 1 second. More recently another way of producing H atoms
has been developed. By illumination of a mixture of hydrogen and
mercury hydrogen atoms are produced by excited Hg atoms, resonance
line 2537Å.

One of the most studied reactions is the reaction with molecular hydrogen.

$$H + H_2 \rightarrow H_2 + H \qquad\qquad (12)$$

$$k_{12} = 5.10^{13} \exp(-7500/RT) \ |cm^3 mole^{-1} sec^{-1}|$$

Hydrogen atoms normally react under hydrogen abstraction with saturated hydrocarbons or hydrogen addition with unsaturated hydrocarbons. Table 3.4 gives the rate constant for some hydrogen abstraction reaction. The rate constants for hydrogen addition to unsaturated compound are given in table 3.5. The activation energy is about 7-9 kcal per mole for hydrogen abstraction, whereas the addition apparently takes place without any activation energy at all. Due to the complexity of the chemical reaction and the inherent weakness of the kinetic theory it is yet not possible to predict the rate constants. Some attempts have been made to correlate the activation energy with the bond strength |19|. The activation energy is often empirically expressed as a fraction of the bond broken minus the bond formed. Tro tman-Dickenson gives an empirical expression for the reaction

$$RH + CH_3 \rightarrow CH_4 + R$$
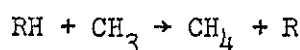
$$Ea = 0.49|D(R-H) - 74.3| \ kcal/mole$$

which is valid for saturated alkanes. For toluene the predicted value is 4.8 kcal/mole (D(R-H) = 84 kcal/mole) which should be compared with the experimental value of 8.3 kcal/mole. So far the prediction of activation energy has been of little value unless one can accept an error of several magnitudes. The approach taken in this report is to calculate average values for the different group of reactions that occurs. With oxygen the main reactions are:

$$H + O_2 \rightarrow OH + O \qquad\qquad (13)$$

TABLE 3.4   HYDROGEN ABSTRACTION

Reaction	$^{10}\log A$ $cm^3 mole^{-1} sec^{-1}$	kcal mole^{-1}	Temp. range
H + H$_2$ → H$_2$ + H	13.7[a], 13.5[b]	7.5[a], 6.2[b]	a) 25-700°C
H + CH$_4$ → H$_2$ + CH$_3$	10.5[a], 13.6[b]	6.6[a], 12[b]	a) 99-163
H + C$_2$H$_6$ → H$_2$ + C$_2$H$_5$	12.5[a], 11.3[b]	6.8[a], 9[b]	a) 80-163
H + C$_3$H$_8$ → H$_2$ + C$_3$H$_7$	-	9[b]	-
H + C$_4$H$_{10}$ → H$_2$ + C$_4$H$_9$	11.0[b]	9[b]	-
H + C$_6$H$_6$ → H$_2$ + C$_6$H$_5$	10.15[b]	9.2[b]	-
H + C$_6$H$_5$CH$_3$ → H$_2$ + C$_7$H$_7$	11.17	8.3	-
CH$_3$ + CH$_4$ → CH$_4$ + CH$_3$	11.5[a], 11.8[b]	14.3[a], 14.65[b]	a) 350-525
CH$_3$ + C$_2$H$_6$ → CH$_4$ + C$_2$H$_5$	11.3[a]	10.4[a], 10.4[b]	a) 25-340
CH$_3$ + C$_3$H$_8$ → CH$_4$ + C$_3$H$_7$	-	5.5[b]	-
CH$_3$ + C$_4$H$_{10}$ → CH$_4$ + C$_4$H$_9$	11.1[a], 11[b]	8.3[a], 8.3[b]	a) 25-340
CH$_3$ + C$_6$H$_6$ → CH$_4$ + C$_6$H$_5$	10.15[a]	9.2[a]	a) 70-340
CH$_3$ + C$_7$H$_8$ → CH$_4$ + C$_7$H$_7$	11.17[a]	8.3[a]	a) 70-340

a) V. Kondrat'ev "Chemical Kinetics of Gas Reactions",

Pergamon Press, London 1964.

b) Z. Szabo   "Advances in the Kinetics of homogeneous Gas Reactions",

Methuen & Co. Ltd, London 1964.

Miscellaneous

H + O$_2$ → HO + O	14.5, 14.1[a]	17.5, 18.8[a]	a) 450-600
H + Cl$_2$ → HC$_1$ + Cl	-	9.4	-
CH$_3$ + CH$_3$CHO → CH$_4$ + CH$_3$CO	-	6.8	-
OH + H$_2$ → H$_2$O + H	10.0	14.15	-

$$K_{HAB} = A \cdot \exp(-E/RT) \quad cm^3 mole^{-1} sec^{-1}$$

$$H + O_2 + M \rightarrow HO_2 + M \tag{14}$$

$$k_{13} = 9.6 \cdot 10^{10} \exp(-16200/RT) \quad |1 \cdot mole^{-1} sec^{-1}|$$

$$k_{14} = 4.3 \cdot 10^9 \quad |1 \cdot^2 mole^{-2} sec^{-1}| \quad (450\text{-}650°C)$$

In the presence of hydrocarbon there is an additional reaction where active hydrogen is replaced with a considerably less active radical.

$$H + RH \rightarrow H_2 + R \tag{15}$$

$$k_{15}(\text{propane}) = 3.6 \cdot 10^{10} \exp(-8300/RT) \quad |1 \cdot mole^{-1} sec^{-1}|$$

Unlike oxygen and nitrogen there is no evidence to support the existence of excited hydrogen molecules. The hydrogen atoms carry too much energy to allow homogeneous recombination, without a third body to remove the excess energy.

TABLE 3.5   HYDROGEN ADDITION

Reaction	$^{10}logA$ $cm^3 mole^{-1} sec^{-1}$	E_a $kcal \, mole^{-1}$
$H + C_2H_4 \rightarrow C_2H_5$	13.5	4.1
$H + C_3H_6 \rightarrow C_3H_7$	14.4	5.0
$H + CH_3 \rightarrow CH_4$		0
$H + C_2H_5 \rightarrow C_2H_6$		0
$H + C_6H_5CH_2 \rightarrow C_6H_5CH_3$		0

3.2 REACTIONS OF ORGANIC COMPOUNDS

Despite the intensive research during the last decade no commercial plant or process has yet been built for organic synthesis and few processes have reached the pilot plant stage. The inhibiting factors seem to be high energy requirement, low pressure and difficulties of scaling-up.

So far it has not been possible to predict the products of the different reactions in the discharge. However, certain characteristics can be recognized. Almost all reactions can be divided into three groups, namely, isomerization or rearrangement, condensation or polymerization and elimination. The energy requirement for these groups are slightly different. Elimination requires the highest energy - about 2-10 kWhr/mole. Isomerization requires about 1-2 kWhr/mole and polymerization or condensation about 0.5-1 kWhr/mole. Most of the knowledge comes from Cvetanovic [64-69], who investigated the reaction of atomic oxygen in the ^3P state with different hydrocarbons, and from H. Suhr [31, 32], who studied reactions of hydrocarbons without oxygen. Pechuro [8] has reported the reactions of alkanes and alkenes in arc and glow discharge.

Among the syntheses attempted in a discharge are acetylene from methane, ammonia from hydrogen and nitrogen, hydrazine from ammonia, and hydrogenperoxide from hydrogen and oxygen.

At the present time there is no rate expression that will include the electrical variable in a simple way. Most of the results are presented as empirical curves when it comes to reaction rates and reaction yields.

3.2.1   Isomerization

Rearrangement in an electrical discharge takes place even under very mild conditions. A typical result is the change in position of substituted groups in organic compounds. Table 3.6 gives the yields and the products for a number of rearrangement reactions in a discharge. |32|. In the isomerization of anisole it was found that the electric variables had little influence on the ratio of ortho to para cresol. However, as the energy was increased more phenol was produced until at high energy, phenol was the major product. Minor traces of m-cresol, benzene, toluene and cyclo pentadiene was also reported. The reaction of other aryl ethers are similar to anisole. If the ortho and para position is reserved by other groups it was found that the migrating group often was eliminated to yield the corresponding phenol. Ethylvinylether was found to yield butenylalcohol and vinyl alcohol. The corresponding amines show similar patterns to the ethers. The reaction products from N,N-dimethylaniline are shown below:
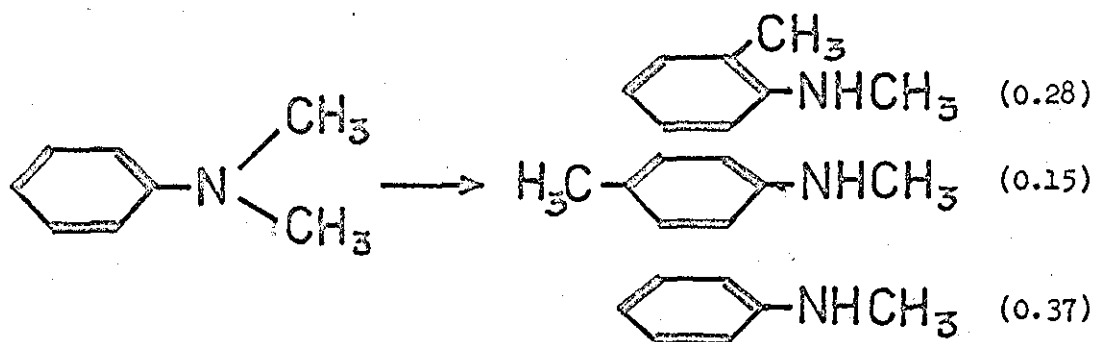
Other types of rearrangement in electrical discharges are aromatic ring closure and dearomatisation by ring opening. Cycloheptatriene isomerizes to yield toluene. Pyrolle gives crotononitrile. A few examples are shown below:

Anisole → o-cresol (0.44), p-cresol (0.27), phenol (0.2)
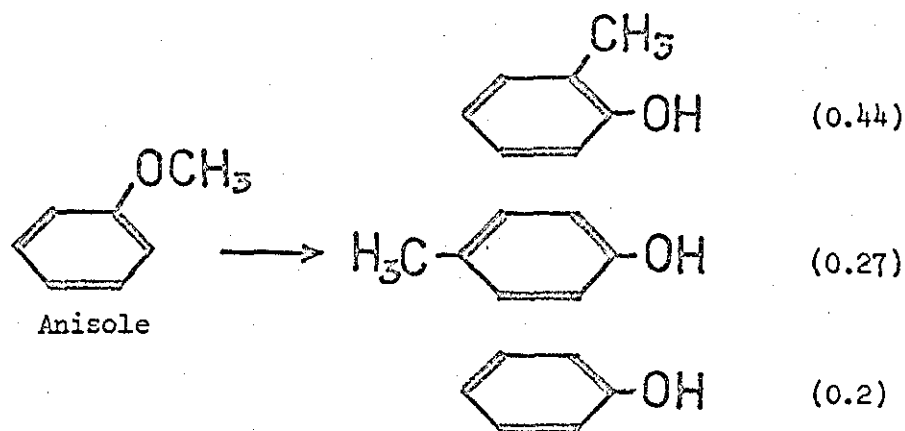
TABLE 3.6 REARRANGEMENTS OF ORGANIC COMPOUNDS

Compound	Products (selectivity)	Yield g/kWhr
Anisole	o-cresol (0.44), p-cresol (0.27)	50
Phenyliso-propylether	o-isopropylether (0.36)	25
	p-isopropylether (0.22)	
p-Tolylmethyl-ether	2,4-dimethylphenol (0.59)	58
1-Naphthylmethyl-ether	2-methyl-1-naphthol (0.51)	55
	4-methyl-1-naphthol (0.31)	
2-Naphthylmethyl-ether	1-methyl-2-naphthol (0.47)	58
Diphenylether	2-phenylphenol (0.53)	180
	4-phenylphenol (0.18)	
N,N-Dimethyl-aniline	N-methyl-o-toluidine (0.28)	23
	N-methyl-p-toluidine (0.15)	

Table 3.7 gives the rate of reaction for some rearrangements. For reactions with normal frequency factor it is often found that E_a is about 40 kcal/mole. For the pseudo first order cis-trans isomerization no such value can be determined.

TABLE 3.7   ISOMERIZATION REACTIONS

Reaction	$^{10}logA$ $cm^3mole^{-1}sec^{-1}$	E kcal $mole^{-1}$
c-butene → 1,3 butadiene	13.08	32.5[b]
1-methylcyclobutene	13.9	35.1[b]
vinylcyclopropane	13.5	49.6[b]
1,1-dimethylcyclopropane	15.05	62.6[b]
2,1,0-bicyclopentane	14.58	46.6[b]
$CH_3NC → CH_3CN$	13.6	38.4[c]
$C_2H_5NC → C_2H_5CN$	13.8	38.2[c]
Cyclo-$C_3H_6 → C_3H_6$	15.4	65.6[c]
Cyclo-$CH_3C_3H_5 → C_4H_8$	15.5	65.0[c]
Cyclo-$C_4H_6 → C_4H_6$	13.4	32.7[c]
$C_4H_7OC_2H_3 → C_5H_9CHO$	11.2	29.1[c]

PSEUDO FIRST ORDER REACTIONS

Reaction	$^{10}logA$ sec^{-1}	E_a kcal $mole^{-1}$
tr-CHD=CHD	12.5	61.3[b]
cis-$CH_3CH=CHCH_3$	13.7	62.8[b]
cis-$C_6H_5CH=CHC_6H_5$	12.8	42.8[b]

b) ref. (19)   c) ref. (2)

3.2.2 Polymerization

The most common type of polymerization is the hydrogen abstraction giving rise to dimerization. The reaction is bimolecular, e.g.

$$R\cdot + R^\cdot \to R - R$$
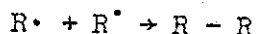
Another type of reaction comes from benzylhalogenes or benzylalcohols which upon condensation yield 1,2-diarylethane. Acetylene yields vinylacetylene, diacetylene, benzene and cuprene.   If the surface to volume ratio is high (heterogeneous reaction?), it is possible to isolate the intermediates. The following products were then obtained from acetylene.

Compound	%
styrene	30-70
phenylacetylene	.15-50
c-octatetraene	1
benzene	5-10
naphthalene	10-20

Apart from polymerization of styrene and butadiene, etc. it is possible to polymerize stable compounds like benzene to yield a polymer, probably "polyphenyl" |49|, under certain circumstances. Dimerization of a few organic compounds are shown in table 3.8 |32|. Aromatic nitrogen compounds like pyrrole, pyridine and aniline react to give unsaturated nitriles, which easily polymerize in a discharge. Polymerization also forms an important part in the many reactions in electrical discharges, where tary substances have been found. Cvetanovic reports formation of a tary substance in the oxidation of toluene with atomic oxygen.

TABLE 3.8   DIMERIZATION OF AROMATIC COMPOUNDS

Compound	Product (selectivity)	Yield g/kWhr
Benzene	diphenyl (0.40)	45
Toluene	dibenzyl (0.90)	8
p-Xylene	dixylyl (0.90)	70
Durene	didurene (0.77)	43
isopropylbenzene	2,3-diphenylbutane (-)	34
t-butylbenzene	2,3-dimethyl-2,3-diphenylbutane	38
1-Methylnaphthalene	1,2-di(1-naphthyl)ethane (0.49)	129
p-Methylbenzoenitrile	1,2-di(4-cyano-phenyl)-ethane (0.90)	170

3.2.3   Elimination

The elimination of the migrating group in the rearrangement reaction under high energy dissipation has been described previously. Other types of group often eliminated in discharges are hydrogen (hydrogen abstraction 3.1.5), carbon monoxide, carbon dioxide and nitrogen. Isocyanates lose carbon monoxide to give a nitrogen complex that decomposes to amines and azo compounds, e.g. phenylisocyanate gives azobenzene and diphenylamine.

phenyl-isocyanate
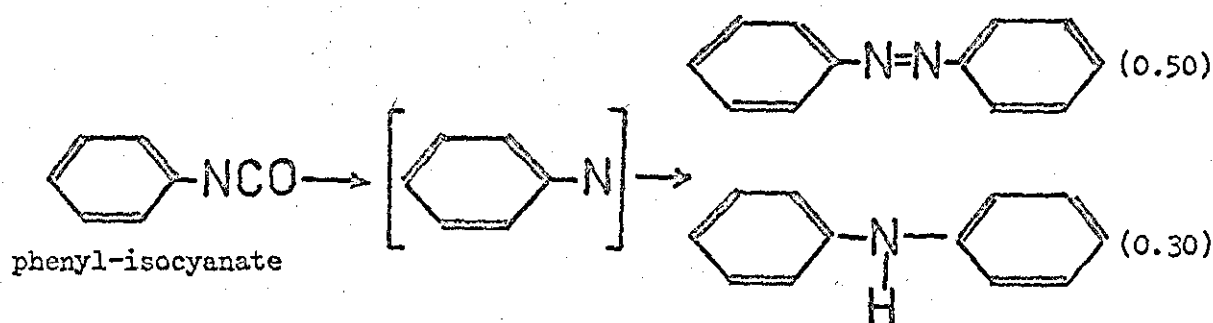
Other groups that eliminate carbonyl are aldehydes and ketones (table 3.9). Benzaldehyde gives benzene and biphenyl. The radical

that is created after carbonyl abstraction is stabilized through hydrogen abstraction or dimerization. Phenols also lose carbon-monoxide under ring fracture. In this way we obtain cyclopentadiene from phenol, methylcyclopentadiene from cresols. Naphthol gives indene.

2-Naphthol $\xrightarrow{\text{-CO} \ (0.95)}$ indene $\xleftarrow{\text{-CO} \ (0.75)}$ 1-Naphthol
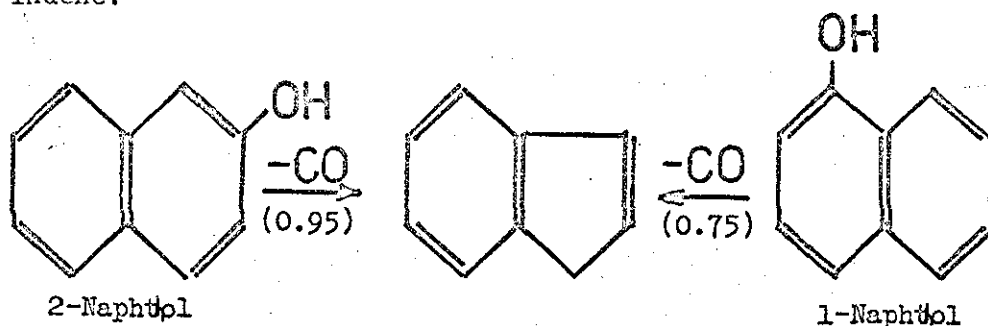
Carboxylic acids react under carbondioxide abstraction to yield the corresponding hydrocarbon. Anhydrides eliminate first carbonyl and thereafter carbondioxide. Concerning esters the picture is more diffuse, but hydrocarbon is a usual product.

TABLE 3.9   CARBONYL ABSTRACTION

Compound	Product (selectivity)		Yield (g/kWhr)
Benzaldehyde	benzene	(0.81)	93
	biphenyl	(0.16)	18
Thiophencarbaldehyde	thiophen	(0.99)	24
Benzophenone	biphenyl	(0.27)	18
	fluorenone	(0.36)	24
	biphenylene	(0.36)	24
2-Pyridinecarbaldehyde	pyridine	(0.70)	–
	2,2-bipyridyle	(0.2)	–
Benzil	biphenyl	(0.98)	27
Fluorenone	biphenylene	(0.99)	43
Camphor	trimethylcyclo-2,1,1,hexane	(0.76)	24

52

From table 3.10 and appendix 1.10 we see that groups like carbonyl and N_2 have very high bond energies. Also the activation energy for elimination is higher than for polymerization and isomerization reactions.

TABLE 3.10 ELIMINATION REACTIONS

Reaction	$^{10}log A$ $cm^3 mole^{-1} sec^{-1}$	E kcal/mole
$CH_4 \rightarrow CH_3 + H$		102
$C_2H_6 \rightarrow 2CH_3$	17.0	84
$C_3H_8 \rightarrow CH_3 + C_2H_5$		84
$C_4H_{10} \rightarrow C_2H_5 + C_2H_5$	17.0[b]	80[b]
$C_2H_5 \rightarrow C_2H_4 + H$	13.8	39.5[a]
$n-C_3H_7 \rightarrow C_3H_6 + H$	14.6	38[c]
$n-C_3H_7 \rightarrow C_2H_4 + CH_3$	9.0	19
$i-C_3H_7 \rightarrow C_3H_6 + H$	14.4[c]	38[b]
$i-C_3H_7 \rightarrow C_2H_4 + CH_3$		26
$n-C_4H_9 \rightarrow C_4H_8 + H$		40
$C_4H_9 \rightarrow C_3H_6 + CH_3$	12.1	27
$C_4H_9 \rightarrow C_2H_4 + C_2H_5$	11.2	22[a]

MISCELLANEOUS

$CH_3CO \rightarrow CH_3 + CO$		13.5
$(COOH)_2 \rightarrow HCOOH + CO_2$	11.9	30.0

CHAPTER FOUR

CHAPTER 4

REACTIONS OF TOLUENE AND OXYGEN

This section contains a survey of homogeneous gas phase reaction, catalytic oxidation of toluene and reactions of toluene in an electrical discharge without oxygen.

The thermal oxidation of toluene starts at about $300^{\circ}C$, but some catalysts may operate at temperatures below $150^{\circ}C$. There appears to be some contradiction about the reaction products. The main products are benzaldehyde and benzoic acid. Since oxidation of toluene is highly exothermic it is difficult to obtain high conversion without producing carbon oxides, the ultimate oxidation products, thereby reducing yield. One must bear in mind that prior to 1960 the analytical methods were not sufficiently advanced to cope with analysis of hydrocarbon isomers for conversions below 1%. It was not until the gaschromathograph and the mass spectrometer were introduced that positive identifications could be done in a routine way. This does not imply that all the analysis performed prior to this approximate date are in error.

Some authors have investigated the reaction kinetics for the oxidation of toluene. The expressions fitted are mostly of pseudo-first order. This approach is probably well-founded when we have low conversions and excess of either oxygen or toluene. At higher conversions these rate expressions are likely to break down, since toluene and oxygen can react with the products to give more complicated reactions.

4.1 HOMOGENEOUS OXIDATION OF TOLUENE IN GAS PHASE

The knowledge on homogeneous oxidation of toluene is not very extensive. Norrish and Taylor |74| studied the cool flames from oxidation of toluene and ethylbenzene at low temperature. A faint glow was observed in both cases. The IR spectrum was photographed and shown to be similar to that of fluorescent formaldehyde. The nature of the cool flame was considered to include the reaction

$$CH_3O + OH \rightarrow HCHO^* + H_2O$$
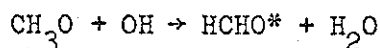
The main products from oxidation of toluene were benzaldehyde and benzoic acid. A diagram showing the ignition of toluene is included below.
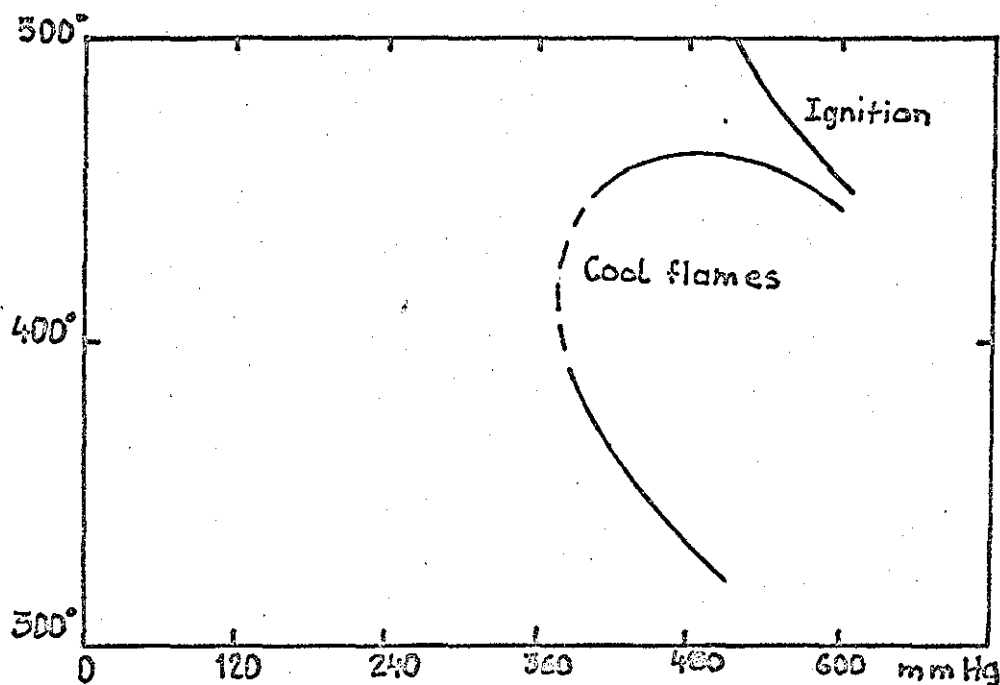
Fig. 4.1   Ignition of toluene/oxygen 4:1 ratio

Kröger and Bigorajski |36| investigated the slow oxidation of aromatics in a batch reaction. The oxidation conditions for toluene were T = 415°C, P_{C7H8} = 50 torr and P_{O2} = 450 torr. The reaction was stopped after the pressure had increased 20 torr. The major products reported were benzene, benzaldehyde, carbon dioxide, carbon

monoxide, water and condensation products.

Burgoyne |73| studied the progressive oxidation of benzene
and its monoalkyl derivatives. The products obtained from toluene
were benzylalcohol, benzaldehyde, benzoic acid, phenols and oxides
of carbon. Traces of peroxides, ethylene, acetylene, paraffins
and hydrogen were also detected. The phenols consisted of di-
hydroxy-derivatives of toluene although cresols were undoubtedly
present in minor amounts. The results are tabulated in table 4.1
for a mixture of 325 mm Hg toluene and 325 mm Hg of oxygen at 408°C.
Minor amounts of ethylene (0.9 torr), hydrogen (1.1) and methane
(0.2) were also found.

Time (min)	11	22	50
Conversion O_2%	34	77	100
CO_2 (torr)	25	60	80
CO	44	116	151
C_6H_5COOH	3	9	11
C_6H_5CHO	15	14	12
$C_6H_5CH_2OH$	15	13	12
$C_6H_3CH_3(OH)_2$	13	27	31

Table 4.1 Oxidation of toluene at 408°C

Burgoyne, Tang and Newitt |72| investigated the slow combust-
ion of toluene at elevated pressures. The following products at
8 atm in a 4.3% mixture of toluene in air at 400°C were obtained:
benzyl alcohol, benzoic acid, benzaldehyde, dihydroxybenzene,
formaldehyde, carbon dioxide, carbon monoxide and water. The ig-
nition temperatures of toluene air mixtures were also reported.

The effect of the ratio of toluene to oxygen were studied by Burgoyne and Newitt |81|. In addition to the previous major reaction products (benzylalcohol, benzaldehyde, benzoic acid and 2,4-dihydroxybenzene), they found traces of formaldehyde, bibenzyl, benzene, p-cresol and salicylic acid. The non-condensable gases obtained contained up to 11% methane. The product distribution at various toluene to oxygen ratios is shown in table 4.2

Ratio toluene/oxygen	Temp ($^{\circ}$C)	Mole%					
		$PhCH_2OH$	PhCHO	PhCOOH	2,4-DHB	CO_2	CO
30	337	6.2	50.5	16.3	9.9	5.2	5.4
20	276	5.9	36.1	12.1	14.7	3.0	1.4
3.7	250	2.8	21.9	26.2	6.1	17.9	6.0
1.0	250	0.7	3.0	59.3	7.1	25.8	3.8

Table 4.2 Various toluene/oxygen mixtures at 20 atm.

From the above results of Burgoyne it seems that homogeneous oxidation of toluene proceeds in three ways: as a result of (1) oxidation of side chain, (2) oxidation of aromatic nucleus or (3) oxidation from the rupture of the ring itself. Thus benzylalcohol, benzaldehyde and benzoic acid are formed by oxidation of the side chain. 2,4-dihydroxybenzene and p-cresol result from oxidation of the aromatic ring. Carbon monoxide and carbon dioxide are formed from the rupture of the aromatic ring.

HETEROGENEOUS OXIDATION OF TOLUENE

In comparison to the homogeneous oxidation we find that more publications have been produced on the catalytic oxidation of toluene. One of the most employed catalysts is vanadium pentoxide. Studies have been done with enrichment of oxygen isotopes in the catalyst. No O^{18} was found when naphthalene was oxidized in the presence of O^{18} labelled vanadium catalyst. This result leads to the conclusion that catalytic oxidation does not involve lattice oxygen via reduction-oxidation mechanism of the catalyst. Dmuchovsky [39] postulated two independent paths of oxygen attack on the benzene ring, one leading directly to oxides of carbon and the other to maleic anhydride. The two modes of attacking are the 1,2 addition and the 1,4 addition as shown below.
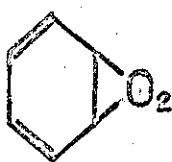
(a)   (b)

Structure (a) has the lowest energy because of conjugated double bonds and leads to carbon oxides, while structure (b) leads to p-bensoquinone and maleic acid. This mode of attack is ascribed to the singlet state of oxygen. The transition of triplet ground state to singlet requires about 23 kcal, or 1eV, and is usually accomplished by sensitation from other molecules in excited state, which themselves upon collision undergo deactivation.

4.2.1   Vanadium pentoxide

Kumar [35] used a continuous flow reactor for the oxidation of toluene. The reaction rates were calculated assuming an ideal plug flow reactor behaviour, and that the different products were formed in consecutive steps. The activation energy for the rate determining step was 29 kcal/mole. The following reaction mechanism was reported.

$$\text{Toluene} \xrightarrow{k_1} \text{Benzaldehyde} \xrightarrow{k_2} \text{Benzoic acid}$$
$$\begin{array}{ccccc} k_5 & & k_4 & & \downarrow k_3 \\ CO_2 \leftarrow & \text{Maleic acid} & \leftarrow & \text{Benzoquinone} \end{array}$$
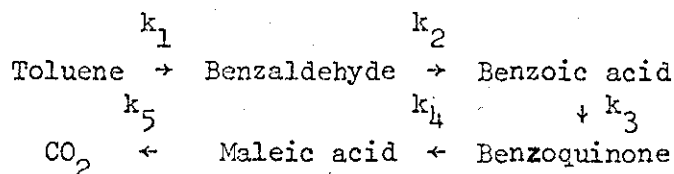
From the kinetic analysis it was concluded that the rate determining step was the oxidation of toluene to benzaldehyde, since this step has the lowest rate constant. It is interesting to compare the activation energy of the rate determining reaction with that of singlet to triplet transition for oxygen (23 kcal).

Downie |37| investigated the oxidation of toluene in a fixed bed reactor at low conversions at temperatures from 300 to 350°C. The rate data in this case were correlated by a model of Hins helwood |13|. It was concluded that the data were well fitted to this expression. The samples were analysed by spectrophotometry and by potentiometric titration. The observed products were benzaldehyde, p-benzoquinone, benzoic acid and maleic anhydride. Table 4.3 shows the selectivity from a run at low conversion. The activation energy was found to be 29 kcal/mole.

Compound	selectivity mole per cent
Benzaldehyde	86
p-Benzoquinone	7
Benzoic acid	4
Maleic anhydride	3

Table 4.3 Selectivity on V_2O_5 catalyst

The values reported by Downie are in good agreement with the values reported by Kumar.

Somewhat different results were reported by Pichler and Obenaus |77|, who found besides benzaldehyde, benzoic acid and maleic anhydride, major amounts of citraconic acid, and smaller

amounts of acetic acid, o-cresol, phthalic anhydride and anthra-
quinone. No traces of formaldehyde or phenol were found. Ssuworow
|79| in an attempt to cover all reported oxidation products
suggested the following reaction scheme.

$$PhCH_3 \longrightarrow PhCH_2OH \xrightarrow{-HCHO} PhOH \longrightarrow p-C_6H_4O_2 \longrightarrow MSA \longrightarrow CSA$$

$$\downarrow {\scriptstyle -H_2O} \qquad \uparrow {\scriptstyle -CO_2} \qquad \searrow$$

$$PhCHO \longrightarrow Ph\underset{O}{\overset{\parallel}{C}}OOH \xrightarrow{-O} PhCOOH \xrightarrow{-CO_2} C_6H_6$$
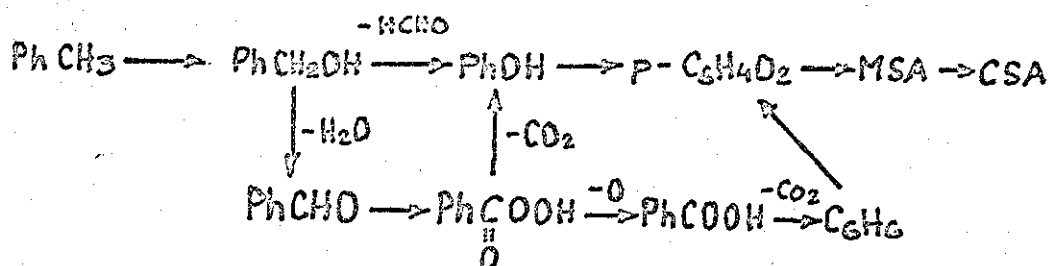
4.2.2   Ceric Molybdate catalyst

Kumar |35| investigated the kinetics for oxidation of toluene
with Ceric molybdate catalyst, using a fluidized catalyst bed. The
same method of analysis of the kinetic data as for vanadium pent-
oxide was employed. The reaction steps are:

$$\text{Toluene} \xrightarrow{k_1} \text{Benzaldehyde} \xrightarrow{k_2} \text{Benzoic acid} \xrightarrow{k_3} CO_2$$
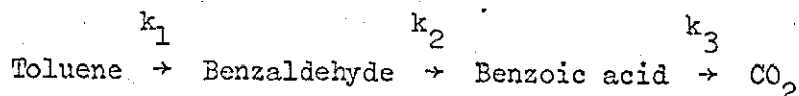
The reaction path in this case is different from that of vanadium
pentoxide. This can be interpreted as a preference for structure (a)
(see section 4.2) in the addition of oxygen to the benzene ring,
thus favouring the conjugated double bond structure. However, the
reported activation energy is lower than the triplet to singlet
state transition (19.7 kcal/mole).

4.2.3   Tin Vanadate catalyst

For the catalytic oxidation of toluene over a fluidized bed
Kumar |35| reported the following reaction steps.

$$\text{Toluene} \xrightarrow{k_1} \text{Benzaldehyde} \xrightarrow{k_2} \text{Benzoic acid} \xrightarrow{k_3} CO_2$$
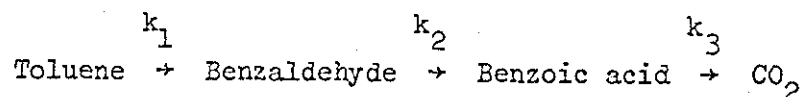
Sasayama |78| found that 47% of the converted toluene reacted to
form maleic anhydride. Maxted |80| found for the same catalyst
33-43% benzoic acid.

4.3 REACTIONS OF TOLUENE WITH ATOMIC OXYGEN

The reaction of toluene with atomic oxygen produced by photo-sensitized decomposition of nitrous oxide was studied by Jones and Cvetanovic |33|. The activation energy was estimated to about 4 kcal/mole. The rate of atomic oxygen consumed could be measured from the nitrogen liberated. Between 15 and 20% of the oxygen atoms reacted were recovered as cresols, water corresponded to about 7%. Carbonmonoxide was measured by oxidation over a copperoxide bed and analysing the carbondioxide formed. The major product was a low volatile polymer. Cresols and carbonmonoxide were also formed in measurable quantities. No trace of dibenzyl was found from gas-chramatographic analysis. The relative amounts of the cresol isomers were 4-5% meta-cresol, 20-25% para-cresol and 70-75% ortho-cresol. The interesting thing about this report is that there is no sign of the ordinary hydrogen abstraction, which would be expected from this type of reaction. No recombination of radicals was detected and only 7% of the reacted oxygen atom did form water. Thus we must conclude that the primary step is an addition of oxygen atoms to the aromatic ring.

4.4 REACTIONS OF TOLUENE IN A DISCHARGE

Kraaijveld and Waterman |30| investigated the chemical effect of an electrical discharge in toluene. At low flow rates the major product was a polymer and at high flow rates they obtained bibenzyl as the main product. At a conversion of 20% they obtained 35% cracking products, 35% bibenzyl and 30% polymer. At the 40% conversion they reported 30% cracking products, 24% bibenzyl and 46% polymer. The energy yield was 20-30 g/kWhr.

Streitwieser and Ward |29| studied the reaction of toluene in Helium/toluene mixtures in a microwave discharge. The volatile

fraction containing about 84% toluene had the following composition: 49% benzene, 30% ethylbenzene, 9% cracking products, 8% phenylacetylene, 3% styrene. The use of argon as a carrier gas in the discharge did not affect the results, whereas hydrogen and methane reduced the tar content below 1%. Experiments with labelled deuterium in the methyl group of toluene showed that most of the deuterium ended up in the ethyl group of the ethylbenzene. The authors suggested the formation of an intermediate anion by electron capture as a possible mechanism.

This result is in contradiction to previous investigations which assume a dominance of radicals in the discharge. Dinan et al |75| showed that free radicals are the dominant species in a 28 Mhz radiofrequency discharge. The following condensable products were obtained from toluene: 35% benzene, 40% ethylbenzene, 16% bibenzyl, 7% diphenylmethane and 2% biphenyl. No change in the composition was observed when helium was used as carrier gas. This demonstrates the difference between the different types of discharges (Kraaijveld's 3 KMHz microwave discharge and Dinan's 28 Mhz radiofrequency discharge).

Experiments with labelled deuteriotoluene provided further support for formation of radicals. It was found that the label remains localized in the side chain of the benzylradical and not distributed throughout the ring. If the tropylium radical was formed we would expect to find a uniform distribution of deuterium label.

Additional experiments were conducted with iodine and toluene. The absence of bibenzyl, biphenyl and diphenylmethane together with the iodine compounds found strongly support the existence of free radicals in the discharge. Table 4.4 shows the condensable products found from iodine and toluene vapour in a 28 Mhz rf-discharge.

Compound	%
Benzyliodide	47
Iodobenzene	14
Ethylbenzene	11
Benzene	13
Methyliodide	6
Unidentified	9

Table 4.4   Condensable products from iodine and toluene

Preliminary studies of the polymeric material formed indicates a different mechanism from that which leads to formation of condensable products.   The polymers appear to be low molecular weight substituted polystyrene.   Hay |76| investigated the polymerization of a number of organic compounds in nitrogen mixtures in a corona discharge.   Infra-red spectra of toluene, benzene and styrene were all similar.   When compared to conventional polystyrene they showed the same strong absorbance but differences were observed in the region 850-1400 cm^{-1}.   It was found that halogens and halogenated compounds when added to styrene had the reversed effect upon the yield.   Bromine reacted to produce the largest yield of all additives.   The author suggests that polymerization does not take place through the vinyl-mechanism, but rather through an ionic or free radical mechanism.

CHAPTER FIVE

CHAPTER 5

EXPERIMENTS IN A BATCH REACTOR

Preliminary runs were made in a batch reactor with the intention of studying the conditions under which the discharge takes place. Although no attempt was made to record the electrical variables in these experiments some valuable results were in fact obtained. Ignition inside the reactor vessel occurred in a few cases, but as the soft glass walls were punctured the reaction ceased. The ignition was seen as a light flash and after dismant ling carbon deposits were found on the reactor walls.

The puncturing of the soft pyrex wall was a serious problem in these earlier experiments. Furthermore, it was found that the electrodes did not make good contact with the reactor walls, but rather point contacts were obtained with very high electric fields, figure 5.1. It was also observed that the thermal reaction was negligible below 300°C for space times less than a few minutes.

Measurements of the temperature profile in the oven (home built) revealed a very large temperature gradient across the reactor. The temperature measured at 300°C was about 30-50°C lower at the reactor ends than in the middle.

5.1 EXPERIMENTAL PROCEDURE

The reactor was charged with 0.30 cc toluene using a 1 cc syringe, and then evacuuated. Oxygen was let in to the reactor, which was subjected to further evacuuations to remove any nitrogen present. After repeating this procedure five times the final oxygen pressure was measured with a manometer (figure 5.3).

The reactor was then placed in the oven with a tap dipping into a thermostated water bath and the electrical connections were fitted
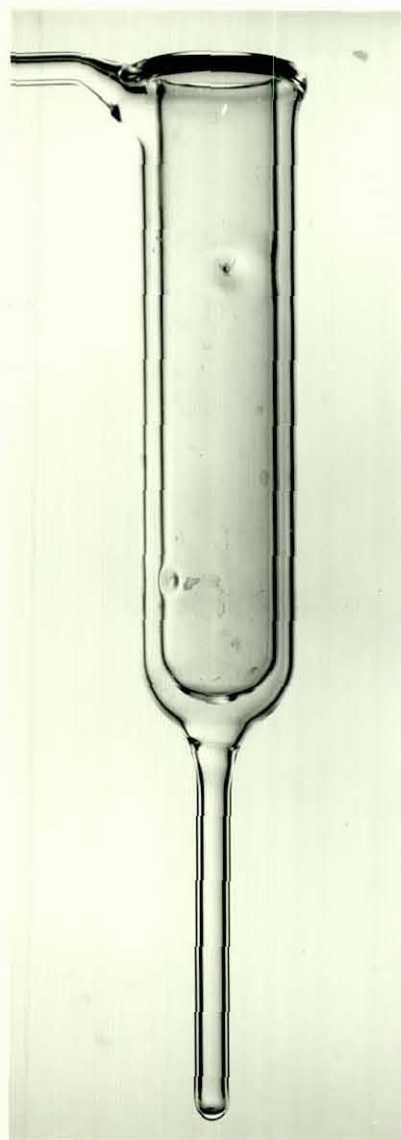
Figure 5.1.a   Batch reactor

Figure 5.1.b   Close-up of a puncture

on. After allowing for an initial heating-up period of five minutes the voltage was switched on for a given time. The reactor was taken out of the oven and cooled to ambient temperature and the pressure was again measured. The liquid fraction was collected and analysed on a gas chromatograph.

The high voltage was obtained from two air cooled high voltage transformers each giving about 5 kV. Frequent problems with insulation breakdown both inside and outside the transformer cage were encountered. The reactor electrodes consisted of brass strips around the cylindrical reactor walls. The outer electrode often fell down when the reactor was placed in the oven. Unsuccessful attempts were made with soldering but in the end the only way to hold the electrodes in place was to twist a couple of strings around the strap.

The qualitative and quantitative analysis is described in section 7. Although cresols can be seen in the chromatograms they were not identified at this early stage and therefore included in the benzyl alcohol peaks.

5.2 EXPERIMENTAL RESULTS

Since the electrical variables were not recorded it was not possible to study their influence upon the reaction rate. Reproducibility of the experiments was poor, partly due to temperature variations and partly due to poor control over the electrical variables.

However, some qualitative conclusions can be found from these preliminary runs. The first and also the most important result is that the reaction rate is greatly increased in the presence of an electrical discharge. Secondly, the capacitive discharge gives a very mild attack on the toluene molecule. The analysis reveals that the side chain is more readily reacted under the conditions employed.

A summary of all experiments is presented in appendix III.

5.2.1 Conversion of toluene

Table 5.1 presents some results obtained with and without the discharge at different residence times, and temperatures. The ratio of oxygen to toluene is greater than 5:1.

Temp. $^\circ$C	Res. time (min)	Conversion without discharge	Conversion with discharge
245	5	-	1.35%
260	6	0.10%	1.26%
255	10	0.03%	1.28%
305	5	0.10%	1.56%
305	10	0.03%	2.03%

Table 5.1. Effect of discharge upon conversion of toluene

The product composition did not show any substantial difference in selectivity for these experiments with and without the discharge as seen in table 5.2 below.

Compound	without discharge (mole %)	with discharge (mole %)
Benzene	5-10	5-10
Phenol	20-30	30-40
"Benzyl alcohol"	0	0-5
Benzaldehyde	50-60	30-50

Table 5.2. Product composition at 300°C

5.2.2 Reaction order of oxygen

In table 5.1 we observed the substantial effect of the electrical variables upon conversion and therefore also the reaction

rate. However, at this early stage we do not have the necessary in-
formation about how the electrical variables influence the rate ex-
pression. To calculate the reaction order of oxygen we will have to
assume that the batch reactor has the same dependence of the electrical
variables as the flow reactor, e.g.

$$-r = kP_{O2}^{\alpha} \, e^{\frac{-68}{E/p}} = \frac{XN_t^0}{V\theta} \quad (\text{moles/l.-sec})$$ (5.2)

where X = conversion of toluene

θ = run time in seconds

V = reactor volume (0.035 litre)

N_t^0 = moles of toluene charged

To counteract the low accuracy of the experiments we will group
the data and calculate the mean of each group. Using the data from
run 21-27 we obtain table 5.2.

$\ln(-r)$	$\ln P_{O2}$	E/p	$68 \, p/E$	mean $\ln(-r)$
-12.4	4.56	50		
-13.2	4.56	50	-1.36	-13.2 ± 0.7
-14.0	4.56	50		
-13.2	5.95	25		
-13.4	5.95	25	-2.72	-13.7 ± 0.7
-14.3	5.95	25		
-13.6	6.64	18.7	-3.64	-13.6

Table 5.2. Reaction order of oxygen

$\ln(-r) - 68 \, p/E$ is plotted atainst $\ln P_{O2}$ in figure 5.2. The
slope of the curve gives the reaction order. From the graph we find
$\alpha = 0.9$. This indicates that the reaction is of first order with

respect to oxygen.

5.2.3 Reaction rate

We will now proceed to find the value of k in expression 5.2 and compare this value with that obtained from the flow reactor $(9.7 \cdot 10^{-8}$ moles $1^{-1} \text{sec}^{-1})$.

Again we will use the same technique as in section 5.2.2. The result obtained from run 35-39 are shown in table 5.3 below.

Conversion mole %	Resid time min.	(-r) moles/1.-sec
0.25	0.5	$67 \cdot 10^{-7}$
0.33	1.0	$44 \cdot 10^{-7}$
0.85	2.0	$57 \cdot 10^{-7}$
1.86	5.0	$41 \cdot 10^{-7}$
2.03	10.0	$27 \cdot 10^{-7}$
	Mean	$47 \cdot 10^{-7}$

Table 5.3. Reaction rate at 300°C

The values of the physical and electrical variables were as follows: V = 10 kV, d = 0.5 cm, p = 300 mm Hg, inserting these values in 5.2 we obtain k = $9.5 \cdot 10^{-8}$ (moles 1^{-1}sec^{-1}). We notice that this value is about the same as that for the flow reactor made in silica. Thus we find the encouraging result that the rate expression is independent upon the type of reactor and also there is no difference between silica and pyrex from a catalytic point of view (heterogeneous reactions).

71
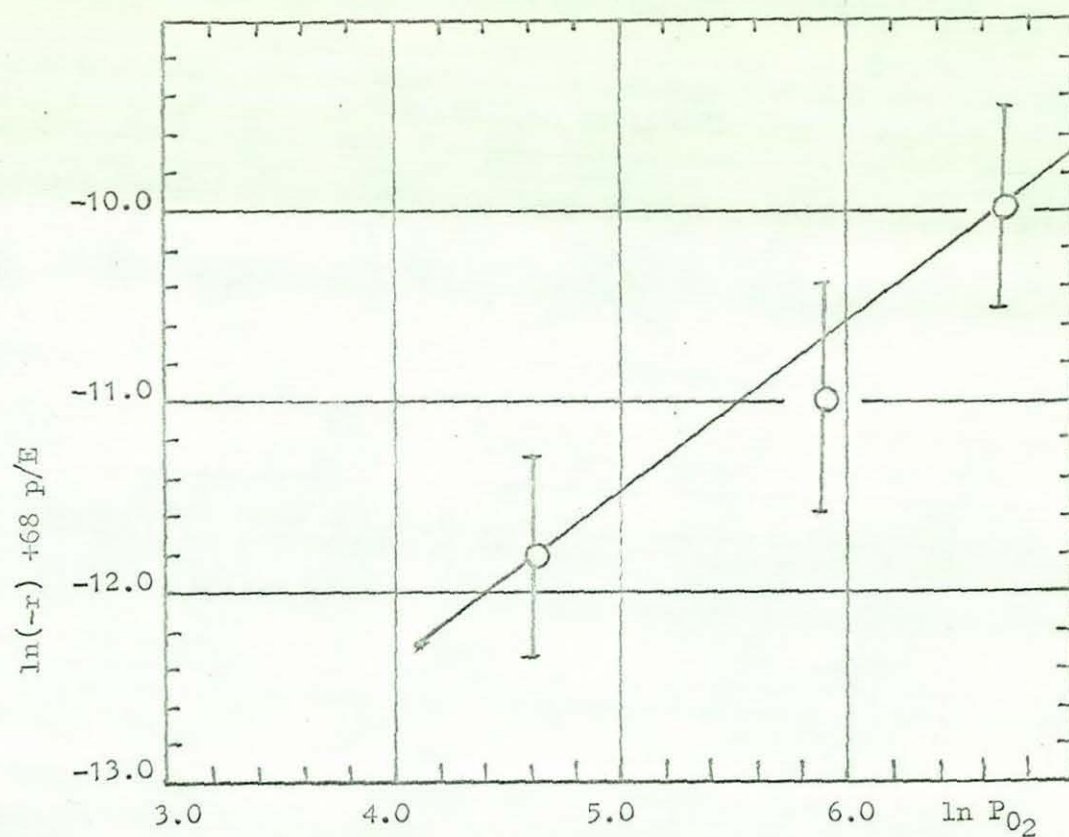
Figure 5.2. Reaction order of oxygen
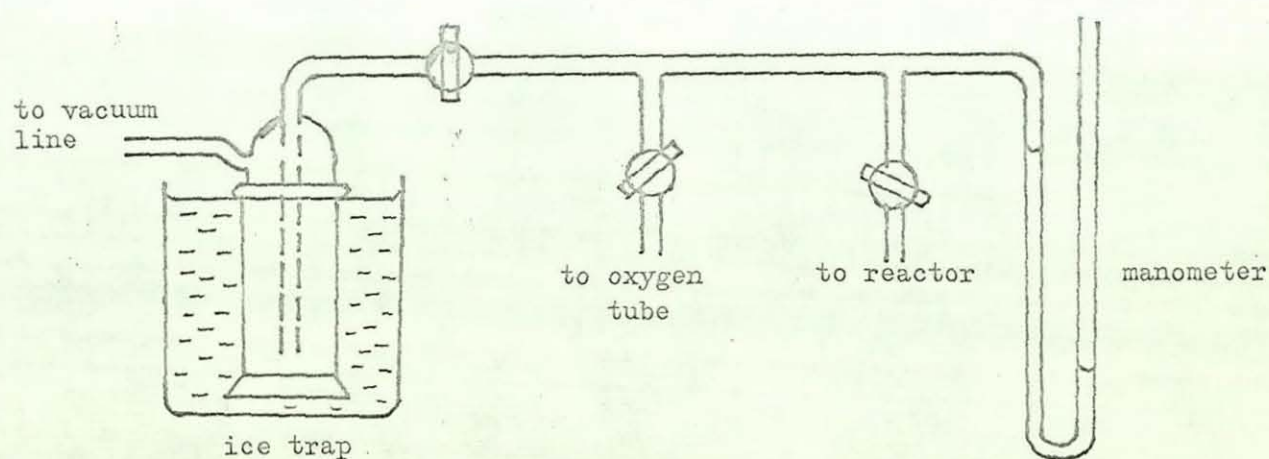
Figure 5.3. Arrangement for charging of batch reactor

5.2.4 Selectivity

From the rate expression it is found that the two variables affecting the rate of reaction is the electric field and the partial pressure of oxygen. The effect of the electric field upon selectivity could not be investigated since these variables were not measured.

The effect of partial pressure of oxygen upon the selectivity are shown in figures 5.4 to 5.8.

At low residence time and low partial pressure of oxygen, benzyl alcohol (including cresols) are the major products; as the residence time increases more benzaldehyde and benzoic acid are produced.

The effect of pressure may be interpreted as follows. At low pressure the kinetic energy of the electrons is high (the mean free path is increased) thus giving rise to atomic oxygen.

5.2.5 Effect of cyclic discharges

In an attempt to increase the energy yield of the reaction, the discharge was operated in cycles. The total run times in all experiments was 5 minutes. $f = 5$ means 5 discharges in 5 minutes, $f = 30$ means 30 discharges in 5 minutes. $f = 5$ and 50% represents 30 seconds on and 30 seconds off. $f = 30$ and 25% represents 2.5 seconds on and 7.5 seconds off.

At $f = 30$ there is an indication of a better yield, but the result may be within the experimental errors, as seen in figure 5.9.
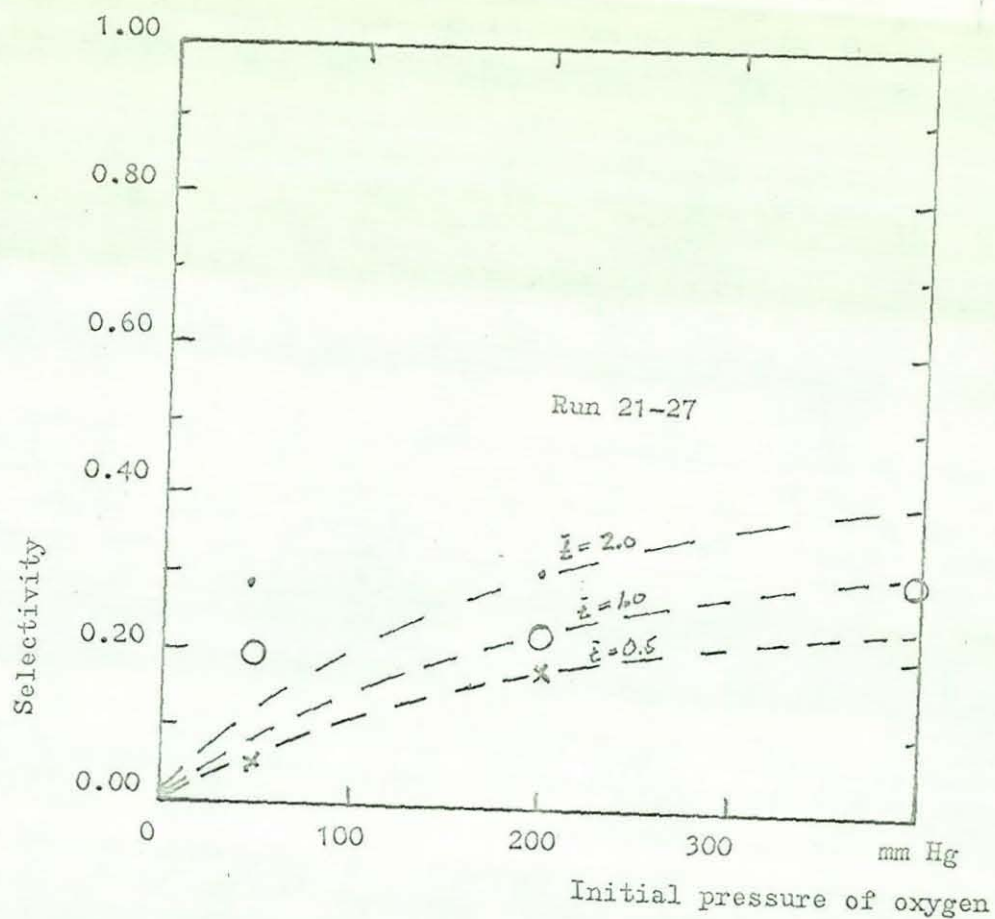
Figure 5.4. Selectivity for benzaldehyde
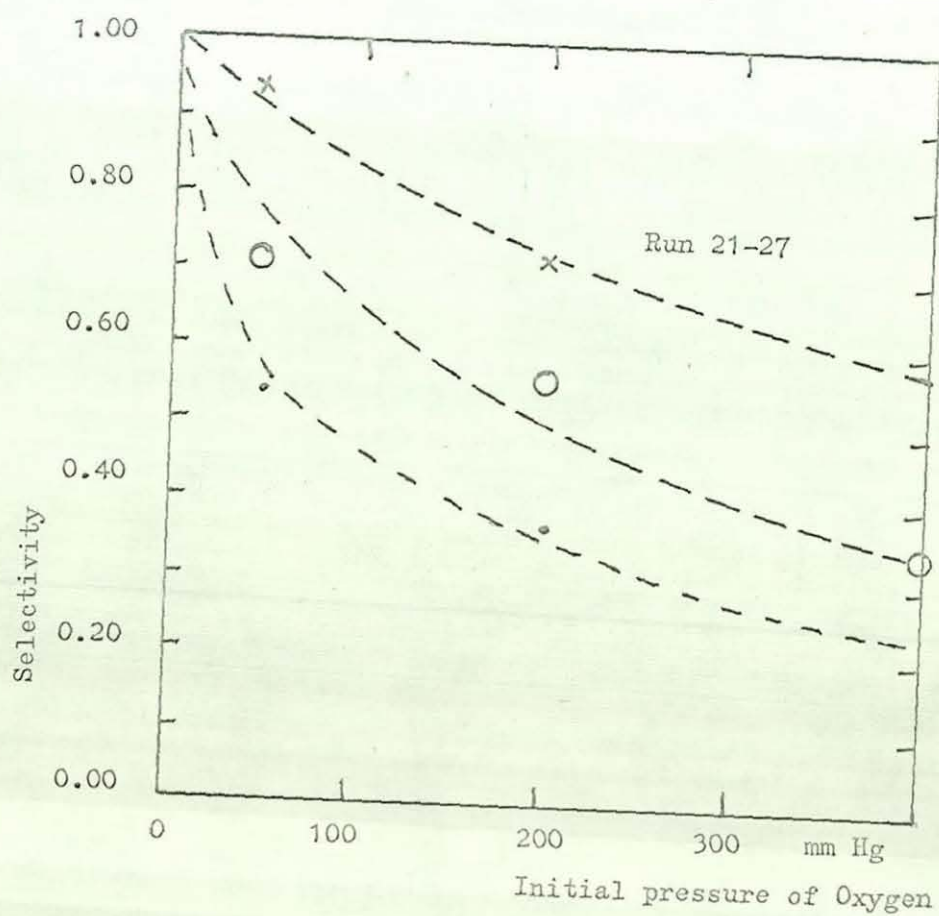
Figure 5.5. Selectivity for C_7H_8O

74
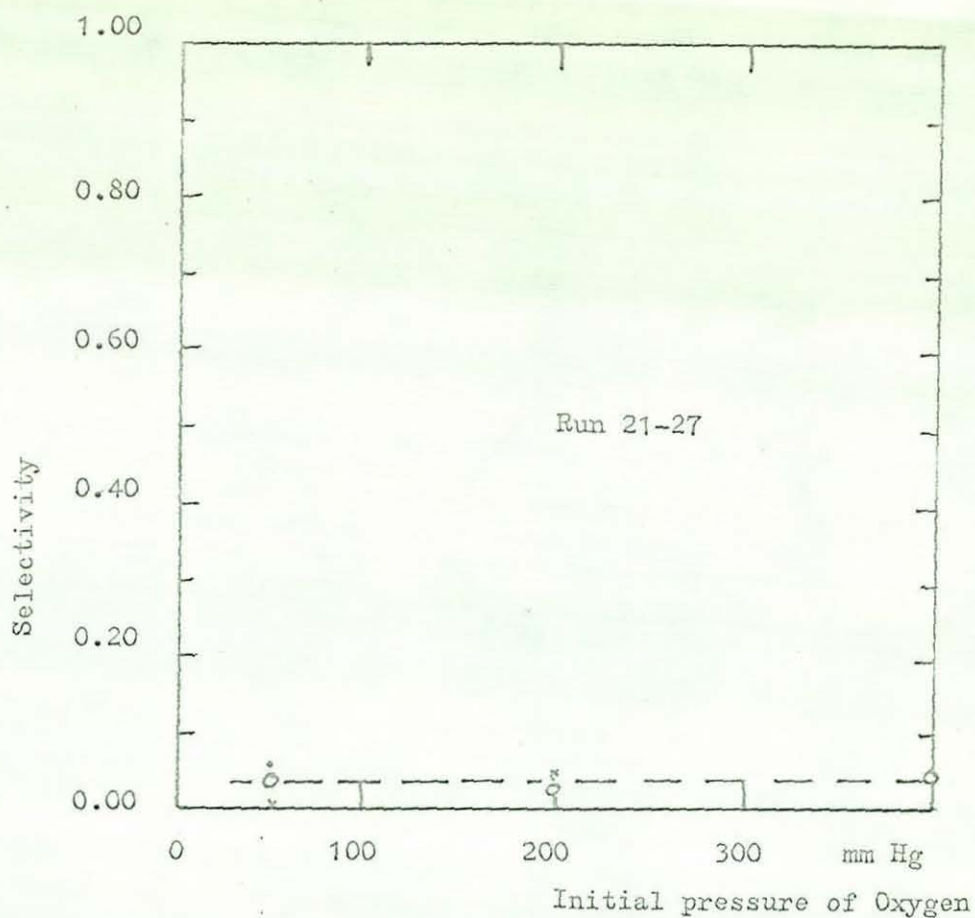
Figure 5.6.   Selectivity for benzene
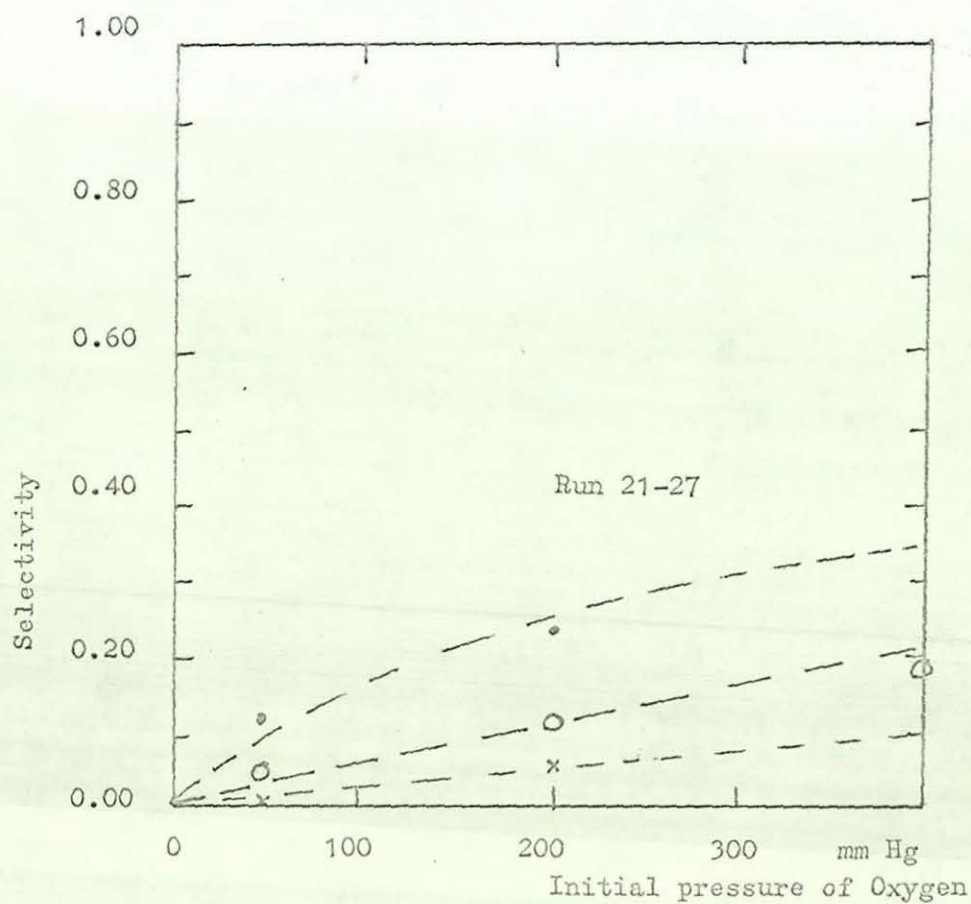
Figure 5.7.   Selectivity for phenol
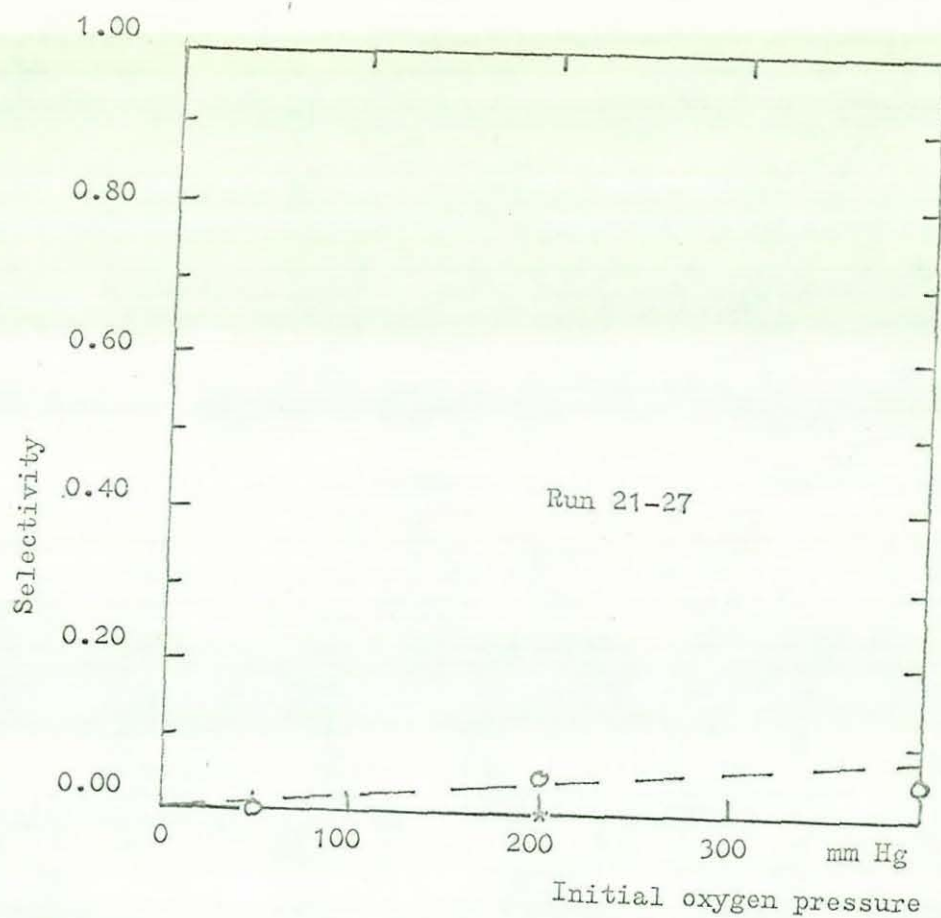
Figure 5.8.   Selectivity for benzoic acid
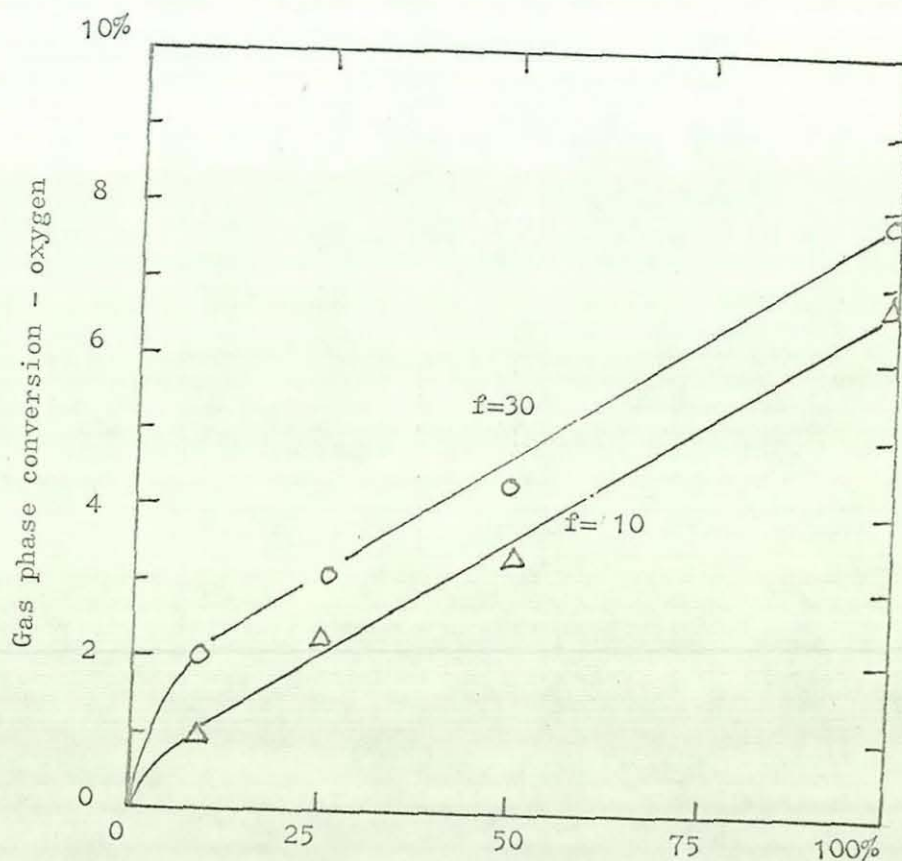
Figure 5.9.   Cyclic discharge

CHAPTER SIX

CHAPTER 6

EXPERIMENTAL REACTOR DESIGN

In the previous section we showed that reaction rate and conversion were controlled by the electrical discharge. This fact will have its implications on the design of the reactor. The electrical properties of the reactor become the dominant design criteria.

The minimum wall thickness to be used is determined by the dielectric strength of the reactor material and the maximum applied voltage.

We suggest here two more parameters to characterise the reactor from an electrical point of view. The first one is the capacitance of the reactor. This property determines the capacitive current in an ac-circuit and also the length of the discharge zone. The second parameter used to characterise the reactor is the Paschen curve (2.1.3). This parameter determines the discharge current and hence the reaction rate.

Unfortunately, in the batch reactor experiments we were not able to measure any of the electrical variables, such as discharge current, phase shift, length of the discharge zone, reactor voltage. Without these variables we have no means of obtaining a good correlation for the reaction rate. The most urgent requirement in the flow reactor experiments was therefore to design a circuit that would enable us to measure these electrical variables. This section describes the development of such a circuit.

6.1 GEOMETRY AND PHYSICAL PROPERTIES OF THE REACTOR

There are several ways in which the geometry and the physical properties of the vessel can affect the reaction rate.

The material in which the reactor has been constructed is important for two reasons, firstly it may affect the reaction rates (heterogeneous reactions), secondly it affects the electrical properties such as dielectric strength and electric capacitance.

The gas gap (i.e. the distance between the walls) is of fundamental importance because it determines the breakdown voltage. It also determines the flow characteristics of the reactor. A narrow gap tends to give plug flow characteristics, whereas a large gap combined with low gas velocity results in deviation from ideal plug flow behaviour.

6.1.1 Geometrical dimensions of the reactors

The batch reactors (section 5) were made of pyrex and had all the following dimensions:

$$r_a = 0.0175 \text{ m} \qquad L = 0.120 \text{ m}$$
$$r_b = 0.0155 \text{ m} \qquad r_c = 0.0140 \text{ m}$$
$$r_d = 0.0120 \text{ m} \qquad \text{Discharge volume} = 0.034 \text{ litre}$$

The flow reactors were made in silica with the following dimensions:

$$r_a = 0.0196 \text{ m} \qquad L = 0.127 \text{ m}$$
$$r_d = 0.01395 \text{ m} \qquad \text{Discharge volume} = 0.035 \text{ litre}$$
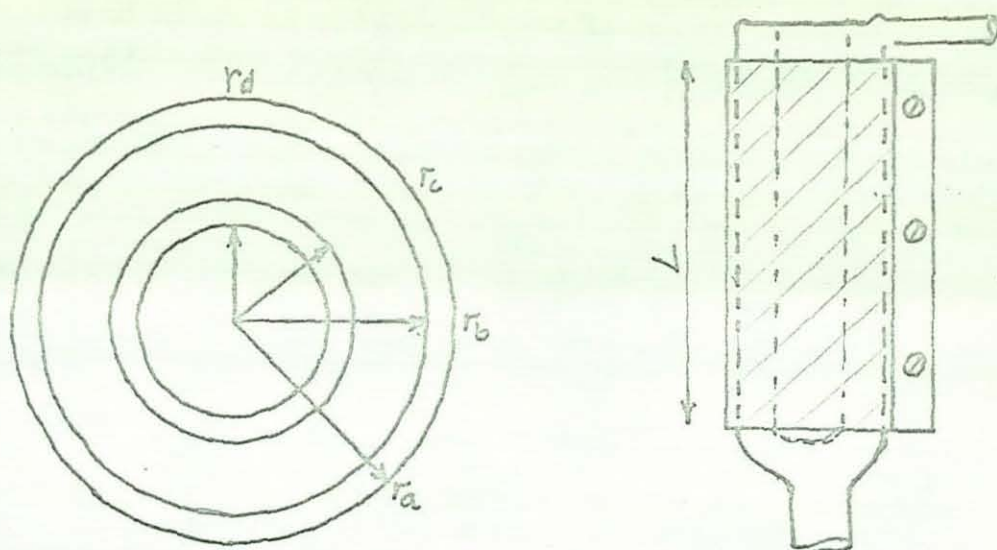
Figure 6.1   Reactor dimension

6.1.2   Residence time distribution

Real reactors never satisfy the flow pattern required for an
ideal reactor. This deviation from ideal behaviour can sometimes
be considerable. In an ideal plug flow reactor each molecule will
have spent exactly the same time in the reactor. Many models for
characterisation of the flow pattern have been suggested. The most
common is probably the dispersion model. This model is based upon
the assumption that dispersion takes place and takes the form of a
diffusion process; no by-passing or stagnant pockets exist. The
dimensionless group used to characterise this mixing is D/uL., which
is called the reactor dispersion number. It varies from zero for
an ideal plug flow reactor to infinity for an ideal CSTR (Continu-
ous Stirred Tank Reactor).

For a closed vessel the dispersion number is found from the
variance according to Levenspiel |12|.

$$\delta = \frac{\delta t^2}{\bar{t}} = 2\left(\frac{D}{uL}\right) - 2\left(\frac{D}{uL}\right)^2\left(1 - e^{-uL/D}\right) \qquad (6.1)$$

$$\delta_t = \frac{\sum t^2 c}{\sum c} - \left(\frac{\sum tc}{\sum c}\right)^2 \qquad (6.2)$$

79

The experimental procedure is to inject a tracer at the inlet of the reactor and then measure the concentration of this tracer at the reactor outlet. In our case we injected 1.0 cc cis-butene as a tracer and recorded the outlet concentration on a gas chromatograph.

In practice it is impossible to avoid dead volumes from connection leads to the reactor and to the analyzing circuit. A couple of runs were therefore made to determine the "dead" volume of the system. The value obtained was 28 seconds.

We repeated the procedure with the reactor in place and the results are seen in figure 6.2. The corresponding voltage as recorded on a digital voltmeter is presented in appendix II:2 table 1.

6.1.2 Residence time distribution

From appendix II:2 table 1 we obtain $\sum c = 37.752 \cdot 10^3$, $\sum tc = 17.429 \cdot 10^6$ and $\sum t^2 c = 8.309 \; 10^9$. The mean residence time is $\bar{t} = \sum tc / \sum c = 462$ seconds. The variance is

$$\delta_t^2 = \frac{8309 \cdot 10^6}{37.752 \cdot 10^3} - (\frac{17.429 \cdot 10^6}{37.752 \cdot 10^3})^2 = 6962$$

$$\delta^2 = \frac{6962}{426} = 0.0326$$

The value of the reactor dispersion number, obtained through iteration, is

$$(\frac{D}{uL}) = 0.01656$$

The value of the dispersion number tells us that we have a fairly small dispersion in our vessel. The effect of the dispersion number upon reactor size for a given conversion has been solved for a first order reaction by Wehner and Wilhelm (1956). For a

80
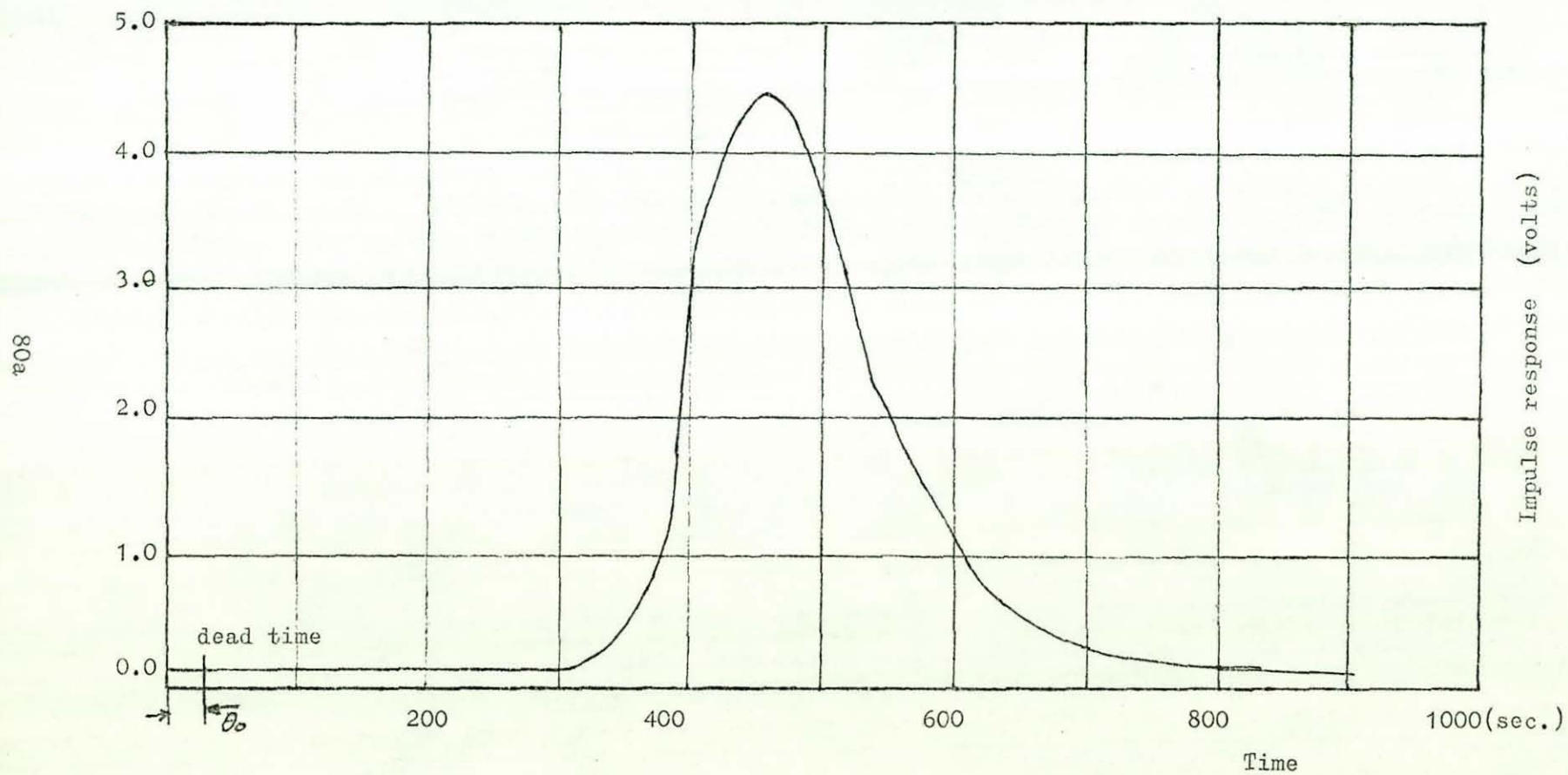
Figure 6.2. Residence time distribution

conversion less than 10% the effect of a small dispersion number is negligible.

The assumption of ideal plug flow is found to hold within experimental error, for our case.

6.2 ELECTRICAL PROPERTIES OF THE REACTOR

The most used material for construction of ozonizers is silica. The main reason for this is its high dielectric strength. The dielectric strength for silica and pyrex is 25 kV/mm, 15 kV/mm respectively. An overdesign factor for the wall thickness of two is recommended but no practice has been found in the literature.

6.2.1 Capacitance of the reactor

From an electrical point of view the chemical reactor consists of two conductors separated by dielectics and is thus a capacitor. The capacitance of the reactor can be calculated from the geometrical dimensions and the physical properties of the reactor material (dielectric constant). The capacitance for a cylindrical reactor shape, neglecting end effects, is:

$$C = \frac{2\pi\varepsilon_0 L}{\ln(r_a/r_b)}$$

A typical configuration is

———||———||———||———

glass   gas   glass

with the capacitance

$$\frac{1}{C} = \frac{1}{2\pi\varepsilon_0 L}\left|\frac{\ln(r_a/r_b)}{K} + \ln(r_b/r_c) + \frac{\ln(r_c/r_d)}{K}\right| \qquad (6.3)$$
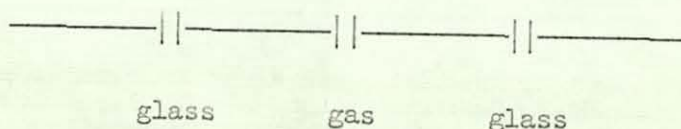
Inserting the geometrical dimensions (6.1.1), noticing that K is approximately equal to 6 for pyrex, we get C = 45 pF. The measured value (by a resistance bridge) was 56.7 pF. The two flow reactors in silica had a capacitance of 31 and 34 pF respectively

6.2.2 Paschen curves for the reactor

From section 2.1.3 we found that the breakdown voltage of a gas gap is dependent only on the product pd for a particular gas. But d (gas gap) is a property of the reactor. Therefore the Paschen curve is a characteristic of the reactor for a given gas. Imperfections of the surfaces tend to lower the breakdown voltage and two similar reactors may therefore have different breakdown voltages. Figure 6.3 shows the Paschen curves for oxygen in a silica reactor at low gas pressure (pd ≤ 150 mm Hg cm). The lower curve represents the extinguishing voltage of the discharge. The curve was obtained by lowering the applied electric field until finally the discharge ceased. A second method of obtaining the extinguishing voltage is to measure the voltage drop when a discharge takes place, figure 6.12. This method is particularly valuable when we have a geometry where the difference in radius is large (i.e. non-uniform fields).

6.3 DISCHARGE MEASUREMENTS

A simple circuit for measuring discharge current and voltage was proposed by the Department of Chemical Engineering, University of Newcastle-upon-Tyne |45|. The circuit consists of a 100 Ohm resistor in series with the reactor, and a voltage attenuator in parallel to the reactor. The circuit is shown in figure 6.4. The main disadvantage with this circuit was that it was difficult to detect the height of the peaks on the oscilloscope. An alternative method is presented in section 6.3.2.

pd ⩽ 150 mm Hg cm
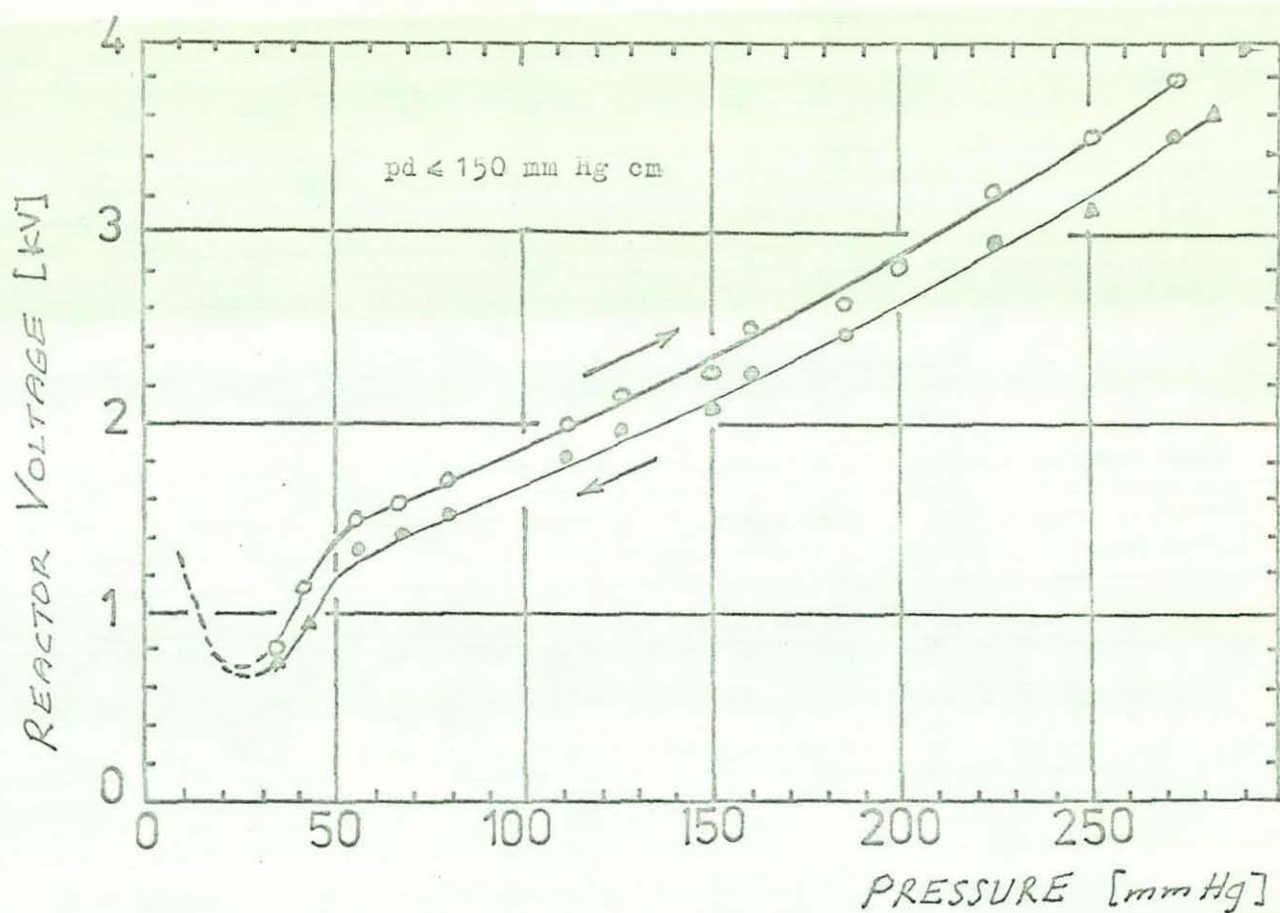
Figure 6.3.a   Paschem curves for oxygen at 20°C
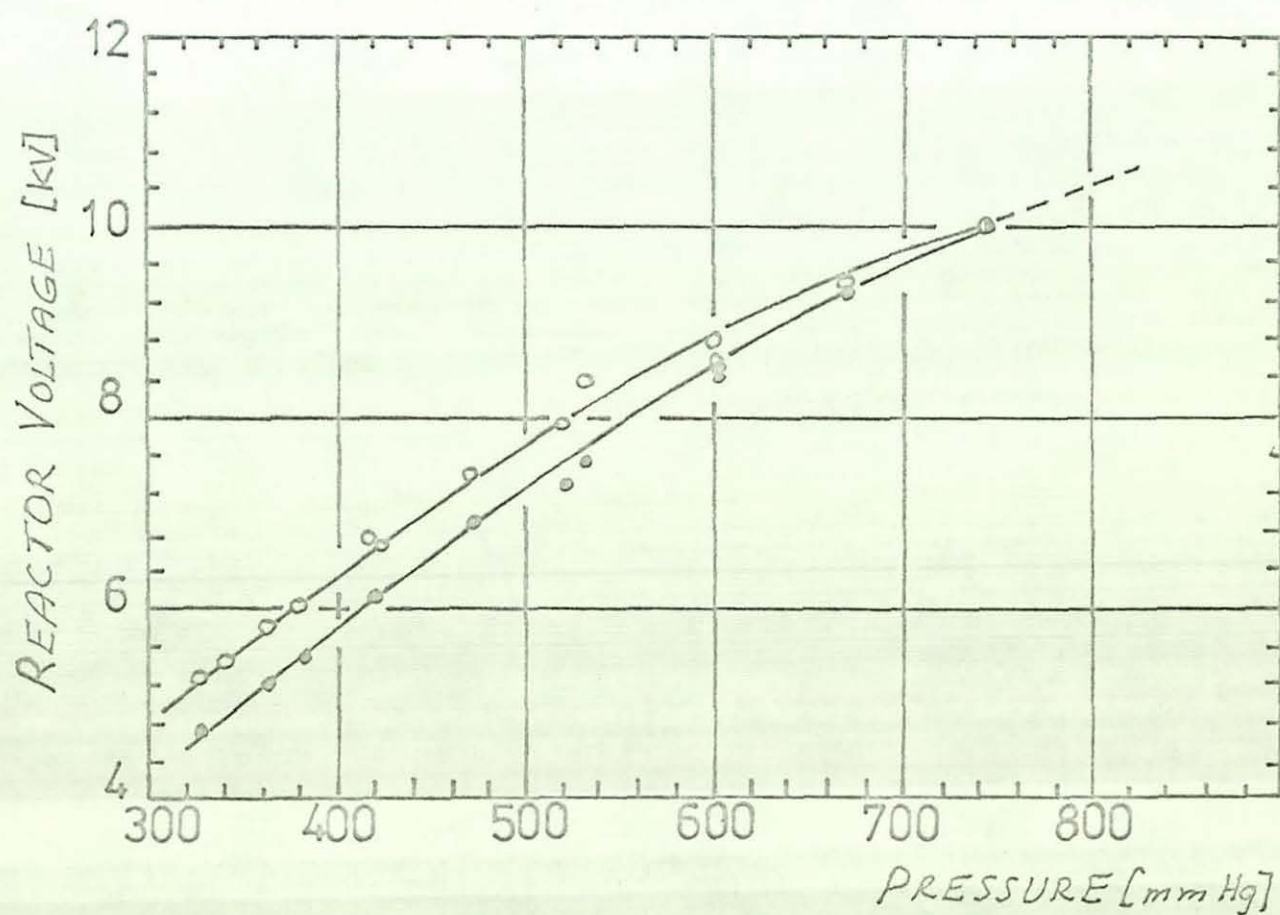
Figure 6.3.b   Paschen curves for oxygen at 20°C

6.3.1 Measurement of the capacitive current

Measurement of the capacitive current presents no problem. The circuit used for the first experiments is shown below.
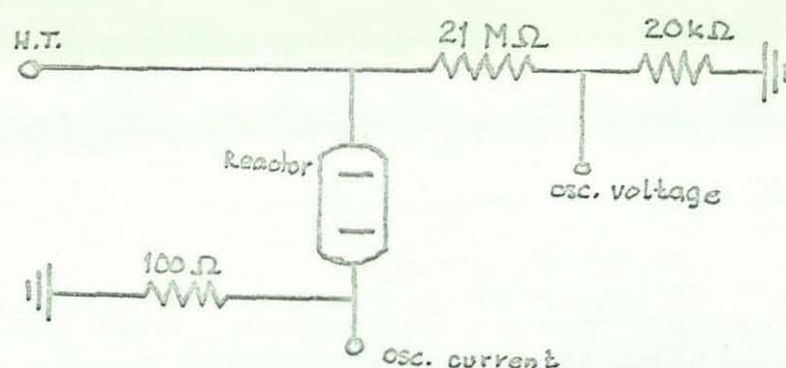
Figure 6.4 Measuring circuit for capacitive current

A photograph of the capacitive current and the voltage taken of air at atmospheric pressure in the pyrex reactor as measured on an oscilloscope is shown in figure 6.11. A comparison between calculated and measured current is presented in table 6.2. The calculated current is based upon equation 6.6.

Time (m sec.)	Reactor voltage (vols)	mA	
		i_c(calc.)	i_c(meas.)
0	0	+0.11	+0.12
2	1600	+0.09	+0.10
4	2700	+0.03	+0.04
6	2700	−0.03	−0.03
8	1600	−0.09	−0.06
10	0	−0.11	−0.12
12	−1600	−0.09	−0.11
14	−2700	−0.03	−0.04
16	−2700	+0.03	+0.02
18	−1600	+0.09	+0.06
20	0	+0.11	+0.11

Table 6.2 Capacitive reactor current

We notice the agreement between calculated and measured values of the current. In fact we may reverse the calculation and calculate the capacitance of the reactor from knowledge of the capacitive current and the applied voltage.

6.3.2 Measurement of the discharge current

The circuit in figure 6.4 has two major disadvantages when we measure the discharge current. The first difficulty is to record the peak height of the pulses on the oscilloscope. The second problem is more fundamental. When we take a photograph over a single cycle, we can only measure the instantaneous current. To find the average discharge current requires several photographs. A way to overcome the first difficulty was suggested by K. Honda[20], who introduced a capacitor across the resistor to catch the current pulse. Figure 6.13 and 6.14 shows the measurements of the current pulses. The RC-circuit must have a time constant that allows the capacitor to fully discharge between successive current pulses, also we want the main current of a pulse to pass through the capacitor. K. Honda suggested a time constant of 26 µseconds with a value of R = 20 kOhm. The second problem was overcome by introducing an RCL-filter. This filtered out the capacitive current and the remaining current was rectified and measured with a d.c. amperemeter.

The procedure for evaluation of the discharge current from photographs is described briefly below. By measuring the voltage across the capacitor on an oscilloscope we can measure the charge transferred in one second (i.e. the discharge current). Since

$$i_d = \frac{dQ}{dt} \quad \text{and} \quad C = Q/V$$

we have
$$i_d = C\sum_i^N U_i$$

RCL-Filter: Murhead D-925A

Oscilloscope: Phillips PM-3250

Figure 6:5   Electrical circuit.

Thus we obtain the discharge current by summing up all peaks over a half cycle and multiplying by 100 (or summing over a cycle, multiplying by 50) and the capacitance of the filter (1500 pF).

6.3.3 Measuring circuit for electrical porperties

The electrical circuit used in the flow reactor experiments is shown in figure 6.5. The circuit consists of a primary transformer, whose energy consumption is measured with a kWhr-meter. The secondary side is fed to a high voltage transformer through a thermal fuse and a microswitch operating on the safety cover. The applied voltage is attenuated and connected to an oscilloscope. The other arm of the high voltage side is connected to a graphite rod inside the reactor, which is packed with graphite. An aluminium foil is wrapped around the reactor and a brass cylinder is screwed tight around the reactor, which is electrically connected to a home built analyser.

The analyser filters out the 50 Hz ac current and the remaining current is rectified and measured with a d.c. ampere meter. The instantaneous discharge current is obtained from an RC-filter with a time constant of 30µs. The voltage rise over the capacitor is recorded on an oscilloscope. Thus we were able to measure the capacitive current, the instantaneous discharge current, the average discharge current and the applied reactor voltage.

6.4 DISCHARGE SIMULATIONS

In this section we propose a model of the discharge, and explain some of the features of the discharge.

6.4.1 Equivalent circuit of the reactor

K. Ogawa|21| proposed an equivalent circuit of the discharge according to
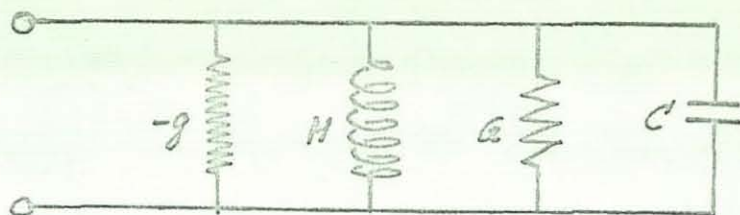
Figure 6.6 Equivalent circuit according to Ogawa

It is now suggested that below the breakdown voltage the circuit simplifies to

Figure 6.7 Simplified circuit

The equation for this circuit is

$$U_0 \cos wt = U_1 + U_2 = iR + U_2 = RC \frac{dU_2}{dt} + U_2 \qquad (6.4)$$

with boundary conditions $U_2 = 0$ when $t = 0$. Equation 6.4 can be solved by Laplace transformation. The transform is

$$U_2(s) = \frac{U_0 s}{RC(s^2 + w^2)(s + 1/RC)}$$

The inverse is found by applying the residue value theorem.

Let $\qquad U(p) = \dfrac{p}{(p^2 + a^2)(p + b)} \qquad$ with poles $+ia$, $-ia$, and $-b$

$$U(x) = \text{Res}\left\{ \lim_{p \to -ia} \frac{pe^{px}(p+ia)}{(p+ia)(p-ia)(p+b)} + \lim_{p \to ia} \frac{pe^{px}(p-ia)}{(p+ia)(p-ia)(p+b)} \right.$$

$$\left. + \lim_{p \to -b} \frac{pe^{px}(p+b)}{(p+ia)(p-ia)(p+b)} \right\}$$

88

$$= \text{Res} \left\{ \frac{(b+ia)e^{-iax} + (b-ia)e^{-iax} - 2be^{-bx}}{2(a^2 + b^2)} \right\}$$

$$= \text{Res} \left\{ \frac{b}{a^2 + b^2} \left[\frac{e^{iax} + e^{-iax}}{2} + \frac{ia(e^{-iax} - e^{iax})}{2b} \right] - e^{-bx} \right\}$$

$$= \frac{b}{a^2 + b^2} \left\{ \cos ax + \frac{a}{b} \sin ax - e^{-bx} \right\}$$

where $\qquad a = w, \qquad b = \frac{1}{RC}$

therefore

$$\frac{b}{a^2 + b^2} = \frac{RC}{w^2 R^2 C^2 + 1} \qquad \frac{a}{b} = RwC$$

and the solution is:

$$U_2(t) = \frac{U_0}{(w^2 R^2 C^2 + 1)} \left[\cos wt + RwC \sin wt - e^{-t/RC} \right] \qquad (6.5)$$

$$i(t) = \frac{U_0/R}{(w^2 R^2 C^2 + 1)} \left[w^2 R^2 C^2 \cos wt - wRC \sin wt + e^{-t/RC} \right] \qquad (6.6)$$

For $w = 0$ (d.c.) we have the solution $U_2 = U_0 (1 - e^{-t/RC})$. This solution is consistent with the ones found from the literature for simple d.c. circuits. We also notice that since $i = C \frac{dU_2}{dt}$ the phase shift is 90°.

Above the breakdown voltage two additional properties must be included, namely the breakdown voltage and the extinguishing voltage. Although the reactor also has some inductance (about 3 µH) it is not important at low frequencies (below the khz-range), the resonance frequency being about 0.5 kHz.

6.4.2 A study of some discharge features

Before we involve ourselves too deeply in the theoretical calculations, let us first find out what the features of the discharge are and what we are trying to explain. Let us look closely at figure 6.12. We notice two unusual features. The first is that there is a discharge at zero applied voltage, which obviously contradicts the physical laws. The second feature is that the discharge ceases at the maximum voltage. Easier to understand is the difference in peak heights between the positive and negative polarity. Recalling figure 2.9 we may explain this difference by assuming two different breakdown voltages due to the effect of a non-uniform field. The difference in peak heights raises the question whether or not the current of the two polarities are equal. Table 6.3 summarises the effect of polarity upon the discharge current.

	Inner electrode	
	negative	positive
number of peaks	33	15
Σ peak heights	30	31
mean height	0.8	2.0
Std deviation	0.4	0.9

Table 6.3   Effect of polarity upon peak heights

Table 6.3 show that the current of the two polarities is not significantly different. Thus we may assume that no accumulation of charge, which could lead to fluctuating currents, occurs.

The distribution of peak heights is shown in figure 6.8.
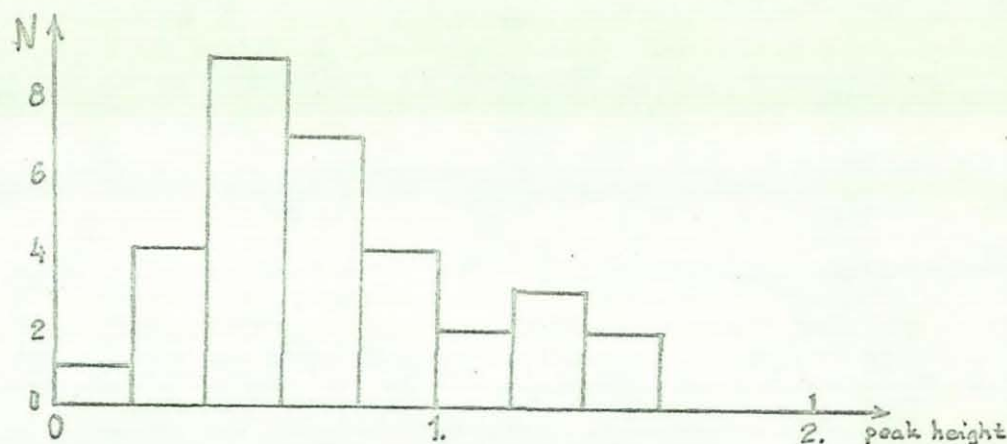
Figure 6.8   Peak height distribution

6.4.3   Phase shift

Returning to the apparent contradiction of a discharge at zero voltage and disruption of the discharge at maximum voltage, we suggest now that a phase shift takes place.

Figure 6.9 shows a hypothetical graph of this phase shift.
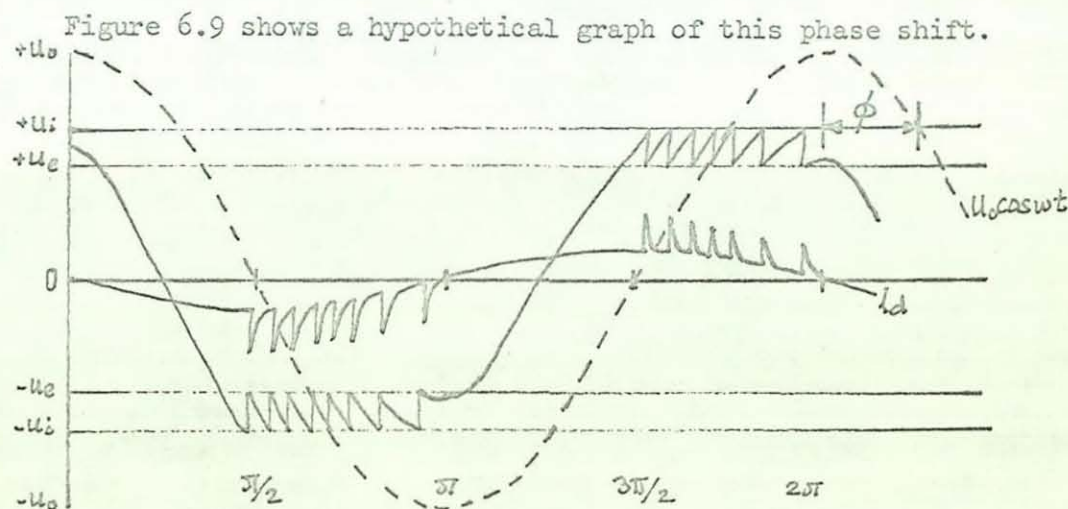
Figure 6.9   Phase shift

Let us now try to quantify the phase shift. The applied voltage is $U_0 \cos wt$. We see first of all that a discharge at zero applied voltage is explained by the phase shift. At the maximum applied voltage we notice that the maximum discharge voltage is U_i (the breakdown voltage of the gas gap); at this

point, however, the current changes its polarity and the voltage starts to decrease. Thus no further discharge can take place. The phase shift, ϕ, can be calculated from equation 6.5.

$$U_i = \frac{U_0}{1 + w^2 R^2 C^2} \left\{ \cos(wt-\phi) + wRC\sin(wt-\phi) - e^{-t/RC} \right\}$$

this simplifies to

$$\frac{U_i}{U_0}(1 + w^2 R^2 C^2) = \cos(-\phi) + wRC\sin(-\phi)$$

since: $p \cos A + q \sin A = \sqrt{p^2 + q^2}\,\sin(A + \theta)$; $\tan \theta = p/q$

we get $\quad \sin(\theta - \phi) = \frac{U_i}{U_0}\,\frac{1}{(1 + w^2 R^2 C^2)^{\frac{1}{2}}}$; $\tan \theta = \frac{1}{wRC}$

and finally

$$\phi = \arctan\left(\frac{1}{wRC}\right) - \arcsin\left\{ \frac{U_i}{U_0}\,\frac{1}{(1 + w^2 R^2 C^2)^{\frac{1}{2}}} \right\} \qquad (6.7)$$

6.4.4 Length of the discharge zone

The phase shift cannot be measured directly from the photographs of the instantaneous current and the applied voltage. But we can measure another property, and that is the length of the discharge zone. The question now is whether or not a relationship between the phase shift and the length of the discharge zone (LDZ) can be found. From figure 6.9 we notice that LDZ is simply the time the voltage exceeds the breakdown voltage (U_i). But ϕ is just half this value and therefore we get

$$LDZ = 2\phi \qquad (6.8)$$

A comparison between calculated and experimental LDZ shows good
agreement. Using figure 6.12 we obtain LDZ = $21/35 \times 180^\circ = 108^\circ$.
Assuming a breakdown voltage of 2000 Volt at 200 mm Hg and $300^\circ C$
(appendix II:3), we get the following values: $U_0 = 3800$ V,
$U_i = 2000$ V, C = 31 pF, w = 314 rad/sec. Replacing R with Z,
putting Z = 0.536 M Ohm, we get $\phi = 57.9^\circ$ and LDZ = 115.8° (or 6.0,
6.4 msec. respectively).

6.4.5 Impulse response of the circuit

To test the response of the RC-filter we will develop a
transfer function of the system. The transfer function will also
enable us to simulate the discharge on a computer. Figure 6.10
shows the measuring circuit used.
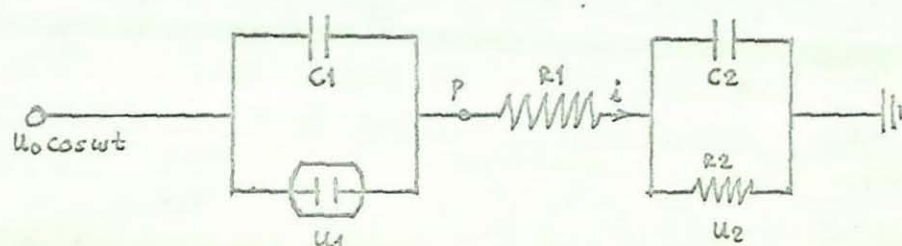
Figure 6.10   Measuring circuit

Using the notation of figure 6.10 we get

$$x = i_1 R1 + U_2 \qquad\qquad x = U_p - U_p^0$$

$$i_1 = C2 \frac{dY}{dt} + \frac{Y}{R2} \qquad\qquad Y = U_2 - U_2^0$$

$$x = R1C2 \frac{dY}{dt} + \frac{R1}{R2} Y + Y$$

The Laplace transform is:

$$x(s) = R1C2sY(s) - 0 + \frac{R1 + R2}{R2} Y(s)$$

$$G(s) = \frac{Y(s)}{x(s)} = \frac{1/R1C2}{\left[S + \frac{R1 + R2}{R1R2C2} \right]}$$

$$\text{Impulse area} = \Delta U_2 \int_0^\infty e^{-t/R1C2} \, dt = R1C2\Delta U_2$$

$$Y(s) = \frac{\Delta}{R1C2} \frac{1}{\left[S + \frac{R1 + R2}{R1R2C2} \right]} \quad ; \quad \Delta U_2 = \frac{\Delta UR2}{R1 + R2}$$

$$\text{and} \qquad \boxed{U_2 = U_e^0 + \frac{\Delta UR2}{R1 + R2} e^{-\frac{(R1 + R2)t}{R1R2C2}}} \qquad (6.9)$$

Equations 6.5 and 6.9 form the basis of a computer program for simulation of the electrical discharge.

A simple way to evaluate the RC-filter is described below. Using photograph 6.13 we find that $U_2 = 40$ V approximately and $t = 0.4$ µseconds. The current passing through the capacitor (C2) is:

$$i_c = 1500 \cdot 10^{-12} \frac{40}{0.4 \cdot 10^{-6}} = 150 \text{ mA}$$

The instantaneous current passing through the resistor is:

$$i_R = \frac{40}{20\ 000} = 2 \text{ mA}$$

The RC-circuit proposed is therefore adequate for our measurements.

6.4.6 Hardware simulations

A physical model was built up out of electrical components to study the features of the discharge. Figure 6.16 shows the circuit for this study.
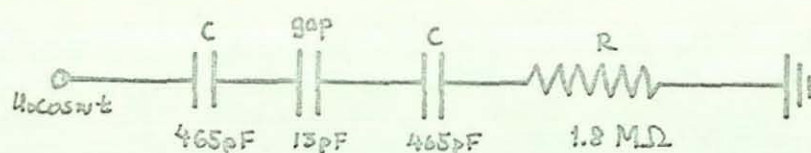
Figure 6.16 Electric circuit for discharge simulations

The middle capacitor consisted of an air gap between two
brass plates about 1 mm apart. Figure 6.17 is a photograph of a
discharge through atmospheric air. The applied voltage was 3500 V
and the discharge current about 80 µA.

We notice that all current peaks have the same height. This
is expected because of the uniform electric field.

6.4.7 Computer simulations

Equations 6.5 and 6.9 form the basis of a computer program
written to calculate the voltage and current for the circuit in
figure 6.10. A listing of the program is shown in appendix II:4.
A brief description of the basic calculation steps in our program
is given below.

The impedance of the circuit, Z, is calculated from

$$Z = R1 + \frac{R2}{(1 + w^2 C2^2 R2^2)^{\frac{1}{2}}}$$

U1 < U$_i$

Below the breakdown voltage, the voltage and current are
calculated from

$$U1 = \frac{U_0}{1 + w^2 Z^2 C1^2} \left\{ \cos wt + wC1Z \sin wt - e^{-t/ZC1} \right\}$$

$$i = \frac{U_0/Z}{1 + w^2 C1^2 Z^2} \left\{ w^2 Z^2 C1^2 \cos wt - wZC1 \sin wt + e^{-t/ZC1} \right\}$$

95

$$Ul = U_i$$

When breakdown occurs the voltage drops to U_e. The voltage is calculated by subtraction of $U_i - U_e$ from Ul. Next time breakdown occurs we subtract $2(U_i - U_e)$ and so on. The current at breakdown is given by

$$i_d = (U_i - U_e)/Z$$

This current will decay with a time constant of 30µs in our measuring circuit. Figure 6.15 shows a simulation of a discharge. The difference in peak heights between the positive and negative period is obtained by assuming different values of the breakdown voltage for the positive and negative cycles. (See figure 2.9.)

U$_1$ (1000V/div)   U$_2$ (10mV/div)

Time (.2 ms/div)
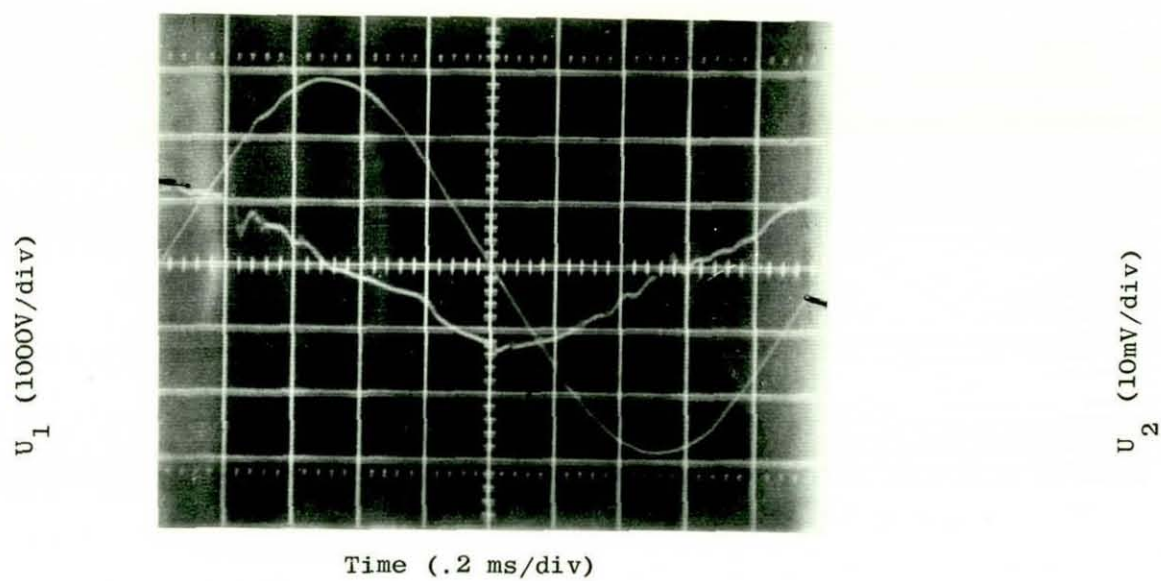
Figure 6.11   Capacitive current

U$_1$ (1000V/div)   U$_2$ (10V/div)

Time (.2ms/div)
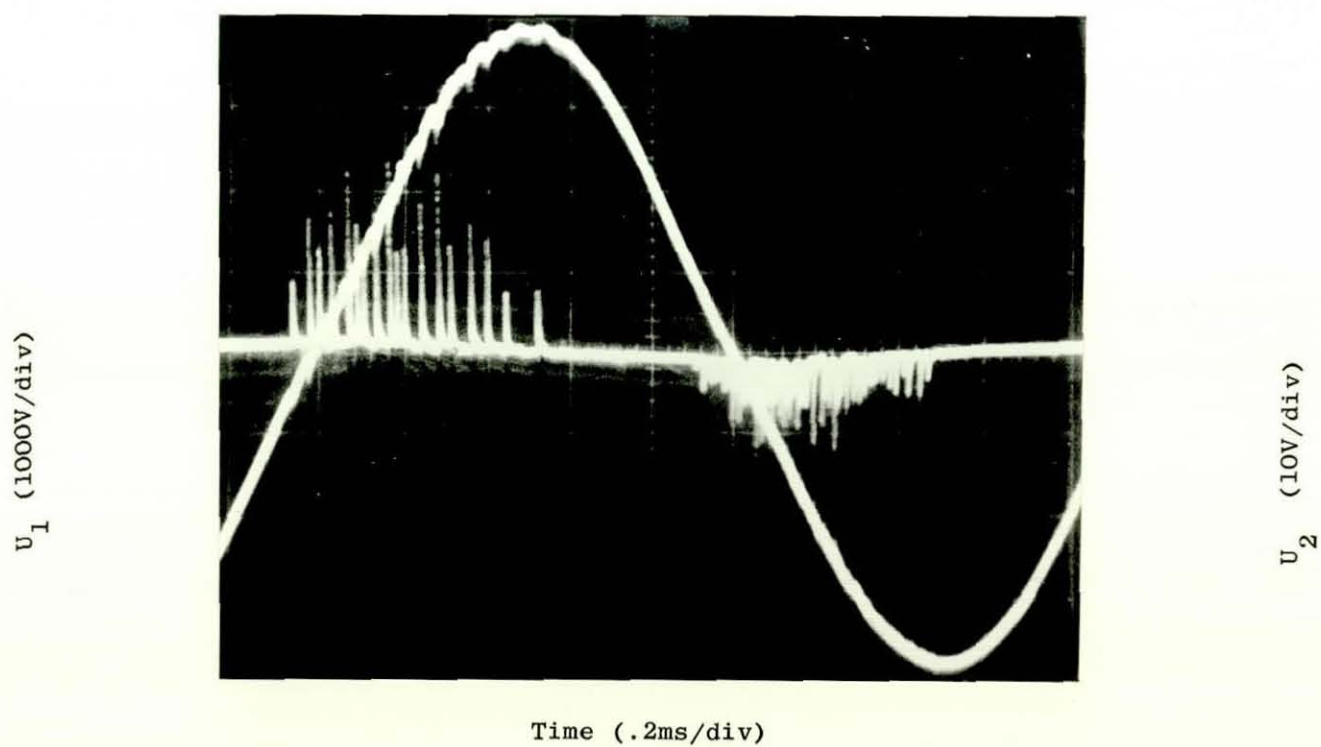
Figure 6.12   Discharge current

97

U₂ (20V/div)
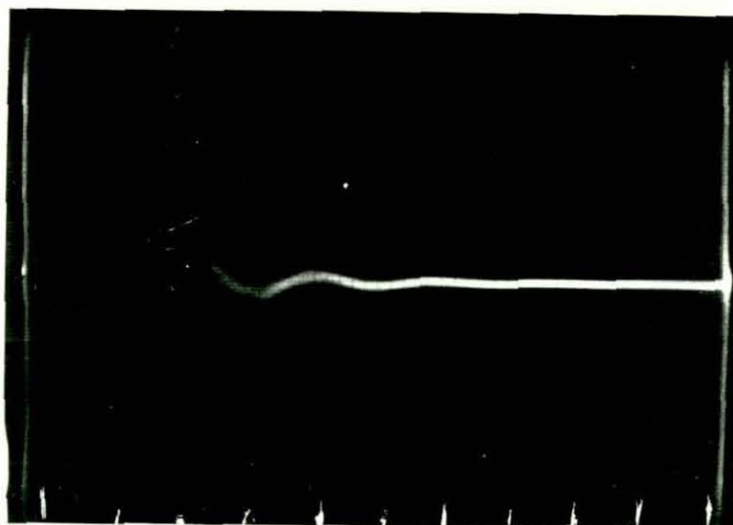
Time (0.2 μs/div)

Figure 6.13   A current pulse

U₁ (200V/div)
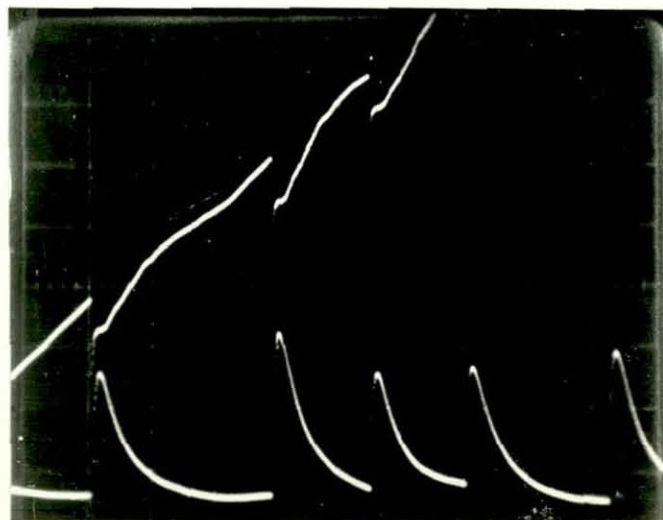
U₂ (10V/div)

Time (100 μs/div)

Figure 6.14   Current pulses

DISCHARGE SIMULATION
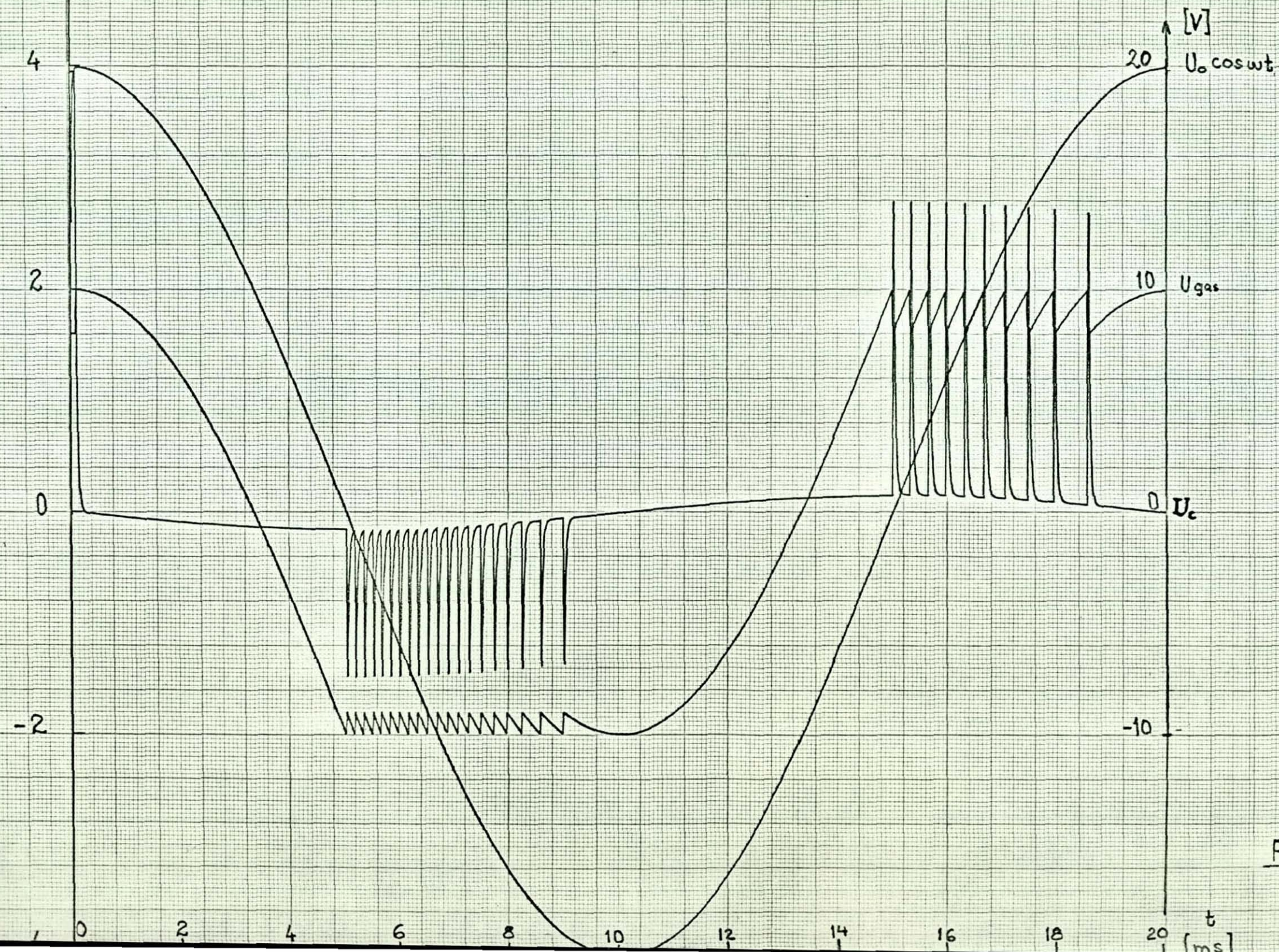
$R1 = 587 k\Omega$

$C1 = 31 pF$

$R2 = 20 k\Omega$

$C2 = 1500 pF$

$U_0 = 4000 V$

$\omega = 314$ rad/sec

$U_i = 2000 V$

$U_e^+ = 1600 V$

$U_e^- = 1800 V$

Figure 6.15.

U$_1$ (200V/div)

U$_2$ (20mV/div)

Time (100 μs/div)
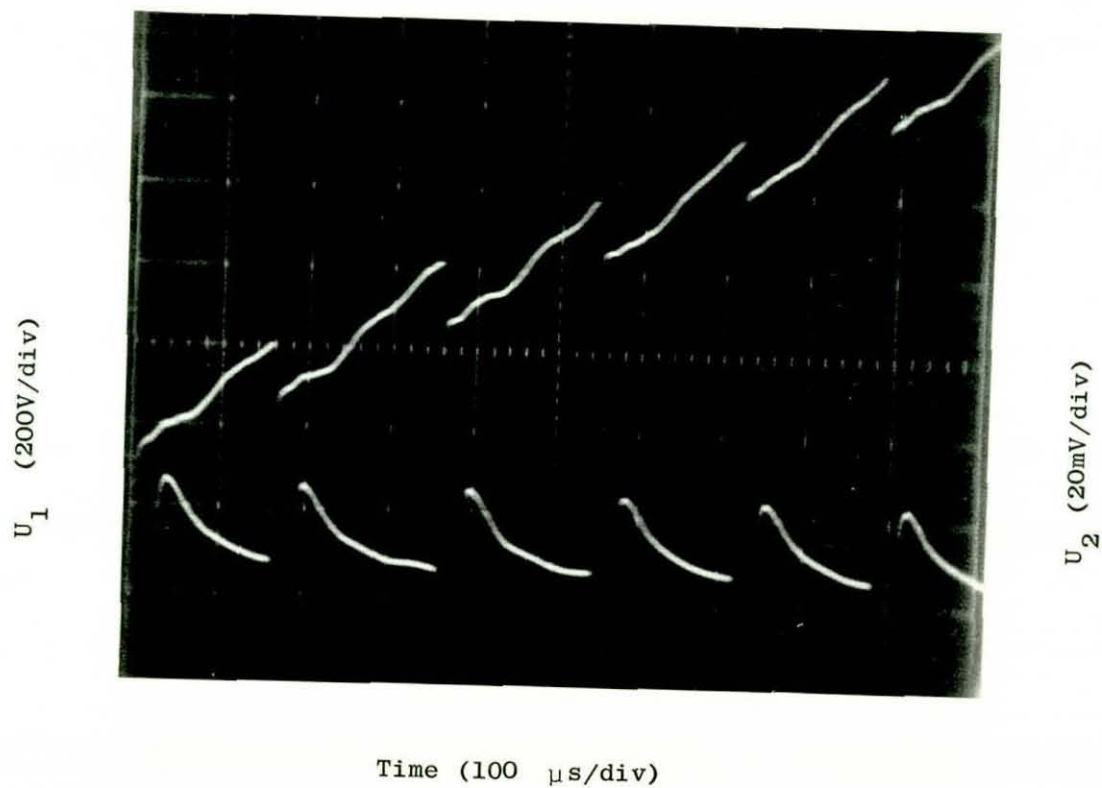
Figure 6.17 Discharge simulation

100

CHAPTER SEVEN

CHAPTER 7

PRODUCT ANALYSIS

One of the simplest and most efficient methods of qualitative

and quantitative analysis is that of gaschromatography.|7|

Chromatography is a physical separation based upon a difference

in distribution between two phases, one of which is stationary and

the other mobile. The gas chromatograph employes a carrier gas

(mobile phase) under pressure to transfer a vapour sample from the

injection port through a stationary phase (column), where separation

takes place, to a detector where the components are recorded as they

come out.

The gas chromatograph used in these experiments was a PYE-104.

The first objective was to find a column that would separate all

components in the sample. We started by trying some polar columns

(Carbowax 20 M, polyethyleneglycol) and some non polar columns

(SE-30, Apiezon L). The most suitable column (giving the most

number of peaks and best separation) was Apiezon L (APL). The

separation is shown in figure 7.1.

For the analysis of the batch reactor experiments we used an

APL column operating at $175^{\circ}C$. A hot wire detector was used with

helium as carrier gas. The quantitative analysis was based on ex-

ternal standards measuring peak heights.

For the analysis of the flow reactor experiments we used the

same APL column operating at $160^{\circ}C$. A flame ionization detector (FID)

was used with nitrogen as carrier gas. The quantitative analysis was

based on internal standards using an electronic integrator to measure

peak areas.
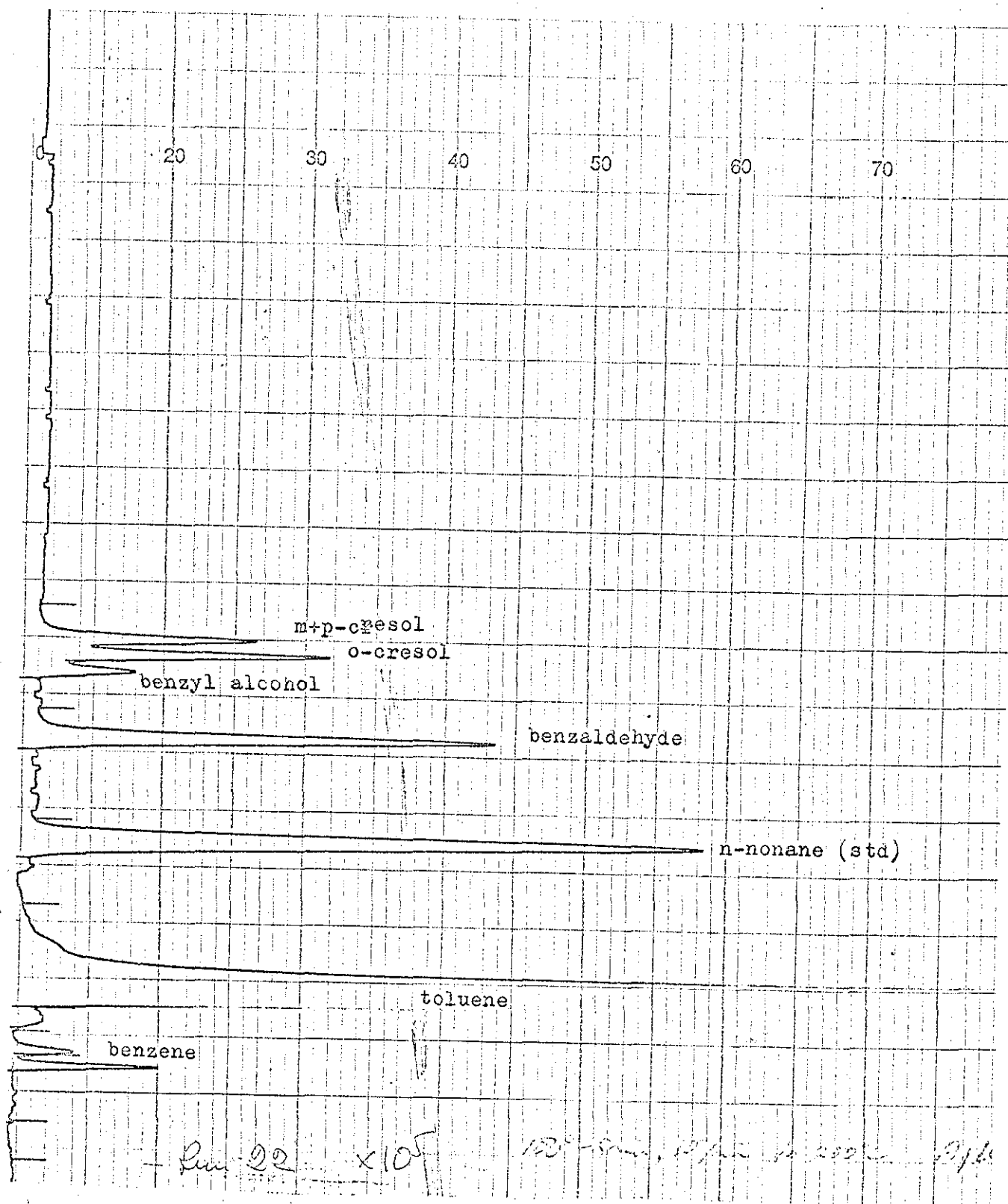
Figure 7.1. Separation on Apiezon L

7.1 QUALITATIVE ANALYSIS

Although it is fairly easy to verify the composition of known or probable mixtures by gas chromatography, it is in itself not sufficient for completely unknown samples. To make a positive identification of the unknown products one must utilize other instrumental or chemical methods like infrared absoprtion (IR), ultraviolet absorption (UV), nuclear magnetic resonance (NMR), mass spectrometry (MS) and solubility properties. The problem with most of these methods is to obtain a fairly pure sample of the component for the analysis.

7.1.1 Gas chromatography

The only parameter available for identification of unknown compounds is the retention time, the time elapsed between injection and appearance of the peak on the recorder. This time is usually called the absolute retention time. It is made up in two parts, the time taken for the carrier gas to flow from the injection point to the detector, and the time taken for the sample to reach the detector, due to its retardation by the stationary phase in the column. The first of these times is called the "dead time", and is a characteristic of the particular instrument and column in use. The difference between the absolute retention time (ART) and the dead time is called the corrected retention time (CRT). It is a characteristic for a given compound at a specific combination of oven temperature, column, liquid phase, carrier gas flow rate, etc. Because of this sensitivity on many parameters, the CRT is difficult to reproduce.

To overcome this difficulty, a concept called relative retention time was introduced. This is the ratio of the corrected retention time of the peak in question to that of some reference peak in the chromatogram. This reference may be present in the sample or it may

be added to the sample.

This freedom of choosing the reference substance causes problems, when we want to find data from the literature. To overcome this problem Kováts introduced a standard set of reference substances for all samples. The set chosen is the normal paraffin s.

The index is defined as

$$I = 100\left\{ n.\frac{\log R_x - \log R_z}{(\log R_{z+n} - \log R_z)} + z \right\}$$

where n is the difference in carbon atoms in the paraffin s

R_z is the corrected retention time of the normal alkane $C_z H_{2z+2}$.

Thus n-hexane has an index of 600, n-heptane 700, etc. The index will depend on the column used and on the column temperature. The advantage with Kováts indices is that data can be transferred. The Kováts indices obtained on Apiezon L at $160^{\circ}C$ for the reaction products is shown in table 7.1.

Compound	Index
Benzene	617
Phenol	1004
Benzaldehyde	1042
Benzyl alcohol	1125
m-Cresol	1171
p-Cresol	1169
o-Cresol	1140
Benzoic acid	1336
p-Benzoequinone	1422

Table 7.1 Kováts indices for the reaction products

7.1.2 Product identification on GC

The identification was made by mixing the suspected component with the sample. An increase of the suspected peak was taken as a proof of identification. Figures 7.2 to 7.9 show the chromatograms recorded from this identification. It was found that two peaks were composite peaks. Thus benzyl alcohol and o-cresol did not separate and similarly m-cresol and p-cresol both had the same retention time. By using temperature programming we were able to resolve benzyl alcohol from o-cresol, but not the meta and para isomers of cresol.

We also made use of the solubility properties of the components.|7| Phenol, cresol and benzoic acid are soluble in a strong base as they are weak acids. The procedure was to shake 5 cc of the sample with 5 cc 2-N NaOH. The water phase and the toluene phase were separated. The water phase was reacidified with HCl and the organic components extracted with ether. Figures 7.10 to 7.13 show the results from these runs. The phenols come out in the right places on the chromatogram, figure 7.13. Benzaldehyde and benzyl alcohol are not soluble in NaOH and are found in the toluene phase, figure 7.12. These runs support the previous results based upon retention times.

7.1.3 Product identification on IR

Because of the low conversion in our experiments, we were not able to prepare samples of the individual components. This made our task much more difficult, since we could not identify the individual IR spectra of the components. To overcome this problem we made up standards of the feed plus the suspected components and compared the IR-spectra of these mixtures with the sample from run number 55. Appendix 4 shows the IR spectra of these standards. Comparing
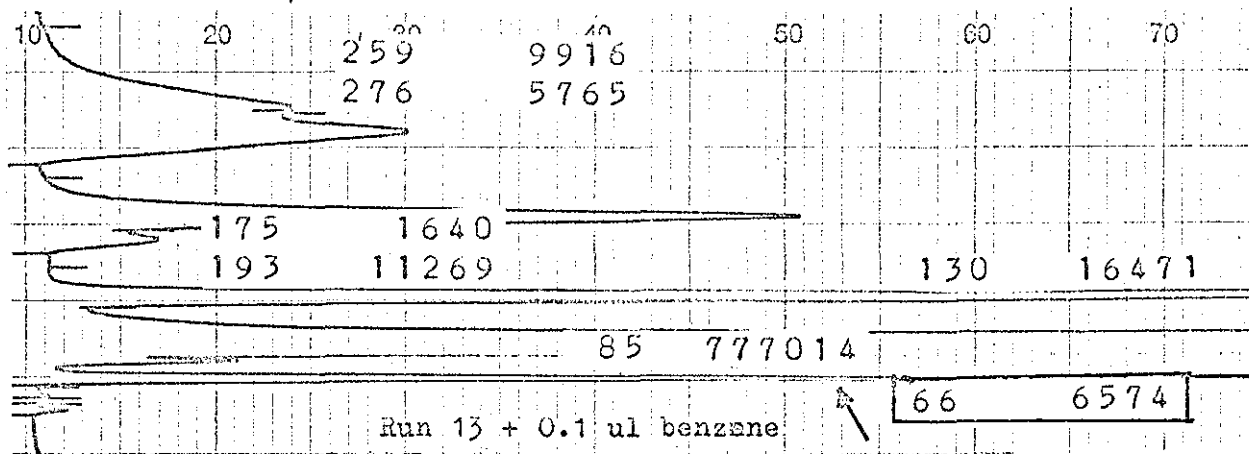
Figure 7.2. Identification of benzene
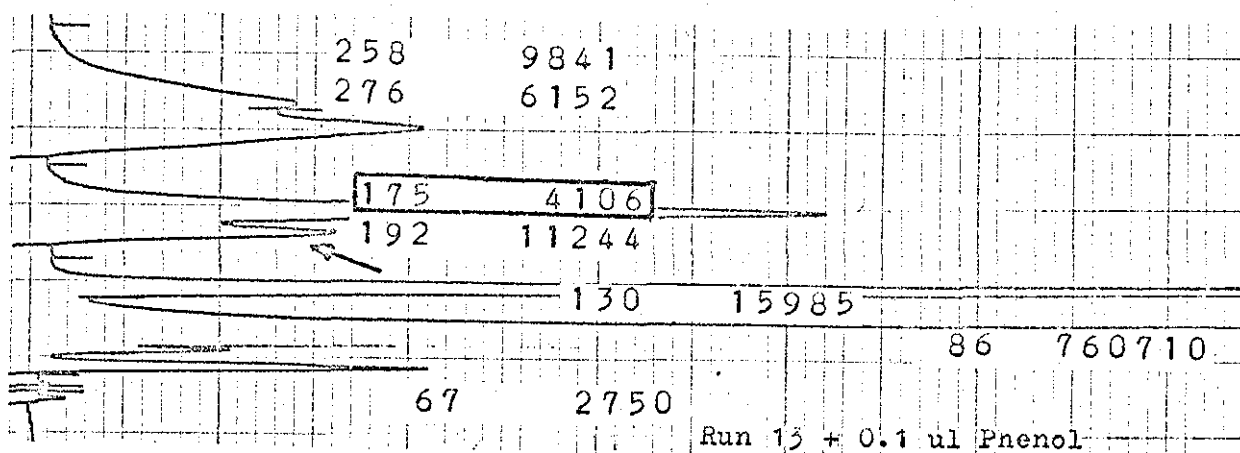
Figure 7.3. Identification of phenol
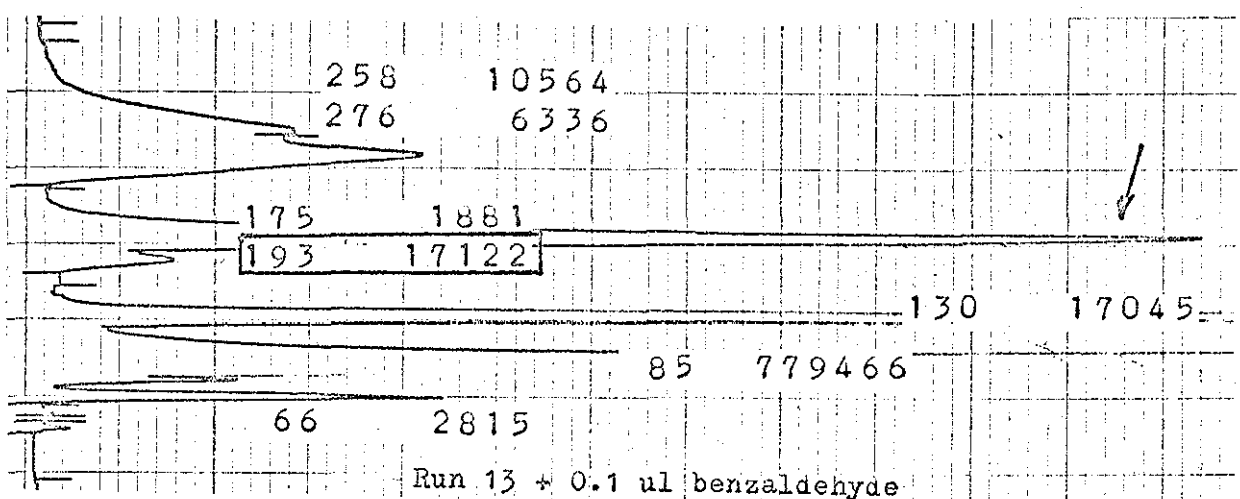
Figure 7.4. Identification of benzaldehyde

256   15110
175   1816
193   10833
130   16565
86   767187
67   2783

Run 13 + 0.1 ul benzyl alcohol
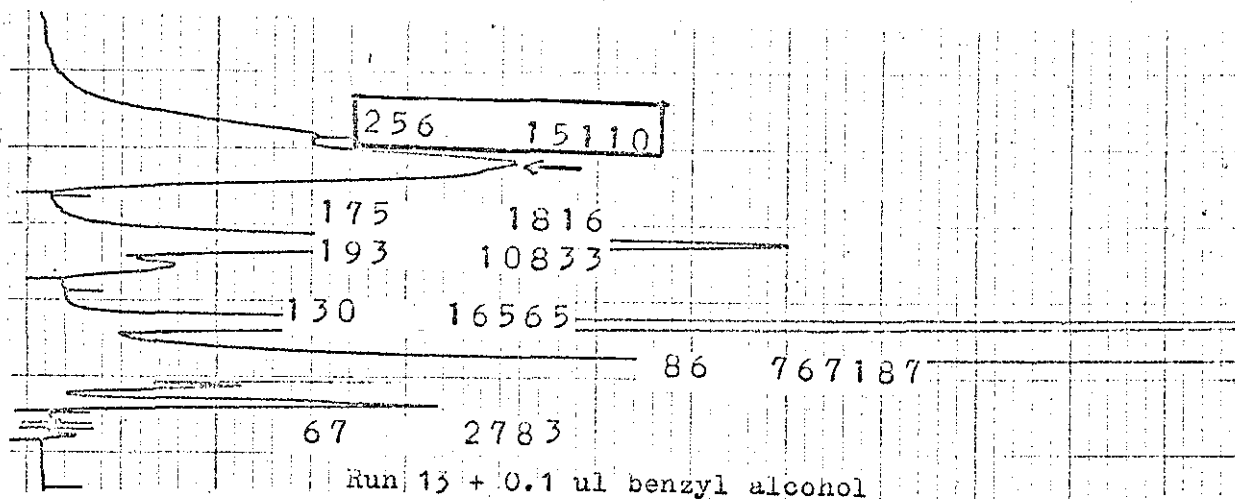
Figure 7.5.   Identification of benzyl alcohol

257   9048
277   11318
174   1729
192   10986
130   16425
86   779512
67   2815

Run 13 + 0.1 ul m-cresol
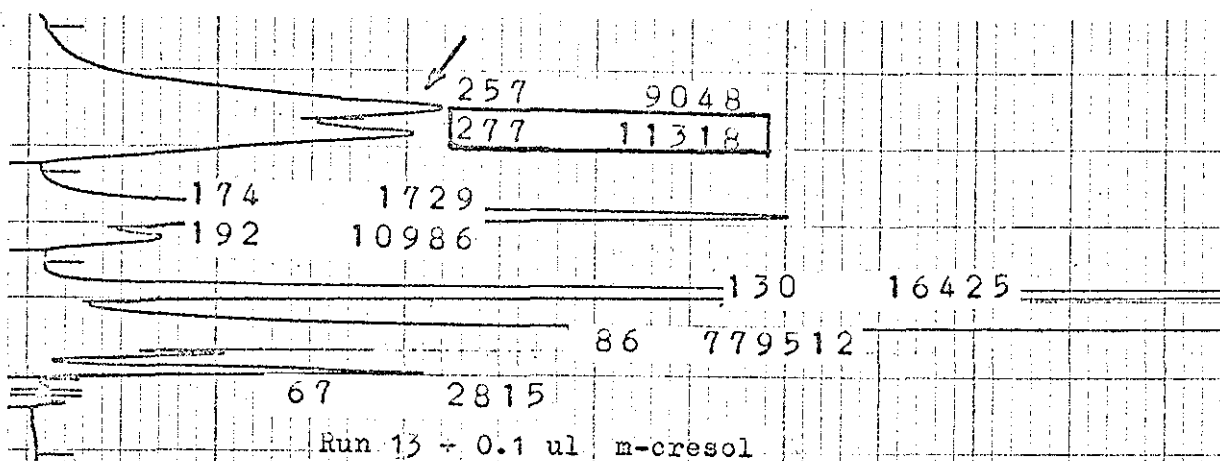
Figure 7.6.   Identification of m-cresol

255   9266
274   7995
191   9762
172   1750
130   16685
85   780317
67   2565

Run 13 + 0.1 ul p- cresol
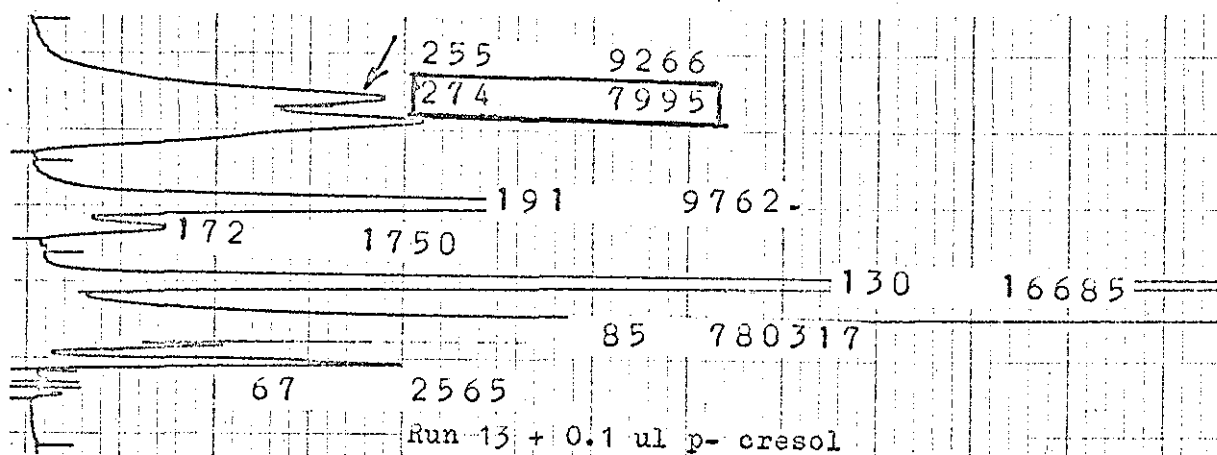
Figure 7.7.   Identification of p-cresol

255   10097
272   6030

172   1784
191   10215

130   14611
86   722334
67   2599

Run 13 + 0.1 ul o-cresol
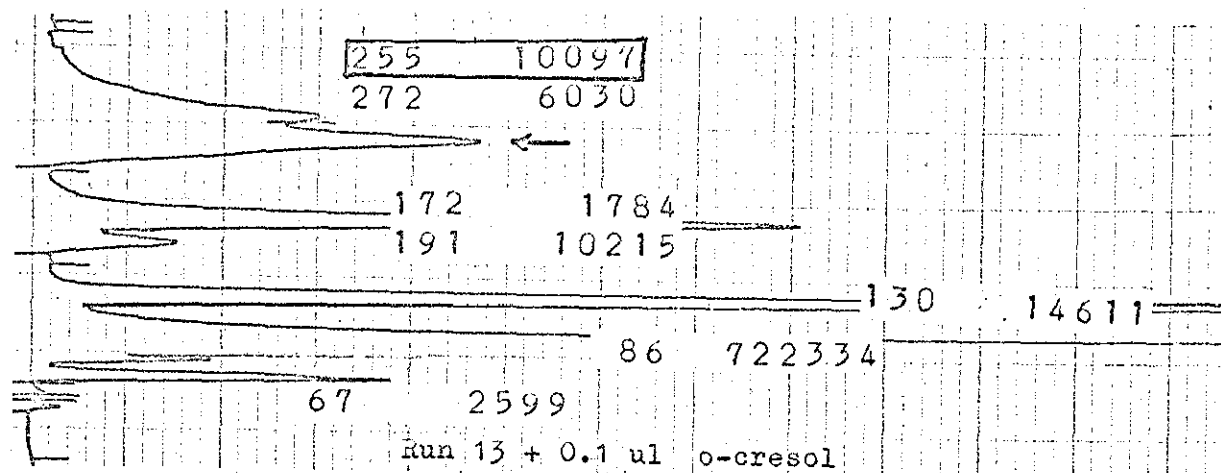
Figure 7.8.   Identification of o-cresol

464   5095

126   16277
83   778301
63   437
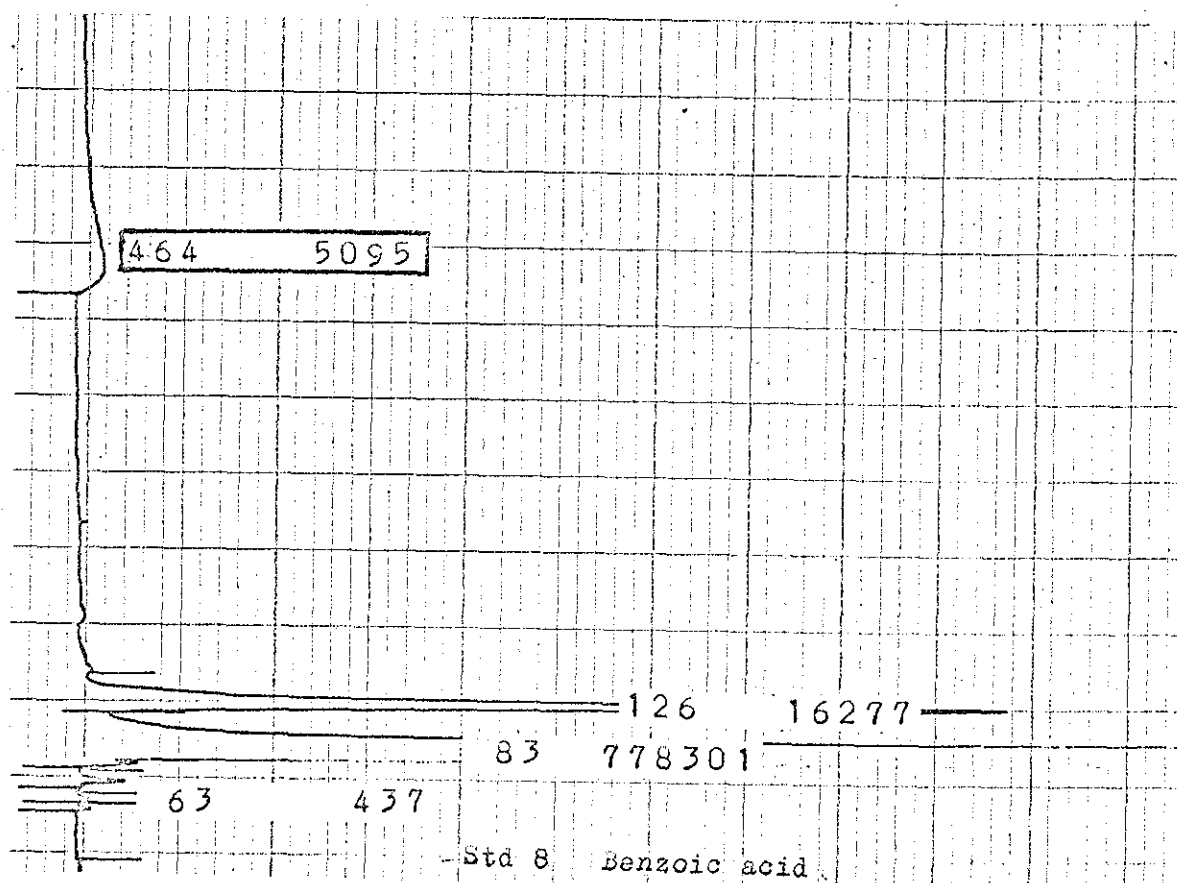
Std 8   Benzoic acid

Figure 7.9.   Identification of benzoic acid
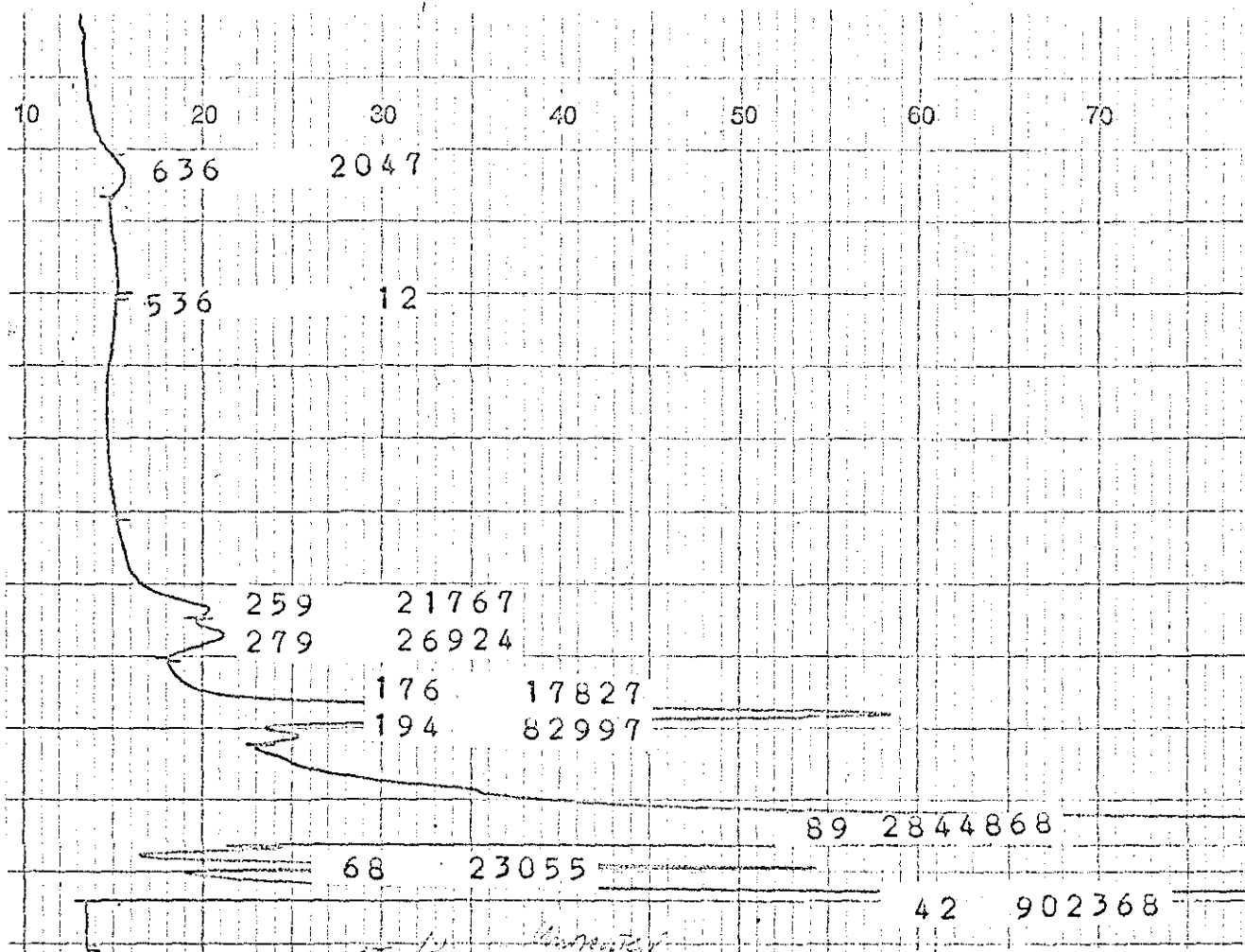
Figure 7.10.   Sample 12 untreated.
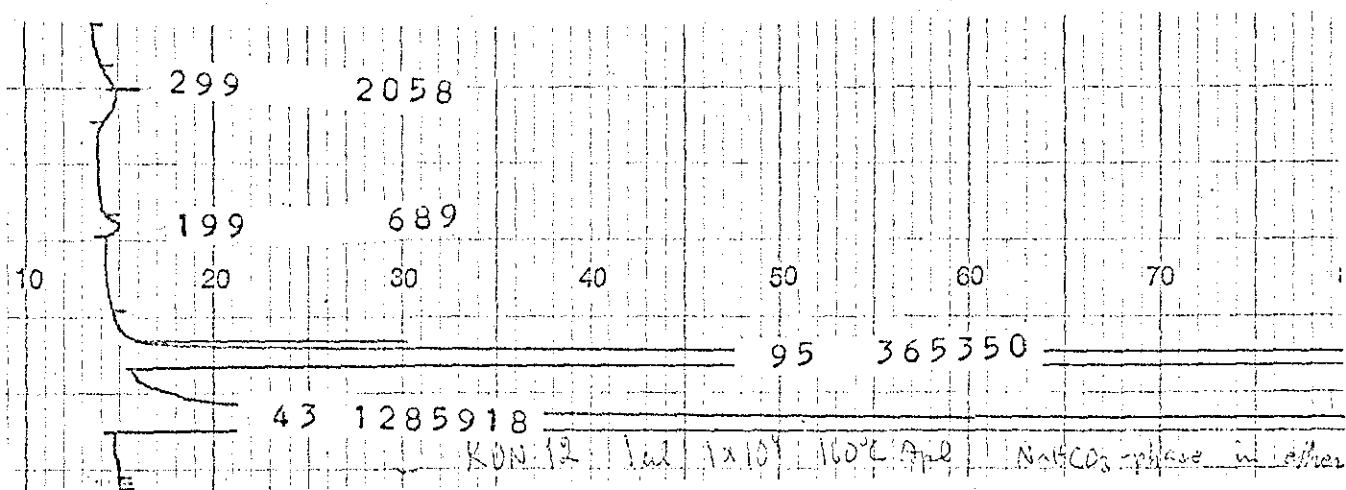
Figure 7.11.   Solubility in saturated NaHCO₃
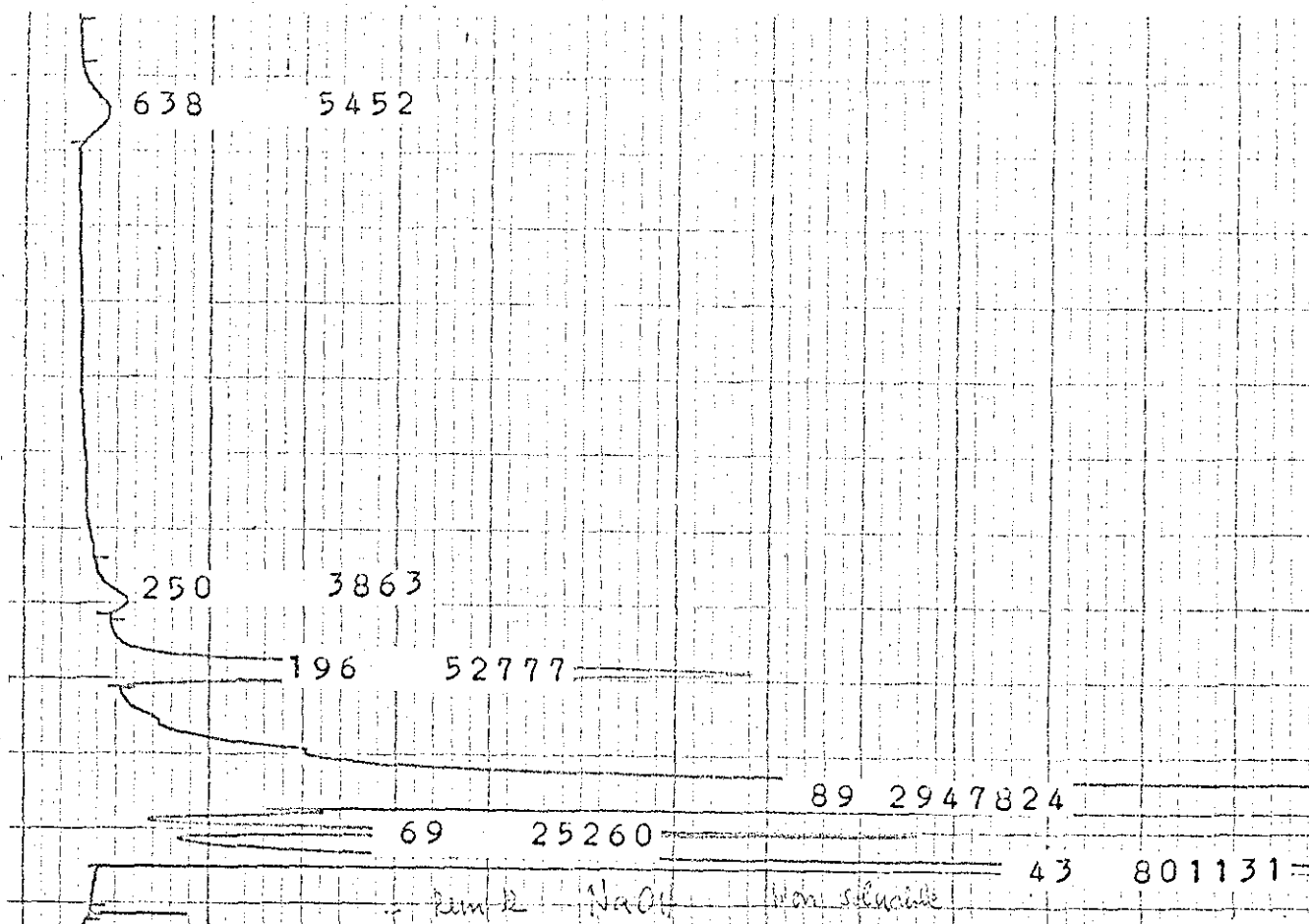
Figure 7.12.   Products not solu ble in 2-N NaOH
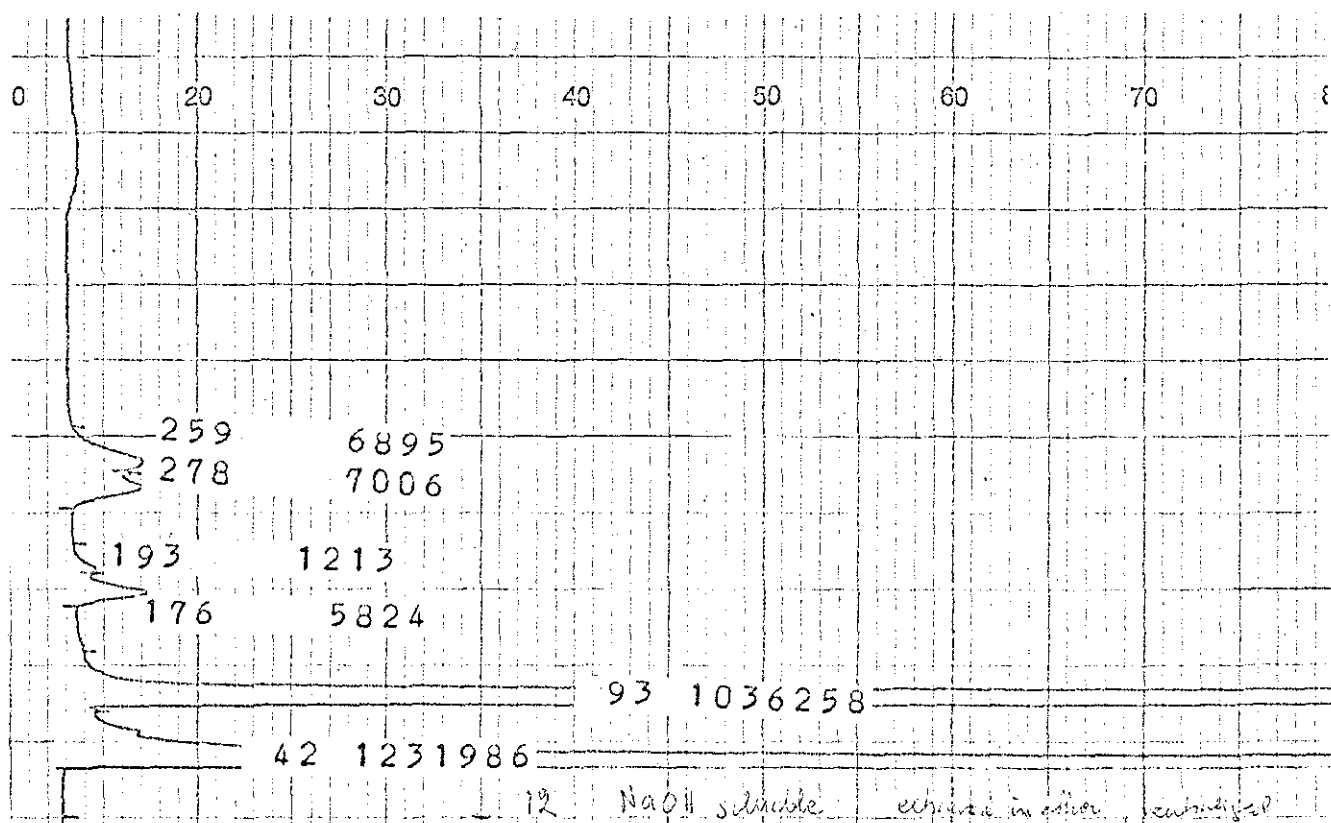
Figure 7.13.   Products solu ble in 2-N NaOH

110

sample 55 with the feed we found new peaks at wavenumbers 3580,
3540, 1710, 1285, 1205 1170 and 830. The standard containing
benzaldehyde (4:3) gave the following peaks: 1710, 1260, 1205, 1170
and 830. We also found that the following peaks had increased in
height: 1740, 1260, 970 and 935. The cresols gave peaks at 1285,
3580 and 3540; so did benzyl alcohol.

At this stage we found that no further information could be
extracted from the graphs, since the pattern of the sample was
matching the prepared standards.

Summarising our results we are confident that benzaldehyde is
present in the sample and smaller amounts of cresol and/or benzyl
alcohol are also present. Benzene may be present but we had no
means of proving that it was.

7.1.4 Product identification of MS

The mass spectrograph is an extremely sensitive instrument for
qualitative analysis. This gave us an opportunity to detect the trace
elements present in our sample. The first run was made by introducing
sample 13 into the mass spectrograph. The results are seen in figure
7.14. The following products were identified, using Massot's
compilation of mass spectral data|10|: phenol, banzaldehyde, cresol
and/or benzyl alcohol, and benzoic acid. Traces were found of
naphtalene (m/e = 128,129), diphenylethane (m/e = 182,183,91), maleic
acid? (m/e = 115), methyl naphtalene? (m/e = 141) and benzyl benzoate?
(m/e = 212,211).

A second run was made using a gaschromatograph/MS interface.
An attempt was made to detect the products as they were separated
on the APL-column. The individual peaks from the gaschromatograph
were not resolved in the MS, but some separation was obtained. The

111

70　　80　　90　　100　　110　　120

68　　77 78　　94　　105 108　　115　　122

(C6H5+)

112

120　　130　　140　　150　　160　　170　　180　　190　　200　　210

122　　128　　152　　165 167　　198
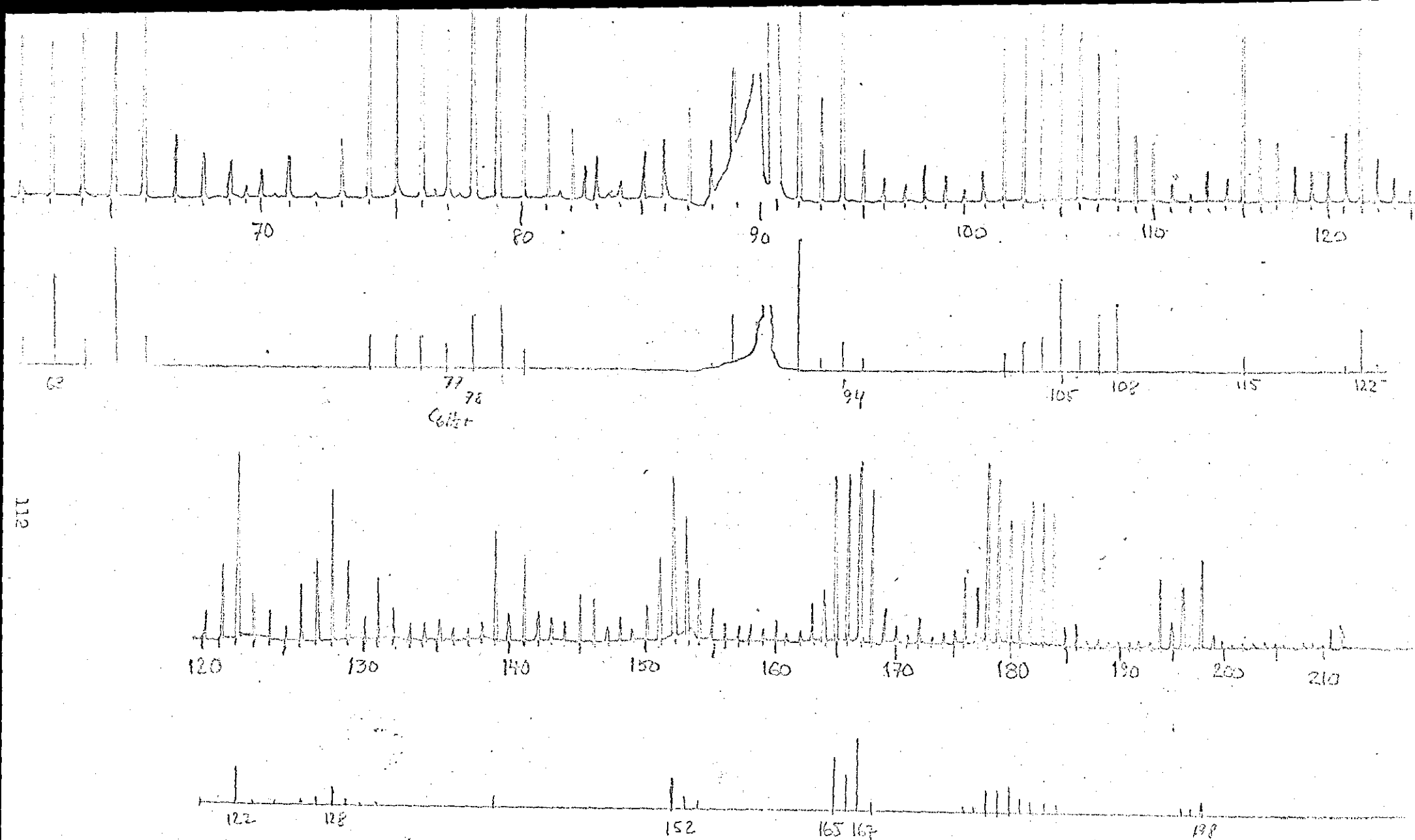
Figure 7.14.　Product identification on MS

second run of sample 13 showed the presence of benzene, phenol, benzaldehyde, cresol and/or benzyl alcohol, and benzoic acid. Traces of naphthalene, methylnaphthalene and citraconic acid? (m/e = 130) were also detected.

We wish to thank Mr Kumar for preparation of the experiments and for analysis of the samples. A special thanks also to Dr. Heaney, Department of Chemistry, Loughborough University of Technology, for allowing us to use the mass spectrometer.

7.2 QUANTITATIVE ANALYSIS

In the previous section we described a number of instrumental methods for qualitative analysis. When we come to quantitative analysis we find that the only method suitable for measuring the concentration is the gaschromatographic analysis.

In this section we give a brief description of the use of external and internal standards.

7.2.1 External standards

One of the methods of quantitative analysis is the method of external standards. The standards are prepared by mixing the substance we are interested in with a solvent to make up solutions of known concentrations. From these standards a calibration curve is prepared, which shows the concentration versus the response of the instrument. By measuring the response of the unknown sample, the concentration may be found from the calibration chart. This method was employed in the analysis of the products from the batch reactor experiments. The response was measured in form of peak heights.

The method of external standard has some drawbacks. For instance, the injected sample size must be exact and the calibration

must frequently be checked, to ensure that no drift has occurred. The last problem is not a great restriction for the hot wire detector, but for the FID detector it is a severe problem.

7.2.2 Internal standards

The internal standard method avoids the problem of having the standard and the sample run at different times, with separate injections. Again, we prepare a calibration mixture containing known amounts of our components plus an added component, which is not present in our sample. From this mixture we can determine the relative response factor. The procedure is as follows. Each area is divided by the concentration of the component. This will give us the response factor. The relative response factor is obtained by dividing the response factor of the components with that of the internal standard. The internal standard used in the flow reactor experiments was n-nonane. The advantage with the internal standard is that the sample of unknowns and the standard are run together in the same injection. Changes in sample size are no longer important. The procedure of evaluating the relative amounts of the components is described below. The first step is to divide the area of each peak with the relative response factors. This compensates for the non-uniformity of the detector. The next step is to divide the corrected area with that of the internal standard. This will give us the relative amounts. To obtain the absolute amounts we multiply each of the relative amounts, previously obtained, by the amount of the internal standard.

7.2.3 Analysis of the gas phase

The gas phase was analysed on a separate PYE-104 gas chromatograph, using a catharometer detector (hot wire detector). The

sample size was 10 cc at system pressure and ambient temperature. Two columns were employed, molecular sieve 5A and silica gel. The first column was used to separate nitrogen, oxygen and carbon monoxide; the second column was used to separate carbon dioxide. The oven temperature for both columns was $50^{\circ}C$ and the carrier gas was helium (30cc/min.). The use of helium increased the sensitivity because of the large difference in thermal conductivity.

The gas sample was taken after the last cold trap, which contained acetone and solid carbon dioxide. The sampling system suffered from air leaks due to the fact that the sampling valves were not designed for vacuum. The mole fraction of nitrogen amounted to 10-40%. It was noticed that the sensitivity for carbon dioxide was not sufficient for our purposes. Only if the conversion was high (above 1%) could we actually detect it.

Attempts were made to increase the sensitivity by collecting the gas in a container and compressing the sample before analysis. Some advantage was gained for compression ratios of 5:1.

No traces of carbon monoxide and methane were found. The relative response factors for the different gases are presented in table 7.2 below.

Gas	Molecular sieve	Silica gel
Oxygen	1.00	1.00
Nitrogen	1.04	1.02
Methane	0.89	0.89
Carbon dioxide	–	1.30

Table 7.2 Relative response factors for some gases

7.2.4 Analysis of the liquid phase

The liquid fraction was analysed on a PYE-104 using an APL column (3ft) and a flame ionization detector. The method of internal standards was employed for the flow reactor experiments while the method of external standards was used in the batch reactor experiments.

A small amount of the n-nonane (internal standard) was diluted with a known amount of the liquid fraction to be analysed. / 1cc of the mixture was injected on the GC with a syringe and the area was measured with an electronic integrator. The following settings of the integrator were used: peak filtering 3 sec., detection level 32 sec., noise filtering normal, base line corrector normal.

Two types of runs were made. The first sample was run isothermally at $160^{\circ}C$ and the second sample with temperature control to measure o-cresol and benzyl alcohol. The following settings were employed. Initial temperature, 5 minutes at $100^{\circ}C$, thereafter a linear increase of $10^{\circ}C$/minute up to $200^{\circ}C$. A printout from an analysis is shown in figure 7.16. The relative response factors for the reaction products are shown in table 7.3. The water content was determined by Karl Fisher titration.[9]

Component	RRF
Benzene	.42
Toluene	.115
Phenol	.47
Nonane	1.00
Benzaldehyde	.48
Benzyl alcohol	.48
o-Cresol	.48
p-Cresol	.48
m-Cresol	.48
Benzoic acid	.45
p-Benzoquinone	1.29
di-Phenyl	1.20

Table 7.3 Relative response factor for the reaction product

CHAPTER EIGHT

EXPERIMENTS IN A FLOW REACTOR

About sixty runs were made with the flow reactor in silica. All runs were made under isothermal conditions with temperatures ranging from 50° to 400°C. The total pressure in the reactor was varied from 100 to 200 mm Hg and the residence time from 0.1 to 15 seconds.

The conversion was kept low so that the initial rates could be obtained from a single run. Not only did this simplify the rate expression (when the product concentration is kept small the reaction can be considered as irreversible), but the assumption of ideal plug flow becomes trivial. A few modifications were made during these experiments. Thus a preheater was introduced in the oven after the first six runs. A new reactor in silica was used after run 29. This reactor had no joints and was sealed into place to avoid air leaks from the joints. At this stage a bubble flow meter was inserted to measure the inlet flow of oxygen.

The only detected compound in the gas product stream apart from oxygen and nitrogen was carbon dioxide.

In the liquid phase we found benzene, phenol, benzyl alcohol, benzaldehyde, cresols, and benzoic acid. Appendix V lists the results of the runs.

8.1 EXPERIMENTAL APPARATUS

The process flowsheet is shown in figure 8.1. Photographs of the system and the flow reactor are included in appendix VI.

Oxygen was fed through a control valve from an oxygen bottle. The inlet pressure of the oxygen was maintained at 400 mm H_2O (1).

From run 29 onwards there was also a bubble flow meter just before the manometer (1). The purpose of this modification was to provide a more accurate measurement of the inlet oxygen flow.

The inlet oxygen flow was dried over silica gel (2) to remove the moisture. The inlet flow rate of oxygen was measured by an orifice meter (3). A calibration curve for the orifice meter is included in appendix VI. The oxygen feed rate was controlled through a precision vacuum valve and the total pressure of the system was measured with a mercury manometer (8). The oxygen was then dispersed in a flask containing toluene (14). The vapour pressure of toluene was determined from the temperature of the water bath (4).

The feed mixture of toluene and oxygen was heated by heating tapes and introduced into a preheater (5), situated in the oven. The mixture of toluene and oxygen was introduced at the top of the reactor (7). The temperature of the outlet product stream was measured with a thermocouple (6). The gaseous product stream was rapidly cooled in an air condenser at first and then by an ice trap. Further cooling was provided in a NaCl/ice trap (9) and finally in a solid carbon dioxide/acetone trap (10).

The outlet flow of the product stream and the pressure was measured with an orifice meter (12) and a vacuum gauge (11), respectively. After the last cold trap with carbon dioxide/acetone samples of the gas stream were taken for analysis on the gaschromatograph. The operating pressure was controlled by a restrictor (13) and an air vent, which was varied to maintain the correct pressure. It was found that a converted gaschromatographic oven (PYE-104) made an ideal oven for our experiments. The temperature profile revealed that deviations within the oven were negligible (about 1° at $300^{\circ}C$). Temperature stability was excellent and amounted to less than 1° over 4 hours.

Variac   E   HT

4

O₂

2

3

8

Water bath(4)   14

Gas chromatograph oven

5   6   7

A-A

A-A

To gas chromatograph

11

To vacuum pump

13

15

9

10

12

Air vent
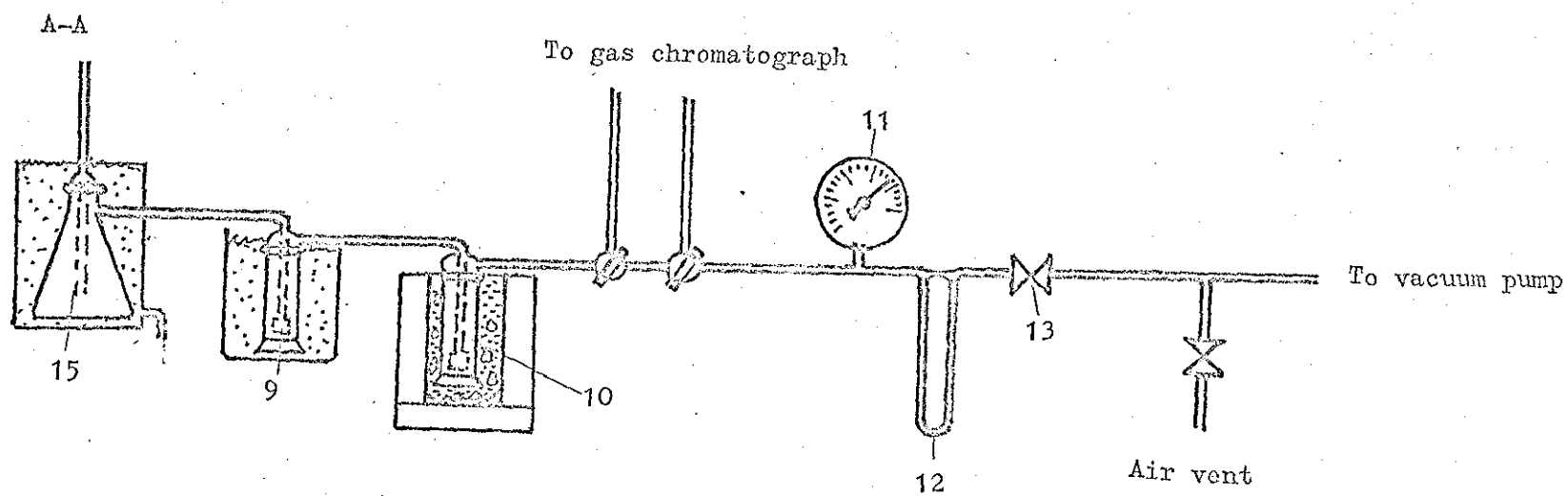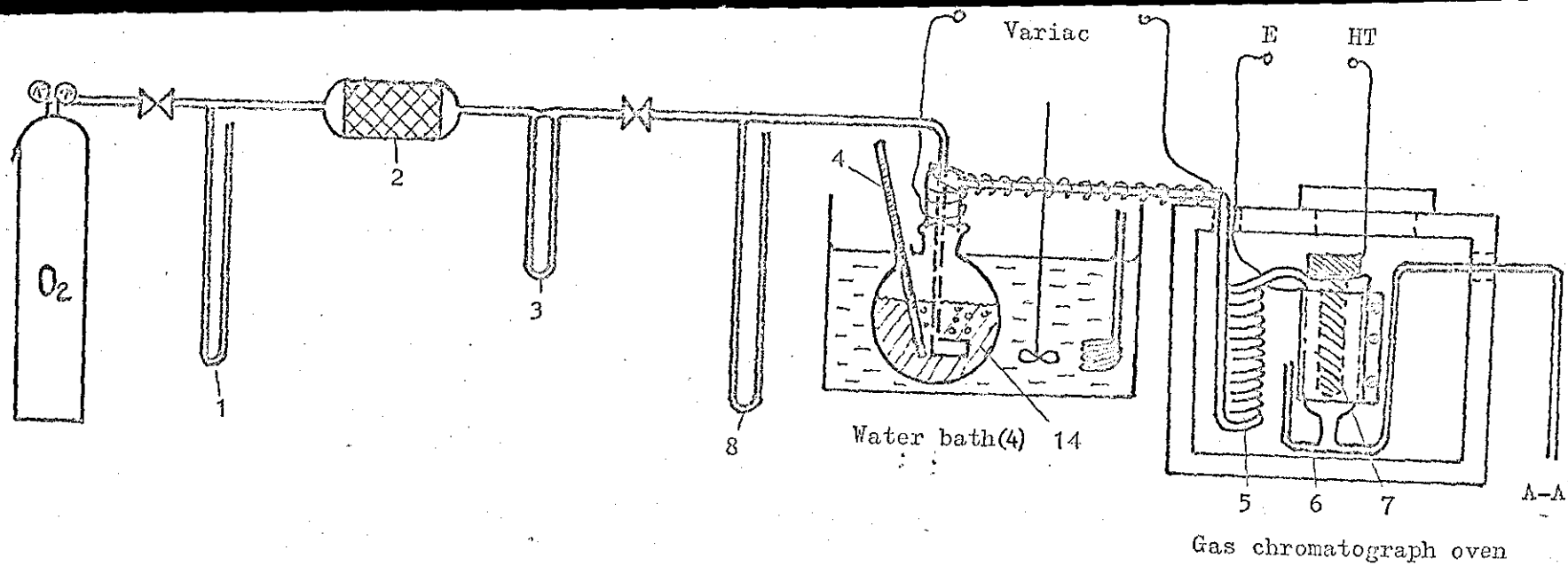
Figure 8.1.   Process flowsheet

It was observed that full saturation was not obtained in runs 1-28 despite efforts to achieve this. The inlet flow meter was suspected and it was decided to insert a redundant bubble flow meter. Figure 8.2 shows a graph of the partial pressure of toluene, calculated from the molar ratio, versus the vapour pressure of toluene, calculated from the bath temperature. It can be seen that full saturation is obtained. The oxygen flow measurements in the first 28 runs are thus biased. The electric circuit for measuring the discharge properties has been described in section 6 and is therefore omitted here.

8.2 EXPERIMENTAL PROCEDURE

8.2.1 Experimental description

The ice cooler (15) and the absorption flasks (9,10) were cleaned and dried and the tare-weight of the flasks determined. The toluene flask was topped up with fresh toluene and weighed. The water bath and the oven temperature were set at the desired temperatures. The coolers were filled with ice and the last absorption flask with solid carbon dioxide/acetone.

When the temperatures had stabilized the vacuum pump was started and with the aid of the air vent the appropriate pressure in the system set. Oxygen was fed to the system at a pressure of 400 mm H_2O controlled by the manometer (1). The vacuum valve was opened and the required flow rate set up.

Every twenty minutes readings of the bath temperature, thermocouple, inlet and outlet flow, and system pressure were taken.

From the oscilloscope we recorded the applied voltage and the instantaneous discharge current. The discharge analyzer gave us the total rectified dc current and the filtered discharge current. Readings of the room temperature and the barometric pressure were taken
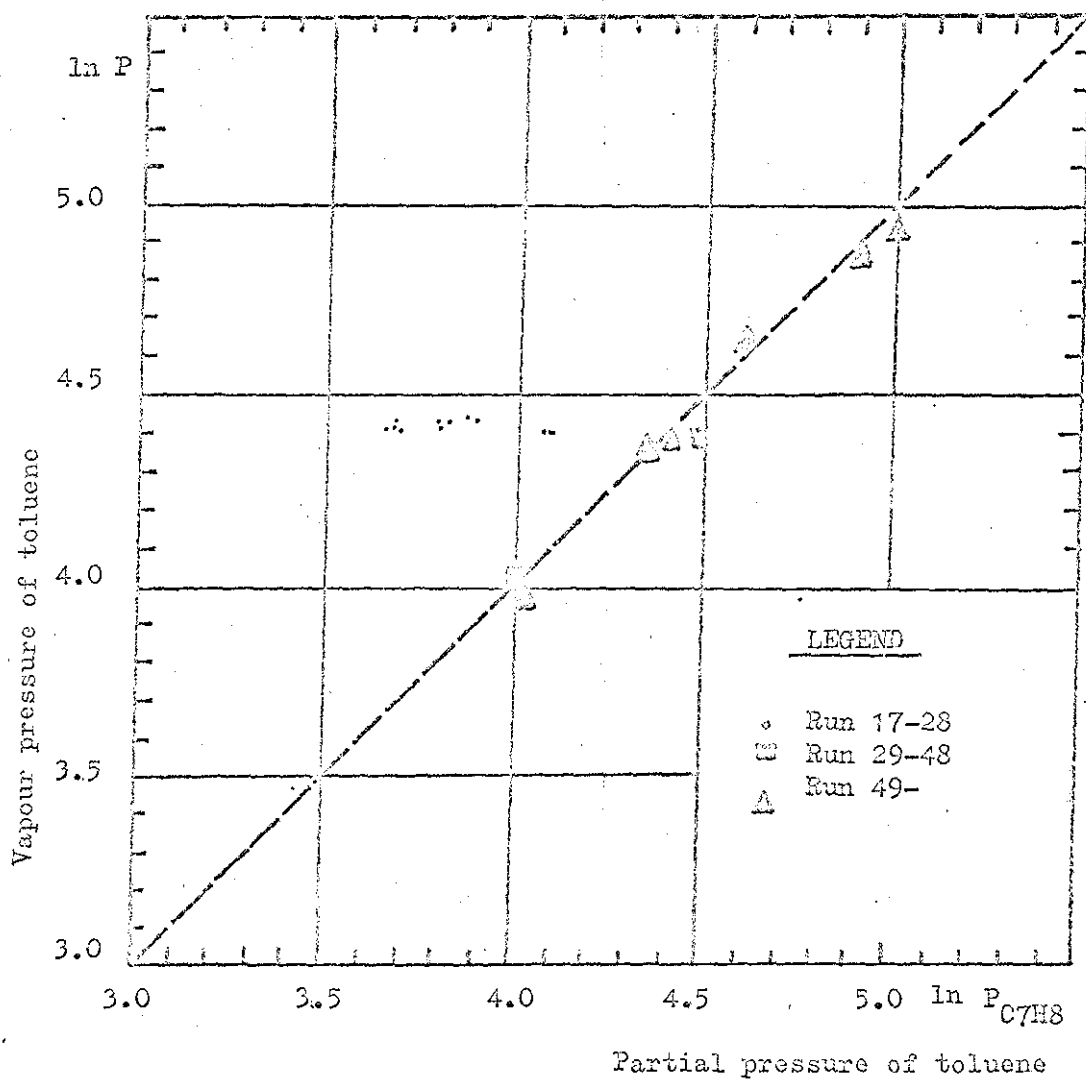
Figure 8.2. Saturation of toluene

at the beginning and end of each run. Gas samples were taken towards the last hour of each run for analysis on the gaschromatograph. These analyses were made "on-line". The details of the analysis have been described previously in section 7.

8.2.2 Calculations of composite variables

The recorded variables were averaged over the total run time. The standard deviation of the measurements were below 2% except for the discharge current and the total rectified current where 5-10% often was observed.

The residence time is calculated from

$$\bar{t} = \frac{P \cdot V \cdot \theta}{R \cdot T_g (N_{O2} + N_{toluene})} \tag{8.1}$$

, where θ is the total run time and V is the reactor volume. This relation expresses the ratio of the reactor volume to that of the total volumetric flow.

The vapour pressure of toluene is calculated from the Antoine equation

$$\log_{10} P_{toluene} = 6.95334 - \frac{1343.9}{218.4 + t} \tag{8.2}$$

, where t is the bath temperature in $^{\circ}C$.

The electric field (E) is given by $E = \frac{V}{r \ln(d_y/d_i)}$.

Assuming a uniform field we have $E = V/d$, where V is the applied voltage and d is the distance between the electrodes.

The error in this assumption is less than 2% and we have therefore adapted the simpler expression of a uniform field. Thus E is given by

$$E = \bar{V}/0.565 \qquad\qquad (8.3a)$$

, where $\bar{V}$ is the root mean square (rms) voltage. $\boxed{\bar{V} = V_{max}/\sqrt{2}}$

The parameter E/N determines the mean kinetic energy of the electrons and is given by

$$E/N = \frac{E \cdot R \cdot T \cdot 760}{p \cdot N} = 1.035 \cdot 10^{-19} \frac{E \cdot T}{p}(V\text{-}cm^{-2}) \qquad (8.3b)$$

, where N is the molecular number density and p is the total pressure in mm Hg.

The instantaneous current is obtained from the photographs. The procedure is to sum up all the peak heights over a second. The method is described in section 6.

The energy dissipation is the product of the rms voltage and the filtered current.

The conversion is obtained from the analysis of the liquid phase. It is assumed that the carbon dioxide found in the gas phase is a result of the oxidation of the side chain and not from breakage of the benzene ring.

The selectivity is obtained from the analysis of the liquid phase, and is expressed as the number of moles produced of the compound per mole of toluene reacted.

The reaction rate finally is obtained from the formula

$$-r_{C_7H_8} = \frac{N_{C_7H_8}(\theta) - N_{C_7H_8}(0)}{\theta \cdot V} \quad mole.l.^{-1}sec.^{-1} \qquad (8.4)$$

This expression is based upon the initial reaction rate and the assumption of ideal plug flow.

123

8.3 EXPERIMENTAL RESULTS

This section describes the correlations obtained between the variables, the disappearance rate of toluene and its dependence on partial pressure of the reactants and the electric field.

The recorded experimental data from the runs is found in appendix V.

Individual reaction rates and other deduced parameters are discussed in section 9.

8.3.1 Mass balance

Unfortunately we found that only three runs showed traces of carbon dioxide. These were all runs at high conversions, about 1% based on toluene. The amount of carbon dioxide in the product gas stream was about 0.2 vol%. The detection limit for carbon dioxide was about 0.05%. The mass balance presented here is only shown for these three samples, which provide a full mass balance. Table 8.1a shows the complete mass balance and a net balance based upon reacted toluene is presented in table 8.1b.

It can be seen in table 8.1b that the carbon dioxide is the result of the oxidation of the side chain to produce benzene and phenol. The hydrogen balance gives further support to this conclusion.

We could not include total oxygen in the net mass balance in table 8.1b. The oxygen consumed in the chemical reaction is only 1% of the inlet oxygen flow. This implies that the flow measurements must be made with an accuracy better than 0.5% in order to obtain a net mass balance for oxygen.

Run number	36		37		55	
	grams	gmoles	grams	gmoles	grams	gmoles
IN						
Toluene charged	10.16	.1102	7.39	.0802	9.97	.1062
Oxygen charged	5.41	.169	2.90	.0908	4.02	.1256
OUT						
Liquid collected	9.77	.1061	6.95	.0754	9.97	.1083
Gas stream	4.50	.141	3.78	.118	5.46	.171
Oxygen	4.49	.141	3.76	.118	5.46	.171
Carbon dioxide	.014	.00032	.018	.00042	.0145	.00033
Liquid phase (Conversion)	0.90%		1.39%		1.10%	
Toluene	9.67	.1049	6.84	.0742	9.84	.1068
Benzene	.016	.00021	.014	.00015	.017	.00022
Phenol	.006	.00006	.008	.00008	.010	.00011
Benzaldehyde	.044	.00041	.050	.00047	.053	.00050
C_7H_8O	.028	.00026	.032	.00030	.031	.00029
Water	.011	.00062	.017	.00095	.018	.00098
Total	9.775	.1064	6.96	0.0803	9.97	0.1089

Table 8.1a   Total mass balance

Run number	36	37	55
IN			
Toluene reacted (mmoles)	1.00	1.11	1.17
Total C in	7.00	7.77	8.19
Total H in	8.00	8.88	9.36
OUT			
Benzene (mmoles)	0.21	0.17	0.22
Phenol	0.06	0.09	0.11
Benzaldehyde	0.42	0.50	0.50
C_7H_8O (cresols + benzyl alcohol)	0.32	0.26	0.30
Carbon dioxide	0.32	0.46	0.33
Water	0.62	0.95	0.98
Total C	6.70	7.76	7.91
Total H	7.94	9.02	9.34

Table 8.1b   Net mass balance

8.3.2 Reaction order

From the kinetic theory it follows that the rate equation is a function of the reactants and reaction products. The form of the rate equation is

$$-r = A \cdot [O_2]^{\gamma} [C_7H_8]^{\delta} \, e^{-\Delta E_a/RT}$$

The exponential term gives the fraction of the molecule whose energy exceeds E_a. Let us substitute RT with E/p, which represents the mean kinetic energy of the electrons as compared with RT, which represents the mean kinetic energy of the molecules and the electrons. This is the case of thermal equilibrium.

The mean kinetic energy of the molecules at room temperature is about 0.04 eV. When breakdown occurs we are in fact approaching the ionization potential of the reactants, about 10-12 eV. This implies that the kinetic energy carried by the molecules can be neglected compared with that carried by the electrons in a cold plasma.

The rate expression is now written as

$$-r = k_0 \cdot p_{O_2}^{\alpha} \, p_{C_7H_8}^{\beta} \, e^{-B/(E/p)} \tag{8.5}$$

If we keep the partial pressure of toluene constant and take the logarithm of 8.5 we obtain

$$\ln(-r) = A + \alpha \ln p_{O_2} - B/(E/p)$$

The first experiments were aimed at finding numerical values of A, α, and B. First we tried to vary one variable at a time. Figure 8.3 shows the correlation of $\ln(-r)$ as a function of p/E. The oxygen
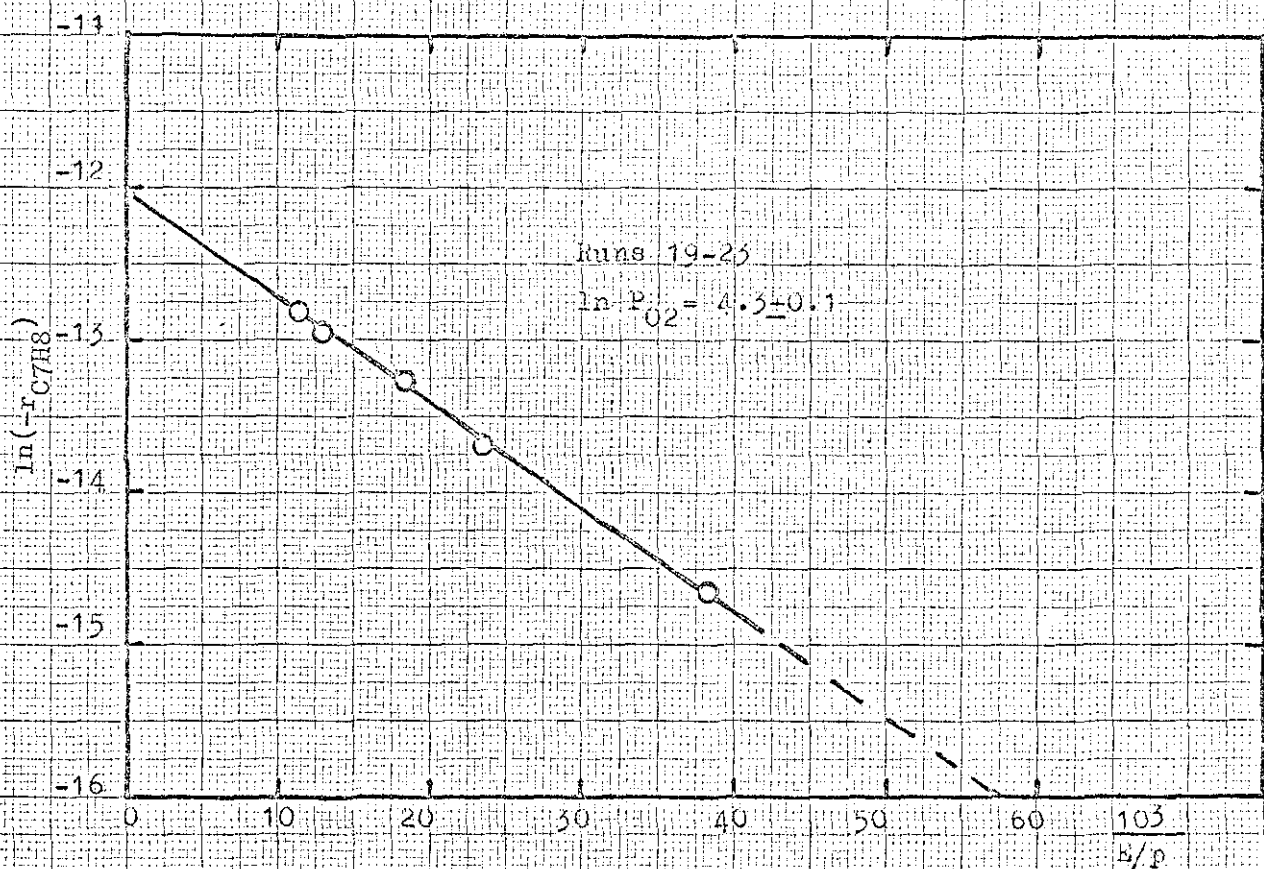
Figure 8.3. Effect of the parameter E/p upon reaction rate.

Runs 19-25

$\ln P_{O_2} = 4.5 \pm 0.1$
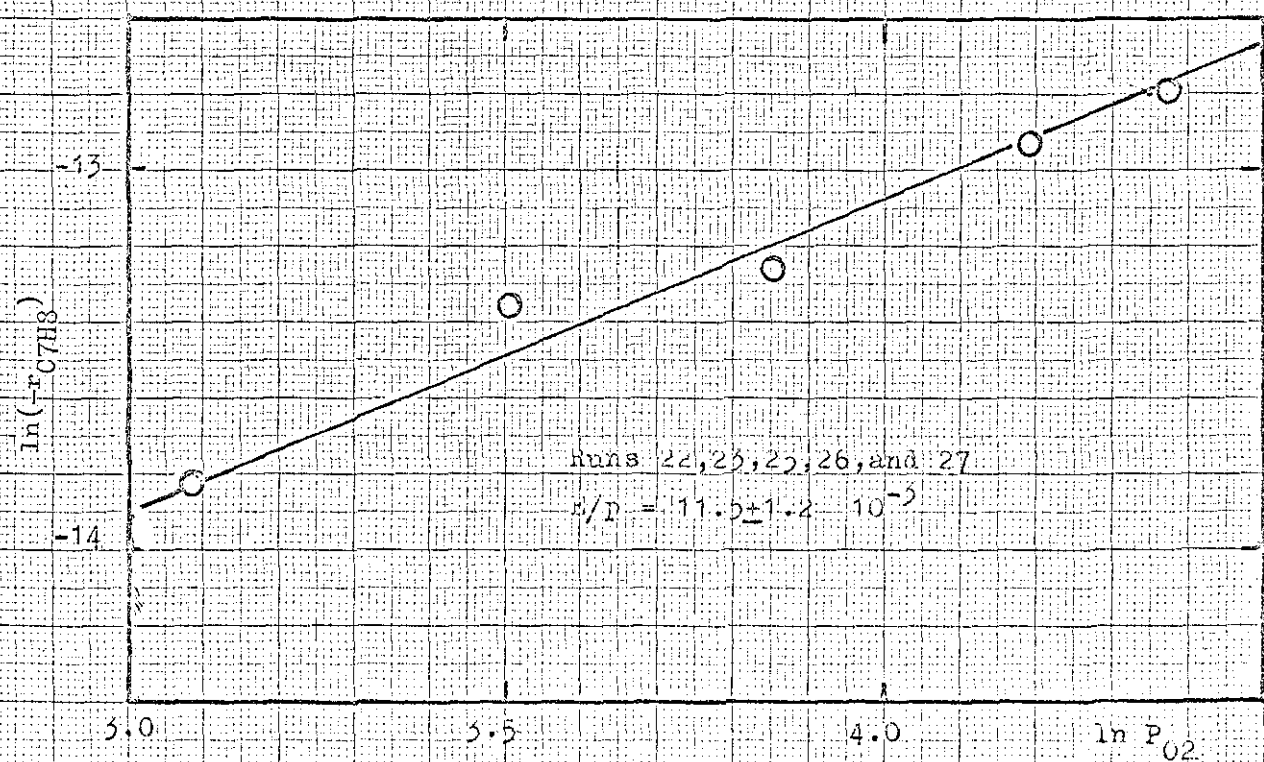
Figure 8.4. Reaction order for oxygen

Runs 22,23,25,26,and 27

$E/p = 11.5 \pm 1.2 \cdot 10^{-3}$

pressure is kept at $\ln p_{O_2} = 4.3 \pm 0.1$. Similarly the toluene

pressure is maintained at 80 mm Hg. We obtain a nice line, which

was expected. The slope found is -69. This is our first approxi-

mate value for B.

To obtain α we kept p/E constant while we varied p_{O_2}. Figure

8.4 shows the correlation obtained. Again we expect a straight line,

which indeed is the case. The slope obtained is about 0.8.

Finally, we tried a least square fit for both variables

simultaneously. The result obtained was

$$\ln(-r) = -16.172 + 0.99 \ln p_{O_2} - \frac{65.86}{E/p}$$

Figure 8.5 shows the goodness of the fit. The data are tabulated in

table 8.2.

Run	$\ln(-r)$	$\ln p_{O_2}$	$1/(E/p)$	$\ln(-r)-\ln p_{O_2}$	$\ln r + 66/(E/p)$
17	-13.42	3.79	0.0134	-17.21	-12.38
18	-13.95	3.92	0.0259	-17.87	-12.24
19	-14.64	4.15	0.0384	-18.79	-12.09
22	-12.94	4.18	0.0128	-17.12	-12.10
24	-12.95	4.30	0.0153	-17.25	-11.94
25	-13.27	3.85	0.0125	-17.12	-12.45
26	-13.34	3.50	0.0111	-16.84	-12.60
27	-13.81	3.08	0.0098	-16.89	-13.16
28	-12.75	4.54	0.0174	-17.29	-11.60

Table 8.2 Rate data for oxygen and p/E

The rate expression can be written more explicitly as

$$(-r) = 9.47 \cdot 10^{-8} \times p_{O_2}^{0.99} \times e^{-66/(E/p)}$$

The rate constant compares favourably with that obtained from

the batch reactor experiments ($9.5 \cdot 10^{-8}$) in a similar analysis.
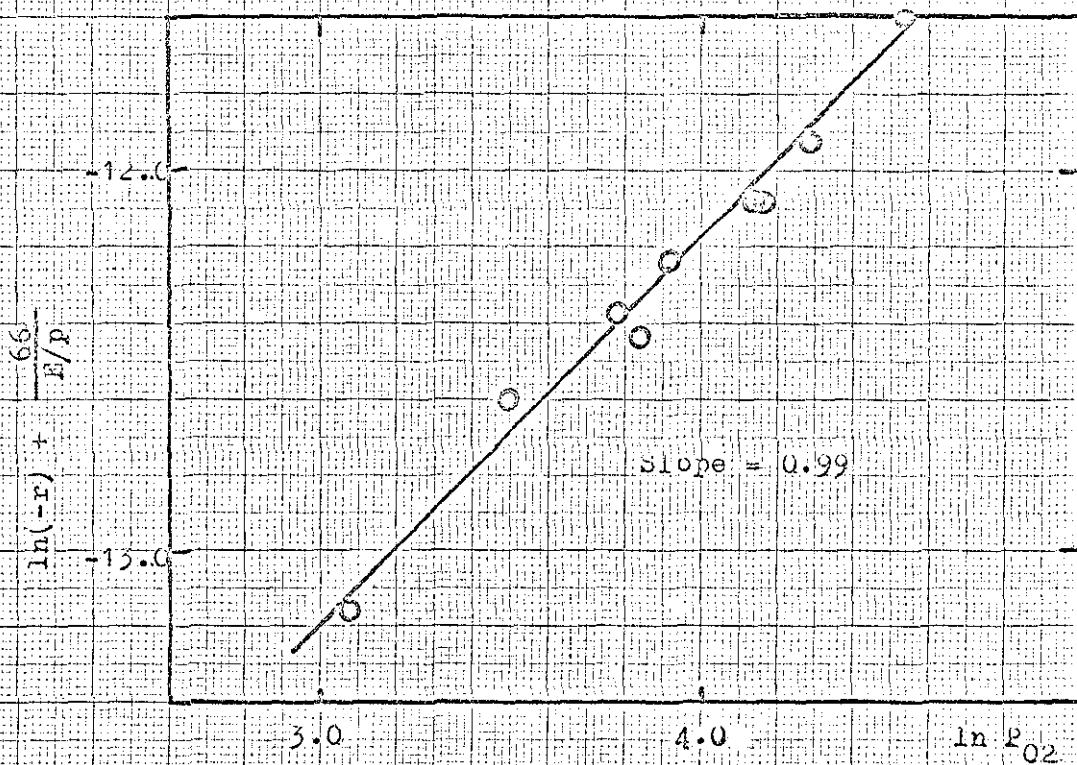
Figure 8.5.a Reaction order of oxygen
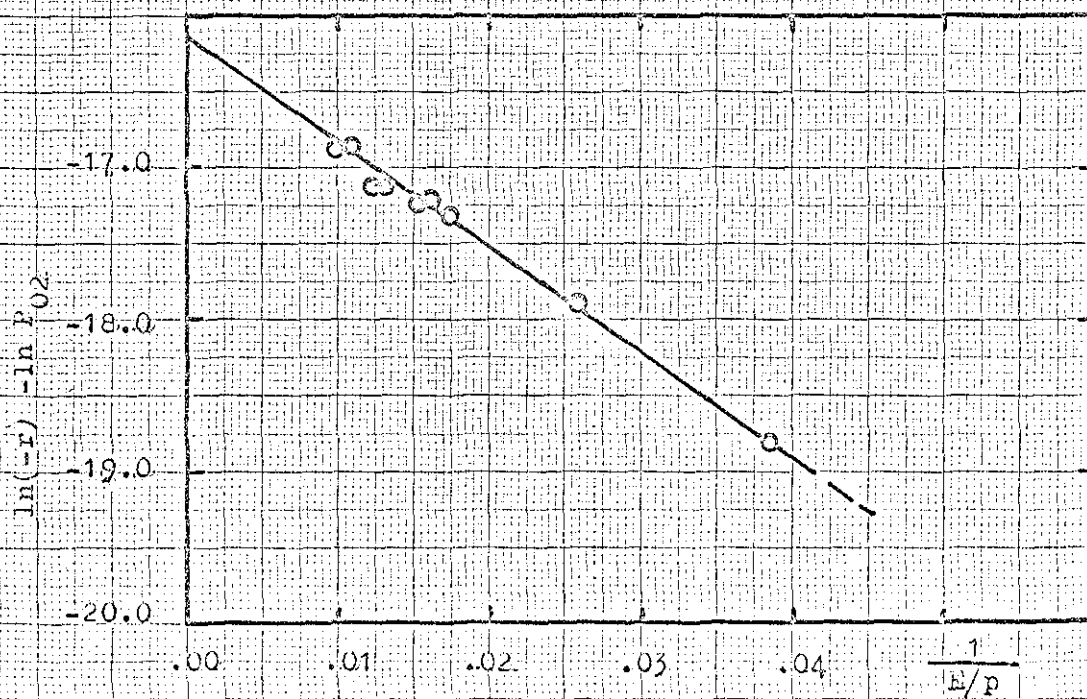
Figure 8.5.b. Effect of the electric field upon reaction rate

Finding the reaction order with respect to toluene is more difficult. Runs 31, 34 and 51 to 54 are the only runs where the partial pressure of toluene was varied. There are a few points which should be mentioned before we present the analysis. The first is that as we extract information from a set of values, we use experimentally measured variables, which have certain errors attached to them. The more variables included, the larger the errors. Secondly, the ratio of oxygen to toluene is important in that it determines the reaction products. This of course is an indication that the reaction paths change. We therefore have to use a good deal of judgement in this analysis. The data used for the analysis have been tabulated in table 8.3, together with conversions and oxygen/toluene ratios.

Run	$\dfrac{p_{O_2}}{p_{C_7H_8}}$	$\ln(-r)$	$\ln p_{C_7H_8}$	$\ln(-r) - \ln p_{O_2} + 66p/E$	Conversion mole%
31	0.8	-12.80	4.38	-16.00	0.33
34	1.3	-12.84	4.02	-16.23	0.41
36	0.8	-12.84	4.32	-16.04	0.90
37	0.8	-12.74	4.38	-15.95	1.39
51	2.1	-13.10	3.93	-16.49	0.43
52	0.5	-12.86	4.65	-15.78	0.19
(53	0.3	-12.71	4.86	-15.16	0.07)
(54	0.1	-11.65	4.93	-13.46	0.04)

Table 8.3   Rate data for toluene

In runs 53 and 54 we have, apart from low accuracy, a different product distribution. Run 54 produces only benzene, and run 53 only 4 mole per cent benzaldehyde and no cresols. These runs have therefore been omitted in the analysis. The correlation thus obtained was

$$\ln(-r) = -19.80 + \ln p_{O_2} + 0.86 \cdot \ln p_{C_7H_8} - 66/(E/p)$$

130

or more explicitly

$$(-r) = 2.5 \cdot 10^{-9} \times p_{O_2}^{0.99} \times p_{C_7H_8} \times e^{-66/(E/p)}$$

However, this relation is more an indication of the reaction order with respect to toluene than a rigorous determination of the order. To make an actual statement of the reaction order for toluene would require substantially more data over different ratios of oxygen/ toluene.

The correlation of the reaction order with respect to toluene is shown in figure 8.6.

8.3.3 Reaction rate

We have already described the variation of reaction rate with partial pressure of the reactants.

In the next set of experiments, with the new silica reactor, we decided to study the influence of temperature upon the reaction rate. Runs 29 and 30 were "blank runs" without a discharge to obtain the thermal reaction rate. The only product found was benzene. The rate was considerably lower than that obtained with the discharge ($\ln(-r) = -16.5$ as compared with -13.0 at $350^{\circ}C$).

Runs 31-50 represent the discharge experiments. The temperature was varied from 50 to $400^{\circ}C$. We did not expect the exponent of p_{O_2} to be different. The collision frequency factor and B were the main interests. Figure 8.7 shows a plot of $\ln(-r) - \ln p_{O_2}$ versus p/E. The kinetic energy is dependent upon the electric field and the mean free path. But the mean free path of the electrons is inversely pro- portional to the molecular number density. Under isothermal condi- tions we may substitute the molecular number density, N, for p.
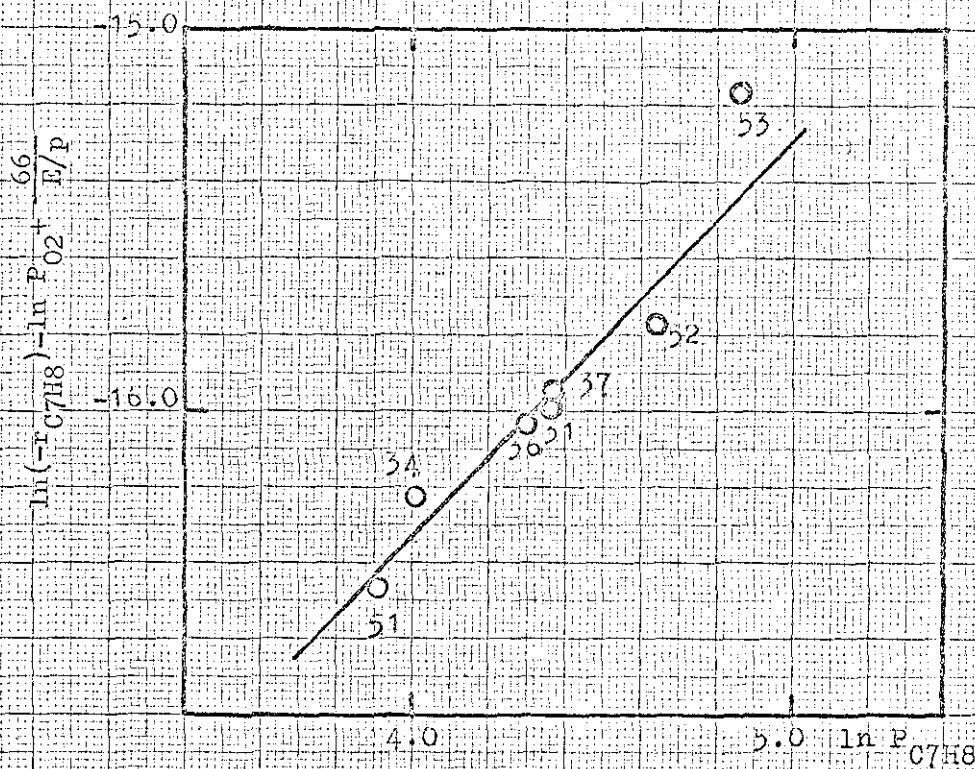
Figure 8.6. Reaction order for toluene
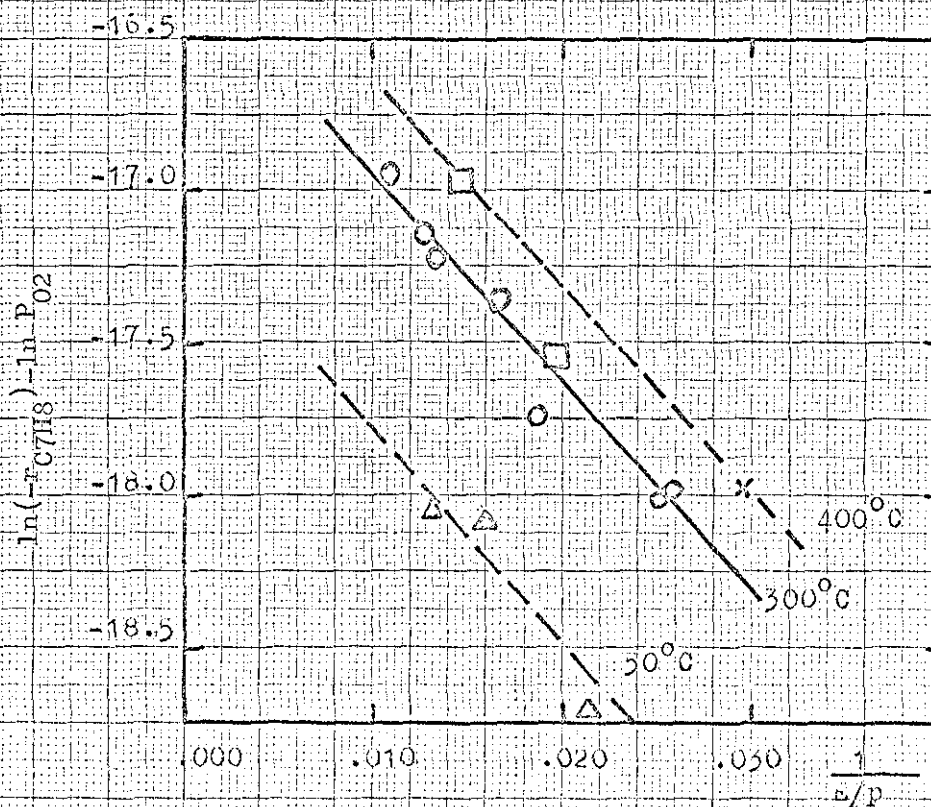
Figure 8.7. Effect of the parameter E/p upon reaction rate.

Therefore we should use N/E instead of p/E, when the temperature is varied. Figure 8.8 shows this plot. The rate expression now becomes

$$(-r) = 1.08 \cdot 10^{-9} \, p_{O_2}^{1.0} \, p_{C_7H_8}^{1.0} \, e^{-3.7 \cdot 10^{-15}/(E/N)} \qquad (8.6)$$

This expression was found to hold well from 50 to 400°C, at oxygen to toluene ratios from 0.5 to 2.0.

Finally we may also correlate a dependent variable, the discharge current, with reaction rate. A linear relationship was found. This agrees with results obtained from other investigators.[45]

8.3.4 Selectivity

Consider the case of two parallel reactions, which are written symbolically

$$A + B \rightarrow X$$

$$A + C \rightarrow Y$$
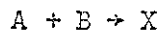
The instantaneous selectivity of X is defined as [11]

$$\phi_X = \frac{d(X)}{d(Y)} = \frac{r_X}{(-r_A)}$$

The total amount of X formed can be expressed as

$$X = \frac{x}{a} \int \phi_X d(A)$$

where a and x are the stoichiometric constants for the reaction.

We have already shown that the rate expression is a function of the partial pressure of oxygen and toluene and the parameter E/p. It can therefore be expected that the selectivity of the products is a function of these variables only. It is not obvious what we should plot on the abscissa. Since we are dealing with reactions of excited

133
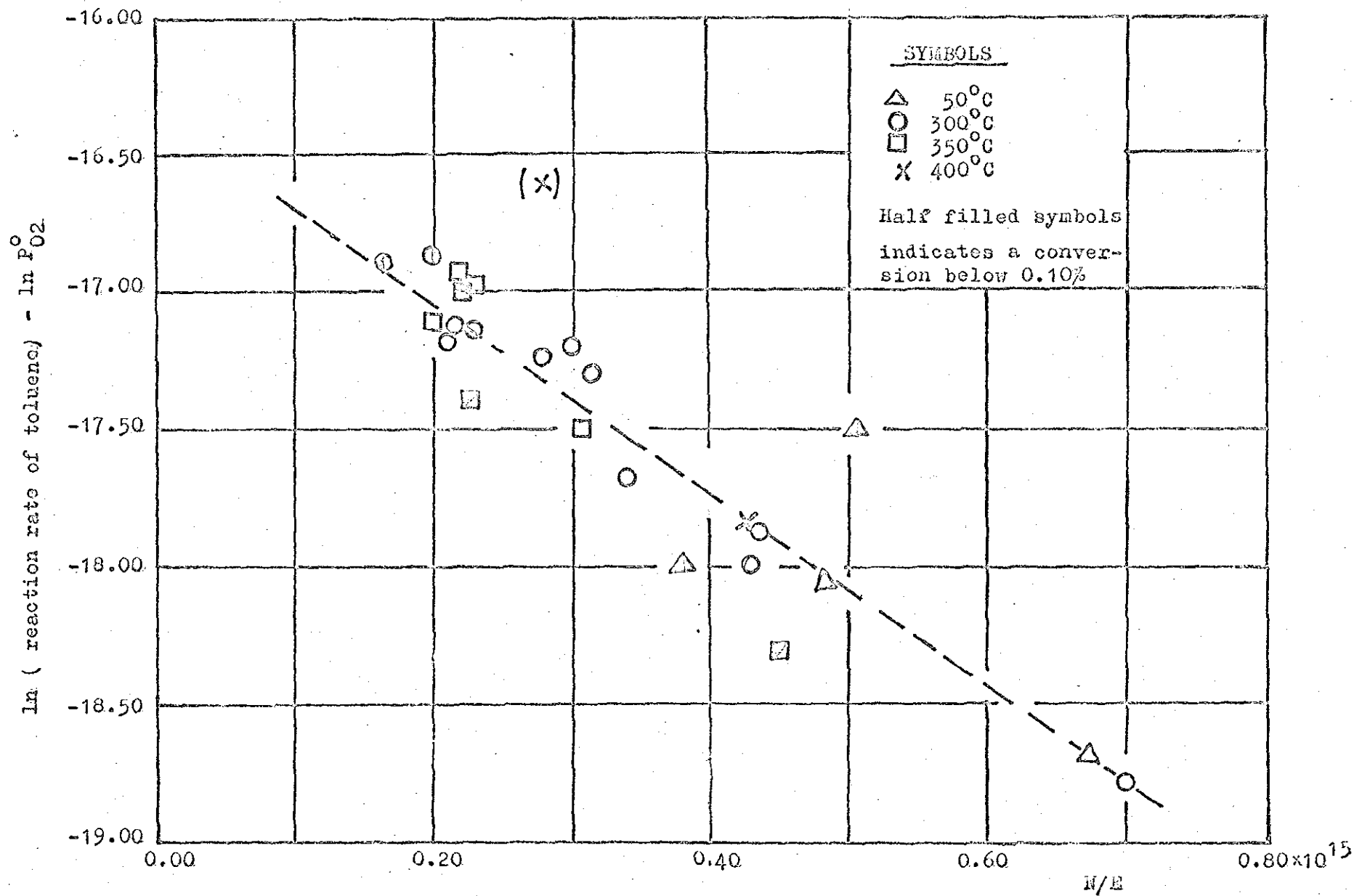
Figure 8.8. Correlation of the parameter E/N vs reaction rate
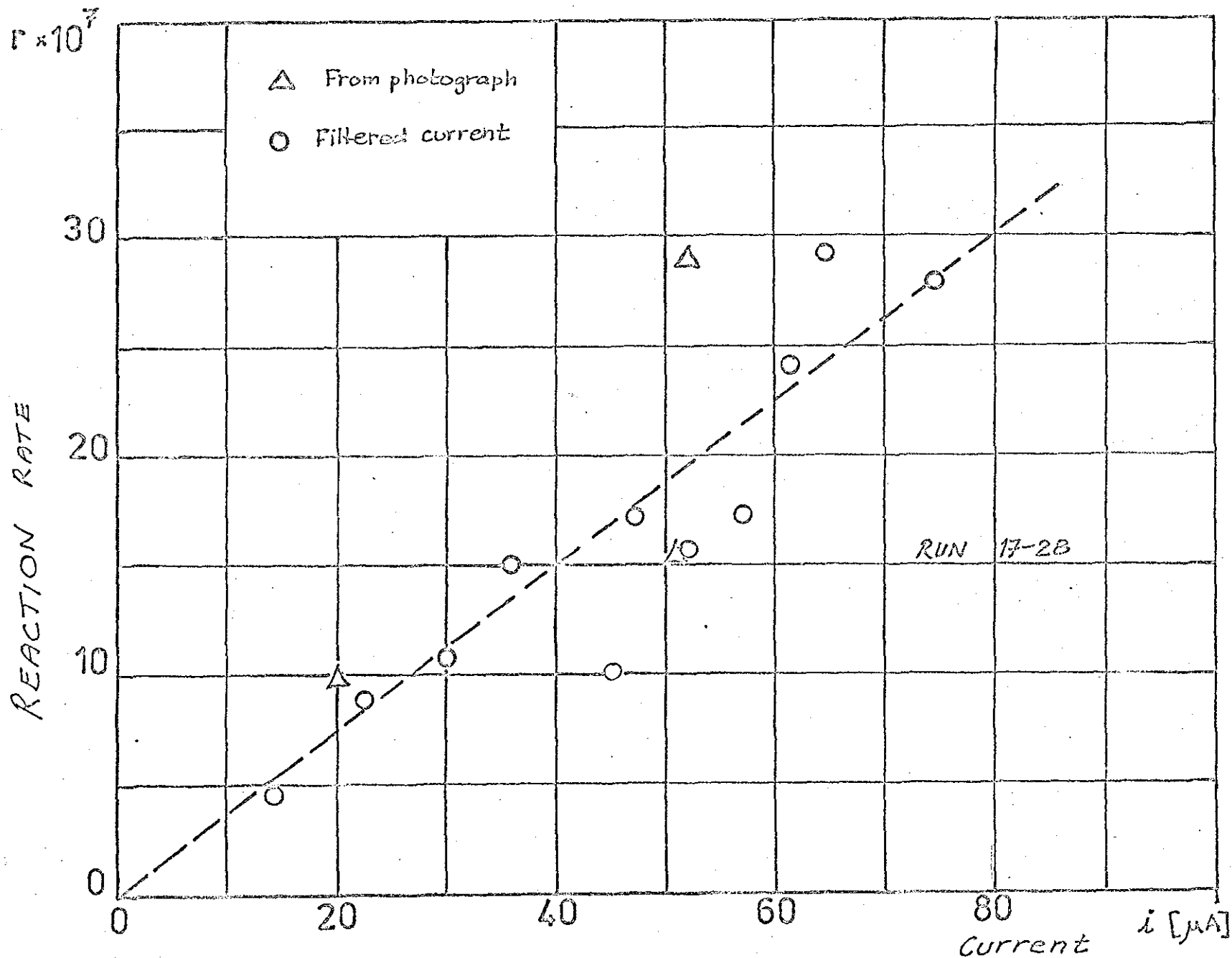
Figure 8.9.   Correlation of discharge current vs reaction rate

species, the ratio of the reactants is important if the excitation energies are about equal. For instance, if toluene is present in large excess, it is more likely that toluene will be excited. This can lead to another type of reaction, which does not involve atomic oxygen. For instance, we may imagine a reaction where excited toluene reacts to give benzene and the CH_2 group reacts with molecular oxygen to produce carbon dioxide and water. We therefore feel that the ratio of oxygen to toluene should be plotted as abscissa rather than the partial pressure of the two components.

The other variable to be plotted against the selectivity of the products is E/p. This group determines the amount of excited species. Figures 8.10 to 18 show these plots.

The selectivity did not show any significant temperature effect. The ratio of the partial pressures of oxygen and toluene had the largest influence upon the selectivity, whereas the effect of E/p was most noticeable for the cresols.

8.3.5 Energy requirement

The energy requirement was defined as the energy consumed per mole of reacted substance. The influence of the parameter E/p upon the energy requirement is shown in figure 8.19. The energy requirement is obtained as the product discharge current and rms voltage divided by the number of moles of toluene reacted. Figure 8.20 shows the effect of the oxygen to toluene ratio. To study the effect of temperature upon energy yield, we must exclude the effect of E/p.

Table 8.4 lists the average energy requirements at different temperatures. A plot of the energy yield against temperature is shown in figure 8.21.
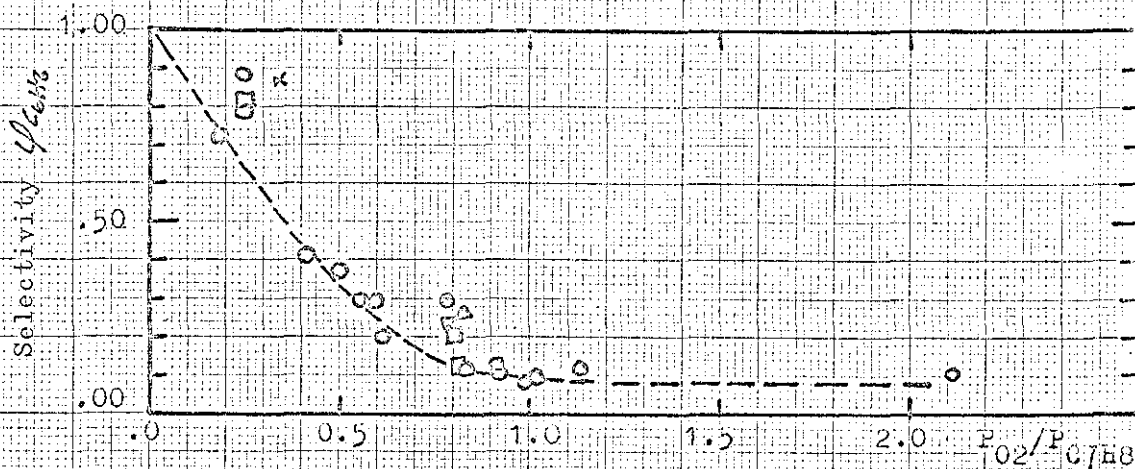
Figure 8.10.   Selectivity for benzene
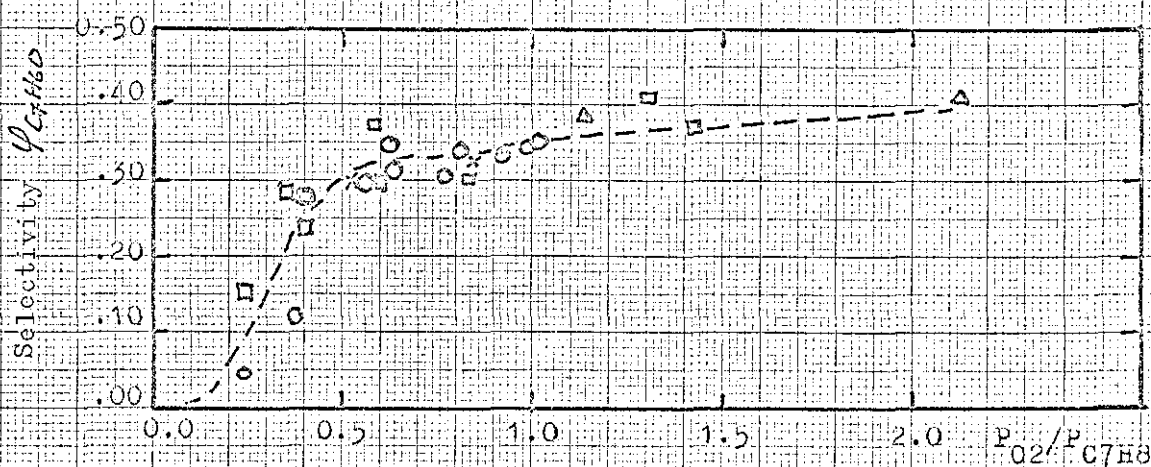
Figure 8.11.   Selectivity for benzaldehyde
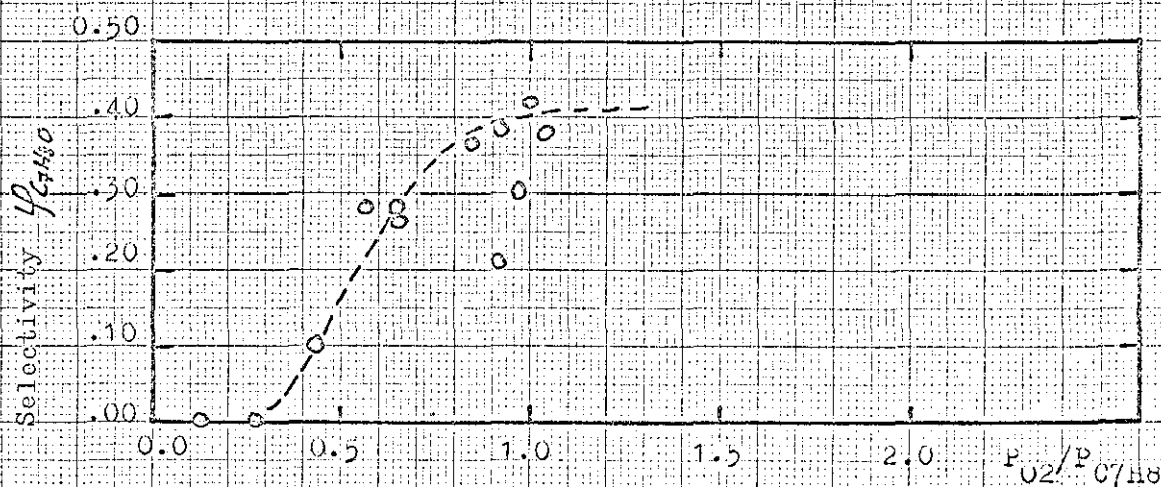
Figure 8.12.   Selectivity for cresol
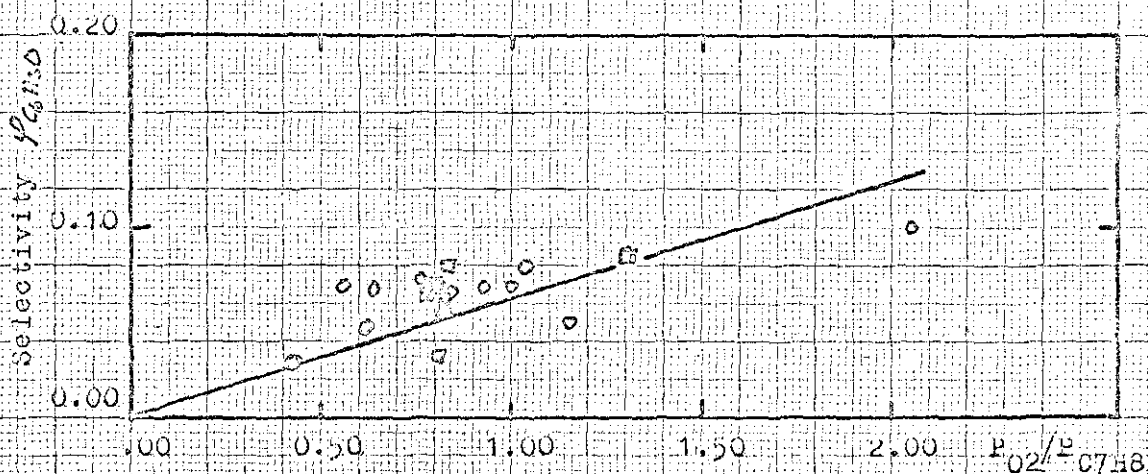
Figure 8.13. Selectivity of phenol
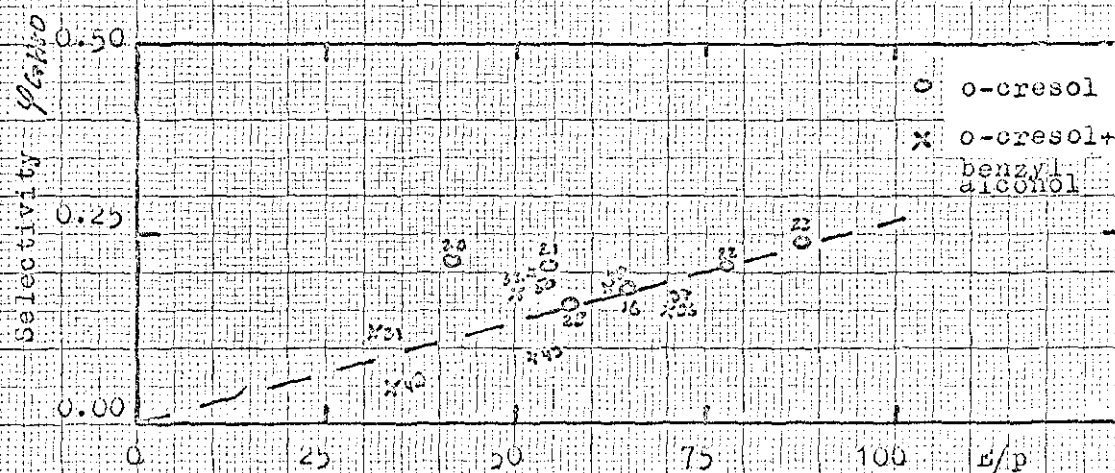
Figure 8.14. Effect of electric field upon selectivity
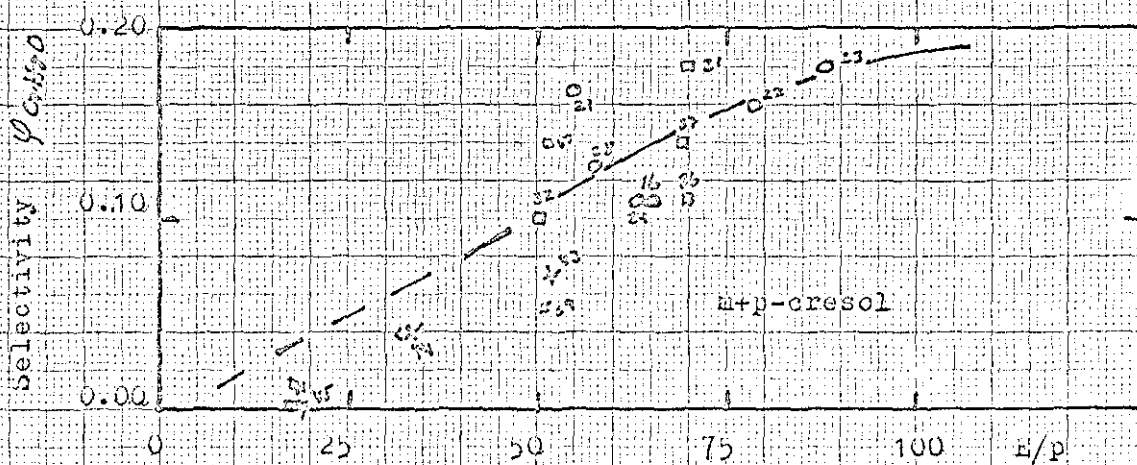
figure 8.15. Effect of electric field upon selectivity
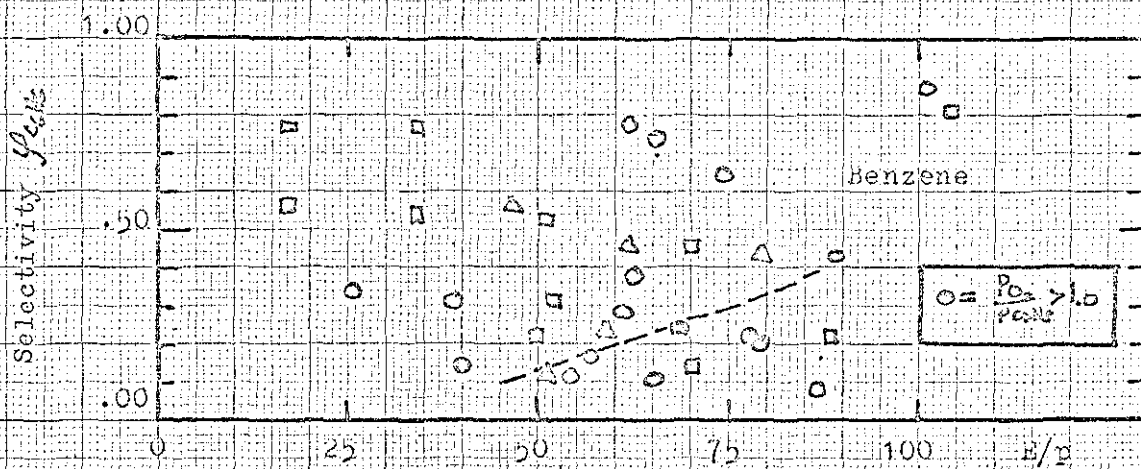
Figure 8.16. Effect of E/p upon selectivity
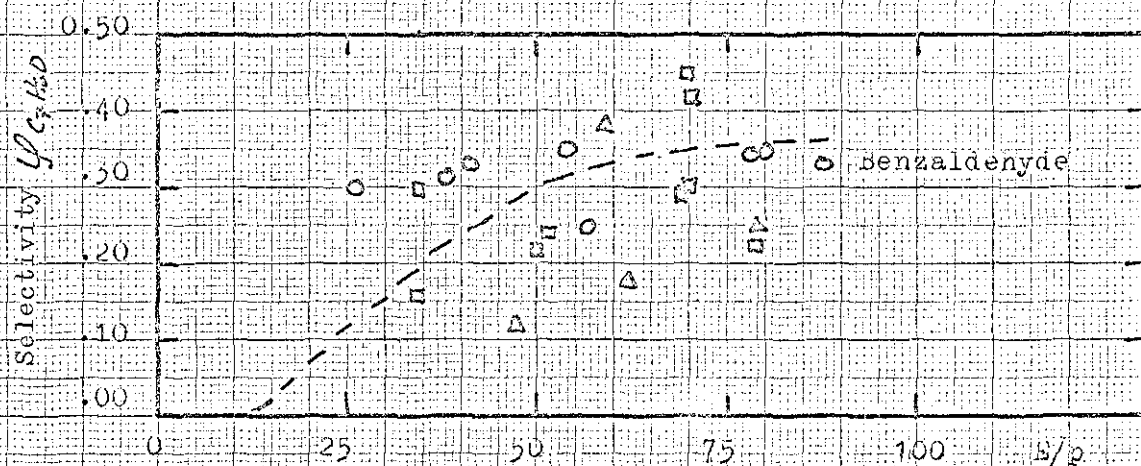
Figure 8.17. Effect of E/p upon selectivity
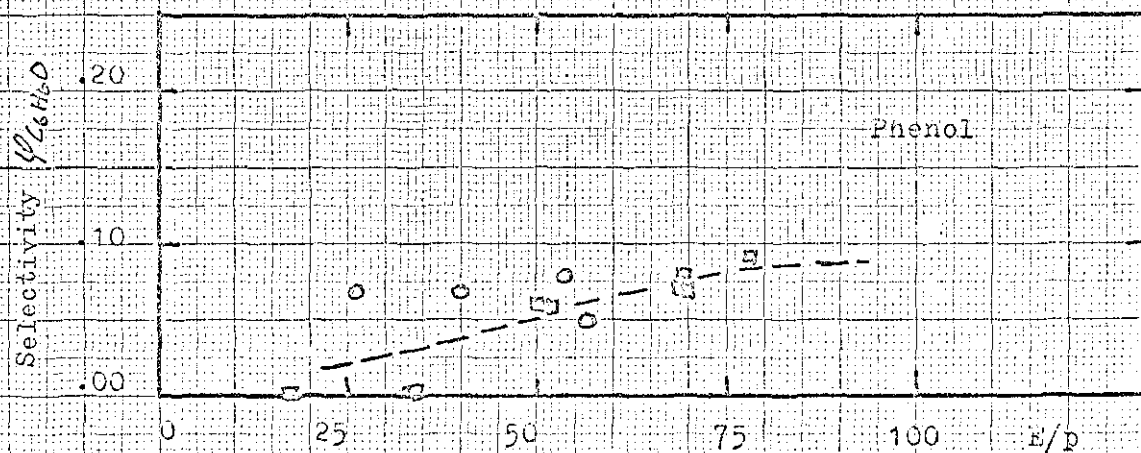
Figure 8.18. Effect of E/p upon selectivity
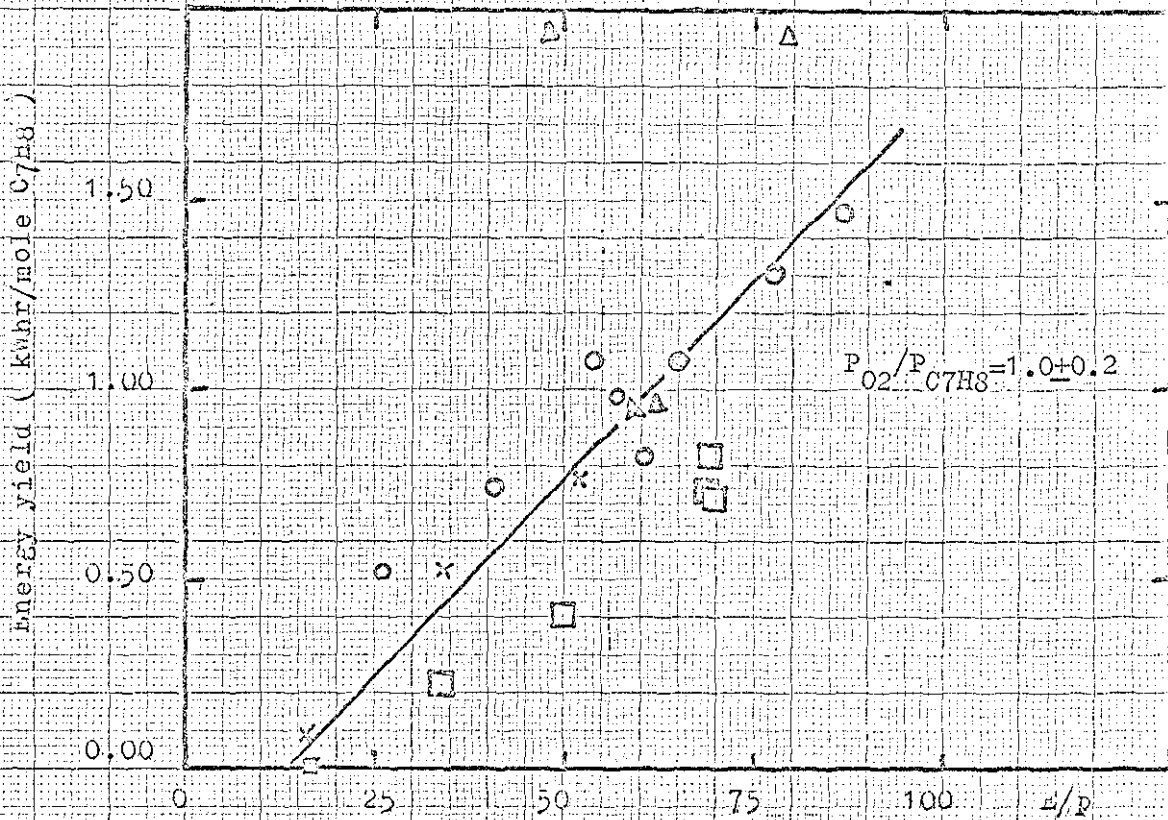
Figure 8.19. Effect of E/p upon energy yield
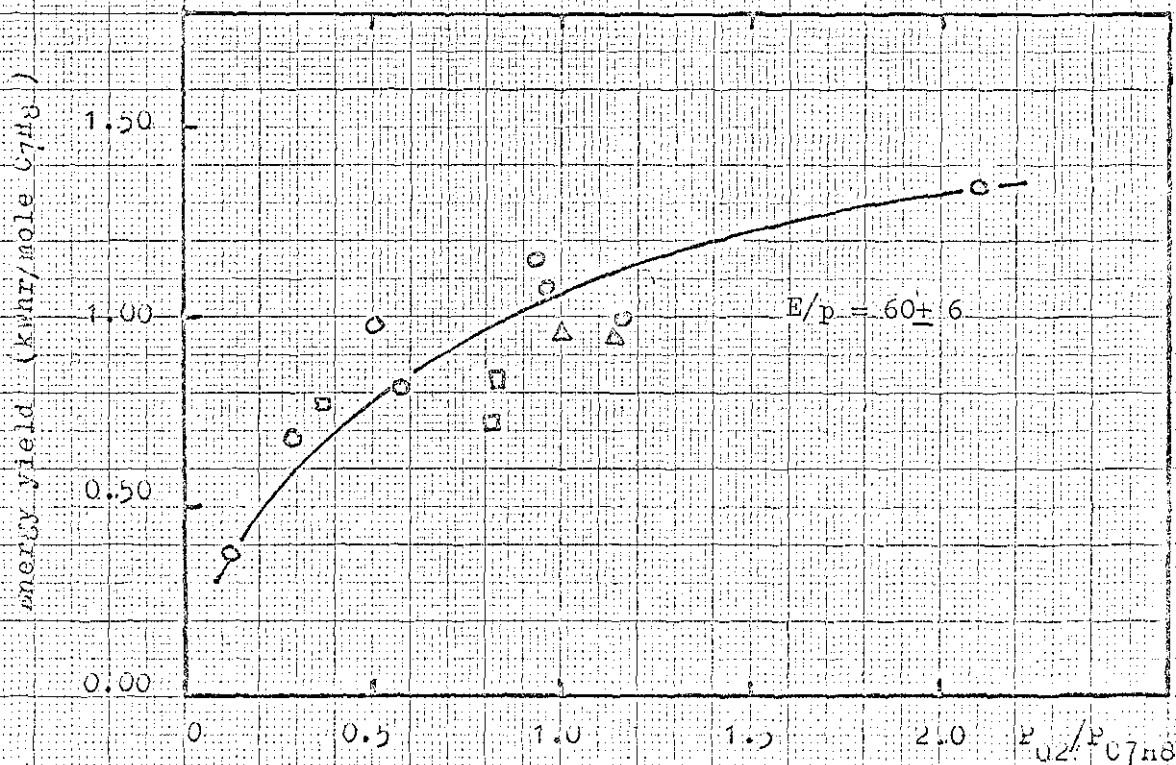
Figure 8.20. Effect of oxygen/toluene ratio upon energy yield

Temperature °C	E/p V/cm mmHg	Energy requirement kWhr/mole
50	63 ± 16	1.45 ± 0.57
300	60 ± 21	1.01 ± 0.36
350	61 ± 16	0.60 ± 0.22
400	43 ± 13	0.46 ± 0.35

Table 8.4 Average energy requirements

The effect of temperature is to promote transition of the reactants to higher vibrational states, and to increase the translation energy (kinetic energy).

8.3.6 Discharge current

It was found earlier that the reaction rate is proportional to the discharge current (figure 8.9). It is therefore not surprising that a plot of $\ln(i_d)$ versus $1/(E/p)$ yields a straight line (figure 8.23).

More interesting perhaps is a comparison between the filtered current and the instantaneous current measured from the photographs. This correlation can be seen in figure 8.24. It was found that the agreement between the two currents was very reasonable. It should be remembered that the breakdown is a statistical phenomena. Two subsequent cycles may have different time lags. This has the consequence that the instantaneous current will fluctuate. If the photographic method is used a number of photographs should be taken to ensure that an average discharge current can be calculated. Finally it should be remembered that the discharge current is a dependent variable and can thus not be used in the reactor design.
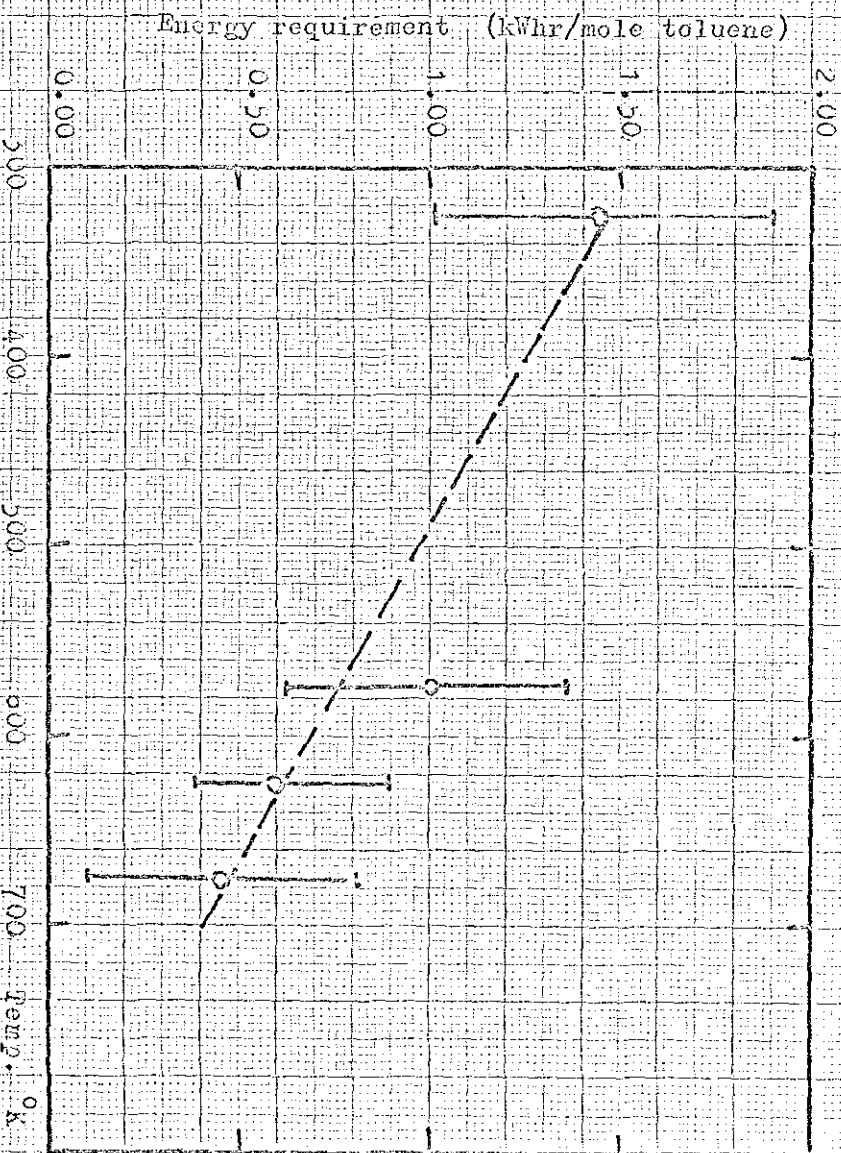
Figure 8.21. Effect of temperature upon energy requirement.
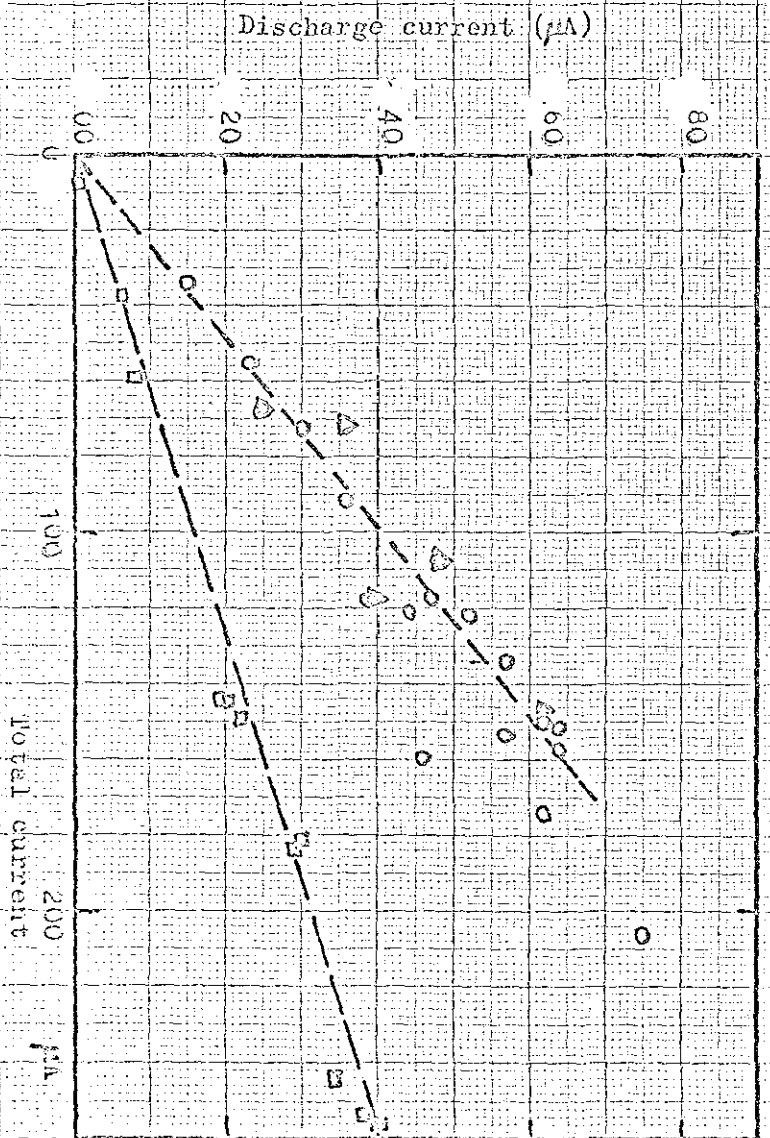
Figure 8.22. Correlation of discharge current.

Run 17-28

$P_{O2}=4.3$ $P_{C7H8}=4.38$
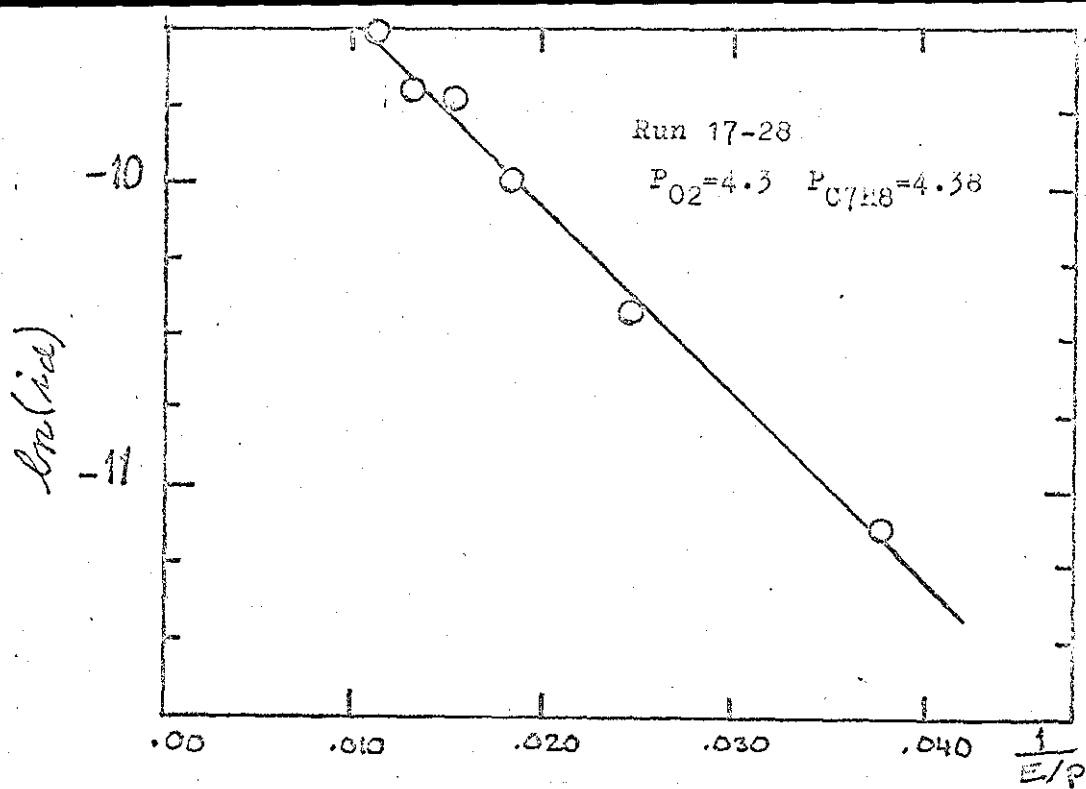
Figure 8.23.   Discharge current vs (p/E)

Photographic current
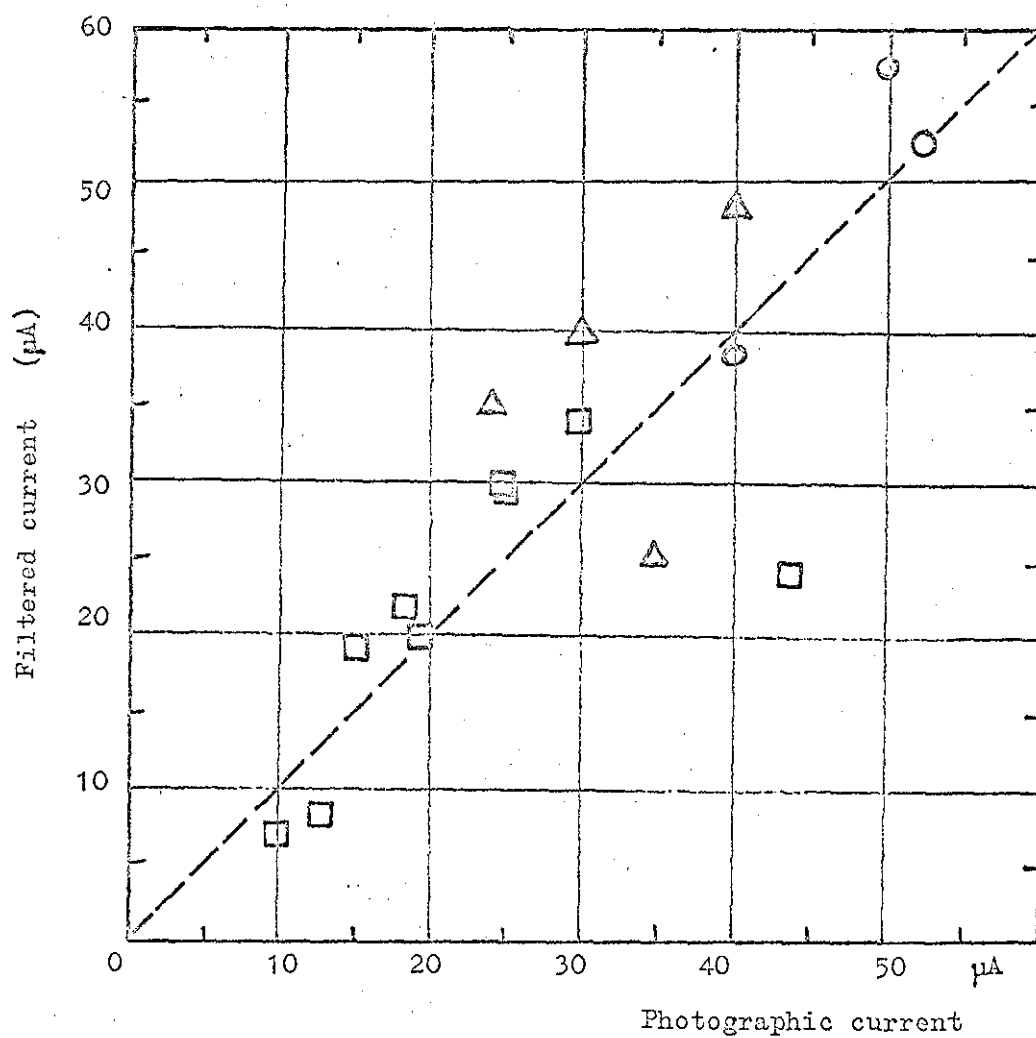
Figure 8.24.   Instantaneous vs filtered discharge current

From figures 8.25 and 8.26 we can calculate the capacitance of the reactor. The difference between the total and the filtered current is the capacitive current and we get di/dV = wC. The capacitance found in this way was 39pF. This compares favourably with the measured values of 31 and 33pF.

The total discharge current includes the capacitive and the discharge current. We may expect the discharge current to be dependent on the total current, since it is a part of it. The correlation is shown in figure 8.22. There is a distinct difference of run 31 to 46 at 350 to 400°C as compared to the other runs at lower temperatures. Photographs taken of the instantaneous discharge current show that the discharge continues after the maximum voltage has been reached. The phase shift is also different from that of runs at lower temperatures. The phase shift in the runs above 300°C is almost zero. Several explanations are possible. The first that comes in mind is that the insulation breaks down at higher temperatures giving rise to an additional resistive load. Another possibility is that of poor connection of the electrodes. Loose connections were reported in runs 32, 33 and 48. This could result in contact resistance of the circuit. This stresses the importance of measuring the true discharge current. Measurements based upon the total current can be completely misleading.
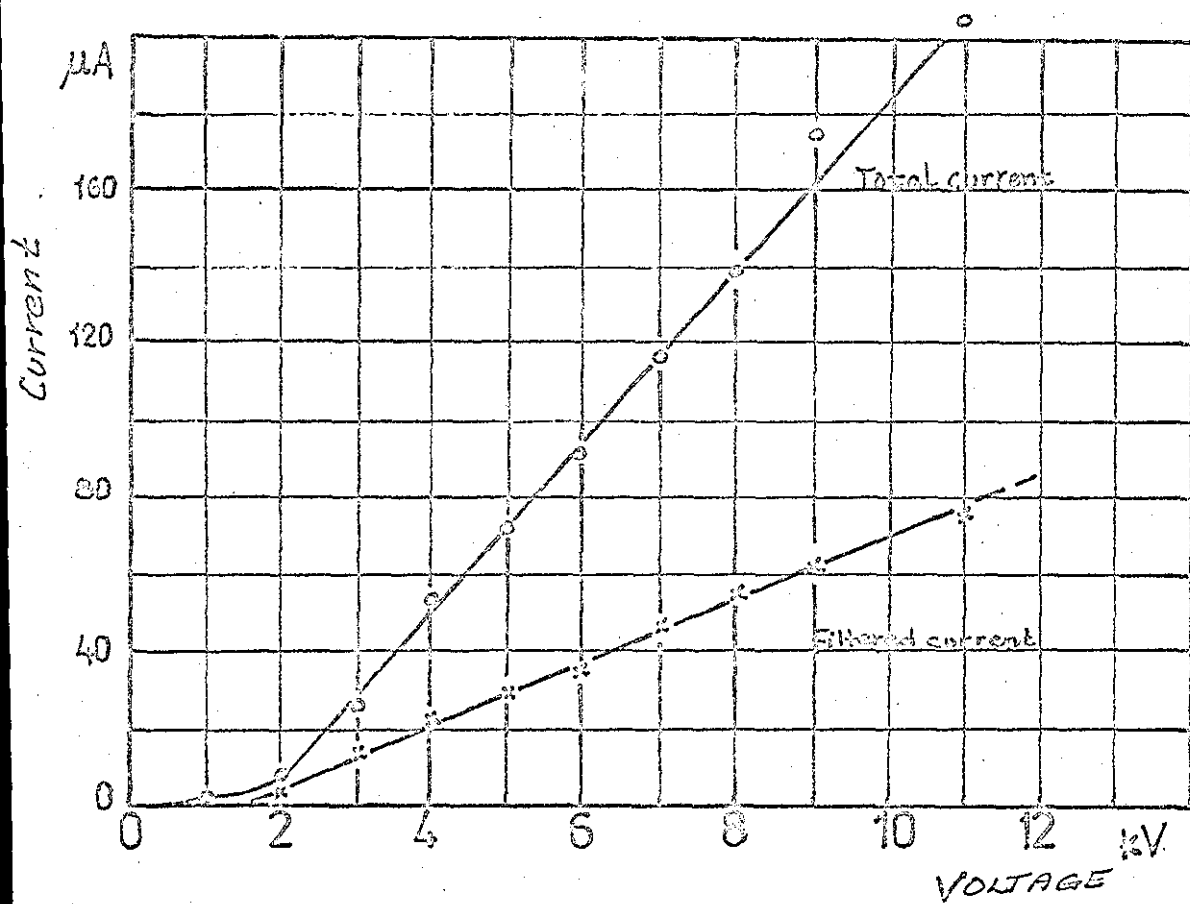
Figure 8.25. Total and filtered current
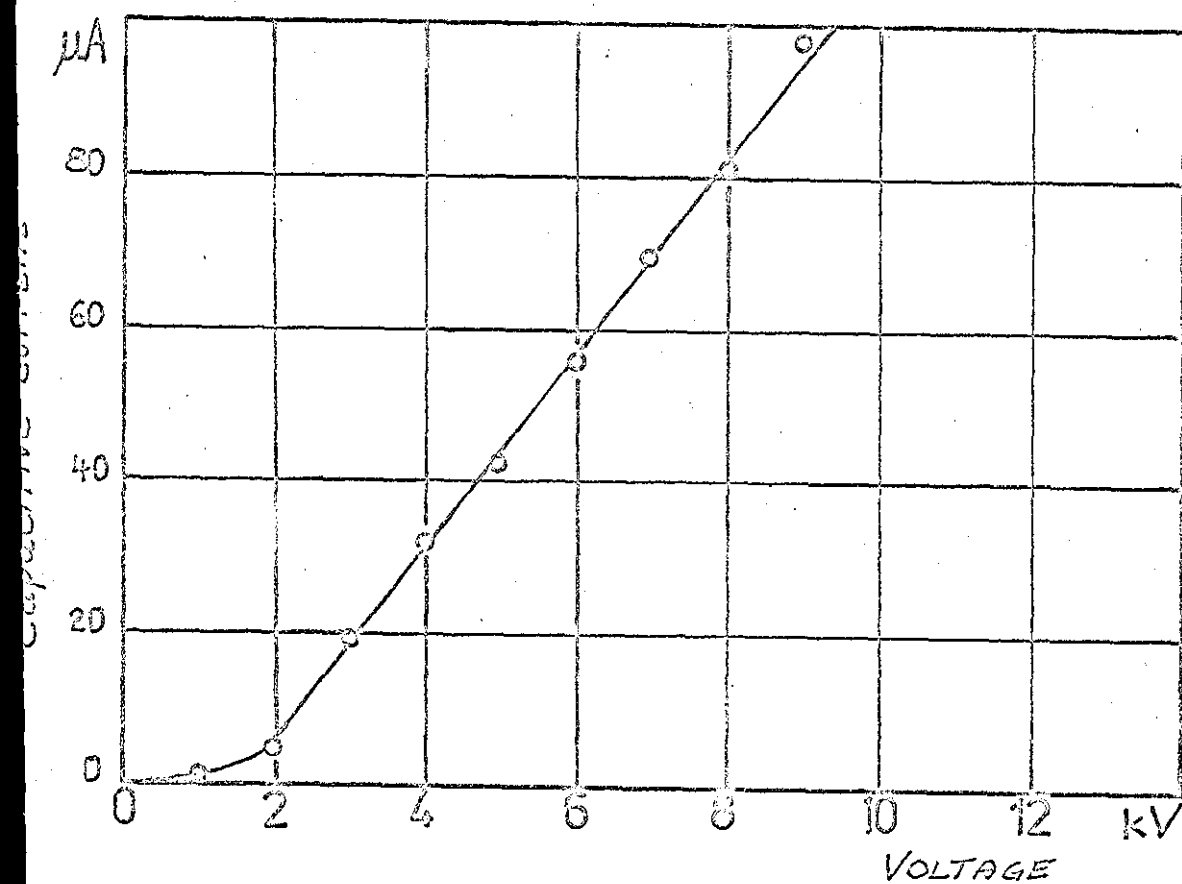
Figure 8.26. Capacitive current

CHAPTER NINE

CHAPTER 9

DISCUSSION OF THE RESULTS

In Chapter 8 we correlated the simple variables, determining the reaction rate. In Chapter 9 we will provide a theoretical explanation of these correlations. We will also calculate the individual rates of the products formed and from these rates deduce a reaction mechanism.

It was found that our derived rate expression gave an excellent agreement with the experimental rates obtained. However, we also found that we did not have sufficient data to resolve the rate mechanism completely.

The mean kinetic energy of the electron was estimated to be about 10 eV, from experimental data.

9.1 DERIVATION OF REACTION RATE

9.1.1 Electron energy

Let us assume that a reaction takes place at every collision for $\lambda \geqslant \lambda_e$. The corresponding mean free path of the electrons can then be calculated from the discharge current. From knowledge of the electric field we can find the threshold (excitation) energy. Figure 9.1 shows the discharge current as a function of reaction rate. First we calculate the number of collisions taken place which lead to reaction. This is given by

$$\frac{90 \cdot 10^{-7} (\text{moles/sec.litre}) \times 1.6 \cdot 10^{-19} (\text{As/e}) 6 \cdot 10^{23} (\text{molecules/gmole})}{100 \cdot 10^{-6} (\text{A})}$$

$= 8640 (\text{molecules/litre} \cdot \text{e})$ The volume of the reactor is 0.035 litre.
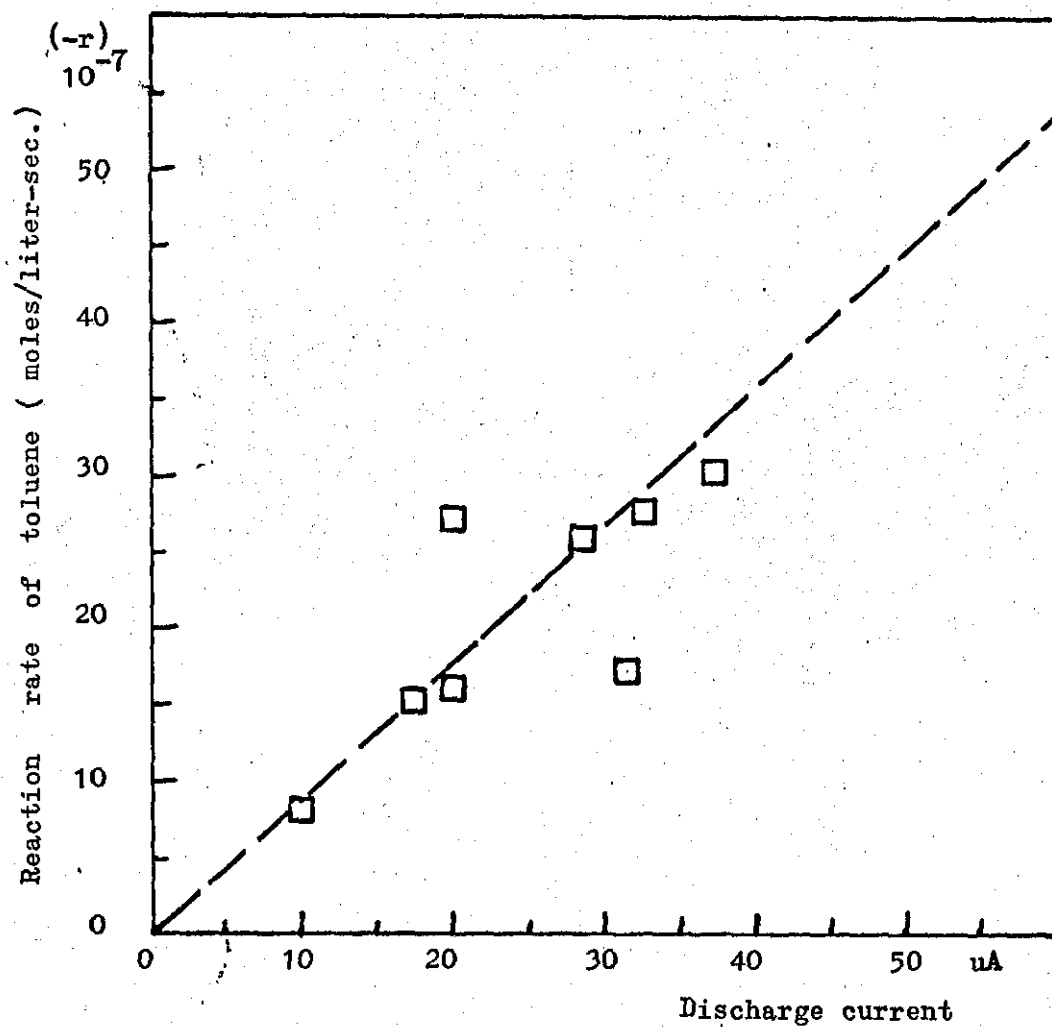
Figure 9.1. Reaction rate vs discharge current
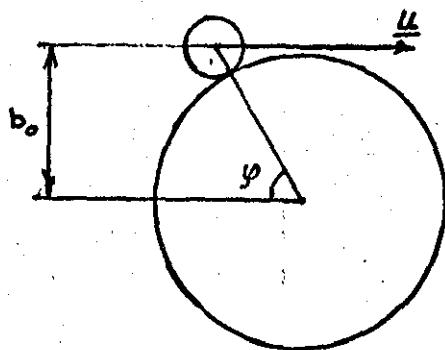
Figure 9.2. Line of centre model

This gives

$$8640 \cdot 0.035 = 300 (\text{collisions/e})$$

The distance of the gas gap is approximately 0.30 cm. Therefore the mean free path of the electrons is

$$\lambda_e = \frac{0.30}{300} = 1 \cdot 10^{-3} \; .$$

Thus the average energy the electrons have gained in the electric field is $E \cdot \lambda_e \cdot e_0$. Hence the threshold energy for the reaction is

$$E \cdot \lambda_e \cdot e_0 = \frac{8000 \cdot 1 \cdot 10^{-3}}{\sqrt{2} \cdot 0.565} = 10 \text{ eV}$$

This excitation energy is slightly lower than the ionization potential for oxygen. It is equal to the ionization potential of toluene, table 1, appendix 1. Electronic excitation of oxygen is described by three processes with threshold energies at 4.5, 8.0, and 9.7 eV. The latter two are larger than the first, and should lead to dissociation, since the upper states have shallow potential minima at larger internuclear distances than the ground state. The combined cross-section for the 8.0 and 9.7 excitation shows a broad peak of $1.1 \cdot 10^{-16} \text{cm}^2$ at 12-15 eV, then drops off and rises again in the 50-100 eV range. [61]

It therefore looks as if our threshold potential could correspond to excited oxygen and/or ionized toluene.

9.1.2 Bimolecular reactions in a cold plasma

In this section we postulate a rate expression for electron collisions in a cold plasma. The expression is derived from the collision theory, neglecting the kinetic energy of the gas molecules in comparison with the high energetic electrons.

Let us imagine a container filled with a gas A, which is activated by electron impact. Let N_A be the number density of A, and N_e the number density of the electrons. We have shown earlier that the kinetic energy of the electrons is in the range of 9-10 eV.

The mean kinetic energy of the gas molecules A at room temperature is about 0.04 eV and at $300^{\circ}C$ approximately 0.07 eV. The velocity of the electrons is thus several magnitudes larger than the velocity of the gas molecules, in a cold plasma. It is therefore reasonable to regard the gas molecules A as being a fixed target for the fast moving electrons.

We define a cross-section such that a reaction will occur if and only if an electron comes within a distance b_r of the molecule, as πb_r^2

$$e + A \rightarrow A^* \hspace{3cm} (9.1)$$

Assume the electron velocity is v (m/sec). In one second an electron will have travelled v meters through the gas; during that second it will react with any A molecules within the volume πb_r^2. The probability of an electron reacting with A in this second is therefore

$$N_A \pi b_r^2 v$$

The number of reactions per unit volume of A in one second is given by the probability of an electron reacting times the number of electrons per unit volume, i.e.

$$-r_A = \pi b_r^2(v) \cdot v \cdot N_A N_e \quad , \hspace{2cm} v = \sqrt{u_x^2 + u_y^2 + u_z^2} \hspace{1cm} (9.2)$$

In a real system the electrons will move with different velocities. The number of electrons having velocity components ranging from u_x to $u_x + du_x$, u_y to $u_y + du_y$, u_z to $u_z + du_z$ is given by

$$N_e f(u_x, u_y, u_z) du_x du_y du_z$$

If the electrons can be considered as being in thermal equilibrium within themselves, then we may assume a Boltzmann distribution for the velocity.

$$N_e f(u_x, u_y, u_z) du_x du_y du_z$$

$$= N_e (m_e/2\pi kT_e)^{3/2} \exp(-m_e \{u_x^2 + u_y^2 + u_z^2\}/2kT_e)$$

$$\pi \delta_r^2(v) \cdot v \cdot du_x du_y du_z$$

The total rate is obtained by integration over all velocities.

$$-r_A = N_e N_A (2\pi kT_e/m_e)^{-3/2} \iiint\limits_{-\infty}^{\infty} \exp(-m_e\{u_x^2 + u_y^2 + u_z^2\}/2kT_e)$$

$$\pi \delta_r^2(v) v du_x du_y du_z$$

Conversion to spherical coordinates gives $du_x du_y du_z = v^2 \sin\phi \sin\theta d\phi d\theta dv$ and integrating gives

$$-r_A = 4\pi N_A N_e (2\pi kT_e/m_e)^{-3/2} \int \exp(-m_e v^2/2kT_e)\pi \delta_r^2(v) v^3 dv \qquad (9.3)$$

We notice that $\frac{1}{2}mv^2$ represents the kinetic energy of a particle moving with a velocity v and mass m. Substitution in 9.3 gives

$$-r_A = (4\pi N_A N_e/m_e)(2\pi kT_e m_e)^{-3/2} \int \exp(-\epsilon/kT_e)\pi \delta_r^2(\epsilon)\epsilon d\epsilon$$

This expression simplifies to

$$\boxed{-r_A = N_A N_e \{8/\pi m_e (kT_e)^3\}^{\frac{1}{2}} \int_0^{\infty} \exp(-\epsilon/kT_e)\pi \delta_r^2(\epsilon)\epsilon d\epsilon} \qquad (9.4)$$

Before we carry out any integration we must find an expression for the reaction cross-section, $\pi\delta_r^2$. We know that the cross-section varies almost linearly with ε for low electron energies, so a hard sphere model would not really be appropriate. The easiest model we can find with an energy dependence is the line of centre cross-section, figure 9.2.18, for which the cross-section is defined as

$$\pi\delta_r^2(\varepsilon) = \pi\delta_r^2(1 - \varepsilon/\varepsilon_0) \qquad \text{for } \varepsilon \geqslant \varepsilon_0$$

$$\pi\delta_r^2(\varepsilon) = 0 \qquad\qquad \varepsilon < \varepsilon_0$$

Inserting the expression for the cross-section and integrating, we get

$$-r_A = \left\{\frac{8}{(\pi m_e (kT_e)^3}\right\}^{\frac{1}{2}} N_A N_e (kT_e)^2 \pi\delta_r^2 \exp(-\varepsilon_0/kT_e)$$

The mean kinetic energy gained by the electrons in the electric field is $E\lambda_e e_0$. But the mean free path of the electrons is given by $\lambda_e = \dfrac{4}{\pi N_A d_A^2}$, assuming a hard sphere model (section 2.2.1). Inserting this, and noticing that the mean kinetic energy is $3/2 kT_e$, we obtain

$$\boxed{-r_A = \{8\pi kT_e/m_e\}^{\frac{1}{2}}\delta_r^2 \cdot N_A N_e \cdot \exp(-3\pi N_A d_A^2 \varepsilon_0/8 e_0 E)} \qquad (9.5)$$

Equation 9.5 may be written more concisely as

$$-r_A = pZ \cdot N_A N_e \cdot e^{(-B/(E/N))} \quad,$$

where Z is the collision frequency and p is the steric factor defined as the ratio of the reaction cross-section to that of the hard sphere model, i.e.

$$p = \frac{\pi\delta_r^2}{\pi\delta_0^2} \quad.$$

Let us now evaluate the numerical value of B, for comparison with our experiments. We showed earlier that the excitation energy for the reaction is about 10 eV. The diameter of the oxygen molecule, d_A, assuming of course that oxygen is activated to about 2 Å or $2 \cdot 10^{-8}$ cm. Inserting these values we obtain

$$\frac{-B}{E/N} = \frac{-3 \cdot \pi \cdot 4 \cdot 10^{-16} \cdot 10 \cdot e_0}{8 \cdot e_0} = -4.7 \cdot 10^{-15} \text{ Volt cm}^{-2} ,$$

or expressed as E/p equal to -70 Volt cm^{-1} mm Hg^{-1}. Our experimental value was -66. This is indeed an excellent agreement between the proposed model and our experiments.

Let us also try to evaluate the collision frequency and make the same type of comparison. The pre-exponential term is

$$p \left(\frac{8 \pi k \cdot T_e}{m_e} \right)^{\frac{1}{2}} b_r^2 .$$

Figure 9.3 shows a graph of the electron temperature versus E/p for oxygen. At a mean kinetic energy of 10 eV, we get $T_e = 85\ 000^{\circ}$K. The cross-section is taken to be $1.1 \cdot 10^{-20} \text{m}^2$, as mentioned earlier in section 9.1.1. Inserting these values we obtain the pre-exponential factor $6.2 \cdot 10^{-14}$ molecules/sec.m^3. To convert these units into gmoles/litre we multiply by $6 \cdot 10^{26}$, which gives $Z = 3.7 \cdot 10^{10}$ moles/l-sec. or $\log_{10} Z = 10.57$. This is the right magnitude for a bimolecular collision.

Our rate expression thus becomes

$$-r_A = p \cdot 3.7 \cdot 10^{10} \cdot N_A' \cdot N_e' \cdot e^{(-70/(E/p))} ,$$

where N_A' is the concentration of A in gmoles/litre. To proceed any further requires a knowledge of the electron density. A common value from the literature seems to be 10^{13} electrons/m^3 |82|. By equating
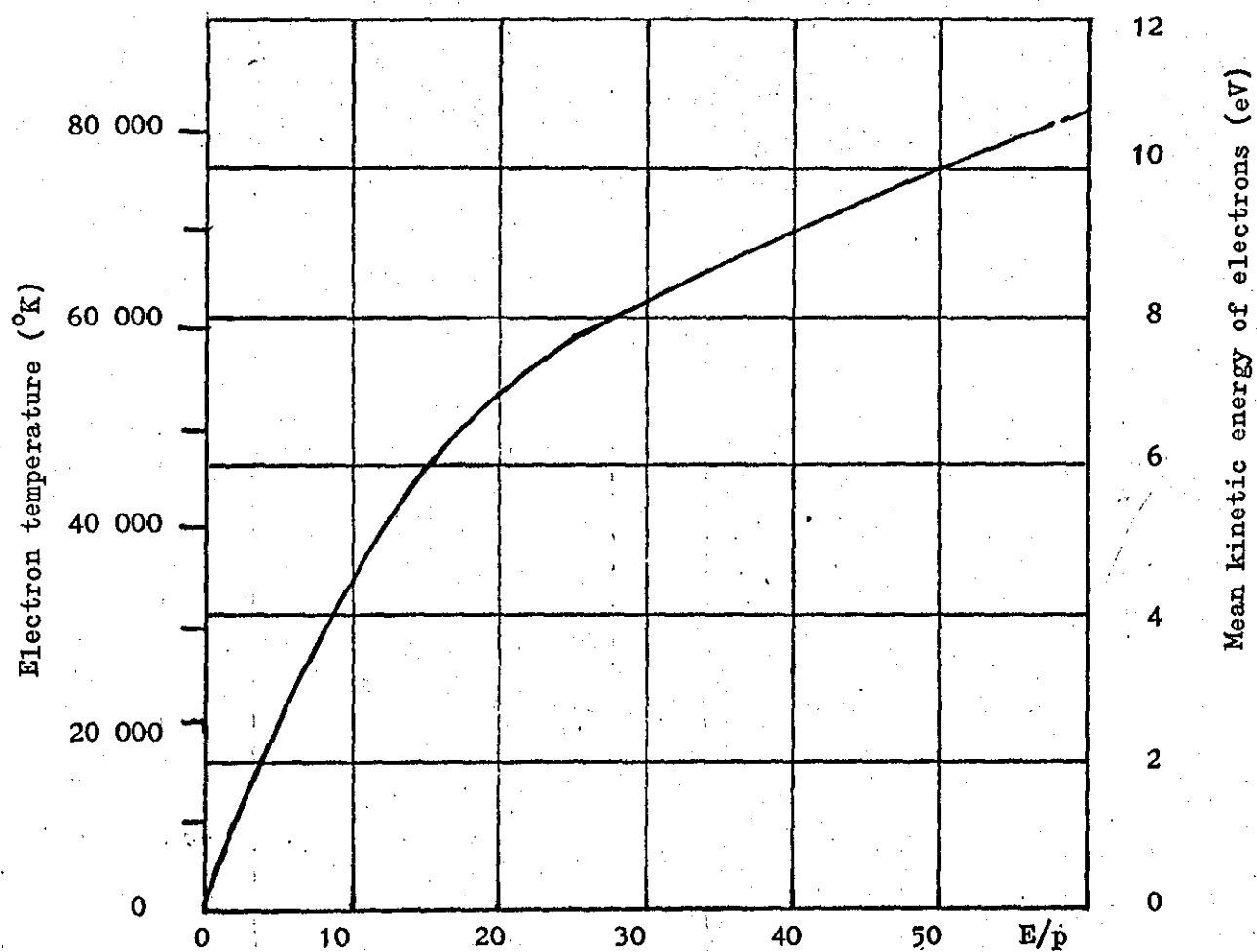
Figure 9.3.   Mean kinetic energy of electrons in oxygen [41]

the theoretical expression with our experimental rate of reaction for benzaldehyde we get,

$$\ln r_{C_7H_6O} = -7.31 + 0.95 \ln[O_2] - \frac{3.82}{E/N}$$

and

$$7.10^{-4} = \frac{p \cdot 4 \cdot 10^{10} \cdot 10^{13}}{6 \cdot 10^{26}} \quad ,$$

which gives p = 1.0. This value of the steric hinderance is not by any means unreasonable. Unfortunately there is no way of computing p, but since p is found to be less than one for all reactions, except the alkali metal reactions, we can obtain the upper limit for the pre-exponential factor. The value of 1.0 implies a perfect fit to the hard sphere model.

9.2 REACTIONS OF TOLUENE AND OXYGEN

From the selectivity and the total reaction rate it is possible to calculate the rate of formation of the products. By looking at the table in appendix V we find that the only consecutive reaction that is likely to occur is the formation of benzoic acid from benzaldehyde. In the majority of the experiments the residence time is so short that this reaction can be neglected. We are thus left with four parallel reactions for benzene, benzaldehyde, cresol plus benzyl alcohol, and phenol. Phenol may of course be formed from atomic oxygen and benzene, but this reaction is not likely to make a significant contribution to the overall yield of phenol, since the concentration of both benzene and atomic oxygen presumably is very small.

The calculated reaction rates for benzene, benzaldehyde, cresol plus benzyl alcohol, and phenol, are presented in table 9.1.

Run	$\ln\ r_{C_6H_6}$	$\ln\ r_{C_7H_8O}$	$\ln\ r_{C_7H_6O}$	$\ln\ r_{C_6H_6O}$
17	-14.80	-14.49	-14.60	-16.11
18	-15.10	-15.18	-15.10	-16.63
19	-15.70	-15.89	-15.80	-17.36
20	-15.56	-14.50	-14.82	-16.39
21	-15.42	-14.08	-14.32	-15.42
22	-15.06	-13.74	-14.01	-15.54
23	-15.16	-13.37	-13.80	-15.27
24	-15.83	-14.24	-13.61	-
25	-14.90	-14.33	-14.30	-16.10
26	-14.20	-	-14.50	-
27	-13.80	-	-	-
28	-15.00	-	-	-
30	-16.54	0	0	0
31	-14.20	-13.98	-14.03	-15.50
32	-14.88	-14.67	-14.40	-
33	-13.10	-	-	-
34	-14.00	-14.45	-13.71	-15.20
35	-13.62	-	-13.95	-
36	-14.37	-14.19	-13.71	-
37	-14.60	-13.95	-13.51	-
38	-14.02	-	-14.46	-
39	-13.96	-	-14.75	-
40	-14.40	-	-15.99	-
41	-14.10	-	-	-
42	-	-	-	-
43	-	-14.21	-13.50	-15.20
44	-14.25	-	-14.90	-
45	-	-	-	-
46	-12.76	-	-	-
47	-14.49	-15.50	-15.00	-
48	-14.45	-15.40	-15.37	-
49	-	-16.00	-16.40	-
50	-14.49	-14.80	-	-
51	-15.16	-14.17	-14.04	-15.40
52	-13.83	-	-13.47	-
53	-12.94	-	-	-
54	-11.95	-	-	-
55	-14.73	-14.45	-13.89	-15.40

Table 9.1 Reaction rates for parallel reactions

9.2.1 Experimental reaction rate for benzene

Several authors investigating reactions of toluene in a micro-wave discharge report benzene and ethylbenzene as the major products, section 4.4. This suggests a mechanism according to

$$C_7H_8^* \rightarrow C_6H_6 + CH_2 \; .$$

$$C_7H_8 + CH_2 \cdot \rightarrow C_6H_5C_2H_5$$
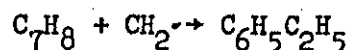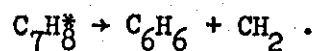
Therefore we expect benzene a priori to be of first order with respect to toluene. The first correlation we tried was not the toluene dependence but the oxygen dependence. The reason was that in the first set of experiments we kept the toluene pressure constant while we varied the oxygen pressure. The correlation obtained can be seen in figure 9.4. The slope obtained was -0.88 for runs 17-28 and -1.13 for runs 31-50. Next we tried a regression analysis of all three variables, O_2, C_7H_8, and E/N, to see if the F-ratio was significant for this correlation. The result is seen in table 9.2.

```
COEFFICIENTS FOR X
                    X( 1 )= .210136
                    X( 2 )=-1.18699
                    X( 3 )= 1.00073
                    X( 0 )=-15.6285


   STANDARD ERROR IN Y= .242698
```

REGRESSION	SS	DF	MS	F
X1-X 3	10.5278	3	3.5093	59.58
X1-X 2	8.7639	2	4.3819	74.39
INCREMENT	1.7640	1	1.7640	29.95
RESIDUAL	0.8835	15	0.0589	
TOTAL	11.4114	18		

```
MORE AVALUES?  YES=1  NO=0
```

Table 9.2 Regression analysis of runs 31-54 for benzene
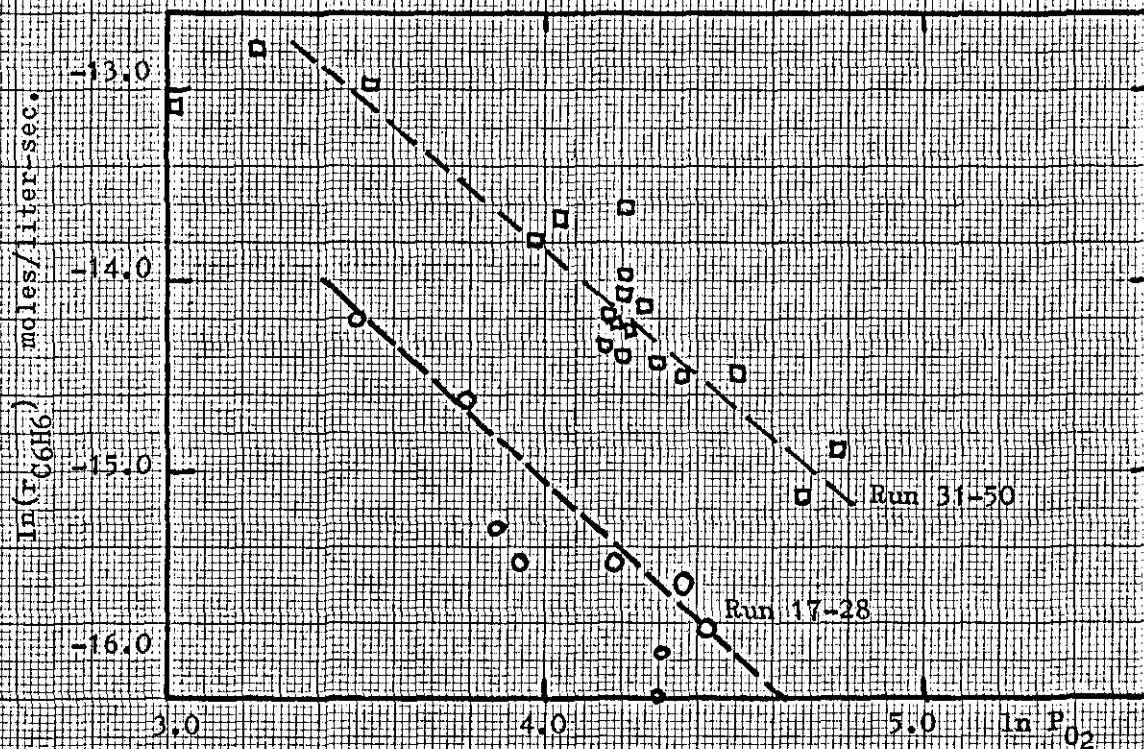
Figure 9.4. Reaction order for oxygen
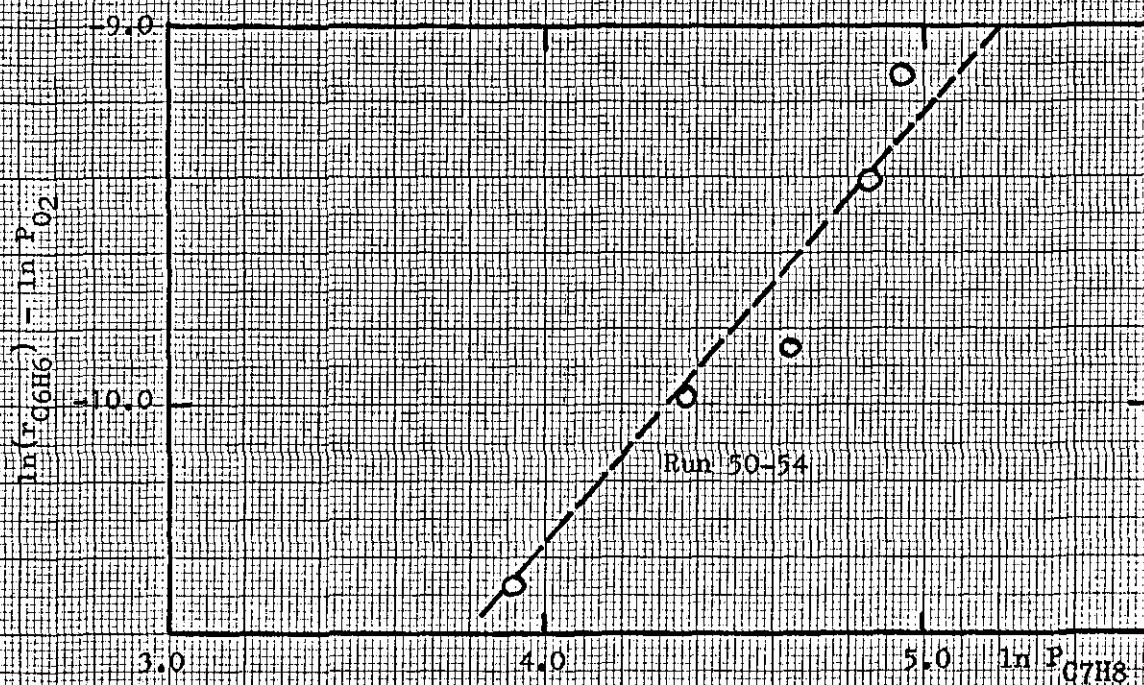
Figure 9.5. Reaction order for toluene
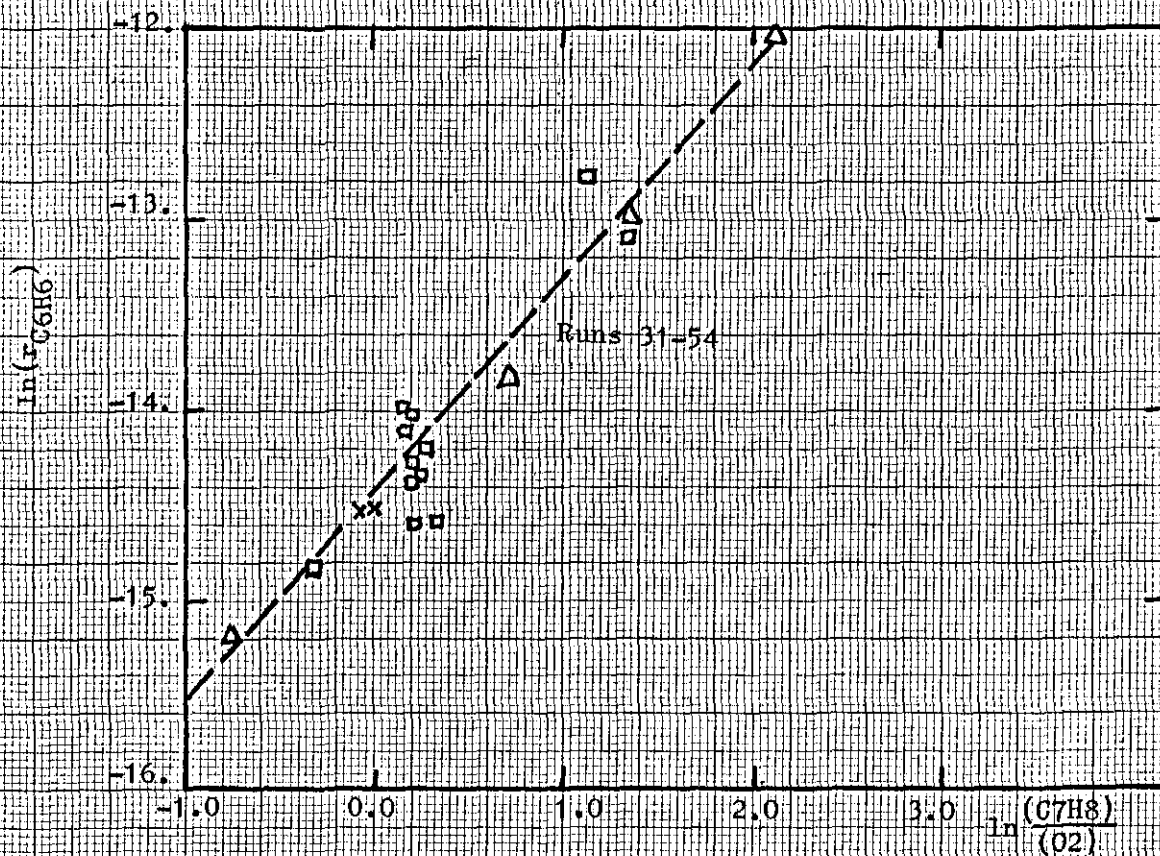
Figure 9.6. Reaction rate vs P_{C7H8}/P_{O2}
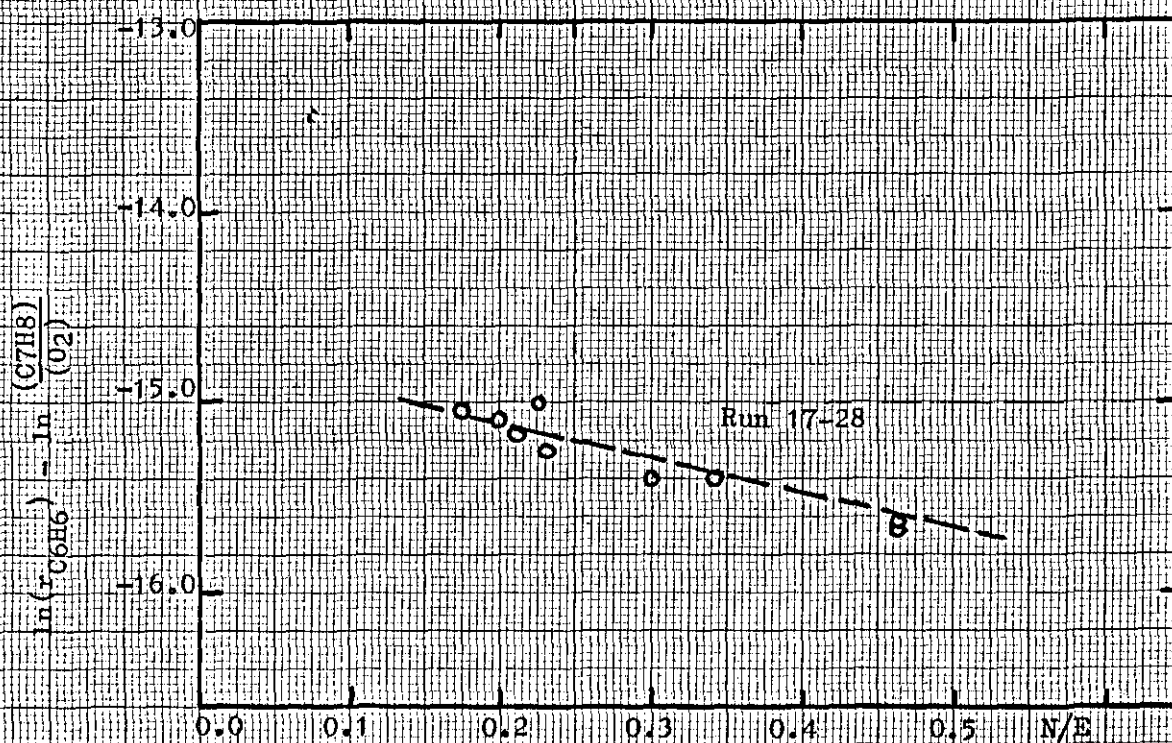
Figure 9.7. Dependence of N/E

The F-ratio for N/E and oxygen was 74, which corresponds to over 99% significance. The addition of the third variable, concentration of toluene, gave an F-ratio of 30. This again is well above 99% significance. We therefore feel sure that the reaction rate is proportional to toluene and inversely proportional to oxygen. The reaction order of -1.18 and 1.00, respectively, indicates a first order for both of them, giving the following reaction rate

$$r_{C_6H_6} = k \frac{\left[C_7H_8\right]}{\left[O_2\right]} e^{-B/(E/N)} .$$

Figures 9.5 and 9.6 show this correlation. The rate equation obtained was:

Runs 17-28: $\quad \ln r_{C_6H_6} = -14.66 + 0.91 \ln \frac{\left[C_7H_8\right]}{\left[O_2\right]} - \frac{1.84 \cdot 10^{-15}}{E/N}$

Runs 31-54: $\quad \ln r_{C_6H_6} = -14.37 + 1.14 \ln \frac{\left[C_7H_8\right]}{\left[O_2\right]} .$

No dependence of N/E was found for the last correlation. We may therefore postulate that the dependence of N/E for benzene is slightly less than half that of the threshold energy found for toluene disappearance ($-3.7 \cdot 10^{-15}$). This gives us an excitation energy of about 5 eV.

9.2.2 Experimental reaction rate for benzaldehyde

In section 4.1 and 4.2 we found that benzaldehyde is the result of a reaction between excited oxygen molecules, in the singular state, and toluene, the excitation energy being about 1 eV. In the event of collision between excited toluene and oxygen we foresee no reason why a reaction should not take place, since the threshold potential is

well above the minimum requirement. Our postulated reaction mechanism is therefore

$$C_7H_8 + O_2(^1\Delta_g) \rightarrow C_6H_5CHO + H_2O$$

$$C_7H_8^* + O_2(^3\Sigma_g) \rightarrow C_6H_5CHO + H_2O$$
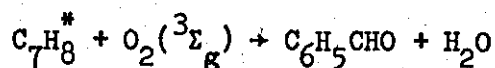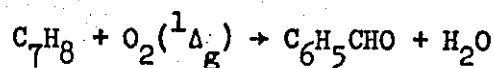
The $O_2(^1\Delta_g)$ state will hereafter be described as O_2^*, similarly $O_2(^3\Sigma_g)$ will be written O_2. The (*) will be used to describe the activated species.

The variable that has the largest significance upon our experimental rate equation is N/E. This indicates that benzaldehyde is indeed formed from an activated complex. Keeping the partial pressure of toluene constant we obtained the following regression,

$$\ln(-r) = -17.08 + 0.96 \ln P_{O_2} - \frac{3.94 \cdot 10^{-15}}{E/N} \quad ,$$

or in terms of concentration,

$$\ln r_{C_7H_6O} = -7.14 + 0.95 \ln[O_2] - \frac{3.82 \cdot 10^{-15}}{E/N} \quad .$$

The F-ratio for including oxygen was 11, which corresponds to about 98% significance. Including toluene in runs 17-26 did not make any significant contribution. The regression analysis is shown in table 9.3 and 9.4. A graph of the results can be seen in figures 9.8 and 9.9. The results from runs 31-51 showed significance in only the first variable N/E. Obviously our experimental errors were such that no further information could be extracted. The correlation obtained from table 9.5 was

$$\ln r_{C_7H_6O} = -13.44 - 0.16 \ln[O_2] + 0.12 \ln[C_7H_8] - \frac{3.38 \ 10^{-15}}{E/N}$$

The standard deviation in ln r was 0.54. Consequently we cannot obtain the toluene dependence from the experimental runs that we have available; this would require further runs varying the partial pressure of toluene.

```
        COEFFICIENTS FOR X
                        X( 1 )=-3.82472
                        X( 2 )= .949588
                        X( 0 )=-7.14639


        STANDARD ERROR IN Y= .186003


        REGRESSION              SS       DF            MS        F
        X1-X 2                 3.5472     2           1.7736    51.27
        X1-X 1                 3.1629     1           3.1629    91.42
        INCREMENT              0.3843     1           0.3843    11.11
        RESIDUAL               0.2076     6           0.0346
        TOTAL                  3.7548     8

        MORE AVALUES?   YES=1   NO=0
```

Table 9.3 Regression analysis of runs 17-26

```
        COEFFICIENTS FOR X
                        X( 1 )=-3.62885
                        X( 2 )= .910704
                        X( 3 )= 2.85728
                        X( 0 )= 9.8861


        STANDARD ERROR IN Y= .186139


        REGRESSION              SS       DF            MS        F
        X1-X 3                 3.5816     3           1.1939    34.46
        X1-X 2                 3.5472     2           1.7736    51.19
        INCREMENT              0.0343     1           0.0343     0.99
        RESIDUAL               0.1732     5           0.0346
        TOTAL                  3.7548     8

        MORE AVALUES?   YES=1   NO=0
        ? 0
```

Table 9.4 Regression analysis for runs 17-26
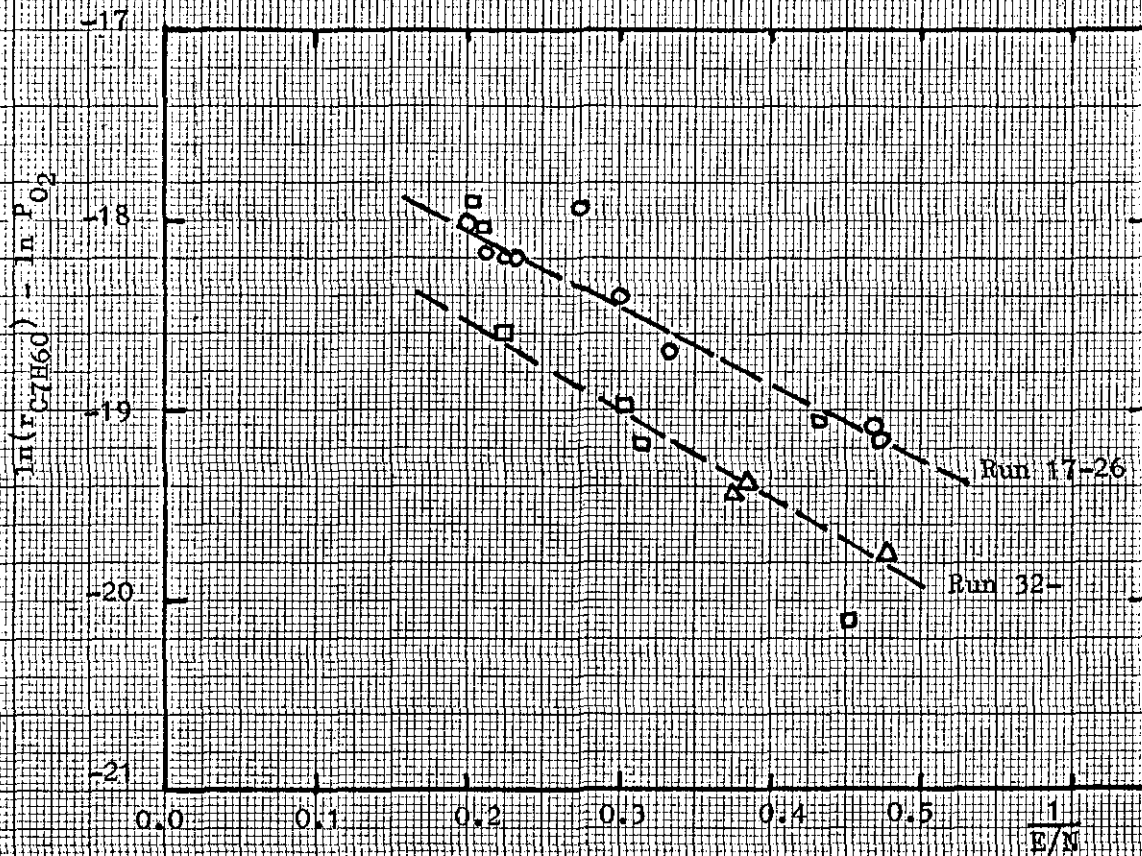
Figure 9.8.   Correlation of N/E for benzaldehyde
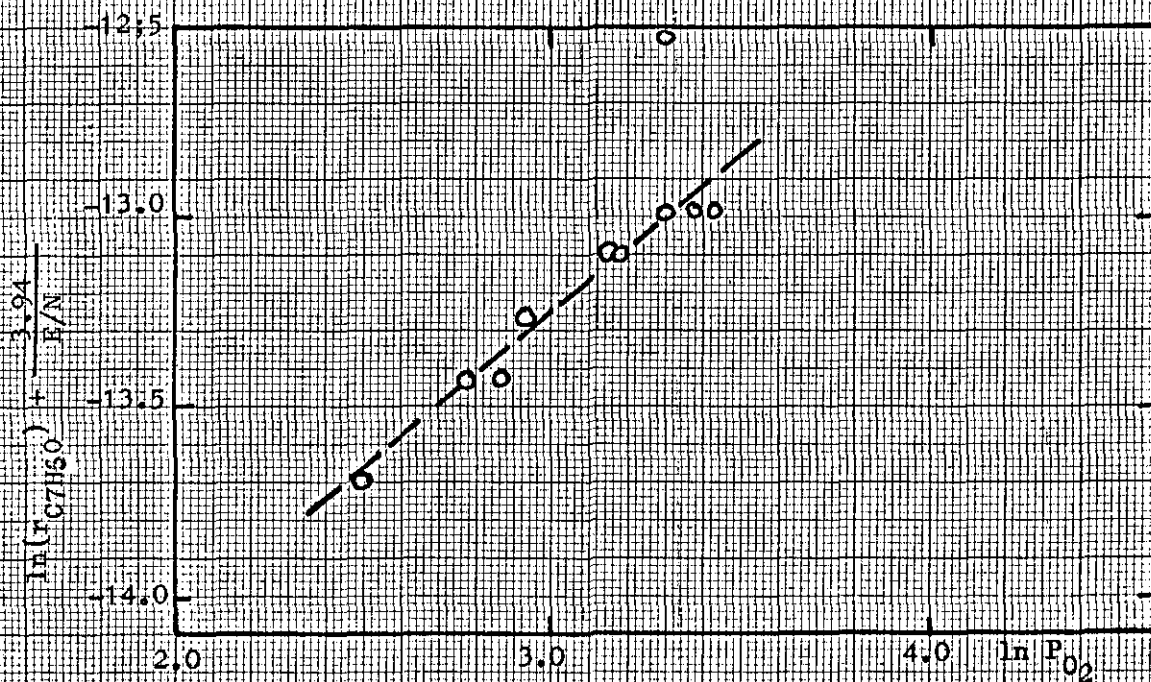
Figure 9.9.   Reaction order for oxygen

163

9.2.3 Experimental reaction rate for cresol and benzyl alcohol

Cvetanovic and Jones investigated the reaction of atomic oxygen in the (^3P) state with toluene. Apart from a low volatile polymer they only found cresol and smaller amounts of carbon monoxide. No trace of benzaldehyde or hydrogen abstraction was found. This indicates that cresols are formed from reactions between atomic oxygen and toluene according to

$$C_7H_8 + O(^3P) \rightarrow C_7H_8O \quad .$$
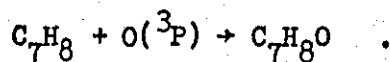
It was shown in section 8.3.4 that the cresol increased with increasing value of N/E. Benzyl alcohol showed a similar trend and we have no reason to assume that benzyl alcohol would be formed by a different reaction. We have therefore in our correlations used grouped data.

The most significant variable was E/N. A correlation of runs 17-25 is shown in figures 9.10 and 9.11. The rate expression obtained was:

$$\ln r_{C_7H_8O} = -17.67 + 1.14 \ln P_{O_2} - \frac{4.23 \cdot 10^{-15}}{E/N}$$

or, in concentration terms,

$$\ln r_{C_7H_8O} = -5.91 + 1.12 \ln [O_2] - \frac{4.12 \cdot 10^{-15}}{E/N} \quad .$$

The F-ratio for including oxygen in the rate expression was 15.6, which gives a 99% significance. The standard deviation was 0.19 (table 9.6).

Again we ran into trouble when we tried to apply the regression on runs 31-51. Table 9.7 shows this regression. The only variable we found significant was E/N. A linear regression of N/E gave the following regression line:

COEFFICIENTS FOR X
                    X(1)=-3.38255
                    X(2)=-.167834
                    X(3)= .123749
                    X(0)=-13.4416

STANDARD ERROR IN Y= .537776

REGRESSION	SS	DF	MS	F
X1-X 3	1.8733	3	0.6244	2.16
X1-X 2	1.8620	2	0.9310	3.22
INCREMENT	0.0113	1	0.0113	0.04
RESIDUAL	3.1812	11	0.2892	
TOTAL	5.0546	14		

MORE AVALUES? YES=1 NO=0
? 0

Table 9.5 Regression of runs 17-26 for benzaldehyde

COEFFICIENTS FOR X
                    X(1)=-4.23427
                    X(2)= 1.14517
                    X(0)=-17.6756

STANDARD ERROR IN Y= .190671

REGRESSION	SS	DF	MS	F
X1-X 2	4.2422	2	2.1211	58.34
X1-X 1	3.6763	1	3.6763	101.12
INCREMENT	0.5659	1	0.5659	15.57
RESIDUAL	0.2181	6	0.0364	
TOTAL	4.4604	8		

MORE AVALUES? YES=1 NO=0
? 0

Table 9.6 Regression of runs 17-26 for C_7H_8O

165
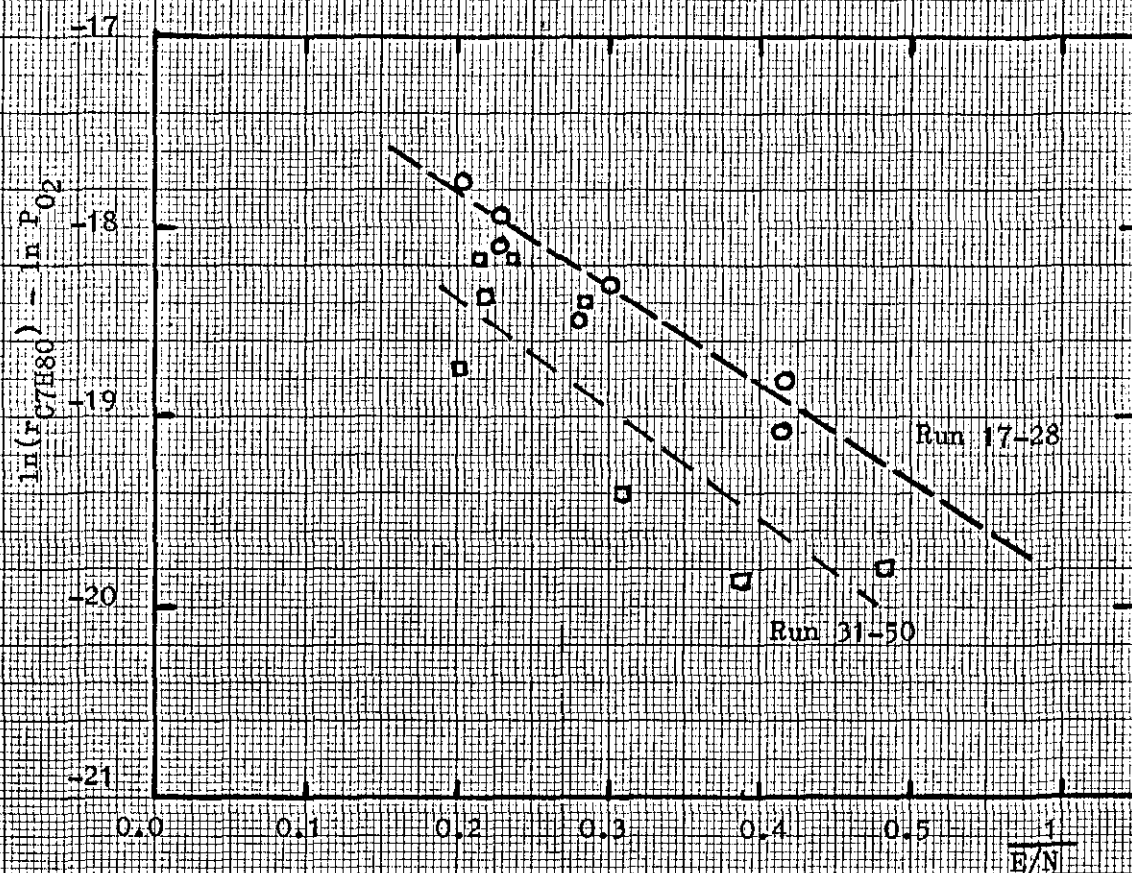
Figure 9.10. Correlation of N/F for cresol and benzyl alcohol
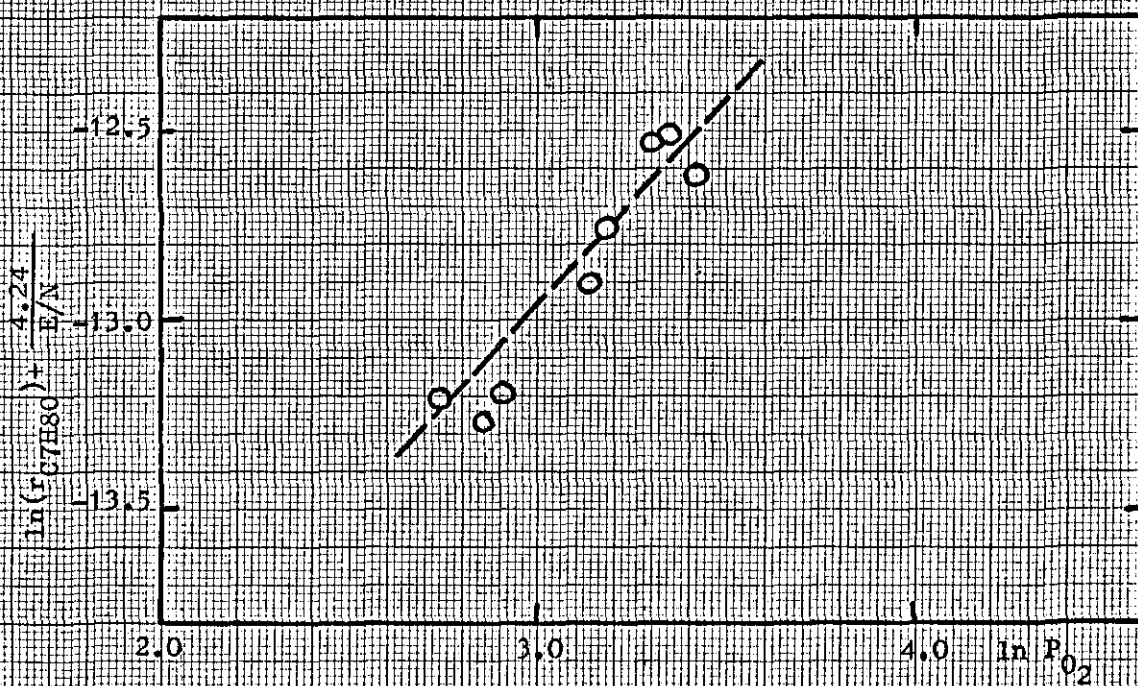
Figure 9.11. Reaction order for oxygen

166

$$\ln r_{C_7H_8O} = -13.33 - \frac{3.89 \cdot 10^{-15}}{E/N} \ .$$

Of course we had no chance whatsoever to see any influence of toluene from runs 31-51, since this would require an additional variable to be included.

9.2.4 Experimental reaction rate of phenol

Many compounds have been found in homogeneous and heterogeneous oxidation of toluene, section 4.1 and 4.2, but phenol is not one of them. The strong dependence of N/E suggests a mechanism over excited oxygen. It is probable that the reaction is very similar to that of cresol as they represent the same type of addition. The proposed mechanism is therefore

$$C_7H_8 + O(^3P) \rightarrow C_6H_5OH + CH_2 \ .$$
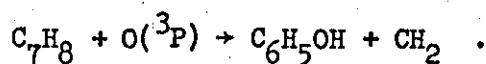
Obtaining a correlation for phenol is simpler, since we do not have to consider the runs 31-51, for which we obviously do not have sufficient data to perform a regression. The correlation obtained from runs 17-23 was

$$\ln r_{C_6H_6O} = -18.87 + 1.031 \ln P_{O_2} - \frac{3.14 \cdot 10^{-15}}{E/N} \ ,$$

or, in concentration terms, from runs 17-25,

$$\ln r_{C_6H_6O} = -7.31 + 1.18 \ln[O_2] - \frac{3.63 \cdot 10^{-15}}{E/N} \ .$$

The correlation is shown in figures 9.12 to 9.13. Table 9.8 gives us an F-ratio of 17. This corresponds to exactly 99% significance. Including toluene in the regression did not improve the correlation since no significance was found for toluene. However, this does not mean that the reaction rate is independent of the toluene pressure, since our variation in the partial pressure of toluene was small, 4.37 ± 0.02. Table 9.9 shows the regression including toluene.
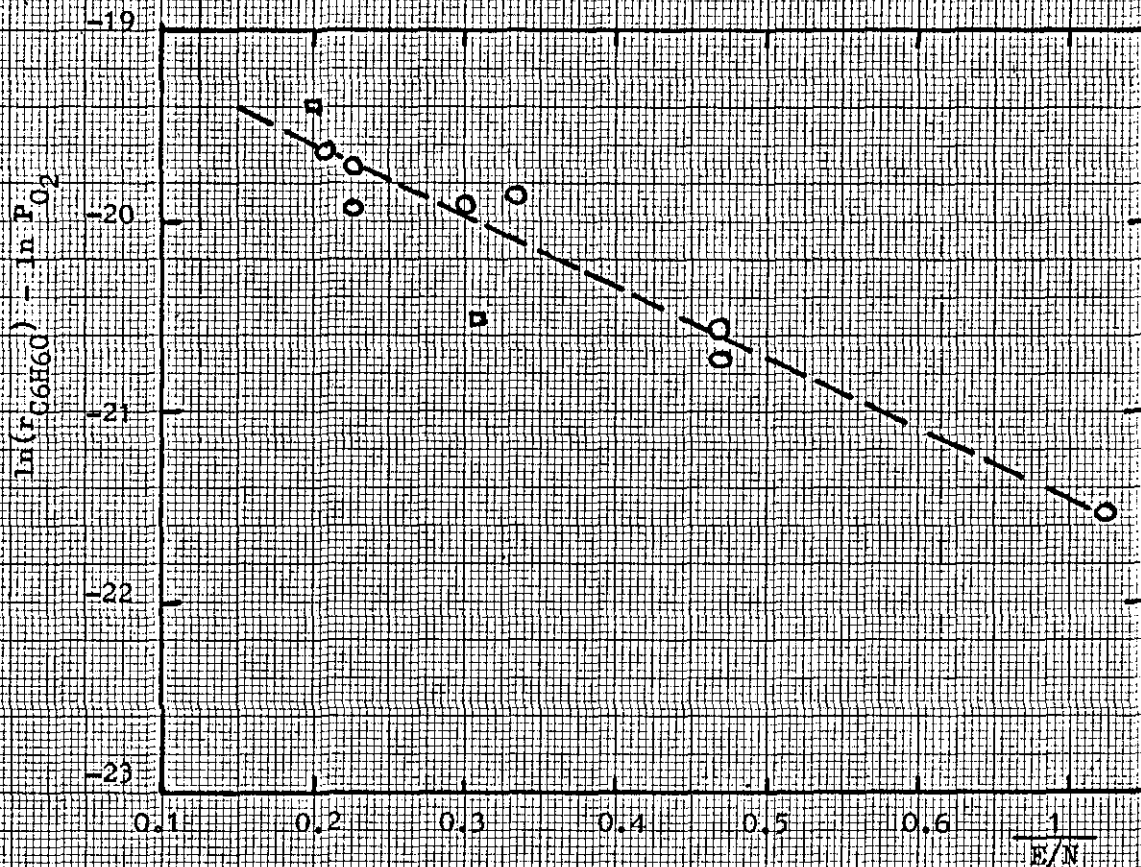
Figure 9.12. Correlation of N/E for phenol
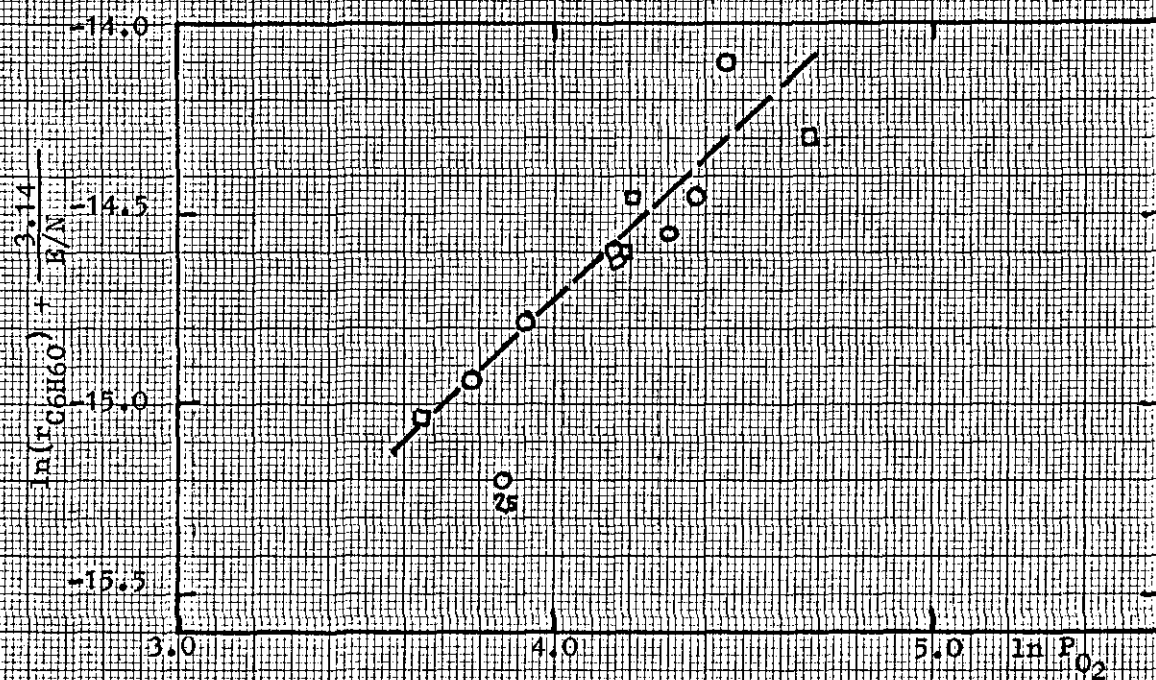
Figure 9.13. Reaction order for oxygen

168

COEFFICIENTS FOR X

$$X(1)=-1.30902$$
$$X(2)=-.766873$$
$$X(0)=-18.736$$

STANDARD ERROR IN Y= .379379

REGRESSION	SS	DF	MS	F
X1-X 2	1.8921	2	0.9460	6.57
X1-X 1	1.6620	1	1.6620	11.55
INCREMENT	0.2301	1	0.2301	1.60
RESIDUAL	1.0075	7	0.1439	
TOTAL	2.8996	9		

MORE AVALUES? YES=1   NO=0
? 0

Table 9.7 Regression of runs 31-50 for C_7H_8O

COEFFICIENTS FOR X

$$X(1)=-3.7421$$
$$X(2)= 1.19799$$
$$X(0)=-19.6846$$

STANDARD ERROR IN Y= .185885

REGRESSION	SS	DF	MS	F
X1-X 2	3.2448	2	1.6224	46.95
X1-X 1	2.6639	1	2.6639	77.10
INCREMENT	0.5809	1	0.5809	16.81
RESIDUAL	0.1728	5	0.0346	
TOTAL	3.4176	7		

MORE AVALUES? YES=1   NO=0

Table 9.8 Regression of runs 17-25 for phenol

```
COEFFICIENTS FOR X
                X( 1 )=-4.31216
                X( 2 )= 1.05687
                X( 3 )= 14.1373
                X( 0 )=-80.7453


   STANDARD ERROR IN Y= .177467


   REGRESSION            SS       DF          MS        F
   X1-X 3             3.2916      3        1.0972     34.84
   X1-X 2             3.2448      2        1.6224     51.51
   INCREMENT          0.0468      1        0.0468      1.49
   RESIDUAL           0.1260      4        0.0315
   TOTAL              3.4176      7

   MORE AVALUES?   YES=1   NO=0
   ? 0
```

Table 9.9 Regression of runs 17-25 for phenol

9.2.5 Reaction mechanism

At this stage we are beginning to accumulate some important information that will help us to find a reaction mechanism. Let us sort out these facts.

(1) Cresols and presumably benzyl alcohol are formed from atomic oxygen. The reaction order with respect to oxygen is ~ 1.0.

(2) Benzaldehyde is formed from excited oxygen, having the same dependence of N/E as atomic oxygen.

(3) Benzene is formed from toluene, being first order with respect to toluene, but inversely proportional to oxygen. The dependence of N/E is lower than that of benzaldehyde, cresol and phenol.

(4) Phenol is first order with respect to oxygen. The N/E dependence is the same as benzaldehyde and cresol.

The conclusions we can make from these facts are as follows. Atomic oxygen is formed from activated oxygen. Two facts support this conclusion. The "activation energy" or threshold potential are identical. The rate of formation of cresol is of first order with respect to oxygen. This gives us reactions 1 and 2.

Oxygen is not involved in the formation of benzene, since the reaction order with respect to oxygen is -1.0. The weak dependence of N/E suggests a complex, probably activated toluene. The oxygen dependence suggests that this activated complex competes for oxygen to form oxygen compounds not involving atomic oxygen, i.e. benzaldehyde.

The proposed mechanism thus becomes:

(1) $$e(1) + O_2 \underset{k_2}{\overset{k_1}{\rightleftharpoons}} O_2^* + e$$

(2) $O_2^* \xrightarrow{k_3} O + O$

(3) $e(2) + C_7H_8 \underset{k_5}{\overset{k_4}{\rightleftharpoons}} C_7H_8^* + e$

(4) $C_7H_8^* \xrightarrow{k_6} C_6H_6 + CH_2\cdot$

(5) $C_7H_8^* + O_2^* \xrightarrow{k_7} C_6H_5CHO + H_2O$

(6) $O_2 + C_7H_8^* \xrightarrow{k_8} C_6H_5CHO + H_2O$

(7) $O_2^* + C_7H_8 \xrightarrow{k_9} C_6H_5CHO + H_2O$

(8) $O + C_7H_8 \xrightarrow{k_{10}} C_7H_8O$

(9) $O + C_7H_8 \xrightarrow{k_{11}} C_6H_5OH + CH_2$

(10) $CH_2\cdot + 3/2\ O_2 \xrightarrow{k_{12}'} CO_2 + H_2O$
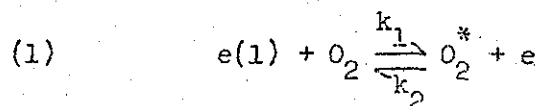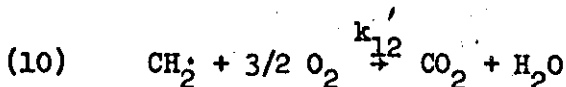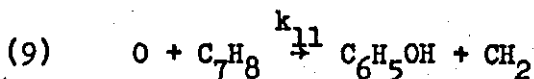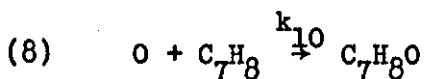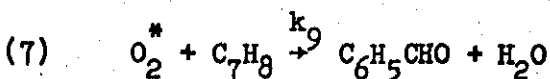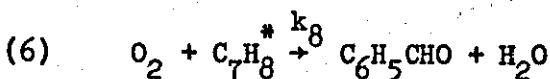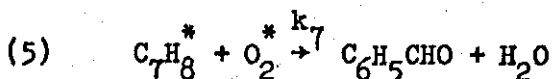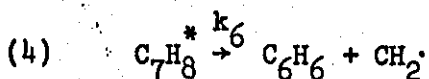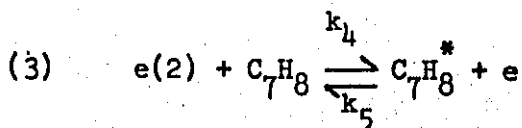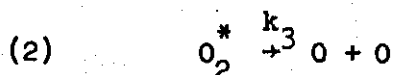
In section 3.1 we discussed the Hinshelwood mechanism. This mechanism assumes that an equlibrium condition for the activated complex is rapidly approached.

$$r_{O_2^*} = k_1[e_1][O_2] - k_2[O_2^*][e_1] - k_3[O_2^*] - k_7[C_7H_8^*][O_2^*] - k_9[O_2^*][C_7H_8] = 0$$

and

$$|O_2^*|_{eq} = \frac{k_1[e_1][O_2]}{k_3 + k_2[e_1] + k_7[C_7H_8^*] + k_9[C_7H_8]}$$

$$r_{C_7H_8^*} = k_4[e_2][C_7H_8] - k_5[C_7H_8^*] - k_6[C_7H_8^*] - k_7[O_2^*][C_7H_8^*] - k_8[C_7H_8^*][O_2] = 0$$

172

and

$$|C_7H_8^*|_{eq} = \frac{k_4[e_2][C_7H_8]}{k_5+k_6+k_7[O_2^*]+k_8[O_2]}$$

$$r_0 = 2k_3[O_2^*]-k_{10}[C_7H_8][O]-k_{11}[C_7H_8][O] = 0$$

$$|O|_{eq} = \frac{2k_3[O_2^*]}{(k_{10}+k_{11})[C_7H_8]}$$

The equilibrium values of the complex are very small and the steady state concentration simplifies to

$$|O_2^*|_{eq} = \frac{k_1[e_1][O_2]}{k_3+k_2[e_1]+k_9[C_7H_8]}$$

$$|C_7H_8^*|_{eq} = \frac{k_4[e_2][C_7H_8]}{k_5+k_6+k_8[O_2]}$$

$$|O|_{eq} = \frac{2k_1k_3[e_1][O_2]}{(k_{10}+k_{11})[C_7H_8]\{k_3+k_2[e]+k_9[C_7H_8]\}}$$

Inserting these concentrations of the complexes, we get the following rate equations.

$$r_{C_6H_6} = \frac{k_6 \cdot k_4[e_2][C_7H_8]}{k_5+k_6+k_8[O_2]}$$

The experimental equation is

$$r_{C_6H_6} = k'\frac{[C_7H_8][e_2]}{[O_2]} \quad .$$

If $k_5 + k_6$ is small compared to $k_8|O_2|$, we get

$$|C_7H_8^*| \simeq \frac{k_4[e_2][C_7H_8]}{k_8[O_2]}$$

173

In other words, deactivation of the complex is mainly done by oxygen.

$$r_{C_7H_8O} = \frac{k_{10} \cdot 2 \cdot k_1 k_3 [e_1][O_2][C_7H_8]}{(k_{10}+k_{11})[C_7H_8]\{k_3+k_2[e]+k_7[C_7H_8]\}}$$

$$\approx \frac{2k_1 k_3 \cdot k_{10}[e_1][O_2]}{(k_{10}+k_{11})\{k_3+k_7[C_7H_8]\}} \ .$$

In other words, first order with respect to oxygen.

$$r_{C_6H_5OH} = \frac{k_{11} \cdot 2k_1 k_3 [e_1][O_2]}{(k_{10}+k_{11})\{k_3+k_2[e_1]+k_7[C_7H_8]\}}$$

$$\approx \frac{2k_1 k_3 \cdot k_{11}[e_1][O_2]}{(k_{10}+k_{11})\{k_3+k_7[C_7H_8]\}} \ .$$

Since the concentration of activated complex is small, we may neglect the product $[O_2^*][C_7H_8^*]$, i.e. there is little chance of collision.

$$r_{C_7H_6O} = \frac{k_8 \cdot k_4 [e_2][C_7H_8][O_2]}{k_8[O_2]} + \frac{k_9 \cdot k_1 [e_1][O_2][C_7H_8]}{k_3+k_2[e_1]+k_7[C_7H_8]}$$

$$r_{C_7H_6O} \approx \frac{k_1 k_9 \cdot [e_1][O_2][C_7H_8]}{k_3+k_2[e_1]+k_9[C_7H_8]}$$

$$r_{C_7H_6O} \approx \frac{k_1 \cdot k_9 [e_1][O_2][C_7H_8]}{k_3+k_7[C_7H_8]} \ .$$

To proceed further we would need information about the reaction order of toluene for either benzaldehyde or cresol. The question of which reaction controls deactivation of oxygen must be guesswork at this stage. The fact that we have substantial amounts of atomic oxygen

in the reactor (formation of cresol, benzyl alcohol) suggests that k_3 has a low activation energy. This suggests that at low partial pressure of toluene we may observe a first order dependence with respect to toluene for the formation of benzaldehyde.

9.2.6 Selectivity from calculated reaction rates

Finally, we compare the selectivity obtained from the calculated rates with our experimental values. To do this we express the instantaneous selectivity as

$$\phi_i = \frac{r_i}{\sum_{i=1}^{N} r_i}$$

Tables 9.11 to 9.14 give the calculated selectivity for three values of E/N at constant toluene pressure (80 mm Hg). The experimental values for runs 17-28 are plotted in figures 9.14 to 9.17.

As can be seen from the graphs, the agreement is very good. We notice that for low ratios of oxygen to toluene, the main product is benzene. The selectivity is almost independent of E/N.

$P_{O_2}/P_{C_7H_8}$	$E/N \cdot 10^{-15} (V\text{-}cm^{-2})$		
	2.0	4.0	6.0
0.125	0.924	0.875	0.853
0.250	0.759	0.644	0.600
0.375	0.588	0.450	0.405
0.500	0.449	0.318	0.279
0.625	0.345	0.232	0.200
0.750	0.269	0.174	0.149
0.875	0.214	0.135	0.115
1.000	0.173	0.107	0.090
1.250	0.119	0.072	0.060
1.500	0.086	0.051	0.043
1.750	0.065	0.038	0.032
2.000	0.051	0.030	0.025

Table 9.11 Selectivity for benzene ($P_{C_7H_8}$ = 80 mm Hg)

$P_{O_2}/P_{C_7H_8}$	$E/N \cdot 10^{-15}(V\text{-}cm^{-2})$		
	2.0	4.0	6.0
0.125	0.040	0.063	0.074
0.250	0.119	0.170	0.189
0.375	0.196	0.254	0.272
0.500	0.256	0.307	0.321
0.625	0.299	0.340	0.350
0.750	0.328	0.359	0.366
0.875	0.349	0.371	0.375
1.000	0.362	0.378	0.381
1.250	0.378	0.385	0.385
1.500	0.385	0.387	0.385
1.750	0.387	0.386	0.384
2.000	0.389	0.385	0.382

Table 9.12 Selectivity for benzaldehyde($P_{C_7H_8}$ = 80 mm Hg)

$P_{O_2}/P_{C_7H_8}$	$E/N \cdot 10^{-15}(V\text{-}cm^{-2})$		
	2.0	4.0	6.0
0.125	0.028	0.049	0.059
0.250	0.098	0.150	0.171
0.375	0.174	0.242	0.265
0.500	0.239	0.308	0.330
0.625	0.290	0.354	0.373
0.750	0.329	0.387	0.404
0.875	0.359	0.411	0.426
1.000	0.382	0.429	0.442
1.250	0.415	0.454	0.466
1.500	0.438	0.472	0.482
1.750	0.454	0.484	0.493
2.000	0.460	0.494	0.502

Table 9.13 Selectivity for C_7H_8O ($P_{C_7H_8}$ = 80 mm Hg)

$P_{O_2}/P_{C_7H_8}$	$E/N \cdot 10^{-15}(V\text{-}cm^{-2})$		
	2.0	4.0	6.0
0.125	0.008	0.012	0.014
0.250	0.024	0.035	0.039
0.375	0.041	0.054	0.057
0.500	0.055	0.066	0.069
0.625	0.065	0.074	0.077
0.750	0.073	0.080	0.081
0.875	0.078	0.083	0.084
1.000	0.082	0.086	0.086
1.250	0.087	0.089	0.089
1.500	0.090	0.090	0.090
1.750	0.092	0.091	0.091
2.000	0.093	0.091	0.091

Table 9.14 Selectivity for phenol ($P_{C_7H_8}$ = 80 mm Hg)
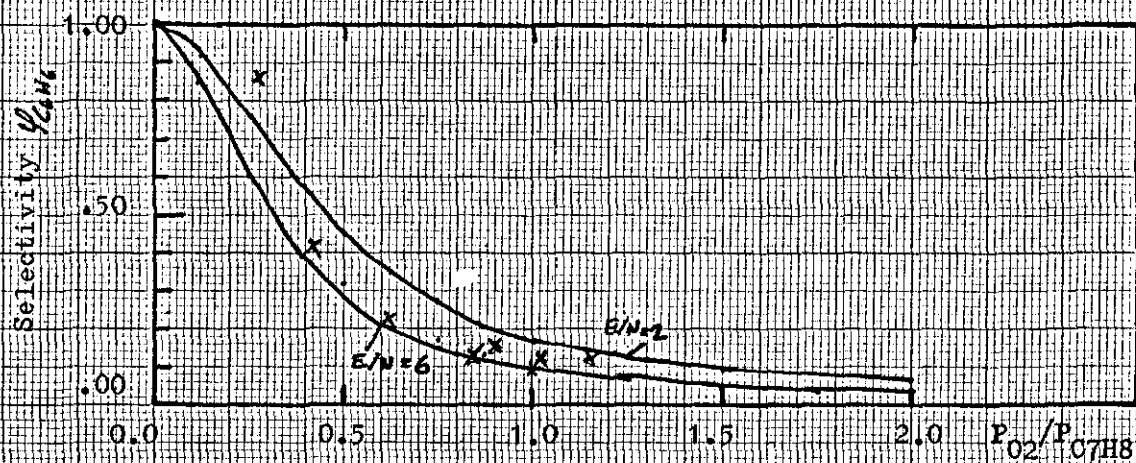
Figure 9.14. Calculated selectivity for benzene
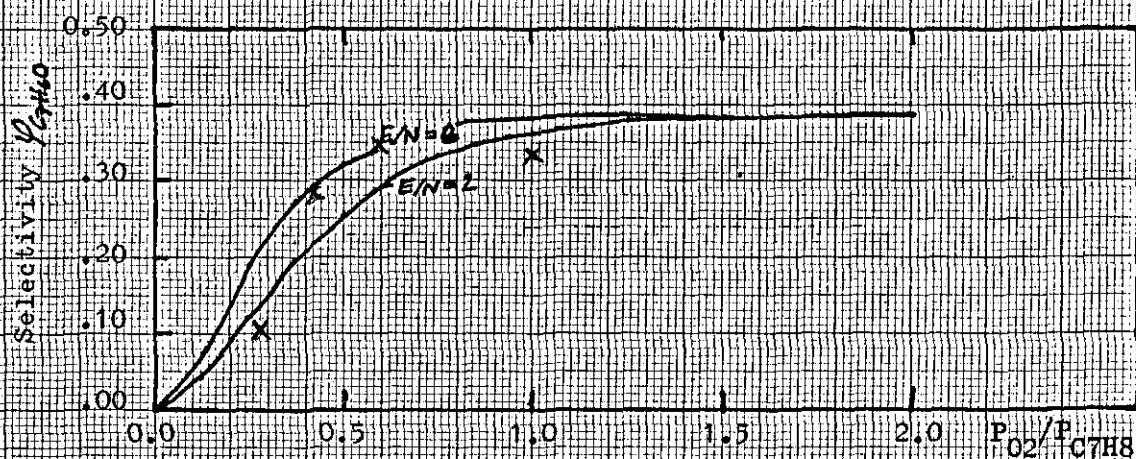
Figure 9.15. Calculated selectivity for benzaldehyde
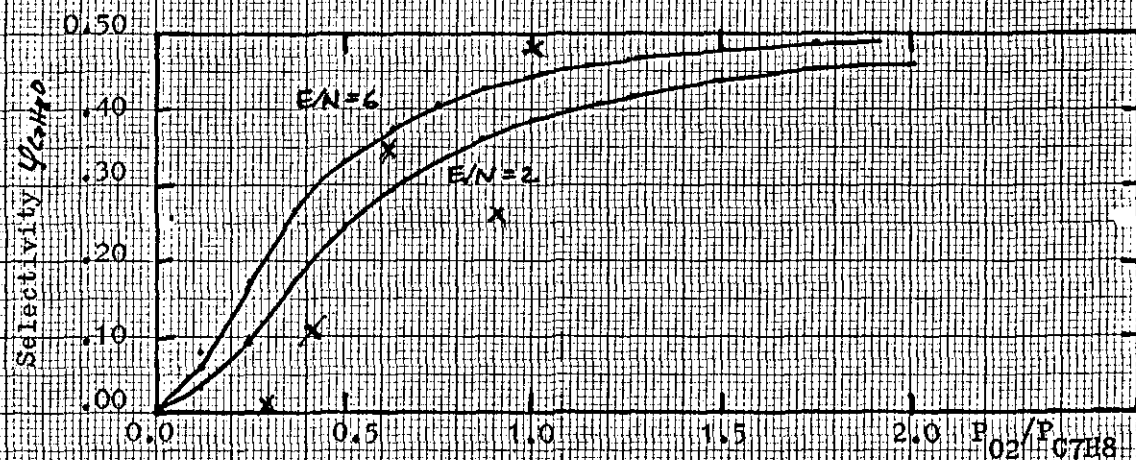
Figure 9.16. Calculated selectivity for C_7H_8O
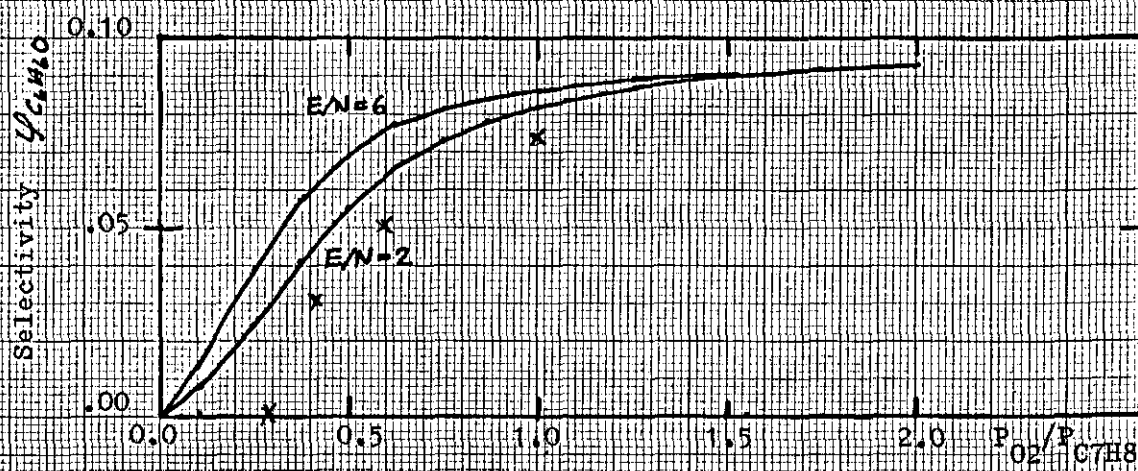
Figure 9.17. Calculated selectivity for phenol

9.2.7 Heat of reaction

Although no temperature increase was noticed, it is still of interest to calculate the heat of reaction for the different reactions. Thermodynamic data of the different reaction products are tabulated in appendix I. No data was found for benzyl alcohol and benzaldehyde, apart from the heat of formation. It was therefore necessary to estimate the thermodynamic values for ΔH^0, and ΔG_r^0. The method used to evaluate these functions is described by Westrum, Sinke and Stull [84]. From the tabulated data we obtained the following values:

$$C_7H_8 \rightarrow C_6H_6 + H_2O + CO_2 \quad \Delta H_{600}^0 = -143.95 \text{ kcal/mole}$$

$$C_7H_8 + O_2 \rightarrow C_7H_7O + H_2O \quad \Delta H_{600}^0 = -77.28 \text{ kcal/mole}$$

$$C_7H_8 + 2O_2 \rightarrow C_6H_6O + H_2O + CO_2 \quad \Delta H_{600}^0 = -186.17 \text{ kcal/mole}$$

$$C_7H_8 + \tfrac{1}{2}O_2 \rightarrow CH_3C_6H_4OH \quad \Delta H_{600}^0 = -41.96 \text{ kcal/mole}$$

$$C_7H_8 + \tfrac{1}{2}O_2 \rightarrow C_6H_5CH_2OH \quad \Delta H_{600}^0 = -43.22 \text{ kcal/mole}$$
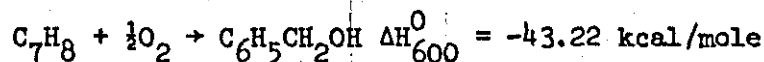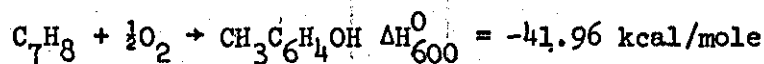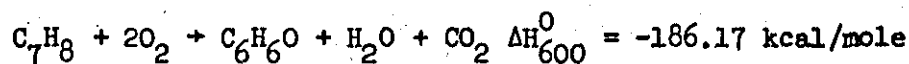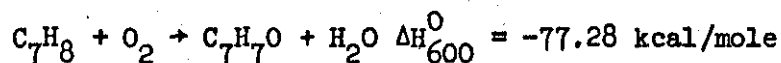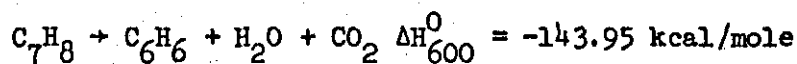
The average selectivity gives the following composition: 15% C_6H_6, 40% C_6H_5CHO, 7% $C_6H_5CH_2OH$, 30% $CH_3C_6H_4OH$, and 8% C_6H_5OH. This gives an average value for the heat of reaction of -83.0 kcal/mole reacted. The heat liberated in the reaction, assuming an average reaction rate of toluene equal to $20 \cdot 10^{-7}$ moles/l.sec., is: $2 \cdot 10^{-6} \times 0.035 \times 83000 = 0.0058$ cal/sec or 0.3 calories per minute. This explains why the temperature effect cannot be seen. The values for the free energy of reaction are all about the same as the heat of reaction, apart from that of cresol and benzyl alcohol for which the values of ΔG_r^0 are -33.6 and -34.2 kcal/mole, respectively.

CHAPTER TEN

CHAPTER 10

CONCLUSIONS AND FUTURE WORK

10.1 GENERAL CONCLUSIONS

The investigation of reactions of toluene and oxygen in an electrical discharge has shown that the chemical reaction is greatly enhanced by the electric field. The disappearance rate of toluene depends on the reactant ratio, the partial pressure of oxygen and the electric field. The effect of the electric field was found to correlate well with the parameter E/N, where N is the number density of the molecules and E is the electric field strength. It was shown that the rate of formation of benzene was proportional to the toluene to oxygen ratio.

The threshold energy of the reaction was estimated at about 10 eV.

The overall reactions occurring in the discharge are represented by the scheme:

$$C_7H_8 + \tfrac{1}{2}O_2 \rightarrow CH_3C_6H_4OH$$

$$C_7H_8 + O_2 \rightarrow C_6H_5CHO + H_2O$$

$$C_7H_8 + 3/2(O_2) \rightarrow C_6H_6 + H_2O + CO_2$$

$$C_7H_8 + 2O_2 \rightarrow C_6H_5OH + H_2O + CO_2$$

$$C_7H_8 + \tfrac{1}{2}O_2 \rightarrow C_6H_5CH_2OH$$
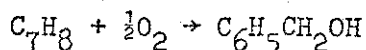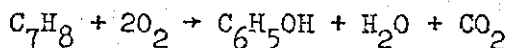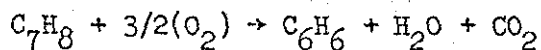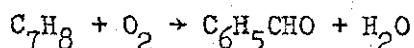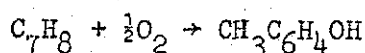
No decomposition of the $\overset{\text{benzene ring}}{\diagup}$ was observed in any of the experiments performed. The electric field was the main controlling factor in production of cresols, phenol, benzyl alcohol, and benzaldehyde, whereas the production of benzene was mainly controlled by the toluene to oxygen ratio.

The features of the discharge were also studied and a model was proposed to explain some unusual characteristics found.

A rate expression was derived for bimolecular reactions in a cold plasma. A comparison was made between the proposed rate expression and the experimental rates. It was found that the simple model agreed extremely well with observed rates.

It was suggested that the chemical reactor should be characterized by two electrical parameters, the electrical capacitance and the Paschen curves. The energy dissipation and the discharge current could be correlated by E/N or at constant temperature by E/p.

It was found that the discharge current could be obtained by filtering of the total current. A comparison was made between discharge current obtained by filtering and discharge current obtained from photographic methods. The average of the photographic current, instantaneous current, was found to agree well with the filtered discharge current.

The energy yield obtained was about 100 grams/kWhr or an energy requirement of about 1 kWhr/mole toluene.

10.2 FUTURE WORK

It is recommended that further work should be carried out to investigate more fully the reaction rates of toluene and oxygen in a capacitive ac discharge reactor with special emphasis directed towards the following effects.

(i) The reaction rate of benzaldehyde and cresols and the dependence on the partial pressure of toluene.

(ii) The effect of inert gases present in reactions of toluene and oxygen, and its effect upon breakdown voltages.

The dilution with an inert gas can provide us with a method of producing electrons of a certain energy. Also it may be interesting from the design aspect to make more accurate determinations of the breakdown and the extinguishing voltages. We feel that such measurements will enable a priori estimations of the discharge current from the Paschen curves for a particular gas.

The effect of frequency is also an area in which future work may be rewarding since this provides us with a way of increasing the power input to an electrical discharge reactor.

It would be interesting to apply the derived rate expression on other reactions in the same type of discharge reactor; for instance, chlorination of hydrocarbons.

Finally, we feel that the only commercial application of the capacitive discharge (cold plasma) will be in the production of active species that would otherwise be unstable or decompose at higher temperatures, although some interesting applications may be found in chemical synthesis of more complex organic molecules.

LITERATURE REFERENCES

LITERATURE REFERENCES

BOOKS

1. McTaggart, F, "Plasma Chemistry in Electrical Discharges". Elsevier, London, 1967

2. Mulcahy, M. R. R., "Gas Kinetics", Nelson & Son Ltd, London, 1973

3. Howatson, A. M., "An Introduction to Gas Discharges", Pergamon Press, London, 1965

4. Llewellyn-Jones, F., "Ionization and Breakdown in Gases", Chapman & Hall, London, 1966

5. Porter, G., "Progress in Reaction Kinetics", Vol. 5, Pergamon Press, London, 1970

6. Burnett, G. M. and NORTH, A. M., "Transfer and Storage of Energy by Molecules", Vol. 1, Wiley, London, 1969

7. Crippen, R. C., "Identification of Organic Compounds with the Aid of Gas Chromatography", McGraw-Hill, London, 1973

8. Pechuro, N. S., "Organic Reactions in Electrical Discharges", Consultants Bureau, New York, 1968

9. Vogel, A. I., "Quantitative Inorganic Analysis", p.944, London, 1961

10. Cornu, A. and Massot, R., "Compilation of Mass Spectral Data", Heyden & Son Ltd, London, 1966

11. Denbigh, K., "Chemical Reactor Theory", Cambridge University Press, London, 1965

12. Levenspiel, O., "Chemical Reaction Engineering", Wiley, New York, 1966

13. Hinshelwood, C. N., "Kinetics of Chemical Change", Oxford University Press, 1949, p.208

14. Fricke, H., Z. Phys. 86 (1933), p.464

15. Meek, J. M. and Craggs, J. D., "Electrical Breakdown of Gases", Oxford University Press, 1953, p.49

16. Loeb, L. B., "Basic Processes of Gaseous Electronics", California, 1955, p.284

17. Kuffel, E., Abdullah, M., "High-voltage Engineering", Pergamon Press, 1966, p.39

18. Gardiner, W. C., "Rates and Mechanism of Chemical Reactions", W. A. Benjamin Inc, New York, 1969

19. Szabo, Z. G., "Advances in the Kinetics of Homogeneous Gas Reactions", Methuen & Co Ltd, London, 1964

JOURNALS

20. Honda, K. and Naito, Y., J. Phys. Soc., Japan, 10 (1955), p.1007

21. Ogawa, K., J. Phys. Soc., Japan, 16 (1961), p.2510

22. Gomet, J. C., Method. Phys. Anal., April (1967), p.71

23. Wexler, S. and Clow, R. P., J. Amer. Chem. Soc. 90 (1968), p.3940

24. Muller, K. G., Chemie-Ing. Techn. 45 (1973), p.122

25. Savage, D., J. Chem. Eng. Univ. Newcastle, No. 5 (1969)

26. Howarth, C. R. and Brown, B. A., J. Chem. Eng. Univ. Newcastle, No. 6 (1970)

27. Herron, J. T., Schiff, H. I., Can. J. Chem. 36 (1958), p.1159

28. Weisbeck, R. and Volkner, A., Z. Angew. Phys. 32 (1971), p.258

29. Streitwieser, A. and Ward, H. R., J. Amer. Chem. Soc. 85 (1963), p.539

30. Kraaijveld, H. J. and Waterman, H. I., Brenn. Chem. 43 (1962), p.15

31. Suhr, H., Z. f. Naturforschg. 23b (1968), p.1559

32. Suhr, H., Angew. Chem. 84 (1972), p.876

33. Jones, G. R. H. and Cvetanovic, R. J., Can. J. Chem. 39 (1961), p.2444

34. Grovenstein, E. and Mosher, A. J., J. Am. Chem. Soc. 92 (1970), p.3811

35. Kumar, R. N. et al., Indian Chem. Eng. 10 (1968), p.16

36. Kröger, C. and Bigorajski, G., Erdöl Kohle 15 (1962), p.109

37. Downie, J. et al., Can. J. Chem. Eng. 39 (1961), p.201

38. Kaeding, W. W., Hydroc. Proc. 43 (1964), p.173, No. 11

39. Dmuchovsky et a-., J. Catal. 4 (1965), p.291

40. Aiba, T. and Freeman, M. P., Ind. Eng. Fundam. 13 (1974), p.179

41. Brown, L. C. and Bell, A. T., Ind. Eng. Chem. Fundam. 13 (1974), p.203

42. Spedding, P. L., Ind. Res. Fell. Rep. No. 5, C.E. 1969, p.17

43. Brooks, B. Sambrook, R.M., J.Appl.Chem.Biotechnol. 22 (1972)p9

44. Townsend, J. S., "The Theory of Ionization of Gases by Collision".
Constable & Co, London, 1910

45. Mearns, A. M., Univ. of Newcastle, private comm.

46. Foner, S. N. and Hudson, R. L., J. Chem. Phys. 25 (1956), p.601

47. Dewhurst, H. A., J. Phys. Chem. 63 (1959), p.1976

48. Harteck, P. and Kopsch, U., Z. Physik Chem. B12 (1931), p.327

49. Weisbeck, R., Chem. Ing. Tech. 43 (1971), p.721

50. Tsakuda, M. and Shida, U., J. Chem. Phys. 77 (1966), p.3130

51. Meek, J. M., Phys. Rev. 57 (1940), p.722

52. Raether, H., Zeit. Phys. 117 (1941), p.375

53. Zeleny, J., J. Appl. Phys. 13 (1942), p.444

54. Fisher, L. H., Phys. Rev. 64 (1943), p.187

55. Brewer, A. K. and Westhaver, J. W., J. Phys. Chem 34 (1930), p.153

56. Peek, F. W., "Dielectric Phenomena in High Voltage Engineering", McGraw-Hill
Co. Inc, 1920

57. Trichel, G. W., Phys. Rev. 55 (1939), p.382

58. Bennett, W. H. and Hudson, G. G. (et al.), Phys. Rev. 60 (1941), p.714

59. Loeb, L. B., "Electrical Coronas", Univ. Calif. Press, 1965

60. Tate, J. T. and Smith, P. T., Phys. Rev. 39 (1932), p.220

61. Kaufman, F., "Progress in Reaction Kinetics", Vol. 1, Pergamon, London,
1961

62. Franklin, F. H., "Electron Impact Phenomena", Acad. Press, N.Y., 1957

63. Reed, R. I., "Ion Production by Electron Impact", Acad. Press, N.Y.,
1962

64. Cvetanovic, R. J., Canad. J. Chem. 34 (1956), p.775

65. Cvetanovic, R. J., Canad. J. Chem. 26 (1958), p.970

66. Cvetanovic, R. J. and Sato, S., Canad. J. Chem. 86 (1958), p.1668

67. Cvetanovic, R. J. and S. Sato, J. Chem. Phys. 30 (1959), p.19

68. Cvetanovic, R. J. and Sato, S., Canad. J. Chem. 37 (1959), p.953

69. Cvetanovic, R. J. and Sato, S., J. Amer. Chem. Soc 81 (1959), p.3223

70. Benson, S. W. and Axworthy, A., J. Chem. Phys. 26 (1957), p.1718

71. Kondratiev, V. N., "Chemical Kinetics of Gas Reactions", Pergamon, London, 1964

72. Burgoyne, J. H., Tang, T. and Newitt, M., Proc. Roy. Soc. A174 (1940), p.379

73. Burgoyne, J. H., Proc. Royal Soc. A175 (1940), p.539

74. Norrish, R. and Taylor, G., Proc. Royal Soc. A238 (1956), p.143

75. Dinan, F., Fridman, S. and Schirmann, P., Advan. in Chem. Ser. 80 (1969), p.289

76. Hay, P., Advan. in Chem. Ser. 80 (1969), p.350

77. Pichler, H. and Obenaus, R., Brennstoff-Chemie 45 (1964), p.97

78. Sasayama, H., J. Soc. Chem. Ind. Janan 46 (1973), p.1229

79. Ssuworow B. et a., Ber. Akad. Wiss. UdSSR 88 (1953), p.79

80. Maxted, E. B., J. Soc. Chem. Ind. 47 (1928), p.101

81. Burgoyne, J. H. and Newitt, D. M., Proc. Roy. Soc. A153 (1936), p.448

82. Vasile, M. and Pottie, R., Advan. in Chem. Ser 80 (1969), p.92

83. Fite, W. L., Advan. in Chem. Ser. 80 (1969), p.1

84. Stull,Westrum,Sinke."The Chemical Thermodynamics of Organic Compounds." Wiley & Sons.London.1969.

APPENDIX I

TABLE 1   IONIZATION POTENTIAL OF HYDROCARBONS |62,63|

Compound	Ionization potential eV	
Methane	13.12	
Ethane	11.65	
Propane	11.21	
Butane	10.80	
Pentane	10.55	
Hexane	10.43	m-Alkanes
Heptane	10.35	
Octane	10.24	
Nonane	10.21	
Decane	10.19	
i-butane	10.79	
i-pentane	10.1	
2-methylbutane	10.6	
i-hexane	10.0	iso-Alkanes
2-methylpentane	10.34	
3-methylpentane	10.30	
2,3-dimethylbutane	10.24	
c-propane	10.23	
c-pentane	11.1	cyclo-Alkanes
c-hexane	10.3	
methylcyclohexane	9.9	
ethylene	10.56	
propylene	9.80	
butene-1	9.72	Alkenes
cis-butene-1	9.34	
trans-butene-1	9.27	
benzene	9.4	
toluene	9.20	
o-xylene	9.0	Aromatics
p-xylene	8.9	
m-xylene	9.0	
oxygen	12.1	
nitrogen	15.60	
hydrogen	15.44	
water	12.67	

PHENOL C_6H_6O (Ideal gas state) Molwt: 94.108

T^0K	cal/(mole deg K)		kcal/mole			log K_p
	C_p^0	S^0	$H^0 - H_{298}^0$	ΔH_f^0	ΔG_f^0	
298	24.75	75.43	0.00	-23.03	-7.86	5.763
300	24.90	75.44	0.05	-23.05	-7.77	5.661
400	32.45	83.82	2.93	-24.09	-2.51	1.369
500	38.64	91.75	6.50	-24.90	2.99	-1.306
600	43.54	99.24	10.61	-25.53	8.62	-3.140
700	47.44	106.26	15.17	-26.01	14.36	-4.482
800	50.62	112.80	20.07	-26.38	20.14	-5.502
900	53.26	118.92	25.27	-26.64	25.98	-6.308
1000	55.49	124.65	30.71	-26.80	31.84	-6.958

Source: Stull, Westrum and Sinke

Table 2 Thermodynamic data for phenol

BENZYL ALCOHOL C_7H_8O (Ideal gas state) Molwt: 108.134

T^0K	cal/(mole deg K)		kcal/mole			log K_p
	C_p^0	S^0	$H^0 - H_{298}^0$	ΔH_f^0	ΔG_f^0	
298	28.2	86.2	0.00	-31.20	-9.54	
300	--	86.4	0.05	-31.23	-9.41	
400	-	95.7	3.32	-32.84	-1.89	
500	-	104.7	7.37	-34.16	6.01	
600	-	113.4	12.12	-35.20	14.14	
700	-	121.7	17.51	-35.99	22.43	

Source: Estimated Values, Janz,"Thermodynamic Properties of Organic Compounds", London, 1967, Academic Press.

Table 3 Thermodynamic data for benzyl alcohol

O-CRESOL   (Ideal gas state)   Molwt: 108.134

T^0K	cal/(mole deg K)		kcal/mole			log K_p
	c_p^0	S^0	$H^0 - H_{298}^0$	ΔH_f^0	ΔG_f^0	
298	31.15	85.47	0.00	-30.74	-8.86	6.491
300	31.31	85.67	0.06	-30.77	-8.72	6.353
400	39.74	95.86	3.63	-32.07	-1.16	0.635
500	46.91	105.52	7.97	-33.11	6.69	-2.923
600	52.77	114.61	12.96	-33.94	14.72	-5.362
700	57.56	123.11	18.49	-34.58	22.89	-7.147
800	61.55	131.06	24.44	-35.06	31.13	-8.503
900	65.25	138.53	30.78	-35.38	39.43	-9.573
1000	68.82	145.99	37.49	-35.50	.45.75	-10.436

Source: Stull, Westrum and Sinke, "The Chemical Thermodynamics
of Organic Compounds", Wiley & Sons, 1969.

Table 4   Thermodynamic properties of o-cresol

BENZALDEHYDE C_7H_6O

T^0K	cal/(mole deg K)		kcal/mole			log K_p
	c_p^0	S^0	$H^0 - H_{298}^0$	ΔH_f^0	ΔG_f^0	
298	26.0	82.3	0.00	-7.60	5.92	
300	26.1	82.5	0.05	-7.62	6.00	
400	33.0	90.9	3.02	-8.83	10.72	
500	39.3	99.0	6.64	-9.87	15.74	
600	45.0	106.7	10.86	-10.76	20.94	
700	49.9	114.0	15.62	-11.48	26.27	

Source: Estimated Values, G. Janz, "Thermodynamic Properties of
Organic Compounds", Academic Press, London 1967.

Table 5   Thermodynamic properties for benzaldehyde

WATER H_2O (Ideal gas state) Molwt: 18.016

$T^0 K$	cal/(mole deg K)		kcal/mole			
	C_p^0	S^0	$H^0 - H_{298}^0$	ΔH_f^0	ΔG_f^0	$\log K_p$
298	8.03	45.11	0.00	−57.80	−54.64	40.049
200	8.03	45.16	0.02	−47.80	−54.62	39.788
400	8.19	47.49	0.83	−58.04	−53.52	29.241
500	8.42	49.35	1.66	−58.28	−53.36	22.887
600	8.68	50.90	2.52	−58.50	−51.16	18.634
700	8.95	52.26	3.40	−58.71	−49.92	15.585
800	9.25	53.48	48.10	−58.91	−48.65	13.290
900	9.55	54.38	48.76	−59.08	−47.36	11.499
1000	9.85	55.61	49.39	−59.24	−46.04	10.062

Source: Stull, Westrum and Sinke

Table 6 Thermodynamic properties of water

CARBON DIOXIDE CO_2 (Ideal gas state) Molwt: 44.010

$T^0 K$	cal/(mole deg K)			kcal/mole			$\log K_p$
	C_p^0	S^0	$-(G^0 - H_{298}^0)/T$	$H^0 - H_{298}^0$	ΔH_f^0	ΔG_f^0	
298	8.87	51.07	51.07	0.00	−94.05	−94.26	69.091
300	8.89	51.13	51.08	0.02	−94.05	−94.26	68.666
400	9.87	53.83	51.44	0.96	−94.07	−94.33	51.535
500	10.66	56.12	52.15	1.99	−94.09	−94.39	41.255
600	11.31	58.12	52.98	3.09	−94.12	−94.45	34.400
700	11.84	59.90	53.84	4.25	−94.17	−94.50	29.503
800	12.29	61.51	54.70	5.45	−94.22	−94.54	25.826
900	12.66	62.98	55.54	6.70	−94.27	−94.58	22.966
1000	12.97	64.33	56.36	7.98	−94.32	−94.61	20.676

Source: Stull, Westrum and Sinke

Table 7 Thermodynamic properties of carbon dioxide

TOLUENE C$_7$H$_8$ (Ideal gas state) Molwt: 92.134

T^{0}K	cal/(mole deg K)			kcal/mole			log K$_p$
	C$_p^0$	S^0	$-(G^0-H_{298}^0)/T$	H^0-H$_{298}^0$	ΔH_f^0	ΔG_f^0	
298	24.77	76.64	76.64	0.00	11.95	29.16	-21.376
300	24.94	76.80	76.65	0.05	11.92	27.27	-21.320
400	33.48	85.17	77.73	2.98	10.34	35.30	-19.287
500	40.98	93.47	80.05	6.71	9.05	41.70	-18.225
600	47.20	101.51	82.96	11.13	8.02	48.32	-17.599
700	52.33	109.18	86.16	16.12	7.24	55.11	-17.205
800	65.61	116.45	89.50	21.57	6.65	61.98	-16.931
900	60.23	123.33	92.88	27.41	6.24	68.93	-16.736
1000	63.32	129.85	96.25	33.60	6.01	75.91	-16.589

Source: Stull, Westrum and Sinke, 1967

Table 8   Thermodynamic properties of toluene

BENZENE C$_6$H$_6$ (Ideal gas state) Molwt: 78.108

T^{0}K	cal/(mole deg K)		kcal/mole			log K$_p$
	C$_p^0$	S^0	H^0-H$_{298}^0$	ΔH_f^0	ΔG_f^0	
298	19.52	64.34	0.00	19.82	30.99	-22.714
300	19.65	64.35	0.04	19.79	31.06	-22.623
400	26.74	71.11	2.37	18.56	35.01	-19.126
500	32.80	77.75	5.36	17.54	39.24	-17.152
600	37.74	84.18	8.89	16.71	43.66	-15.901
700	41.75	90.31	12.87	16.04	48.21	-15.051
800	45.06	96.11	17.22	15.51	52.84	-14.434
900	47.83	101.58	21.86	15.10	57.53	-13.970
1000	50.16	106.74	79.98	26.77	14.82	-13.608

Source: Stull, Westrum and Sinke, 1967

Table 9   Thermodynamic properties of benzene

195

Bond	D(R-X)	Bond	D(R-X)
		kcal/mole	
H-H	104	H_3C-CH_3	88
H-CH$_3$	103	$H_3C-C_2H_5$	85
H-C$_2$H$_5$	98	$H_3C-C_2H_4$	26
H-C$_2$H$_4$	39	$H_3C-COCH_3$	81
H-CH(CH$_3$)$_2$	94	H_3C-CO	11
H-CHCH$_2$	106	$C=O$	257
H-CH$_2$CHCH$_2$	87	$OC=O$	127
H-C$_6$H$_5$	110	H_3C-OH	90
H-CH$_2$C$_6$H$_5$	85	H_3C-F	108
H-COCH$_3$	86	H_3C-Cl	81
H-NH$_2$	104	$N\equiv N$	226
H-O	102	H_2N-NH_2	59
H-O$_2$	47	$N=O$	151
H-OH	119	$O=O$	119
H-OCH$_3$	100	HO-OH	51
H-F	136	$O=SO$	132
H-SH	91	F-F	39
H-Cl	103	Cl-Cl	58
H-Br	87	Br-Br	46
H-I	71	I-I	36

Table.10.   Bond dissociation energies

APPENDIX II

Degrees of freedom for numerator

	1	2	3	4	5	6	7	8	9	10	12	15	20	24	30	40	60	120	∞
1	161	230	216	225	230	234	237	239	241	242	244	246	248	249	250	251	252	253	254
2	18.5	19.0	19.2	19.2	19.3	19.3	19.4	19.4	19.4	19.4	19.4	19.4	19.4	19.5	19.5	19.5	19.5	19.5	19.5
3	10.1	9.55	9.28	9.12	9.01	8.94	8.89	8.85	8.81	8.79	8.74	8.70	8.66	8.64	8.62	8.59	8.57	8.55	8.53
4	7.71	6.94	6.59	6.39	6.26	6.16	6.09	6.04	6.00	5.96	5.91	5.86	5.80	5.77	5.75	5.72	5.69	5.66	5.63
5	6.61	5.79	5.41	5.19	5.05	4.95	4.88	4.82	4.77	4.74	4.68	4.62	4.56	4.53	4.50	4.46	4.43	4.40	4.37
6	5.99	5.14	4.76	4.53	4.39	4.28	4.21	4.15	4.10	4.06	4.00	3.94	3.87	3.84	3.81	3.77	3.74	3.70	3.67
7	5.59	4.74	4.35	4.12	3.97	3.87	3.79	3.73	3.68	3.64	3.57	3.51	3.44	3.41	3.38	3.34	3.30	3.27	3.23
8	5.32	4.46	4.07	3.84	3.69	3.58	3.50	3.44	3.39	3.35	3.28	3.22	3.15	3.12	3.08	3.04	3.01	2.97	2.93
9	5.12	4.26	3.86	3.63	3.48	3.37	3.29	3.23	3.18	3.14	3.07	3.01	2.94	2.90	2.86	2.83	2.79	2.75	2.71
10	4.96	4.10	3.71	3.48	3.33	3.22	3.14	3.07	3.02	2.98	2.91	2.85	2.77	2.74	2.70	2.66	2.62	2.58	2.54
11	4.84	3.98	3.59	3.36	3.20	3.09	3.01	2.95	2.90	2.85	2.79	2.72	2.65	2.61	2.57	2.53	2.49	2.45	2.40
12	4.75	3.89	3.49	3.26	3.11	3.00	2.91	2.85	2.80	2.75	2.69	2.62	2.54	2.51	2.47	2.43	2.38	2.34	2.30
13	4.67	3.81	3.41	3.18	3.03	2.92	2.83	2.77	2.71	2.67	2.60	2.53	2.46	2.42	2.38	2.34	2.30	2.25	2.21
14	4.60	3.74	3.34	3.11	2.96	2.85	2.76	2.70	2.65	2.60	2.53	2.46	2.39	2.35	2.31	2.27	2.22	2.18	2.13
15	4.54	3.68	3.29	3.06	2.90	2.79	2.71	2.64	2.59	2.54	2.48	2.40	2.33	2.29	2.25	2.20	2.16	2.11	2.07
16	4.49	3.63	3.24	3.01	2.85	2.74	2.66	2.59	2.54	2.49	2.42	2.35	2.28	2.24	2.19	2.15	2.11	2.06	2.01
17	4.45	3.59	3.20	2.96	2.81	2.70	2.61	2.55	2.49	2.45	2.38	2.31	2.23	2.19	2.15	2.10	2.06	2.01	1.96
18	4.41	3.55	3.16	2.93	2.77	2.66	2.58	2.51	2.46	2.41	2.34	2.27	2.19	2.15	2.11	2.06	2.02	1.97	1.92
19	4.38	3.52	3.13	2.90	2.74	2.63	2.54	2.48	2.42	2.38	2.31	2.23	2.16	2.11	2.07	2.03	1.98	1.93	1.88
20	4.35	3.49	3.10	2.87	2.71	2.60	2.51	2.45	2.39	2.35	2.28	2.20	2.12	2.08	2.04	1.99	1.95	1.90	1.84
21	4.32	3.47	3.07	2.84	2.68	2.57	2.49	2.42	2.37	2.32	2.25	2.18	2.10	2.05	2.01	1.96	1.92	1.87	1.81
22	4.30	3.44	3.05	2.82	2.66	2.55	2.46	2.40	2.34	2.30	2.23	2.15	2.07	2.03	1.98	1.94	1.89	1.84	1.78
23	4.28	3.42	3.03	2.80	2.64	2.53	2.44	2.37	2.32	2.27	2.20	2.13	2.05	2.01	1.96	1.91	1.86	1.81	1.76
24	4.26	3.40	3.01	2.78	2.62	2.51	2.42	2.36	2.30	2.25	2.18	2.11	2.03	1.98	1.94	1.89	1.84	1.79	1.73
25	4.24	3.39	2.99	2.76	2.60	2.49	2.40	2.34	2.28	2.24	2.16	2.09	2.01	1.96	1.92	1.87	1.82	1.77	1.71
30	4.17	3.32	2.92	2.69	2.53	2.42	2.33	2.27	2.21	2.16	2.09	2.01	1.93	1.89	1.84	1.79	1.74	1.68	1.62
40	4.08	3.23	2.84	2.61	2.45	2.34	2.25	2.18	2.12	2.08	2.00	1.92	1.84	1.79	1.74	1.69	1.64	1.58	1.51
60	4.00	3.15	2.76	2.53	2.37	2.25	2.17	2.10	2.04	1.99	1.92	1.84	1.75	1.70	1.65	1.59	1.53	1.47	1.39
120	3.92	3.07	2.68	2.45	2.29	2.18	2.09	2.02	1.96	1.91	1.83	1.75	1.66	1.61	1.55	1.50	1.43	1.35	1.25
∞	3.84	3.00	2.60	2.37	2.21	2.10	2.01	1.94	1.88	1.83	1.75	1.67	1.57	1.52	1.46	1.39	1.32	1.22	1.00

Degrees of freedom for denominator

Degrees of freedom for numerator

	1	2	3	4	5	6	7	8	9	10	12	15	20	24	30	40	60	120	∞
1	4052	5000	5403	5625	5764	5859	5928	5982	6023	6056	6106	6157	6209	6235	6261	6287	6313	6339	6366
2	98.5	99.0	99.2	99.2	99.3	99.3	99.4	99.4	99.4	99.4	99.4	99.4	99.4	99.5	99.5	99.5	99.5	99.5	99.5
3	34.1	30.8	29.5	28.7	28.2	27.9	27.7	27.5	27.3	27.2	27.1	26.9	26.7	26.6	26.5	26.4	26.3	26.2	26.1
4	21.2	18.0	16.7	16.0	15.5	15.2	15.0	14.8	14.7	14.5	14.4	14.2	14.0	13.9	13.8	13.7	13.7	13.6	13.5
5	16.3	13.3	12.1	11.4	11.0	10.7	10.5	10.3	10.2	10.1	9.89	9.72	9.55	9.47	9.38	9.29	9.20	9.11	9.02
6	13.7	10.9	9.78	9.15	8.75	8.47	8.26	8.10	7.98	7.87	7.72	7.56	7.40	7.31	7.23	7.14	7.06	6.97	6.88
7	12.2	9.55	8.45	7.85	7.46	7.19	6.99	6.84	6.72	6.62	6.47	6.31	6.16	6.07	5.99	5.91	5.82	5.74	5.65
8	11.3	8.65	7.59	7.01	6.63	6.37	6.18	6.03	5.91	5.81	5.67	5.52	5.36	5.28	5.20	5.12	5.03	4.95	4.86
9	10.6	8.02	6.99	6.42	6.06	5.80	5.61	5.47	5.35	5.26	5.11	4.96	4.81	4.73	4.65	4.57	4.48	4.40	4.31
10	10.0	7.56	6.55	5.99	5.64	5.39	5.20	5.06	4.94	4.85	4.71	4.56	4.41	4.33	4.25	4.17	4.08	4.00	3.91
11	9.65	7.21	6.22	5.67	5.32	5.07	4.89	4.74	4.63	4.54	4.40	4.25	4.10	4.02	3.94	3.86	3.78	3.69	3.60
12	9.33	6.93	5.95	5.41	5.06	4.82	4.64	4.50	4.39	4.30	4.16	4.01	3.86	3.78	3.70	3.62	3.54	3.45	3.36
13	9.07	6.70	5.74	5.21	4.86	4.62	4.44	4.30	4.19	4.10	3.96	3.82	3.66	3.59	3.51	3.43	3.34	3.25	3.17
14	8.86	6.51	5.56	5.04	4.70	4.46	4.28	4.14	4.03	3.94	3.80	3.66	3.51	3.43	3.35	3.27	3.18	3.09	3.00
15	8.68	6.36	5.42	4.89	4.56	4.32	4.14	4.00	3.89	3.80	3.67	3.52	3.37	3.29	3.21	3.13	3.05	2.96	2.87
16	8.53	6.23	5.29	4.77	4.44	4.20	4.03	3.89	3.78	3.69	3.55	3.41	3.26	3.18	3.10	3.02	2.93	2.84	2.75
17	8.40	6.11	5.19	4.67	4.34	4.10	3.93	3.79	3.68	3.59	3.46	3.31	3.16	3.08	3.00	2.92	2.83	2.75	2.65
18	8.29	6.01	5.09	4.58	4.25	4.01	3.84	3.71	3.60	3.51	3.37	3.23	3.08	3.00	2.92	2.84	2.75	2.66	2.57
19	8.19	5.93	5.01	4.50	4.17	3.94	3.77	3.63	3.52	3.43	3.30	3.15	3.00	2.92	2.84	2.76	2.67	2.58	2.49
20	8.10	5.85	4.94	4.43	4.10	3.87	3.70	3.56	3.46	3.37	3.23	3.09	2.94	2.86	2.78	2.69	2.61	2.52	2.42
21	8.02	5.78	4.87	4.37	4.04	3.81	3.64	3.51	3.40	3.31	3.17	3.03	2.88	2.80	2.72	2.64	2.55	2.46	2.36
22	7.95	5.72	4.82	4.31	3.99	3.76	3.59	3.45	3.35	3.26	3.12	2.98	2.83	2.75	2.67	2.58	2.50	2.40	2.31
23	7.88	5.66	4.76	4.26	3.94	3.71	3.54	3.41	3.30	3.21	3.07	2.93	2.78	2.70	2.62	2.54	2.45	2.35	2.26
24	7.82	5.61	4.72	4.22	3.90	3.67	3.50	3.36	3.26	3.17	3.03	2.89	2.74	2.66	2.58	2.49	2.40	2.31	2.21
25	7.77	5.57	4.68	4.18	3.86	3.63	3.46	3.32	3.22	3.13	2.99	2.85	2.70	2.62	2.53	2.45	2.36	2.27	2.17
30	7.56	5.39	4.51	4.02	3.70	3.47	3.30	3.17	3.07	2.98	2.84	2.70	2.55	2.47	2.39	2.30	2.21	2.11	2.01
40	7.31	5.18	4.31	3.83	3.51	3.29	3.12	2.99	2.89	2.80	2.66	2.52	2.37	2.29	2.20	2.11	2.02	1.92	1.80
60	7.08	4.98	4.13	3.65	3.34	3.12	2.95	2.82	2.72	2.63	2.50	2.35	2.20	2.12	2.03	1.94	1.84	1.73	1.60
120	6.85	4.79	3.95	3.48	3.17	2.96	2.79	2.66	2.56	2.47	2.34	2.19	2.03	1.95	1.86	1.76	1.66	1.53	1.38
∞	6.63	4.61	3.78	3.32	3.02	2.80	2.64	2.51	2.41	2.32	2.18	2.04	1.88	1.79	1.70	1.59	1.47	1.32	1.00

Degrees of freedom for denominator

Interpolation should be performed using reciprocals of the degrees of freedom.

Table 1   F-distribution

Time sec.	Net time sec.	Voltage mV	Net voltage mV	E(θ)	θ
0	–	134	–		
20	–	137			
40	10	144	0		
60	30	138	0		
80	50	130	0		
100	70	130	0		
120	90	130	0		
140	110	125	0		
160	130	123	0		
180	150	122	0		
200	170	121	0		
220	190	116	0		
240	210	115	0		
260	230	114	0		
280	250	114	0		
300	270	113	0		
320	290	118	5	.00	.65
340	310	222	109	.07	.69
360	330	704	591	.38	.73
380	350	1725	1612	1.05	.77
400	370	2977	2864	1.86	.81
420	390	3727	3614	2.35	.85
440	410	4276	4163	2.71	.89
460	430	4430	4317	2.81	.94
480	450	4218	4105	2.75	0.978
500	470	3756	3643	2.37	1.018
520	490	3147	3034	1.97	1.059
540	510	2300	2187	1.42	1.100
560	530	1990	1877	1.22	1.141
580	550	1525	1412	0.92	1.181
600	570	1157	1044	0.68	1.222
620	590	888	775	0.50	1.262
640	610	690	577	0.38	1.303
660	630	540	427	0.28	1.344
680	650	434	321	0.21	1.385
700	670	358	245	0.16	1.426
720	690	301	188	0.12	1.466
740	710	258	145	0.09	1.507
760	730	227	114	0.07	1.55
780	750	302	89	0.06	1.59
800	770	184	71	0.05	1.63
820	790	169	56	0.04	1.67
840	810	159	46	0.03	1.71
860	830	150	37	0.02	1.75
880	850	142	29	0.02	1.79
900	870	137	24	0.01	1.83
920	890	130	17	0.01	1.87
940	910	127	14	0.01	1.91

Table 2 Residence time distribution

P mm Hg	V_{ign} volts	V_{ext} volts	P mm Hg	V_{ign} volts	V_{ext} volts
34.0	800	750	327.0	5300	4700
43.0	1150	950	363.0	5800	5200
55.5	1500	1350	381.0	6000	5400
67.0	1550	1400	418.0	6800	5700
78.5	1700	1500	424.0	6700	6100
111.5	2000	1800	475.0	7400	6900
126.5	2150	1950	523.0	6800	7200
150.0	2250	2050	534.0	8200	7500
161.5	2500	2250	605.0	8500	8400
184.0	2600	2450	605.0	8700	8500
199.5	2800	2600	673.0	9400	9400
225.5	3250	2950	675.0	9200	9100
251.0	3500	3100	750.0	9900	9900
273.0	3800	3500			

Table 3 Breakdown voltage in oxygen/toluene at 20°C

250°C			300°C			350°C		
P mm Hg	V_{ign} volts	V_{ext} volts	P mm Hg	V_{ign} volts	V_{ext} volts	P mm Hg	V_{ign} volts	V_{ext} volts
69.0	1350	1000	52.0	1000	900	50.0	800	790
95.5	1500	1200	72.0	1150	1050	67.5	900	890
121.0	1675	1350	90.0	1300	1200	115.5	1200	1175
148.5	1850	1550	106.0	1400	1300	156.5	1400	1390
168.0	2000	1650	143.0	1650	1550	174.5	1500	1490
197.5	2250	1775	128.0	1500	1400	200.0	1625	1600
			175.0	1850	1750			
			197.0	1950	1800			

Table 4 Breakdown voltage in toluene and oxygen

```
LIST
SIMUL    08:25 PM           06-NOV-74
5   OPEN "DATA.SIM" AS FILE 1
8   OPEN "SCRAP" AS FILE 2
10  DIM #2,U(1000),C(1000),V(1000)
20  DIM #1,X(1000),Y(1000),S(2)
30  PRINT"GIVE VALUES FOR R1,C1,R2,C2,U0,W"
40  INPUT R1,C1,R2,C2,U0,W1
50  PRINT" GIVE VALUES FOR UI,UE"
60  INPUT V1,V2
65  Z1=R1*C1+R2*C1/SQR((W1*R2*C2)**2+1)
70  Z2=1+(W1*Z1)**2 :   U3=0
75   Z3=SQR((W1*R2*C2)**2+1)
80  FOR I=1 TO 1000
90  W2=2E-5*I*W1 : W5=2E-5*I/Z1
100 IF W5>50 THEN W5=50
110 U(I)=U0/Z2*(COS(W2)+W1*Z1*SIN(W2)-EXP(-W5))-U3
120 C(I)=(W1*Z1)**2*COS(W2)-W1*Z1*SIN(W2)+EXP(-W5)
130 C(I)=C(I)*U0*C1/Z1/Z2
140 V(I)=C(I)*R2/Z3
150 IF ABS(U(I))>V1 THEN 200
160 GOTO 500
200 K=I+1 : S1=U(I)/ABS(U(I)) : V3=(V2*(3+S1)+V1*(1-S1))/4
205 U(I)=V3*S1 : C(I)=S1*(V1-V3)/Z1*C1
210 V(I)=V(I)+R2/(R1+R2)*(V1-V3)*S1
220 U2=S1*(V1-V3) :   U3=U3+U2
300 FOR J=K TO 1000
310 I1=J+1-K : W4=J*2E-5*W1 : W5=I1*2E-5
315 W6=50
330 U(J)=U0/Z2*(COS(W4)+W1*Z1*SIN(W4)-EXP(-W6))-U3
340 C(J)=(W1*Z1)**2*COS(W4)-W1*Z1*SIN(W4)+EXP(-W6)
345 C(J)=C(J)*U0*C1/Z1/Z2
348 W7=(R1+R2)*W5/R1/R2/C2 : IF W7>50 THEN W7=50
350 V(J)=C(J)*R2/Z3+R2/(R1+R2)*(V1-V3)*S1*EXP(-W7)
360 I=J
370 IF ABS(U(J))<V3 THEN 500
380 IF ABS (U(J))>V1 THEN 200
390 NEXT J
500 NEXT I
510 FOR I=1 TO 1000
520 X(I)=2E-5*I*100
530 Y(I)=U(I)/2000+2
540 NEXT I
550 S(1)=2 : S(2)=5 : CLOSE 1 : KILL "SCRAP"
999 END
```

Figure 5.   Computer program for discharge simulation

```
LIST
STAT      02:15 PM         21-AUG-75
50  DATA 4.16,4.76,4.29,4.04,4.14,4.17,4.17,4.20,4.19RENAME
55   DATA 200,190,220
60  DATA 90,90,100,100,110,110,120,120,130,130
70   DATA 0.65,0.76,0.673,0.735,0.74,0.9,0.71,0.905,0.731
75   DATA 0.875,0.76,0.85,0.737,0.9,0.8,0.932
90   DATA 80,80,90,90,100,100,110,110,120,120,130,130,140
95   DATA 140,150,150
100!   MASTER PROGRAM REGRESSION
110   DIM Y(16),S(5),R(5),U(5),B(5),A(4,5),X(4,16)
115   PRINT"VALUES FOR N,M?":INPUT N,M
120   PRINT" START MATRIX X? X(1,1),X(1,2),,,,,"
124   MAT READ X(N,M)
129   MAT READ Y(M)
130   GOTO 145
135   PRINT"NEW X MATRIX?":MAT INPUT X(N,M)
140   INPUT "Y";Y(M)
145   N1=N
150   GO SUB 600!       MEAN
155   GOSUB  500!        MATRIX SETUP
160   GOSUB  700!        SQUARE
165   GOSUB  800!        MATRIX INVERSION
170   GOSUB 750!      MAT MULT
175   T4=0 : FOR I=1 TO N
180   T4=T4+B(I)*R(I)  : NEXT I
185   T4=T2-T4 : T4=T4/(M-N-1)
190   T4=SQR(T4)
192   PRINT:PRINT
195   PRINT" STANDARD ERROR IN Y=";T4
197   GOSUB 900!
200   PRINT:PRINT"MORE AVALUES?  YES=1   NO=0"
205   INPUT T6
210   IF T6=1 THEN 135
215   GOTO 999
500!      MATRIX SET-UP
505   FOR I=1 TO N1: FOR J=1 TO N1
510   A(I,J)=0  : FOR K=1 TO M
515   A(I,J)=A(I,J)+(X(I,K)-S(I))*(X(J,K)-S(J))
518   NEXT K:NEXT J:NEXT I
520   IF T7=M-N-1 THEN 525
521   PRINT:PRINT:PRINT"MATRIX SET-UP"
522   FORI=1 TO N1:FOR J=1 TO N1
523   PRINT"                 A(";I;J;")=";A(I,J)
524   NEXT J:NEXT I
525   RETURN
600!       SUBROUTINE MEAN VALUES
605   FOR I=1 TO N1 :S(I)=0 : NEXT I
610   FOR I=1 TO N1 : T1=0
615   FOR J=1 TO M
620   S(I)=S(I)+X(I,J)  ! SUM X
625   T1=T1+Y(J)         ! SUM Y
630   NEXT J
635   S(I)=S(I)/M        !  MEAN X
640   NEXT I
642   T1=T1/M   !   MEAN Y
644   IF T7=M-N-1 THEN 650
646   PRINT:PRINT:PRINT"MEAN VALUES"
647   FOR I=1 TO N1
648   PRINT"           X(";I;")=";S(I)
649   NEXT I: PRINT"          Y=";T1
650   RETURN
```

Figure 6.   Computer program for regression analysis

```
705   FOR I=1 TO N : R(I)=0 : NEXT I
710   FOR I=1 TO N1 : T2=0 : FOR J=1 TO M
715   R(I)=R(I)+(Y(J)-T1)*(X(I,J)-S(I)) !SQUARE XY
720   U(I)=U(I)+(X(I,J)-S(I))↑2            !SQUARE X↑2
725   T2=T2+(Y(J)-T1)↑2  : NEXT J
728   NEXT I
730   IF T7=M-N-1 THEN 735
731   PRINT:PRINT:PRINT" SQUARES"
732   FOR I=1 TO N
733   PRINT"            X(";I;")↑2=";U(I),"X(";I;")*Y=";R(I)
734   NEXT I:PRINT"            Y↑2=";T2
735   RETURN
750!          MATRIX MULTIPLICATION
752   T8=0
755   FOR I=1 TO N1 : T6=0
760   FOR J=1 TO N1
765   T6=T6+A(I,J)*R(J)
770   NEXT J : B(I)=T6
773   T8=T8+S(I)*B(I)
775   NEXT I
776   IF T7=M-N-1 THEN 785
777   PRINT:PRINT:PRINT"COEFFICIENTS FOR X"
778   FOR I=1 TO N1
780   PRINT"                  X(";I;")=";B(I)
782   NEXT I
784   PRINT"                  X( 0 )=";T1-T8
785   RETURN
800!          SUBROUTINE MATRIX INVERSION
805   FOR I=1 TO N1
810   T3=A(I,I) : A(I,I)=1
815   FOR J=1 TO N1:A(I,J)=A(I,J)/T3
820   NEXT J:FOR K=1 TO N1
825   IF K=I THEN 845
830   T3=A(K,I):A(K,I)=0
835   FOR J=1 TO N1: A(K,J)=A(K,J)-T3*A(I,J)
840   NEXT J
845   NEXT K
848   NEXT I
850   IF T7=M-N-1 THEN 855
851   PRINT:PRINT:PRINT" MATRIX INV"
852   FOR I=1 TO N1:FOR J=1 TO N1
853   PRINT"          A(";I;J;")=";A(I,J)
854   NEXT J:NEXT I
855   RETURN
900!          SUBROUTINE  VARIANCE ANALYSIS
902   PRINT:PRINT
905   PRINT"REGRESSION        SS        DF        MS        F"
910   F$="#####.####    ##    #####.####    ###.##  "
915   T4=0 :FOR I=1 TO N1
920   T4=T4+B(I)*R(I) : NEXT I
925   T7=M-N-1
927   IF N1< N THEN 930
928   B(N)=T4
930 PRINT"X1-X";N1,:PRINT USINGF$,T4,N1,T4/N1,T4/N1*T7/(T2-B(N))
932   N1=N1-1
935   IF N1=N-1 THEN 950
936   T9=B(N)-T4
940 PRINT"INCREMENT",:PRINTUSINGF$,T9,1,T9,T9/(T2-B(N))*T7
945   PRINT"RESIDUAL",:PRINT USINGF$,T2-B(N),T7,(T2-B(N))/T7
947   GOTO 970
950   B(N)=T4 : GOSUB 600
955   GOSUB 500 : GOSUB 700
960   GOSUB 800 : GOSUB 750
965   GOTO 915
970   PRINT"TOTAL",:PRINT USING F$,T2,M-1
975   RETURN
999   END
```

READY

CALIBRATION OF INLET FLOWMETER
FOR OXYGEN

$P_{or} = 741.5$ Torr.

$t_1 = 19.5 \,°C$

$P_1 = 766.8$ Torr.

$\rho_0 = \dfrac{766.8 \cdot 273}{760 \cdot}$

G.O2/MIN

0.4

0.3

0.2

0.1

$\dfrac{\Delta P_r \cdot P_0}{RT}$

h

1   2   3   4   5

202 a

CALIBRATION OF OUTLET FLOWMETER FOR OXYGEN

$\dfrac{\Delta P_1}{P_2}$ [mm/torr]

0.8

0.6

0.4

0.2

0

Ⅱ

ΔP_{π} [mm

0   10   20

APPENDIX III

EXPERIMENTS IN A BATCH REACTOR

EXPERIMENTS IN A BATCH REACTOR

	Run number	1	2	3	4	5
REACTOR	Temperature (^{o}C)	245	260	255	260	260
	Residence time (min)	8	10	10	6	6
	Partial pressure O2 (mm Hg)	521	530	525	268	268
	Partial pressure Toluene (mm Hg)	37	37	37	68	54
FEED	cc toluene	0.3	0.3	0.3	0.3	0.3
	Pressure O2 (mm Hg)	300	300	300	150	150
	Bath temp. (^{o}C)	30	30	30	43	38
DISCHARGE	Discharge time (min)	5	10	0	5	0
	Frequency	–	–	–	–	–
	% discharge	–	–	–	–	–
G.C. ANALYSIS vol %	Benzene	.23	.09	.01	.14	.00
	Phenol	.36	.51	.00	.45	.07
	Benzaldehyde	.45	.35	.02	.51	.03
	Benzyl alcohol	.29	.27	.00	.15	.00
	Benzoic acid	.00	.04	.00	.00	.00
RESULTS	Total pressure after reaction (mm Hg)	336	336	336	168	165
	oxygen/toluene ratio	14	14	14	4.0	5.0
	CONVERSION					
	Gas phase (Mol %)	74	73	2	39	4
	Liquid phase (mol %)	1.35	1.28	0.03	1.26	0.10
	SELECTIVITY					
	Benzene	.01	.01	–	.01	–
	Phenol	.17	.07	–	.11	–
	Benzaldehyde	.33	.27	–	.41	–
	Benzyl alcohol	.22	.21	–	.12	–
	Benzoic acid	.00	.03	–	.00	–

EXPERIMENTS IN A BATCH REACTOR

	Run number	6	7	8	9	10
REACTOR	Temperature (°C)	240	260	310	315	350
	Residence time (min)	5	7	5	10	5
	Partial pressure O2 (mm Hg)	86	90	196	197	209
	Partial pressure toluene (mm Hg)	47	43	66	91	93
FEED	cc toluene	0.3	0.3	0.3	0.3	0.3
	Pressure O2 (mm Hg)	50	50	100	100	100
	Bath temp. (°C)	35	33	42.5	49.5	50
DISCHARGE	Discharge time (min)	2	0	0	0	0
	Frequency	–	–	–	–	–
	% discharge	–	–	–	–	–
G.C. ANALYSIS vol %	Benzene	.02	.01	.005	.01	.01
	Phenol	.11	.00	.00	.00	.00
	Bensaldehyde	.16	.02	.01	.11	.01
	Benzyl alcohol	.03	.00	.00	.00	.00
	Benzoic acid	.00	.00	.08	.00	.00
RESULTS	Total pressure after reaction	68	50	158	122	136
	oxygen/toluene ratio	1.8	2.1	3.0	2.1	2.2
	CONVERSION					
	Gas phase (mol %)	14	1	3	3.5	.5
	Liquid phase (mol %)	.32	.03	.10	.12	.02
	SELECTIVITY					
	Benzene	.06	.00	.00	.00	.00
	Phenol	.34	–	–	–	–
	Benzaldehyde	.50	–	–	–	–
	Benzyl alcohol	.10	–	–	–	–
	Benzoic acid	.00	–	–	–	–

EXPERIMENTS IN A BATCH REACTOR

	Run number	11	12	13	14	15
REACTOR	Temperature (°C)	340	345	346	345	400
	Residence time (min)	10	5	20	65	10
	Partial pressure O2 (mm Hg)	205	311	309	311	338
	Partial pressure Toluene (mm Hg)	96	170	178	186	218
FEED	cc toluene	0.3	0.3	0.3	0.3	0.3
	Pressure O2 (mm Hg)	100	150	148	150	150
	Bath temp (°C)	50.5	64.5	66	67.5	71
DISCHARGE	Discharge time (min)	0	0	0	0	0
	Frequency	–	–	–	–	–
	% discharge	–	–	–	–	–
G.C. ANALYSIS vol %	Benzene	.01	.02	.02	.07	.04
	Phenol	.00	.00	.03	.17	.06
	Benzaldehyde	.02	.04	.12	.35	.14
	Benzyl alcohol	.00	.00	.00	.00	.00
	Benzoic acid	.00	.00	.00	.00	.00
RESULTS	Total pressure after reaction (mm Hg)	136	190	184	179	186
	oxygen/toluene ratio	2.1	1.8	1.7	1.7	1.6
	CONVERSION					
	Gas phase (Mol %)	.7	.9	2.3	7.8	3.1
	Liquid phase (mol %)	.03	.06	.17	.60	.26
	SELECTIVITY					
	Benzene	–	–	–	.11	.15
	Phenol	–	–	–	.28	.23
	Benzaldehyde	–	–	–	.58	.54
	Benzyl alcohol	–	–	–	.00	.00
	Benzoic acid	–	–	–	.00	.00

EXPERIMENTS IN A BATCH REACTOR

	Run number	16	17	18*	19	20*
REACTOR	Temperature (°C)	290	300	300	310	295
	Residence time (min)	4	4	4	5	5
	Partial pressure O2 (mm Hg)	189	288	385	195	95
	Partial pressure Toluene (mm Hg)	141	141	140	141	141
FEED	cc toluene	0.3	0.3	0.3	0.3	0.3
	Pressure O2 (mm Hg)	100	150	200	100	50
	Bath temp (°C)	60	60	59.5	60	60
DISCHARGE	Discharge time (min)	.5	2.0	1.0	2.0	2.0
	Frequency	–	–	–	–	–
	% discharge	–	–	–	–	–
G.C. ANALYSIS vol %	Benzene	.10	.09	.06	.09	.06
	Phenol	.16	.42	.00	.31	.19
	Benzaldehyde	.21	.41	.00	.34	.15
	Benzyl alcohol	.05	.17	.00	.13	.03
	Benzoic acid	.00	.00	.00	.00	.00
RESULTS	Total pressure after reaction (mm Hg)	144	183	530	133	760
	oxygen/toluene ratio	1.3	2.0	2.8	1.4	0.7
	CONVERSION					
	Gas phase (mol %)	9.0	19	.9	15	7.3
	Liquid phase (mol %)	.58	1.17	.06	.91	.46
	SELECTIVITY					
	Benzene	.17	.08	–	.10	.13
	Phenol	.28	.36	–	.34	.41
	Benzaldehyde	.36	.35	–	.37	.33
	Benzyl alcohol	.09	.15	–	.14	.07
	Benzoic acid	.00	.00	.00	.00	.00

* Light flash inside

EXPERIMENTS IN A BATCH REACTOR

	Run number	21	22	23	24	25
REACTOR	Temperature (°C)	300	300	305	300	300
	Residence time (min)	2	4	10	2	2
	Partial pressure O2 (mm Hg)	96	96	97	385	385
	Partial pressure Toluene (mm Hg)	288	288	298	298	298
FEED	cc toluene	0.3	0.3	0.3	0.3	0.3
	Pressure O2 (mm Hg)	50	50	50	200	200
	Bath temp (°C)	79	79	79.5	79.5	79.5
DISCHARGE	Discharge time (min)	.5	1.0	2.0	.5	1.0
	Frequency	–	–	–	–	–
	% discharge	–	–	–	–	–
G.C. ANALYSIS vol %	Benzene	.02	.05	.06	.03	.03
	Phenol	.00	.08	.16	.04	.13
	Bensaldehyde	.07	.27	.33	.11	.23
	Benzyl alcohol	1.47	.99	.65	.47	.59
	Benzoic acid	.00	.00	.02	.00	.06
RESULTS	Total pressure after reaction (mm Hg)	68	65	72	238	242
	oxygen/toluene ratio	.3	.3	.3	1.3	1.3
	CONVERSION					
	Gas phase (mol %)	12.1	10.9	9.3	4.9	8.0
	Liquid phase (mol %)	1.56	1.40	1.22	.65	1.06
	SELECTIVITY					
	Benzene	.01	.04	.05	.05	.03
	Phenol	.00	.06	.13	.06	.12
	Benzaldehyde	.05	.20	.27	.17	.22
	Benzyl alcohol	.94	.70	.53	.72	.56
	Benzoic acid	.00	.00	.02	.00	.06

	Run number	26	27	28	29	30
REACTOR	Temperature (°C)	305	300	300	300	300
	Residence time (min)	5	2	10	5	5
	Partial pressure O2 (mm Hg)	388	770	192	193	192
	Partial pressure Toluene (mm Hg)	298	298	286	286	286
FEED	cc toluene	0.3	0.3	0.3	0.3	0.3
	Pressure O2 (mm Hg)	200	400	100	100	100
	Bath temp. (°C)	79.5	79.5	79.5	79.5	79.5
DISCHARGE	Discharge time (min)	2.0	1.0	5.0	5.0	5.0
	Frequency	–	–	5.0	5.0	5.0
	% discharge	–	–	100	50	25
G.C. ANALYSIS vol %	Benzene	.03	.03	.41	.07	.04
	Phenol	.16	.16	.60	.19	.12
	Benzaldehyde	.20	.26	.59	.31	.23
	Benzyl alcohol	.25	.30	.20	.18	.17
	Benzoic acid	.04	.08	.08	.04	.04
RESULTS	Total pressure after reaction (mm Hg)	244	429	191	136	136
	oxygen/toluene ratio	1.3	2.6	.7	.7	.7
	CONVERSION					
	Gas phase (mol %)	5.2	6.7	16.9	6.4	4.7
	Liquid phase (mol %)	.69	.88	2.15	.81	.60
	SELECTIVITY					
	Benzene	.04	.03	.19	.09	.07
	Phenol	.23	.18	.28	.24	.20
	Benzaldehyde	.29	.30	.27	.38	.38
	Benzyl alcohol	.36	.34	.09	.22	.28
	Benzoic acid	.00	.04	.12	.01	.00

EXPERIMENTS IN A BATCH REACTOR

	Run number	31	32*	33	34	35
REACTOR	Temperature ($^{\circ}$C)	300	300	300	300	300
	Residence time (min)	5	5	15	10	5
	Partial pressure O2 (mm Hg)	192	192	192	192	190
	Partial pressure Toluene (mm Hg)	286	286*	264	270	273
FEED	cc toluene	0.3	0.3*	0.3	0.3	0.3
	Pressure O2 (mm Hg)	100	100	100	100	99
	Bath temp. ($^{\circ}$C)	79.5	79.5	76	77	77.5
DISCHARGE	Discharge time (min)	5.0	2.0	.1	.2	.5
	Frequency	5	–	–	–	–
	% discharge	10	–	–	–	–
G.C. ANALYSIS vol %	Benzene	.01	.01	.01	.01	.02
	Phenol	.00	.01	.00	.00	.04
	Benzaldehyde	.10	.20	.01	.01	.14
	Benzyl alcohol	.05	–*	.00	.00	.00
	Benzoic acid	.00	.04	.00	.00	.00
RESULTS	Total pressure after reaction (mm Hg)	133	103	125	125	121
	oxygen/toluene ratio	.67	.67*	.73	.71	.70
	CONVERSION					
	Gas phase (mol %)	1.3	3.0	.1	.1	2.1
	Liquid phase (mol %)	.16	.38	.02	.02	.25
	SELECTIVITY					
	Benzene	–	.02	–	–	.08
	Phenol	–	.01	–	–	.16
	Benzaldehyde	–	.53	–	–	.56
	Benzyl alcohol	–	–*	–	–	.20
	Benzoic acid	–	.10	–	–	.00

* feed is 0.3 cc benzyl alcohol

EXPERIMENTS IN A BATCH REACTOR

	Run number	36	37	38	39	40
REACTOR	Temperature (°C)	300	310	305	305	280
	Residence time (min)	5	5	5	5	5
	Partial pressure O2 (mm Hg)	190	195	194	194	184
	Partial pressure Toluene (mm Hg)	273	276	276	276	284
FEED	cc toluene	0.3	0.3	0.3	0.3	0.3
	Pressure O2 (mm Hg)	99	100	100	100	100
	Bath temp. (°C)	77.5	78	78	78	79
DISCHARGE	Discharge time (min)	1	2	5	10	20*
	Frequency	–	–	–	–	–
	% discharge	–	–	–	–	–
G.C. ANALYSIS vol %	Benzene	.02	.05	.14	.22	.24
	Phenol	.08	.23	.57	.89	.55
	Benzaldehyde	.17	.37	.41	.38	.18
	Benzyl alcohol	.06	.15	.22	.21	.13
	Benzoic acid	.00	.04	.19	.30	.20
RESULTS	Total pressure after reaction (mm Hg)	135	136	136	122	129
	oxygen/toluene ratio	.70	.71	.70	.70	.65
	CONVERSION					
	Gas phase (mol %)	2.7	6.9	12.7	16.5	10.9
	Liquid phase (mol %)	.33	.85	1.56	2.03	1.38
	SELECTIVITY					
	Benzene	.06	.06	.09	.11	.17
	Phenol	.24	.27	.37	.44	.40
	Benzaldehyde	.51	.44	.26	.19	.13
	Benzyl alcohol	.18	.18	.14	.10	.09
	Benzoic acid	.00	.05	.12	.15	.15

*   electrodes loose

EXPERIMENTS IN A BATCH REACTOR

	Run number	41	42	43	44	45
REACTOR	Temperature (°C)	300	300	300	300	300
	Residence time (min)	10	5	5	5	10
	Partial pressure O2 (mm Hg)	192	192	192	192	192
	Partial pressure Toluene (mm Hg)	284	284	284	284	284
FEED	cc toluene	0.3	0.3	0.3	0.3	0.3
	Pressure O2 (mm Hg)	100	100	100	100	100
	Bath temp. (°C)	79	79	79	79	79
DISCHARGE	Discharge time (min)	5	5	5	5	5
	Frequency	10	10	10	30	30
	% discharge	10	25	50	50	25
G.C. ANALYSIS vol %	Benzene	.01	.05	.05	.04	.01
	Phenol	.03	.19	.20	.23	.12
	Benzaldehyde	.07	.24	.19	.19	.13
	Benzyl alcohol	.05	.14	.13	.13	.10
	Benzoic acid	.00	.00	.04	.00	.00
RESULTS	Total pressure after reaction (mm Hg)	122	136	136	133	144
	oxygen/toluene ratio	.68	.68	.68	.68	.68
	CONVERSION					
	Gas phase (mol %)	1.3	4.3	5.0	4.7	2.9
	Liquid phase (mol %)	.16	.54	.63	.59	.37
	SELECTIVITY					
	Benzene	–	.09	.08	.07	.03
	Phenol	–	.35	.32	.39	.32
	Benzaldehyde	–	.45	.30	.32	.35
	Benzyl alcohol	–	.26	.21	.22	.27
	Benzoic acid	–	.00	.06	.00	.00

EXPERIMENTS IN A BATCH REACTOR

	Run number	46	47	48	49	50
REACTOR	Temperature (°C)	300	300	300		
	Residence time (min)	30	10	10		
	Partial pressure O2 (mm Hg)	192	192	192		
	Partial pressure Toluene (mm Hg)	284	284	284		
FEED	cc toluene	0.3	0.3	0.3		
	Pressure O2 (mm Hg)	100	100	100		
	Bath temp. (°C)	79	79	79		
DISCHARGE	Discharge time (min)	5	5	5		
	Frequency	30	10	10		
	% discharge	10	25	100		
G.C. ANALYSIS vol %	Benzene	.02	.02	.05		
	Phenol	.06	.06	.17		
	Benzaldehyde	.12	.08	.08		
	Benzyl alcohol	.09	.03	.05		
	Benzoic acid	.00	.00	.00		
RESULTS	Total pressure after reaction (mm Hg)	–	151	–		
	oxygen/toluene ratio	.68	.68	.68		
	CONVERSION					
	Gas phase (mol %)	2.5	1.5	2.8		
	Liquid phase (mol %)	.31	.19	.35		
	SELECTIVITY					
	Benzene	.06	–	.14		
	Phenol	.19	–	.49		
	Benzaldehyde	.39	–	.23		
	Benzyl alcohol	.28	–	.14		
	Benzoic acid	.00	–	.00		

APPENDIX IV

WAVELENGTH MICRONS

Wavenumber

Catalogue No. 20604

WITH INDEX	SAMPLE	Toluene feed	FORMULA		PHASE		SCAN SPEED	Medium
RECORDER					THICKNESS		DATE	4-8-75
	REFERENCE				REMARKS		OPERATOR	RE

WAVELENGTH MICRONS

WAVE INDEX	SAMPLE	Feed +0.5 vol% Benzaldehyde	FORMULA		PHASE		SCAN SPEED	Medium
RE RECORDER					THICKNESS		DATE	4-8-75
	REFERENCE				REMARKS		OPERATOR	RE

Catalogue No. 606041

Wavenumber

			6	8	10	12	14

WAVENUMBER

2000   1750   1500   1250   1000   750   650

Catalogue No. 60504I

WITH INDEX	SAMPLE Feed +0.5% Benzaldehyde +0.25% m-Cresol	FORMULA	PHASE	SCAN SPEED Medoum
RECORDER			THICKNESS	DATE 4-8-75
	REFERENCE		REMARKS	OPERATOR RE

219 4

Wavenumber

Catalogue No. 60404
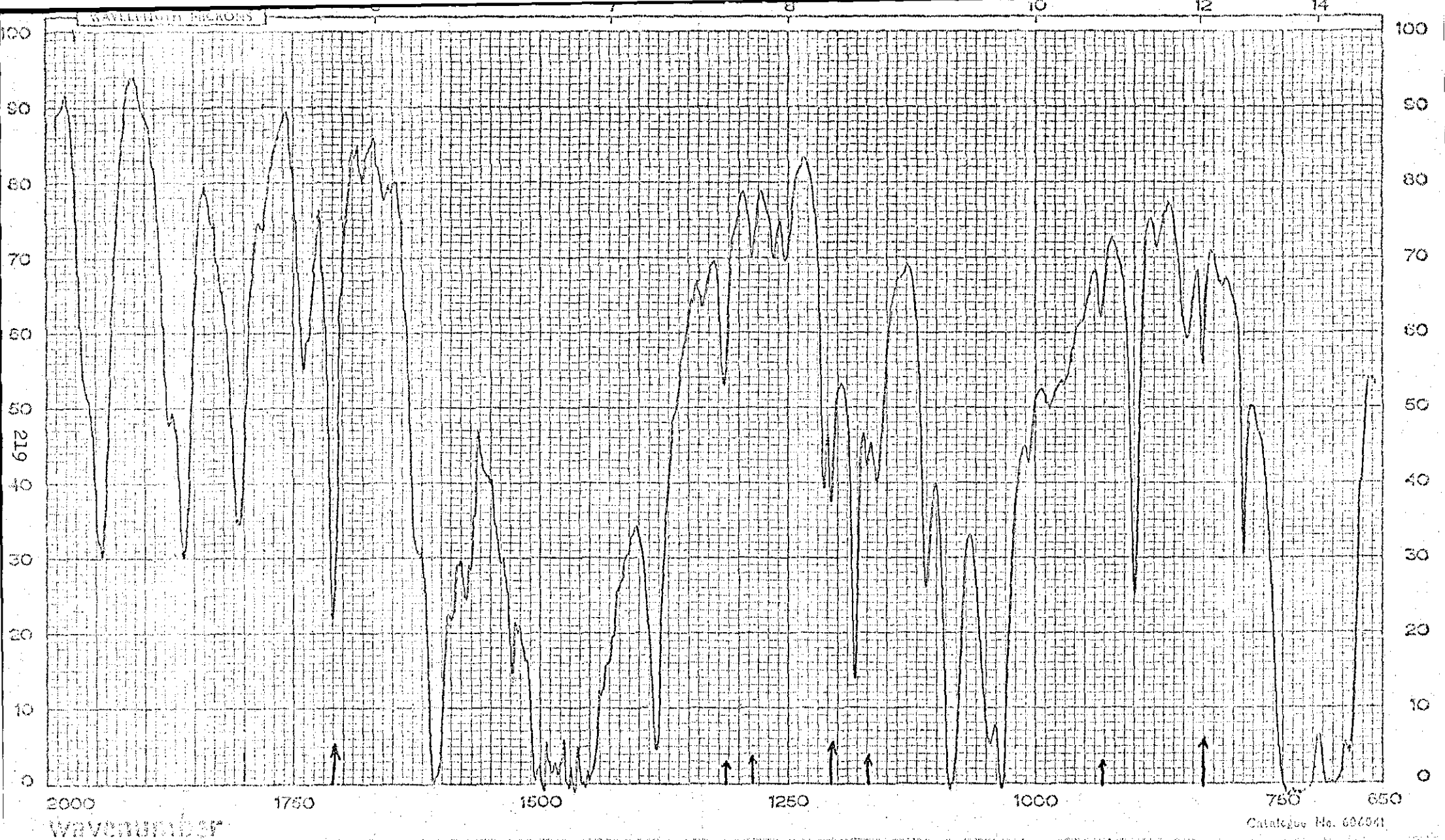
WITH INDEX	SAMPLE	Feed +0.5% Benzaldehyde +0.25% m-Cresol+0.25% Benzyl alcohol+0.25% Benzene	FORMULA		PHASE		SCAN SPEED	Medium
RE RECORDER					THICKNESS		DATE	4-8-75
	REFERENCE				REMARKS		OPERATOR	RE

WAVELENGTH MICRONS

wavenumber

Catalogue No. 606040
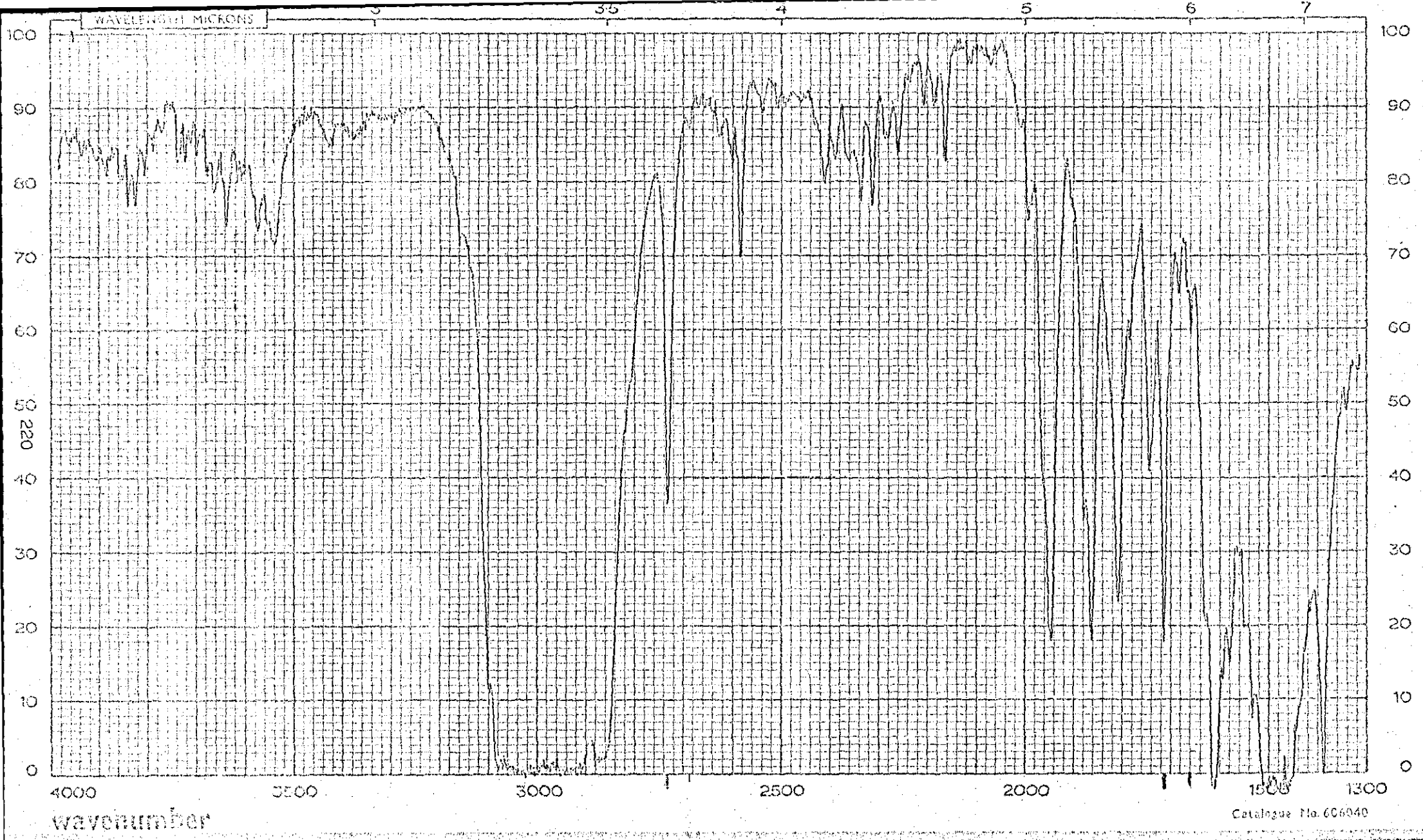
WITH INDEX	SAMPLE Run 55	FORMULA	PHASE	SCAN SPEED Medium
RE RECORDER			THICKNESS	DATE 4-8-75
	REFERENCE		REMARKS	OPERATOR RE

Toluene feed

WAVELENGTH MICRONS					

WaVenumber

Catalogue No. 40404

	Toluene feed	FORMULA	PHASE	SCAN SPEED	Medium
REFR. INDEX	SAMPLE		THICKNESS	DATE	4-8-75
THE RECORDER			REMARKS	OPERATOR	RE
	REFERENCE				

WAVELENGTH MICRONS

wavenumber

Catalogue No. 606040

IR Spectrum

Top axis: WAVELENGTH MICRONS — 3, 3.5, 4, 5, 6, 7

Left/right axis: 100, 90, 80, 70, 60, 50, 40, 30, 20, 10, 0

Bottom axis: wavenumber — 4000, 3500, 3000, 2500, 2000, 1500, 1300

Catalogue No. 606040

WITH INDEX	SAMPLE Feed+0.5% Benzaldehyde+	FORMULA	PHASE	SCAN SPEED	Medium
THIS RECORDER	0.25% m-Cresol		THICKNESS	DATE	4-8-75
	REFERENCE		REMARKS	OPERATOR	RE

WAVELENGTH MICRONS

wavenumber

224

Catalogue No. 606040

WAVELENGTH IN MICRONS

wavenumber

Catalogue No. 606040

ON WITH INDEX	SAMPLE Feed+0.5%Benzaldehyde+	FORMULA	PHASE	SCAN SPEED Medium
THE RECORDER	0.25%m-Cresol+0.25%Benzyl		THICKNESS	DATE 4-8-75
V	alcohol+0.25% Benzene		REMARKS	OPERATOR RE

wavenumber

Catalogue No. 608040

		SAMPLE Standard.15 o-Cresol	FORMULA		PHASE	SCAN SPEED Medium
ON WITH INDEX						
THE RECORDER					THICKNESS	DATE 4-8-75
					REMARKS	OPERATOR RE

WAVENUMBER

Catalogue No. 606040
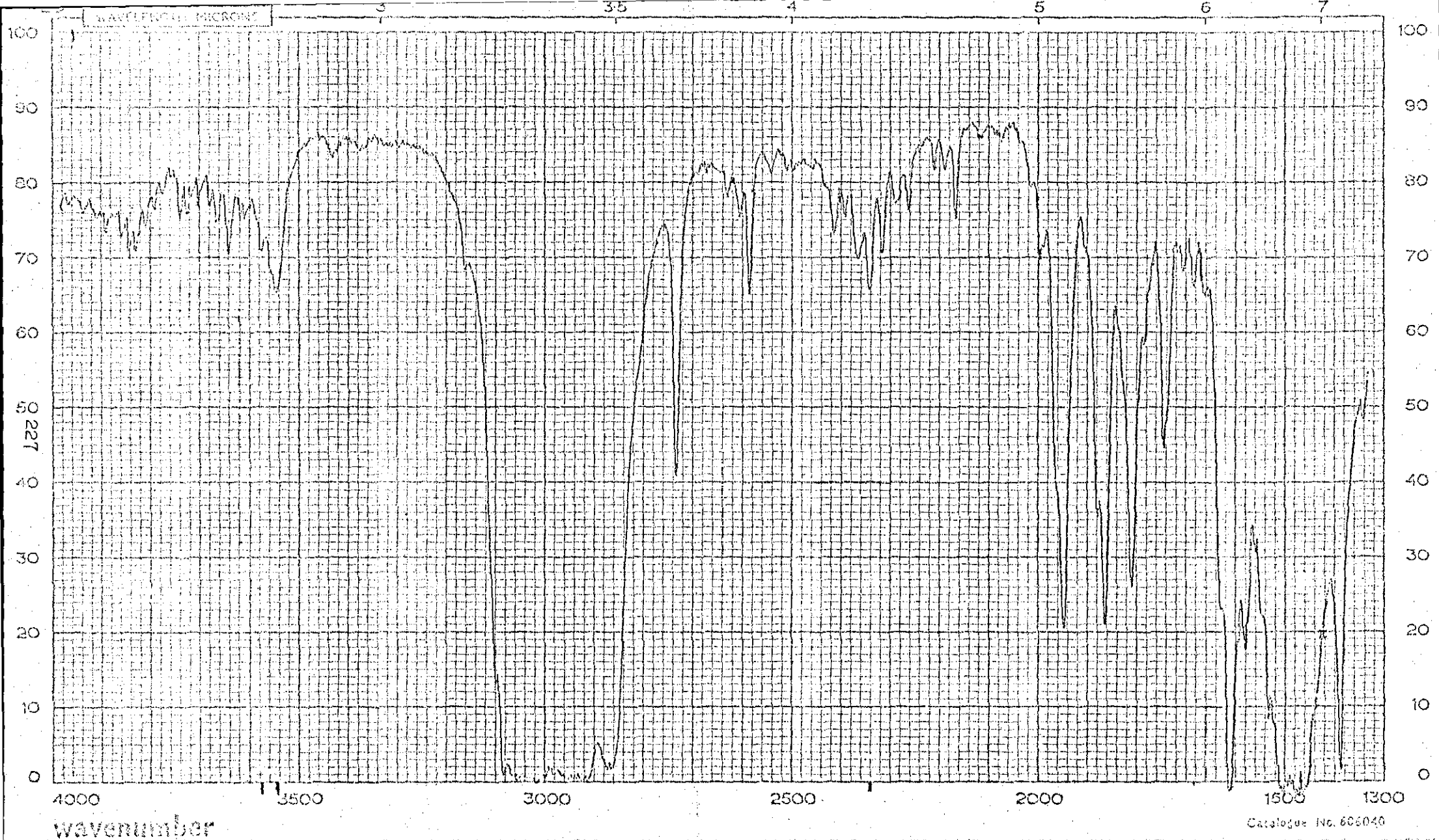
WITH INDEX	SAMPLE	p-Cresol	FORMULA		PHASE		SCAN SPEED	Medium
RE RECORDER					THICKNESS		DATE	4-8-75
	REFERENCE				REMARKS		OPERATOR	RE

APPENDIX V

EXPERIMENTS IN A FLOW REACTOR

Run number	1	2	3	4	5	6
Total run time (min.)	120	150	200	185	90	100
Residence time (sec.)	.25	.74	1.00	2.0	.4	1.3
Oxygen pressure (mm Hg)	74	47	51	50	110	98
Vapour pressure of toluene (mm Hg)	67	56	49	50	90	105
Total pressure (mm Hg)	141	103	100	101	200	203
Reactor temperature ($^\circ$C)	302	301	300	301	301	301
Applied voltage (kV)	0	0	0	0	0	0
E/p (volt mm Hg^{-1}cm^{-1})	0	0	0	0	0	0
E/N 10^{15} (volt cm^{-2})	0	0	0	0	0	0
Total current (uA)	0	0	0	0	0	0
Filtered current (uA)	0	0	0	0	0	0
Instantaneous current from photographs (uA)	0	0	0	0	0	0
Toluene charged (grams)	185	144.4	53.8	23.1	49.7	27.9
Liquid collected (grams)	119	123.8	51.7	21.8	48.3	26.3
Oxygen charged (gmoles)	1.958	.942	.619	.286	1.096	.616
Toluene charged (gmoles)	2.01	1.56	.584	.251	.540	.303
Energy dissipation (Whr)	0	0	0	0	0	0
Charge dissipated (As)	0	0	0	0	0	0
Conversion of toluene (mol %)	0	0	0	0	0	0
SELECTIVITY						
Benzene	—	—	—	—	—	—
Phenol	—	—	—	—	—	—
Benzyl alcohol	—	—	—	—	—	—
Benzaldehyde	—	—	—	—	—	—
Benzoic acid	—	—	—	—	—	—
Energy yield (kWhr/mole)	—	—	—	—	—	—
Reaction rate 10^{-7} (moles C7H8/l.sec)	0	0	0	0	0	0
ln (-r)	—	—	—	—	—	—

Run number	7	8	9	10	11	12
Total run time (min.)	120	60	260	165	180	120
Residence time (sec.)	4.5	1.6	12.4	0.6	1.3	0.6
Oxygen pressure (mm Hg)	78	69	65	75	75	–
Vapour pressure of toluene (mm Hg)	52	78	79	75	79	–
Total pressure (mm Hg)	130	147	144	150	154	144
Reactor temperature (^{o}C)	273	271	263	266	312	360
Applied voltage (kV)	10	10	10	10	9	7.5
E/p (volt mm $Hg^{-1}cm^{-1}$)	96	85	87	83	73	65
E/N 10^{15} volt cm^{-2})	5.44	4.79	4.82	4.64	4.43	–
Total current (uA)	213	212	224	225	488	1613
Filtered current (uA)	102	108	81	90	202	711
Instantaneous current from photographs (uA)	–	–	–	–	–	–
Toluene charged (grams)	6.88	9.64	7.31	99.50	44.20	–
Liquid collected (grams)	5.54	7.52	5.61	96.6	42.20	131.7
Oxygen charged (gmoles)	.128	.229	.098	1.536	.664	.435
Toluene charged (gmoles)	.075	.105	.079	1.08	.480	–
Energy dissipation (Whr)	.73	.76	2.5	1.75	3.9	11.2
Charge dissipation (As)	.734	.388	1.26	.891	2.18	7.68
Conversion of toluene (mol %)	.49	.52	1.88	.39	.63	–
SELECTIVITY						
Benzene	.09	.18	.09	.18	.14	–
Phenol	.06	.07	.08	.00	.06	–
Benzaldehyde	.45	.30	.39	.38	.38	–
Benzyl alcohol	} .20	} .24	} .21	} .41	} .14	–
o-Cresol						–
m+p-Cresol	.18	.17	.20		–	–
Benzoic acid	.00	.00	.00	.00	.00	–
Energy yield (kWhr/mole)	2.0	1.40	1.67	.42	1.00	–
Reaction rate 10^{-7} (moles C7H8/l.sec)	38	34	38	117	82	2
ln(-r)	-12.48	-12.59	-12.48	-11.35	-11.71	-15.00

Run number	13	14	15	16	17	18
Total run time (min.)	120	270	330	120	240	300
Residence time (sec.)	6.7	5.2	2.0	3.5	2.3	2.6
Oxygen pressure (mm Hg)	81	70	36	76	44	51
Vapour pressure of toluene (mm Hg)	80	80	78	79	80	79
Total pressure (mm Hg)	161	150	114	155	124	130
Reactor temperature (^{o}C)	358	177	220	261	300	264
Applied voltage (kV)	7.5	10	10	8	6	4
E/p (volt mm Hg^{-1}cm^{-1})	58	83	110	65	61	38
E/N 10^{15} (volt cm^{-2})		3.88	5.60	3.57	3.34	2.14
Total current (uA)	1800	161	162	139	92	55
Filtered current (uA)	590	92	84	58	36	23
Instantaneous current from photographs (uA)	-	-	-	-	-	-
Toluene charged (grams)	4.00	12.6	58.8	7.18	27.6	26.7
Liquid collected (grams)	2.91	10.6	56.3	4.73	24.8	24.7
Oxygen charged (gmoles)	.101	.321	.598	.236	.458	.578
Toluene charged (gmoles)	.043	.137	.638	.078	.299	.290
Energy dissipation (Whr)	5.9	2.9	3.3	.66	.61	.32
Charge dissipation (As)	4.25	2.61	1.66	.42	.52	.41
Conversion of toluene (mole %)	5.18	1.23	.25	.45	.25	.19
SELECTIVITY						
Benzene	.10	.08	.31	.22	.29	.31
Phenol	.14	.06	.02	.08	.07	.07
Benzaldehyde	.39	.33	.26	.36	.30	.31
Benzyl alcohol	.16	.30	.14	.03	.07	.04
o-Cresol	.18			.18	.15	.15
m+p-Cresol	-	19	.09	.11	.13	.11
Benzoic acid	.02	.00	.00	.00	.00	.00
Energy yield (kWhr/mole)	2.6	1.73	2.0	1.08	.81	.58
Reaction rate 10^{-7} (moles C7H8/l.sec.)	89	27	23	14	15	8.7
ln(-r)	-11.63	-12.82	-12.98	-13.48	-13.41	-13.95

Run number	19	20	21	22	23	24
Total run time (min.)	300	240	240	240	210	240
Residence time (sec.)	3.3	3.5	3.8	3.1	3.7	3.3
Oxygen pressure (mm Hg)	64	74	83	66	79	74
Vapour pressure of toluene (mm Hg)	81	80	80	79	79	80
Total pressure (mm Hg)	145	154	163	145	158	154
Reactor temperature (^{o}C)	300	300	300	264	262	264
Applied voltage (kV)	3	5	7	9	11	8
E/p (volt/cm-mm Hg)	26	41	54	78	87	65
$E/N \; 10^{15}$ (volt cm^{-2})	1.43	2.24	2.96	4.32	4.82	3.61
Total current (uA)	34	72	117	174	206	150
Filtered current (uA)	15	30	47	62	75	62
Instantaneous current from photographs (uA)	–	–	–	–	–	–
Toluene charged (grams)	19.6	15.3	13.4	16.6	11.8	17.7
Liquid collected (grams)	18.2	14.5	12.1	15.6	10.7	16.6
Oxygen charged (gmoles)	.571	.450	.450	.472	.400	.490
Toluene charged (gmoles)	.213	.167	.145	.180	.128	.193
Energy dissipation (Whr)	.145	.42	.93	1.56	2.0	1.4
Charge dissipation (As)	.26	.43	.67	.88	.94	.89
Conversion of toluene (mole %)	.13	.34	.60	.67	1.07	.62
SELECTIVITY						
Benzene	.34	.15	.12	.12	.08	.11
Phenol	.07	.07	.08	.07	.07	.52
Benzaldehyde	.30	.33	.35	.34	.33	
Benzyl alcohol		.05	.07	.07	.07	.05
o-Cresol	.28	.22	.21	.21	.24	.10
m+p-Cresol		.17	.17	.16	.18	.11
Benzoic acid	.00	.00	.00	.00	.00	.02
Reaction rate 10^{-7} (moles C7H8l.sec.)	4.4	11.2	17.3	24.0	27.0	23.7
ln(-r)	-14.64	-13.70	-13.27	-12.94	-12.81	-12.95

EXPERIMENTS IN A FLOW REACTOR

Run number	25	26	27	28	29	30
Total run time (min.)	285	240	180	240	240	240
Residence time (sec.)	2.0	1.5	.33	3.6	3.0	5.9
Oxygen pressure (mm Hg)	48	33	22	94	73	81
Vapour pressure of toluene (mm Hg)	78	79	76	81	82	83
Total pressure (mm Hg)	126	112	98	175	155	164
Reactor temperature (^{o}C)	264	264	276	263	345	346
Applied voltage (kV)	8	8	8	8	0	0
E/p (volt mm Hg^{-1}cm^{-1})	79	89	102	57	0	0
E/N 10^{15} (volt cm^{-2})	4.42	4.97	5.81	3.17	0	0
Total current (uA)	153	122	160	151	0	0
Filtered current (uA)	57	52	46	64	0	0
Instantaneous current from photographs (uA)	–	52	21	52	0	0
Toluene charged (grams)	47.7	52.9	255	16.9	22.69	12.86
Liquid collected (grams)	46.7	51.4	254	16.0	22.51	12.19
Oxygen charged (gmoles)	.565	.504	.364	.507	.457	.246
Toluene charged (gmoles)	.518	.575	2.771	.184	.246	.140
Energy dissipation (Whr)	3.7	1.17	.78	1.45	0	0
Charge dissipation (As)	.98	.75	.50	.92	0	0
Conversion of toluene (mole %)	.20	.14	.017	.80	.03	.02
SELECTIVITY						
Benzene	.20	.43	.87	.16	.93	.93
Phenol	.05	.03	.00	.05	.00	.00
Benzaldehyde	.35	.28	.11	.25	.00	.00
Benzyl alcohol	.06	.01	.00	.06	.00	.00
o-Cresol	.15	.07	.00	.16	.00	.00
p+m-Cresol	.13	.03	.00	.13	.00	.00
Benzoic acid	.00	.00	.00	.00	.00	.00
Energy yield (kWhr/mole)	1.47	1.46	1.67	.99	–	–
Reaction rate 10^{-7} (moles C7H8/l.sec.)	17.3	16	10	29	1.7	.65
ln(-r)	-13.27	-13.34	-13.81	-12.75	-16	-16.5

Run number	31	32[*]	33[*]	34	35	36
Total run time (min.)	240	240	120	240	120	180
Residence time (sec.)	2.2	4.0	.5	2.1	1.7	5.0
Oxygen pressure (mm Hg)	64	117	20	73	–	63
Vapour pressure of toluene (mm Hg)	82	83	76	56	–	79
Total pressure (mm Hg)	146	200	96	129	136	142
Reactor temperature (^{o}C)	344	346	344	354	357	350
Applied voltage (kV)	8	8	8	8	8	8
E/p (volt mm $Hg^{-1} cm^{-1}$)	69	50	104	78	74	70
$E/N \cdot 10^{15}$ (volt cm^{-2})	4.38	3.21	6.66	5.05	4.80	4.55
Total current (uA)	149	144	181	276	254	256
Filtered current (uA)	22	19	30	44	38	40
Instantaneous current from photographs (uA)	18	15	24	22	–	–
Toluene charged (grams)	38.53	19.34	226.7	30.40	27.43	10.16
Liquid collected (grams)	36.28	18.68	226.0	29.52	26.91	9.77
Oxygen charged (gmoles)	.426	.441	.231	.447	.233	.169
Toluene (gmoles)	.418	.210	2.434	.331	.298	.110
Energy dissipation (Whr)	.497	.429	.339	.984	.429	.685
Charge dissipation (As)	.32	.27	.22	.63	.27	.44
Conversion of toluene (mole %)	.33	.36	.03	.41	.25	.90
SELECTIVITY						
Benzene	.25	.23	.81	.22	.42	.22
Phenol	.07	.06	.00	.09	.05	.07
Benzaldehyde	.29	.37	.04	.42	.30	.42
Benzyl alcohol	}.13	}.18	.00	}.12	}.06	}.15
o-Cresol			.00			
m+p-Cresol	.18	.10	.00	.08	.02	.11
Benzoic acid	.00	.00	.00	.00	.00	.00
Energy yield (kWhr/mole)	.36	.57	.46	.73	.57	.69
Reaction rate 10^{-7} (moles C7H8/l.sec.)	27.6	15.1	26.1	26.6	29.2	26.5
$\ln(-r)$	-12.80	-13.40	-12.85	-12.84	-12.74	-12.84

* Loose electrodes!

Run number	37	38	39	40	41	42
Total run time (min.)	180	150	120	120	135	180
Residence time (sec.)	8.3	1.3	2.1	2.1	2.2	3.5
Oxygen pressure (mm Hg)	65	65	67	66	70	53
Vapour pressure of toluene (mm Hg)	80	79	79	80	80	80
Total pressure (mm Hg)	145	144	416	146	150	133
Reactor temperature ($^{\circ}$C)	355	351	350	352	348	389
Applied voltage (kV)	8	8	6	4	2	0
E/p (volt mm Hg^{-1}cm^{-1})	69	70	51	34	17	0
E/N 10^{15} (volt cm^{-2})	4.49	4.50	3.30	2.22	1.07	0
Total current (uA)	273	244	143	59	7	0
Filtered current (uA)	46	34	20	8	.3	0
Instantaneous current from photograph (uA)	--	30	19	13	--	--
Toluene charged (grams)	7.39	32.97	20.25	21.24	22.00	17.56
Liquid collected (grams)	6.95	32.82	19.35	21.00	21.48	17.17
Oxygen charged (gmoles)	.091	.552	.229	.226	.254	.154
Toluene charged (gmoles)	.080	.358	.220	.231	.239	.191
Energy dissipation (Whr)	.790	.480	.165	.043	.001	0
Charge dissipation (As)	.50	.31	.14	.05	.002	0
Conversion of toluene (mole %)	1.39	.16	.19	.08	.12	.08
SELECTIVITY						
Benzene	.14	.46	.53	.77	.77	.86
Phenol	.08	.03	.00	.00	.00	.00
Benzaldehyde	.45	.30	.24	.16	.00	.00
Benzyl alcohol o-Cresol	}.16	}.06	}.05	}trace	}.00	}.00
m+p-Cresol	.14	.06	.03	--	.00	.00
Benzoic acid	.001	.00	.00	.00	.00	.00
Energy yield (kWhr/mole)	.71	.84	.39	.23	.00	--
Reaction rate 10^{-7} (moles C7H8/l.sec.)	29.4	17.6	16.2	7.2	9.7	3.9
ln(-r)	-12.74	-13.25	-13.33	-14.14	-13.84	-14.76

Run number	43	44	45	46	47	48
Total run time (min.)	120	160	120	60	120	150
Residence time (sec.)	2.2	2.0	2.0	.4	4.9	4.8
Oxygen pressure (mm Hg)	65	67	68	26	78	80
Vapour pressure of toluene (mm Hg)	79	80	80	77	80	80
Total pressure (mm Hg)	144	147	418	103	158	160
Reactor temperature ($^{\circ}$C)	386	387	390	384	52	52
Applied voltage (kV)	6	4	2	6	10	8
E/p (volt mm Hg^{-1}cm^{-1})	52	34	17	73	79	62
E/N 10^{15} (volt cm^{-2})	3.55	2.32	1.16	4.96	2.66	2.09
Total current (uA)	488	183	37	403	118	68
Filtered current (uA)	94	29	6.5	68	40	25
Instantaneous current from photographs (uA)	57	24	10	–	30	34
Toluene charged (grams)	16.95	28.63	21.39	63.97	17.70	22.64
Liquid collected (grams)	16.35	27.65	20.81	63.80	17.13	22.36
Oxygen charged (gmoles)	.217	.294	.214	.110	.211	.275
Toluene charged (gmoles)	.184	.311	.232	.694	.192	.246
Energy dissipation (Whr)	.797	.215	.018	–	.561	.354
Charge dissipation (As)	.68	.27	.05	–	.29	.23
Conversion of toluene (mole %)	.56	.13	.10	.06	.15	.15
SELECTIVITY						
Benzene	.31	.55	.56	.88	.44	.46
Phenol	.06	.00	.00	.00	.00	.00
Benzaldehyde	.41	.30	.32	.00	.25	.18
Benzyl alcohol						
o-Cresol						
m+p-Cresol	.07		.00	.00		
Benzoic acid	.00	.00	.00	.00	.00	.00
Energy yield (kWhr/mole)	.77	.53	.08	–	1.95	.96
Reaction rate 10^{-7} (moles C7H8/l.sec.)	40.9	11.7	9.2	32.5	11.7	11.4
ln(-r)	-12.41	-13.65	-13.19	-12.63	-13.66	-13.69

Run number	49	50	51	52	53	54
Total run time (min.)	150	160	150	150	150	60
Residence time (sec.)	4.9	5.3	3.4	2.0	.9	.2
Oxygen pressure (mm Hg)	80	91	108	53	34	17
Vapour pressure of toluene (mm Hg)	80	80	51	105	129	138
Total pressure (mm Hg)	160	171	159	158	613	155
Reactor temperature (^{o}C)	51	50	291	291	294	299
Applied voltage (kV)	6	8	8	8	8	8
E/p (volt mm Hg^{-1}cm^{-1})	47	59	51	63	61	65
E/N 10^{15} (volt cm^{-2})	1.57	1.96	3.67	3.71	3.61	3.83
Total current (uA)	71	107	147	134	121	118
Filtered current (uA)	36	48	62	57	44	38
Instantaneous current from photographs (uA)	24	39	52	49	–	40
Toluene charged (grams)	22.46	23.51	13.81	39.40	119.87	226.29
Liquid collected (grams)	21.93	22.86	13.38	38.92	117.03	264.53
Oxygen charged (gmoles)	.266	.281	.263	.263	.269	.106
Toluene charged (gmoles)	.244	.255	.150	.428	1.30	2.89
Energy dissipation (Whr)	.382	.724	.873	.800	.622	.215
Charge dissipation (As)	.32	.43	.55	.51	.39	.14
Conversion of toluene (mole %)	.08	.30	.43	.19	.07	.04
SELECTIVITY						
Benzene	.56	.23	.13	.38	.79	.74
Phenol	.00	.00	.10	.00	.00	.00
Benzaldehyde	.13	.38	.40	.54	.04	.00
Benzyl alcohol	.18	.30	.21	.00	.00	.00
o-Cresol						
m+p-Cresol			.14	.00	.00	.00
Benzoic acid	.00	.00	.00	.00	.00	.00
Energy yield (kWhr/mole)	1.96	.95	1.35	.98	.68	.13
Reaction rate 10^{-7} (moles C7H8/1.sec.)	6.0	22.6	20	26	30	87
ln(-r)	-14.32	-13.00	-13.10	-12.86	-12.71	-11.6

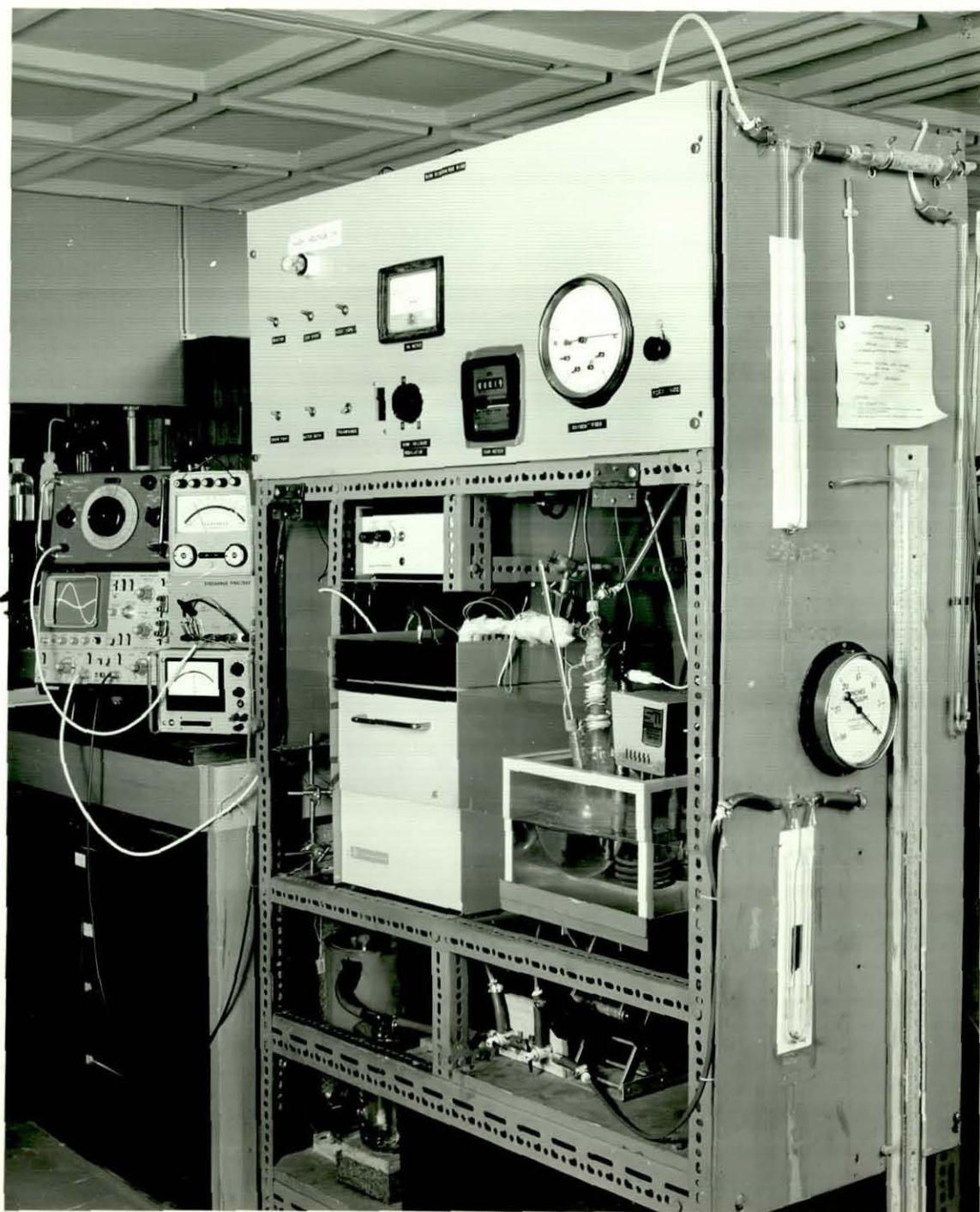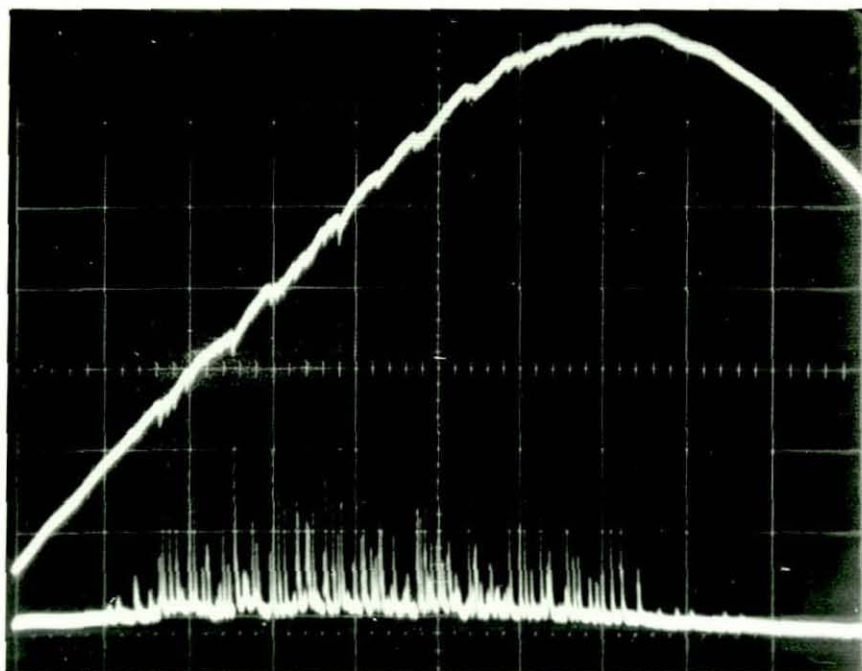APPENDIX VI

Figure 1   Experimental equipment
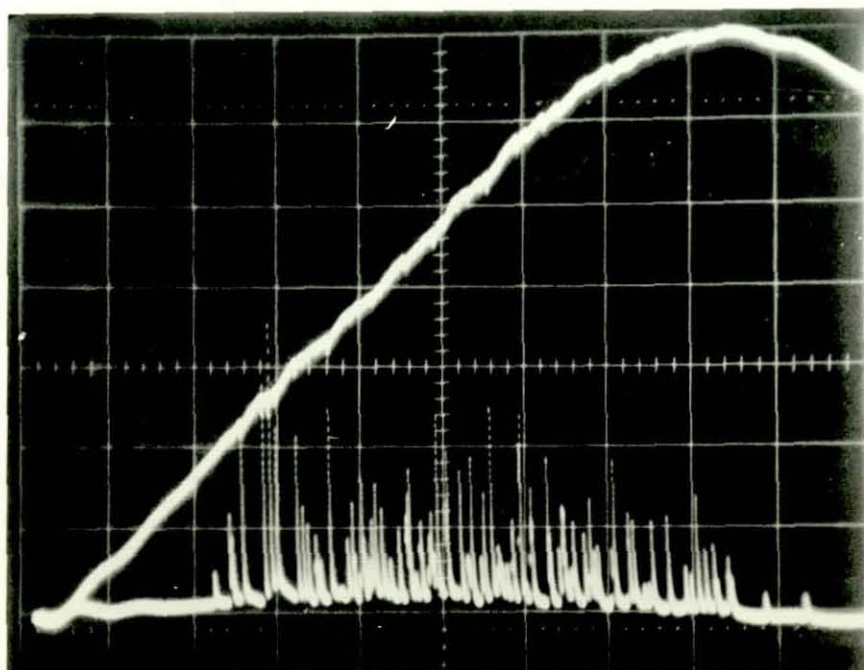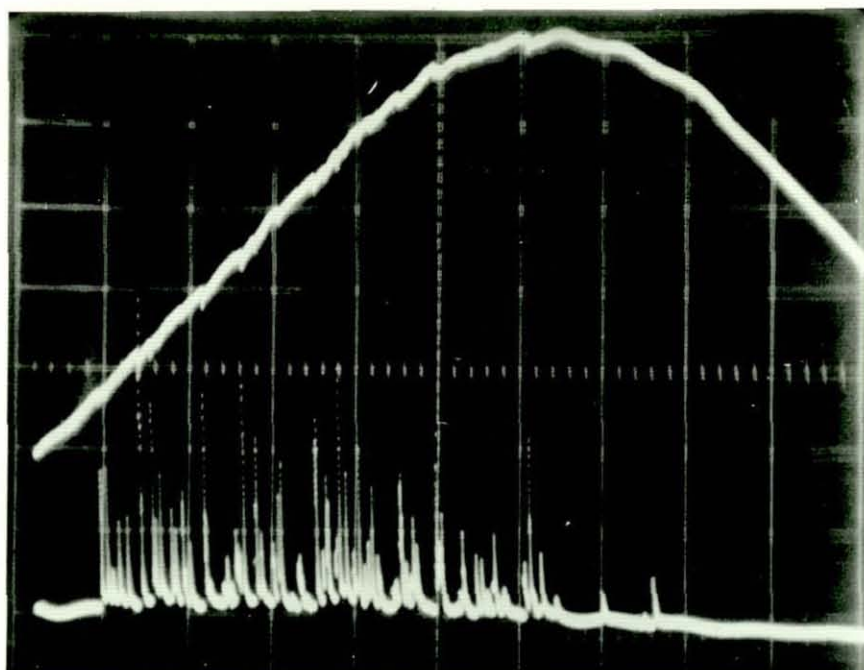
238

Figure 2   Flow reactor

239

U_1 (2000V/div) U_2 (5V/div)

Figure 3   Instantaneous current from Run 28

U_1 (2000V/div) U_2 (5V/div)
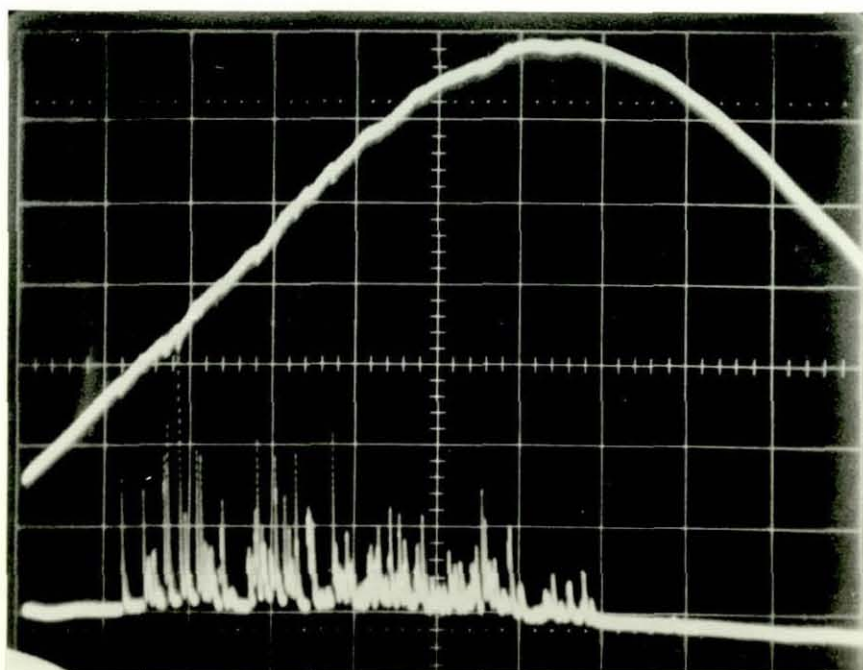
Figure 4   Instantaneous current from Run 5 1

240

Figure 5   Instantaneous current from Run 52

Figure 6   Instantaneous current from Run 54

241